DEVELOPING NOVEL BLOOD-STAGE MALARIA VACCINES

Thesis submitted for the degree of Doctor of Philosophy

Trinity Term 2012

Alexander Douglas

Wadham College

Word count: c. 48,000 words excluding bibliography, tables of contents and acknowledgments

DEVELOPING NOVEL BLOOD-STAGE MALARIA VACCINES

Thesis submitted for the degree of Doctor of Philosophy, Trinity Term 2012

Alexander Douglas, Wadham College, University of Oxford

Abstract

Natural exposure to *Plasmodium falciparum's* asexual blood-stage results in protection against severe disease, but no vaccine using the widely-studied blood-stage antigens apical membrane antigen 1 (AMA1) or merozoite surface protein 1 (MSP1) has proven convincingly protective in clinical trials. Challenges include antigenic polymorphism, the apparent requirement for exceptionally high antibody concentrations for protection, and clinical-grade production of conformationally-accurate recombinant protein antigens followed by formulation with a human-compatible adjuvant.

This thesis describes the generation of viral-vectored vaccines targeting ten less-studied blood-stage antigens, focusing upon antigens implicated in erythrocyte invasion. These vaccines were immunogenic in mice and rabbits. The rabbit antibodies raised were functionally active in the in vitro assay of parasite growth inhibitory activity (GIA). GIA with antibodies against one antigen, RH5, exceeded that achieved with antibodies against the 'gold standard' AMA1 or MSP1 antigens. This antigen's amino acid sequence is relatively conserved between parasite strains. Importantly, and unlike anti-AMA1 and MSP1 antibodies, the GIA effects transcend genetically diverse strains.

It was hypothesised that blockade of the interaction of RH5 with its receptor basigin was likely to be a mechanism of action of anti-RH5 antibodies. Vaccine-induced polyclonal anti-RH5 serum was found to be capable of blocking this interaction, as well as merozoite attachment to erythrocytes. A panel of RH5-specific monoclonal antibodies were raised: those which block the RH5-receptor interaction were capable of neutralising parasites. Minimal linear epitopes recognised by these antibodies were mapped, and are likely to be within or close to RH5's receptor binding site.

These data support prompt clinical testing of RH5-based vaccines, and shed light upon the mechanism of action of anti-RH5 antibodies. However substantial challenges remain in establishing whether this antigen, selected on the basis of the in vitro assay of GIA, will be capable of achieving *in vivo* protection against *P. falciparum*. Further work presented in this thesis addresses the use of quantitative PCR data to assess blood-stage vaccine efficacy in experimental human challenge with *P. falciparum*, and the use of surface plasmon resonance to establish more detailed characterisation of vaccine-induced antibody responses. Finally, the results of *P. falciparum* challenge of RH5-vaccinated Aotus nancymaae non-human primates are presented.

Acknowledgments

The results presented in this thesis could not have been generated without the extensive scientific assistance of a large number of colleagues and collaborators. This is explained in more detail in the authorship statements preceding each chapter. Here, I would like to give particular thanks to a few individuals who have given me especially valuable help- both scientific and personal- over the past three years.

I could not have asked for better supervisors than Simon Draper, Adrian Hill and Quentin Sattentau. Simon combines exceptional scientific talent with integrity, sensitivity and patience. He has provided me with level-headed direction and support, supplying both encouragement and restraint to ensure that I've seen (at least some!) projects through to completion rather than leaving only a trail of over-enthusiastically initiated projects abandoned due to premature doubts. Few DPhil students can have had such conscientious supervision or rigorous, constructive criticism of their output. Although I'm sure Simon is currently enjoying respite from my email barrage, I hope this will be only temporary and we can continue to work productively together for years to come. Adrian has established, in the Jenner Institute, an outstanding environment in which to work, and an inspiring genuinely translational ethos; I can't think of anywhere else I would rather have studied. I am particularly grateful for his advice and support regarding my return to clinical work.

In the laboratory, the blood-stage group and the wider Jenner team have been fantastic colleagues. I would like to single out two individuals for special thanks. Firstly, Andrew Williams performed many of the labour-intensive, tedious and frustrating parasitological assays reported here, sacrificing many evenings and weekend to 'parasite-whispering', and latterly led the development of more advanced parasitological techniques in the Jenner for the first time. This thesis would not have been possible without his support. Secondly, Julie Furze is not only an exceptionally capable laboratory manager, but also seems to have endless hidden talents- notably in the area of hybridoma generation and culture. It's nice to be able to put in writing what is frequently said by many in the group: Julie really is 'worth her weight in gold'. Thank you both.

More personally, I have had some quite difficult times leading up to and during my DPhil. I am grateful to those (relatively few!) people who provided me with encouragement to 'go for it' when the idea of extending my short AFP project into a DPhil arose- notably Alain Townsend- and to Profs Thakker and Klenerman for taking a chance by giving me the Fellowship before I had started specialist training. At various times, I have been extremely lucky to have the support of Paul Riley, Sophie MacDougall, Claire Humphrey, Abigail Gaunt, Tom Cahill, Alexander Finlayson, Sundee Soe-Naung and Rachel Clarke, among others. At all times, my parents and family have offered me love, support and belief. Thank you.

Publications arising from this thesis

To date, the following manuscripts based upon work described in this thesis have been accepted for publication:

1.

Douglas, A. D., A. R. Williams, J. J. Illingworth, G. Kamuyu, S. Biswas, A. L. Goodman, D. H. Wyllie, C. Crosnier, K. Miura, G. J. Wright, C. A. Long, F. H. Osier, K. Marsh, A. V. Turner, A. V. Hill and S. J. Draper. "The blood-stage malaria antigen PfRH5 is susceptible to vaccine-inducible cross-strain neutralizing antibody." Nature Communications 2: 601 (2011).

2.

Williams, A.R., A.D. Douglas, K. Miura, J. J. Illingworth, P. Choudhary, L.M. Murungi, J. M. Furze, A. Diouf, O. Miotto, C. Crosnier, G. J. Wright, D. P. Kwiatkowski, R. M. Fairhurst, C. A. Long and S .J. Draper. "Enhancing blockade of Plasmodium falciparum erythrocyte invasion: assessing combinations of antibodies against PfRH5 and other merozoite antigens." PLoS Pathogens, in press

(ARW and ADD are co-first authors on this manuscript)

Table of Contents

Table of Figures

Table of Tables

Abbreviations

3D7	*Plasmodium falciparum* parasite clone, derived from NF54 isolate
aa	Amino acid
ACT	Artemisinin combination therapy
ADCI	Antibody-dependent cellular inhibition
AdHu5	Adenovirus human serotype 5
ADRB	Antibody-dependent respiratory burst
AMA1	Apical membrane antigen 1
AS01, AS02	Adjuvant system 1 and 2, developed by GlaxoSmithKline
ASTMH	American Society of Tropical Medicine and Hygiene
AVEXIS	Avidity-based extracellular interaction screen
BCG	Bacillus Calmette-Guerin
BS	Blood-stage
BSG	Basigin
BSV	Asexual blood-stage vaccine
CD	Cluster of differentiation
CD4d3+4	Rat CD4 domain 3 and 4
CDF	Cumulative density function
CFA	Complete Freund's adjuvant
CFCA	Calibration-free concentration analysis
ChAd63	Chimpanzee adenovirus serotype 63
CHMI	Controlled human malaria infection
CI	Confidence interval
CSP	Circumsporozoite protein
CV	Coefficient of variation
DDT	Dichlorodiphenyltrichloroethane
DiSH	Direct selection of hybridomas
DMSO	Dimethylsulphoxide
DNA	Deoxyribonucleic acid
EBA	Erythrocyte binding antigen
EC_{50}	50%-effective concentration
ELISA	Enzyme linked immunosorbent assay
ELISPOT	Enzyme linked immunosorbent spot
Fab	Fragment, antigen binding, region of immunoglobulin molecule
FACS	Fluorescence-activated cell sorting
Fc	Fragment, crystallisable- non-antigen-binding region of immunoglobulin molecule
FCS	Foetal calf serum
FMP2.1	AMA1-based recombinant protein antigen developed by WRAIR
FVO	*P. falciparum* Vietnam Oak Knoll strain
GIA	Growth Inhibitory Activity
GMP	Good Manufacturing Practice
GSK	GlaxoSmithKline
HBS	HEPES-buffered saline
HEK293	Human embryonic kidney 293 cell line
Hib	Haemophilus influenzae type b

HIV	Human immunodeficiency virus
HBsAg	Hepatitis B surface antigen
HBV	Hepatitis B virus
IEM	Immuno-electron microscopy
IFA	Immunofluorescent assay *or* Incomplete Freund's adjuvant
IFN-γ	Interferon gamma
IgA/E/G/M	Immunoglobulin A/E/G/M
IM	Intramuscular
iRBC	Infected red blood cell
IU	Infectious units
IV	Intravenous
LBI	Liver-to-blood inoculum
LCP	Log_{10}(cumulative parasitaemia)
LIPS	Luciferase immunoprecipitation system
LOOCV	Leave-one-out cross-validation
LU	Light units
mAb	Monoclonal antibody
MACS	Magnetic ell separation
ME-TRAP	Multi-epitope thrombospondin-related adhesive protein (vaccine antigen)
MHC	Major histocompatibility complex
MR4	Malaria Research and Reference Reagent Resource Center
MSP	Merozoite surface protein
MVA	Modified vaccinia virus Ankara
NAI	Naturally acquired immunity
NAMRU-6	US Naval Medical Research Unit 6, Lima.
NIAID	National Institute of Allergy and Infectious Diseases
NIH	National Institutes of Health
OD	Optical density
PATH-MVI	Programme for Appropriate Technology in Health - Malaria Vaccine Initiative
PBMC	Peripheral blood mononuclear cell
PBS	Phosphate buffered saline
PBS/T	0.05% Tween 20 in phosphate buffered saline
PCR	Polymerase chain reaction
Pf	Plasmodium falciparum
PfEMP1	Plasmodium falciparum erythrocyte membrane protein 1
PFU	Plaque forming units
PHA	Phytohaemagglutinin
p/ml	Parasites per millilitre
PMR	Parasite multiplication rate
PVM	Parasitophorous vacuole membrane
Py235	Plasmodium yoelii 235 kilodalton protein family
QC	Quality control
qPCR	Quantitative polymerase chain reaction
R_0	Basic reproductive number
RAP	Rhoptry associated protein

RBC	Red blood cell
RH	Reticulocyte binding protein homologue
RH5FL	Reticulocyte binding protein homologue 5, full-length antigen
RMSE	Root mean square error
RON	Rhoptry neck protein
RTS,S	*P. falciparum* circumsporozoite protein - HBsAg fusion-protein based antigen developed by GlaxoSmithKline
RU	Response units
SC	Subcutaneous
SEB	Staphylococcal enterotoxin B
SEM	Standard error of mean
SFU	Spot forming units
SPF	Specified pathogen free
SPR	Surface plasmon resonance
SSP2	Sporozoite surface protein 2, a.k.a. TRAP
SUB	Subtilisin-like protease
TB	Tuberculosis
TBV	Transmission-blocking vaccine
TJ	Tight junction
TRAP	Thrombospondin-related adhesive protein
USD	United States dollars
WHO	World Health Organisation
WRAIR	Walter Reed Army Institute of Research

1. Introduction

1.1. Hypothesis

In vivo protection against *Plasmodium falciparum* could in principle be achieved by vaccines which induce antibodies capable of Fc-independent merozoite neutralisation *in vitro*. The major obstacles to the success of this approach are antigenic polymorphism and the apparent requirement for exceptionally high antibody concentrations to achieve an *in vivo* effect. Novel antigens, or antigen combinations, may help to overcome these challenges.

1.2. Human vaccinology

1.2.1. Past successes and current challenges

It has been claimed that vaccines have improved public health more than any other biomedical intervention, including antibiotics (Plotkin, Orenstein et al. 2008). Investment in vaccination programmes has risen substantially over the past decade, resulting in clearly measurable global falls in vaccine-preventable disease (Maurice and Davey 2009).

Certain recurring themes are evident among the successful vaccines of the past. Firstly, most such vaccines target diseases which themselves induce long-lasting protection in survivors. Secondly, the most striking success has been achieved by vaccines based upon live attenuated organisms (or, less commonly, targeting a pathogen-derived toxin rather than the pathogen itself). In other words, vaccines which closely resemble pathogens - and have frequently been developed empirically by microbiologists - have proven successful in recapitulating highly-protective natural immune responses.

In recent decades, molecular cloning, recombinant protein production technology, and increasing understanding of molecular immunology have led to considerable hopes of a new generation of

rationally-designed 'subunit' vaccines based upon single antigens. The considerable fruits of this approach have included the licensure of vaccines against hepatitis B virus and human papillomavirus and the development of pneumococcal polysaccharide-conjugate vaccines to improve upon polysaccharide-only vaccines. Relatively recently-developed vaccines against pneumococcus, *Haemophilus influenzae* type B (HiB), meningococcus and rotavirus have the potential to make considerable inroads into mortality due to diarrhoeal, respiratory and central nervous system infections in childhood.

These considerable advances contrast somewhat with the situations in the fields of malaria, human immunodeficiency virus (HIV) and tuberculosis (TB) vaccinology – the so-called 'big three' of global infectious disease. The RTS,S malaria vaccine appears likely to prove around 50% effective in phase III trials, albeit with caveats around the duration of protection and the endpoint used to quantify protection. This will represent a considerable scientific achievement and will probably have value as a public health tool, but it does not seem likely to provide the long-lasting, high-level protection which would be required in order to achieve eradication of *P. falciparum*. It has now been 15 years since the first published report of the success of RTS,S in a clinical trial (Stoute, Slaoui et al. 1997). In that time, despite considerable investment in a 'pipeline' of candidate vaccines, many of which have reached early-phase clinical trials, no other malaria vaccine has convincingly demonstrated comparable protection in the clinic, let alone improved upon RTS,S. There is no 'heir apparent', and no candidate which currently appears likely to achieve the Malaria Vaccine Technology Roadmap's goal of a vaccine achieving 80% protection lasting more than 4 years by 2025 (http://www.malariavaccineroadmap.net/). The HIV and TB vaccine fields may face even greater challenges – notably due to the lack of a human challenge model rendering efficacy trials expensive and slow. To date, no HIV or post-BCG TB vaccine has demonstrated unequivocal protection of humans.

P. falciparum, HIV and TB - a protozoan parasite, a virus and a mycobacterium - are dramatically different pathogens which cause dramatically different diseases, and the vaccine approaches being pursued to target them are widely varied. However, these efforts share an important goal: a successful vaccine against any one of these diseases must achieve an immune response which is *more effective than the natural response to the pathogen itself.* Unlike the targets of virtually all current effective vaccines, the natural history of these pathogens is to establish chronic infection in the majority of infected humans. Vaccinologists aiming to target these diseases thus face a truly grand and exciting scientific challenge: to identify Achilles' heels in the armour of some of humanity's most feared foes.

1.2.2. Requirements for vaccine development

The Programme for Appropriate Technology in Health - Malaria Vaccine Initiative (PATH-MVI) identifies four elements necessary for successful development of a highly effective malaria vaccine: an antigen, or antigens; evaluation technologies; immunogenic adjuvants/formulations; and an appropriate delivery/administration platform. Of these, the latter two elements can potentially draw upon technology developed for vaccines against other diseases. Antigens and evaluation methods, however, are largely disease-specific, and in the case of malaria, often lifecycle-stage specific.

The aim of the work reported in this thesis is to advance development of blood-stage malaria vaccines, not only by identifying novel antigens, but also by improving the techniques used to evaluate the potential of candidate blood-stage vaccines.

Simply because of development costs, it is inevitable that candidates must be prioritised at every stage of development. Information from *in vitro* assays and animal vaccination-challenge models must be used to select candidates to proceed to early-phase clinical trials. Immunogenicity information and the results of experimental human challenge studies must be used to select candidates to proceed from early-phase clinical trials into field efficacy studies. The accuracy of the

tools used to make these decisions is imperative: inappropriately advancing a poor candidate vaccine can incur substantial costs for little gain; the consequences of discarding a potentially efficacious candidate would be even worse. Here, alongside antigen-identification work, I will therefore describe the results of efforts to refine certain aspects the blood-stage vaccine candidate selection 'pipeline': the quantitative measurement of vaccine-induced antibody responses; and the measurement of blood-stage vaccine efficacy in experimental human challenge infection.

1.3. *P. falciparum* epidemiology and immunity

1.3.1. Epidemiology and existing control measures

Reputable recent estimates of annual global malaria mortality vary widely between 650,000 (World Health Organization. 2011) and 1.2 million (Murray, Rosenfeld et al. 2012) deaths for the year 2010, with the confidence intervals for these estimates including an even wider potential mortality range. Whichever end of this range the true figure lies at, it is clear that malaria, particularly *P. falciparum*, is one of the world's most substantial public health problems. The World Health Organisation (WHO) ranks malaria among the top five global causes of childhood death (World Health Organization. 2011). Recurrent malaria infection during childhood hinders cognitive development, and has substantial indirect socio-economic consequences in addition to direct morbidity and mortality (Sachs and Malaney 2002).

The WHO's Global Malaria Eradication Programme of the 1950s and 1960s, which largely involved the widespread use of chloroquine monotherapy and DDT insecticide indoor residual spraying, is viewed in many quarters as having been a discouraging failure. It did, however, eliminate malaria in a number of areas with relatively high levels of socio-economic development, and reduced global malaria mortality by around 40% (Carter and Mendis 2002). Undoubtedly though, it failed in its central aim of global eradication, and was eventually abandoned in the face of prohibitive costs,

parasite resistance to chloroquine, and vector resistance to insecticide. Despite substantial investment and political will, the scientific knowledge and technology available at the time were insufficient to achieve malaria elimination in high-transmission areas with poor infrastructure, notably sub-Saharan Africa. Following the abandonment of the Global Malaria Eradication Programme, global malaria mortality rose progressively until the end of the 20th century (Carter and Mendis 2002).

More recently, increasing investment in malaria control by international donors combined with improved control technologies (notably long-lasting insecticide treated bednets and artemisinin combination therapies [ACTs]) have yielded major reductions in global malaria burden. Dependent upon the transmission context, these existing tools appear capable of achieving reductions of up to 90% in hospital admissions and mortality, and up to 80-fold reductions in *P. falciparum's* basic reproductive number (R_o) (Greenwood and Targett 2009; Gething, Smith et al. 2010). Most sources estimate global mortality reductions of 25-30% over the past decade, with larger reductions in the areas where interventions have been most intensively implemented (World Health Organization. 2011; Murray, Rosenfeld et al. 2012). Such decreases in malaria-attributable mortality have been accompanied by large falls in all-cause childhood mortality, suggesting that malaria may contribute to a substantial proportion of childhood mortality otherwise attributed to other proximate causes.

Calls for the development of a highly effective malaria vaccine have been prominent for many years, encouraged by early observations of the protection of humans by the bites of irradiated infected mosquitoes (Hoffman, Goh et al. 2002). During the period prior to the availability of bednets and ACTs (and the evidence base and investment to support their use), the development of a malaria vaccine may have appeared to be an appealingly straightforward quick fix for an otherwise intractable problem. More recently, confidence in the development of a highly effective vaccine has been tempered by repeated failures of promising candidates in clinical trials, and the assumption

that a vaccine would be required to achieve global eradication has been challenged by the dramatic and highly cost-effective impact of bednet, ACT and indoor residual spraying implementation.

In the light of this experience, and extensive mathematical modelling efforts to assess the likely impacts of malaria vaccines with various efficacy profiles (Smith, Killeen et al. 2006), more nuanced opinions regarding the likely value and desirable characteristics of a malaria vaccine have emerged in recent years (Greenwood and Targett 2009). There has been a shift in research effort away from disease-preventing vaccines (typified by asexual blood-stage vaccines [BSVs]) and towards transmission-blocking vaccines (TBVs – typically designed to act against sexual stages in the mosquito host), in the belief that the latter offer an appealing route to elimination, without the problems of antigenic polymorphism which have dogged the BSV field.

As the focus of malaria control efforts has swung towards elimination, it has been recognised that the tools required to achieve this will vary in different contexts. Any new vaccine will enter a market of available public health expenditure options, in which it will only be deployed and used if its cost-efficacy is superior to alternative investments; thus as well as a vaccine's efficacy, its cost and the effectiveness of other malaria control measures in a particular area will critically affect its utility and uptake. Under circumstances in which other control measures reduce transmission to low levels (~2 infectious bites per annum), mathematical modelling has suggested that population-wide (as opposed to child-targeted) administration of a partially effective pre-erythrocytic vaccine such as RTS,S may be sufficient to halt transmission; in higher transmission settings, such a vaccine would have little effect (Brooks, Briet et al. 2012). Similarly, the prospects of success of a sexual-stage TBV will critically depend upon local transmission intensity (Carter 2001). Asexual BSVs may have the greatest impact in settings in which transmission levels remain highest, particularly where poor infrastructure or vector behaviour render other control measures less cost-effective (Greenwood and Targett 2009).

Such debate, however, is implicitly based upon two assumptions: firstly, that existing non-vaccine control measures will maintain their current levels of efficacy; and secondly, that vaccines will, for the foreseeable future, remain modestly rather than highly effective. There is now considerably more awareness of the need to safeguard the efficacy of insecticides and drugs than there was in the mid-20th century (for example by the use of combination drug therapy rather than monotherapy). Nonetheless, the development of widespread high-level resistance of either *Anopheles* to pyrethroids, or *Plasmodium* spp. to artemisinin, remains a plausible and alarming prospect; meanwhile, there are emerging reports from some areas in which control measures have been thoroughly implemented of a rebound of malaria morbidity and mortality in older children lacking immunity (K Marsh, personal communication). Failure of existing control measures, or the development of a truly highly-effective vaccine (no matter which lifecycle stage it targets), could result in a decisive swing towards vaccine-mediated control of malaria. Strenuous and continued efforts to develop such a vaccine are thus surely justified.

1.3.2. Overview of malaria vaccine development to date

Robust (>80%) and repeatable artificial immune protection of humans against *P. falciparum* has been clearly demonstrated using only two strategies:

- Repeated bites by heavily sporozoite-infected mosquitoes (after either irradiation of the mosquito, or administration of chloroquine to the human host) are capable of inducing sterile protection, most probably via $CD8^+$ T cell-mediated pre-erythrocytic immunity (Hoffman, Goh et al. 2002; Roestenberg, McCall et al. 2009). Viral-vectored ME-TRAP vaccines probably act via a similar mechanism (Hill, Reyes-Sandoval et al. 2010), albeit achieving lower levels of sterilising efficacy.
- Passively transferred immunoglobulin from malaria-exposed adults is capable of controlling blood-stage parasites in malaria-infected children (Cohen, McGregor et al. 1961; Sabchareon, Burnouf et al. 1991).

In both cases, the immune response is raised by whole *P. falciparum* organisms (in the donors, in the case of passive transfer). Ongoing attempts are being made to generate live Good Manufacturing Practice (GMP) grade *P. falciparum* parasites which elicit a protective response. However, recent experience with GMP radiation-attenuated sporozoites has been disappointing, likely due to inefficient delivery of the parasites to the liver (Epstein, Tewari et al. 2011) (Sheehy et al, manuscript in preparation). Both the optimisation of administration routes and the use of genetically attenuated sporozoites rather than radiation attenuated sporozoites may elicit stronger immune responses 'per sporozoite delivered'. Nonetheless, considerable challenges will remain in mass production and delivery of sporozoites obtained by mosquito dissection and requiring liquid nitrogen cryopreservation.

Both live-attenuated and killed whole blood-stage parasites have been proposed as vaccine strategies, but there is no clear proof that such approaches could achieve parasite strain-transcending immunity in humans. A study widely cited as demonstrating control of *P. falciparum* by a human cellular immune response induced by exposure to low doses of blood-stage parasites was confounded by the presence of extremely high levels of antimalarial drugs in the subjects' plasma at the time of 'challenge' (Pombo, Lawrence et al. 2002; Edstein, Kotecka et al. 2005).

The 'mainstream' of malaria vaccine development over the past three decades has thus comprised a variety of subunit vaccine approaches:

In the case of pre-erythrocytic vaccine development, the principal foci of this effort have been the antigens circumsporozoite protein (CSP) and thrombospondin-related adhesive protein (TRAP, also known as sporozoite surface protein 2 [SSP2]). The cloning of the *P. falciparum* CSP gene, and hence the development of antibody-inducing CSP-based subunit vaccines, followed from the identification of protective monoclonal antibodies (mAbs) against the homologous protein from *P. berghei*(Potocnjak, Yoshida et al. 1980; Dame, Williams et al. 1984). This strand of research has led

directly to the RTS,S vaccine (Casares, Brumeanu et al. 2010). The realisation that protection induced by radiation-attenuated sporozoites was largely $CD8^+$ T cell-mediated led, in another direction, to the demonstration that both CSP and TRAP-specific $CD8^+$ T cells were protective in rodent models (Khusmith, Charoenvit et al. 1991; Khusmith, Sedegah et al. 1994). Subsequent efforts to translate this finding into vaccines capable of protecting humans have resulted in progressively more immunogenic DNA and viral-vectored T cell-inducing vaccines, among which the most successful have been those encoding the antigen ME-TRAP(Hill, Reyes-Sandoval et al. 2010) (Ewer et al, manuscript submitted).

Early efforts to identify antigens for blood-stage vaccines developed from the recognition that immunisation with adjuvanted whole blood-stage parasites (in particular, merozoites) protected animals from malaria challenge (Mitchell, Butcher et al. 1974). Subsequent studies attempted to identify the targets of protective mAbs, and to isolate increasingly pure fractions of culture-derived parasite material which were capable of inducing protection (Freeman, Trejdosiewicz et al. 1980; Holder and Freeman 1981; Schofield, Bushell et al. 1986). The antigens merozoite surface protein 1 (MSP1, in particular the 19 kDa and 42 kDa C-terminal regions $MSP1_{19}$ and $MSP1_{42}$), and apical membrane antigen 1 (AMA1) were identified as a result of such efforts, and following extensive pre-clinical research, a number of GMP vaccines based upon these antigens have been tested in clinical trials (Goodman and Draper 2010). Additional protective merozoite antigens identified by these early studies have received considerably less attention: the Py235-related antigens were not favoured because they constitute a large multi-gene family and because their *P. falciparum* homologues (the PfRH family) were only recently identified (Holder and Freeman 1981; Rayner, Vargas-Serrato et al. 2001); the rhoptry-associated proteins (RAPs) were not favoured largely because they proved refractory to soluble protein expression in a GMP-compliant manner using 1990s technology (Collins, Walduck et al. 2000) (Allan Saul, personal communication).

The results of clinical trials of blood-stage vaccine candidates have been comprehensively reviewed elsewhere (Ellis, Sagara et al. 2010; Goodman and Draper 2010). In summary, both human and non-human primate evidence suggests that antibody-mediated protection induced by the antigens studied to date will require exceptionally high antibody titres and, due to antigenic polymorphism, is likely to be parasite strain-specific (Lyon, Angov et al. 2008; Dutta, Sullivan et al. 2009; Goodman and Draper 2010; Thera, Doumbo et al. 2011). Most clinical trials have not assessed vaccine efficacy in either controlled human malaria infection (CHMI), or in adequately powered field trials. No vaccine has demonstrated an unequivocal or repeatable effect upon the primary trial endpoint, but some trials have reported possible effects upon secondary endpoints, such as strain-specific efficacy. Most recently, the 3D7-strain PfAMA1-based FMP2.1 vaccine, adjuvanted with the proprietary adjuvant AS01 or AS02 from GSK, has been reported to have an effect upon PCR-measured parasitaemia during CHMI, and to have achieved a 64% reduction in clinical malaria episodes due to vaccine-homologous parasite strains in a field efficacy study (Spring, Cummings et al. 2009; Thera, Doumbo et al. 2011). The field efficacy trial has generated some controversy in the field, relating both to the genetic definition of 'vaccine-homologous parasite strains' and to the marginal statistical significance of the result (p=0.03, with correspondingly wide 95% confidence intervals for efficacy- 14-92%). Efficacy in this trial has been said to have been associated with high levels of vaccine-induced antibody and GIA (Thera, ASTMH oral presentation, 2011).

1.3.3. Immunity to blood-stage *P. falciparum*

As stated in section 1.2, most successful vaccines have recapitulated protective responses induced by pathogen exposure. Understanding of the mechanism(s) of natural immunity to malaria is therefore often considered to be of importance to malaria vaccine developers.

Naturally-acquired immunity (NAI) against malaria develops progressively over the course of repeated infections, and is generally agreed to be directed principally against the asexual blood-

stage (Langhorne, Ndungu et al. 2008). Repeated sporozoite-initiated infections administered for the treatment of neurosyphilis resulted in reduced levels of blood-stage parasitaemia but not prolonged pre-patent periods, suggesting that exposure to fully viable parasites does *not* typically result in effective pre-erythrocytic immunity (Collins and Jeffery 1999). The observation that adults in malaria-endemic areas frequently have sub-patent parasitaemia supports the belief that NAI is capable of controlling blood-stage parasitaemia, but that it does not confer sterilising protection at the pre-erythrocytic stage (Bottius, Guanzirolli et al. 1996; Douglas, Andrews et al. 2011).

The mechanism by which NAI protects against the blood-stage is less clear. There is good evidence that cellular immunity, for example mediated by blood-stage-antigen-specific $CD4^+$ T cells, can contribute to the control of blood-stage infections with some rodent malaria models, particularly *P. chabaudi* (Grun and Weidanz 1981). However the evidence is considerably weaker for the control of other rodent malarias (notably *P. berghei* and *P. yoelii*). As stated above, unexpected antimalarial drug persistence probably invalidated a major study which remains widely cited as the only demonstration of control of blood-stage *P. falciparum* by a human cellular immune response in the absence of detectable antibodies (Pombo, Lawrence et al. 2002; Edstein, Kotecka et al. 2005). Moreover, vaccines inducing high levels of MSP1-specific or AMA1-specific $CD4^+$ and $CD8^+$ T cells (2500-5000 SFU per million PBMC by *ex-vivo* IFN-γ ELISPOT assay) had no measurable effect upon blood-stage parasite multiplication following mosquito-bite CHMI (Sheehy, Draper et al, manuscript in preparation).

In contrast, it is generally agreed that antibody is a major effector of NAI, supported by the results of the seminal passive transfer experiments of Cohen and McGregor (Cohen, McGregor et al. 1961). Within the asexual cycle, there are two potential targets for antibody-mediated immunity: the surfaces of the infected red blood cell (iRBC) and the merozoite, each displaying a different antigenic repertoire. Although McGregor argued that the effects of intramuscularly-administered immune IgG may not have manifested themselves until the time of schizogony(McGregor 1964), more recent

studies with intravenously-administered immune IgG observed a rapid onset of action(Sabchareon, Burnouf et al. 1991): the passive transfer studies themselves therefore do not conclusively indicate which stage(s) of the asexual cycle, are targeted by NAI.

Field studies provide fairly robust evidence for an important contribution of anti-iRBC-surface antibodies to NAI. The parasite antigens displayed on the iRBC surface, notably *P. falciparum* erythrocyte membrane protein 1 (PfEMP1), are notoriously variable within and between parasite strains. Anti-iRBC-surface antibodies are acquired in a largely PfEMP1-variant-specific manner following episodes of *P. falciparum* infection(Marsh and Howard 1986; Newbold, Pinches et al. 1992). The parasite's strategy of clonally heritable PfEMP1 expression appears to allow parasites to expand into niches of ineffective immunity. PfEMP1 variants expressed during episodes of clinical malaria are less likely to be recognised by the infected child's pre-existing antibody repertoire than by that of children of the same age from the same community(Bull, Lowe et al. 1998). Importantly this prospective trial demonstrated that a heterologous parasite isolate was just as likely to be recognised by infected and non-infected children, a good control to demonstrate that susceptibility to non-immune-covered variants was independent of pre-existing levels of immunity(Bull, Lowe et al. 1998). Taken together, these studies strongly suggest that disease can arise from parasites expressing a PfEMP1 variant which is not covered by an individual's repertoire of anti-PfEMP1 responses *and* that disease *does not* arise in hosts with pre-existing responses to the expressed variant.

The evidence for a causal link between anti-merozoite antibody responses and NAI is considerably weaker. It is important to note that the duration of exposure of the surfaces of the merozoite and iRBC to serum antibody is very different. Each iRBC is present in the circulation for around 48 hours, expressing the PfEMP1 and sequestered for the majority of that. In contrast, following *in vitro* iRBC rupture, *P. falciparum* merozoites typically re-invade a new target cell in around one minute(Gilson and Crabb 2009). Under *in vivo* conditions of high hematocrit, blood flow and red cell rosetting, re-

invasion may occur even more rapidly (particularly with regard to the period between red cell release and primary contact with the next target cell). Such speed of invasion imposes a requirement for high antibody concentration and association rate to saturate a merozoite antigen within the available time(Saul 1987). Consistent with this, most mAbs which neutralise parasites in the assay of GIA have EC_{50}s in excess of 100µg/mL (there is one credible report of a mAb with an EC_{50} of 15µg/mL[*](Schofield, Bushell et al. 1986)), and the attainment in animal models of anti-merozoite-antibody-mediated protection by either active immunisation or passive transfer requires high antibody titres(Saul 1987; Dutta, Sullivan et al. 2009).

Numerous field studies, recently meta-analysed by Fowkes et al, have reported associations between naturally-acquired antibody to various merozoite surface antigens and protection against subsequent disease(Fowkes, Richards et al. 2010). Similarly, associations have been reported between protection and functional assays of both Fc-dependent and Fc-independent anti-merozoite antibody activity (antibody dependent respiratory burst [ADRB]/ antibody-dependent cellular inhibition [ADCI][†] and GIA respectively)(Druilhe and Perignon 1997; Crompton, Miura et al. 2010; Joos, Marrama et al. 2010). In some cases, such associations remain present in multivariate statistical models which attempt to adjust for levels of other anti-parasite antibodies, and for likely markers of malaria exposure and risk (such as age, location, and haemoglobin genotype). Nonetheless, the measured anti-merozoite responses are likely to be multicollinear with both exposure to parasites and a range of other (unmeasured) responses. In this context, no statistical analysis can reliably determine whether any one response is simply a marker of the acquisition of other immune responses, versus a major causal contributor to protection or, as is perhaps quite likely, whether each individual antibody specificity makes a minor contribution, alongside many others, to a multifaceted protective response.

[*] This mAb was directed against the rhoptry associated protein [RAP] complex

[†]Both ADRB and ADCI are assays of antibody-mediated activation of Fc-receptor-bearing cells: ADRB is assayed using neutrophils, while ADCI is assayed using monocytes.

Indeed, certain strands of evidence suggest that naturally-acquired anti-merozoite antibody responses are *not* effective in preventing disease. The high frequency of pregnancy-associated malaria among women in stable-transmission areas suggests that adhesion of iRBCs to placental chondroitin sulphate A is sufficient to evade NAI, and hence that NAI does not have a substantial effect upon merozoites (which are not known to differ antigenically between pregnant and non-pregnant women)(Hviid 2010). Moreover, recent trials of blood-stage vaccines have achieved levels of GIA and concentrations of anti-$MSP1_{42}$ and anti-AMA1 antibodies which compare favourably with those seen in malaria-experienced subjects with a considerable degree of NAI (Spring, Cummings et al. 2009; Crompton, Miura et al. 2010; Duncan, Sheehy et al. 2011) (Choudhary et al in preparation). The failure of these vaccines to recapitulate the substantial impact of NAI upon pre-patent BS parasite multiplication rate (PMR) in CHMI studies further undermines the notion that these antibody specificities or GIA are major contributors to NAI (Spring, Cummings et al. 2009; Douglas, Andrews et al. 2011).

For reasons of statistical power, many field studies (notably some of the most important studies of iRBC-surface responses) examine the relationships between immune responses and episodes of clinical malaria rather than severe malaria or death (Bull, Lowe et al. 1998; Crompton, Miura et al. 2010). It remains possible that, whilst iRBC-surface responses are the major contributors to protection against mild febrile malaria, non-iRBC-surface responses play a more important role in protection against death. Indeed, evidence from both field studies and malariatherapy of neurosyphilis patients suggests relatively rapid acquisition of a degree of strain-transcending immunity.

Parasitaemia in neurosyphilis patients followed a relapsing and remitting course (Figure 1.3.3.1) (Collins and Jeffery 1999; Collins and Jeffery 1999). The initial wave of infection typically peaked

after around 13 days of blood-stage parasite multiplication[‡] in non-drug-treated patients (Collins and Jeffery 1999; Dietz, Raddatz et al. 2006). Subsequently, a pattern of recrudescences was observed approximately every 20 days, with the level of each successive peak of parasitemia tending to diminish (Collins and Jeffery 1999). It seems quite unlikely that the control of each peak is mediated primarily by anti-merozoite responses – there is no known mechanism by which the parasite could frequently and explosively escape such responses to establish subsequent recrudescences. Instead, the infection time-profile is consistent with control of each wave of parasitaemia by a variant-specific primary adaptive immune response, and recurrent escape from this control by PfEMP1 antigenic switching, as suggested by the immuno-epidemiological field data. The reason for the downward trend in the height of parasitaemia over the course of primary infection is unclear, and may well reflect the acquisition of variant-transcending immunity, such as anti-merozoite antibody. Moreover, a degree of strain-transcending immunity was apparent upon re-infection of the patients with heterologous parasites (Collins and Jeffery 1999).

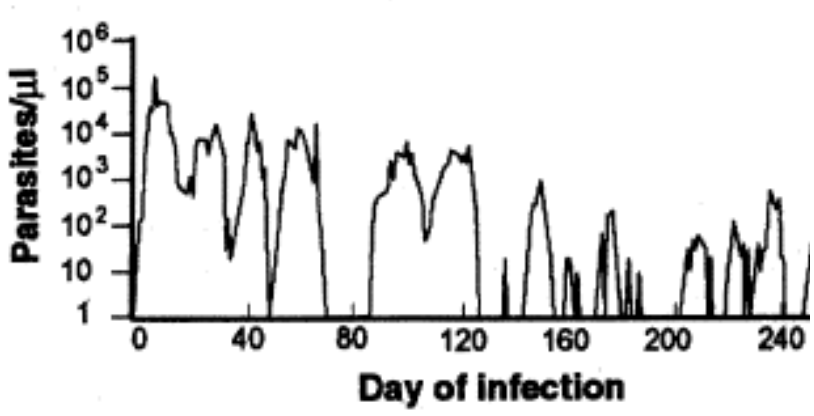

Figure 1.3.3.3.1 Timecourse of untreated *P falciparum* parasitaemia in a human subject.
P. falciparum density in the blood fluctuates for hundreds of days after a single infection by mosquito inoculation of parasites.(Miller, Good et al. 1994)

In the field, mathematical modelling of observed age-specific incidences of severe disease has suggested that one or two episodes of infection may be sufficient to confer substantial immunity against death and severe disease (Gupta, Snow et al. 1999). Thus both malaria therapy and field

[‡] Median time to first peak was 9 days after patency, with a median pre-patent period of 11 days. The estimate of 13 days of blood-stage growth prior to first peak thus assumes a 7 day liver stage.

study evidence suggest some strain-transcending protection against high-level parasitaemia and severe disease. Whether this protection is related to responses against the merozoite or the iRBC surface is not clear.

In summary, anti-merozoite antibody responses face substantial kinetic challenges and seem unlikely to be effective without reaching high concentrations; the major challenge for anti-iRBC-surface responses, however, is antigenic variability. As discussed above, there is convincing passive transfer evidence that antibody can mediate blood-stage protection, and reasonably strong evidence for a causal relationship between PfEMP1 variant-specific antibody and protection. Although anti-merozoite responses are undoubtedly *associated* with protection, the evidence that they *cause* natural immunity is arguably weak. Developers of merozoite-targeting subunit BSVs may therefore be attempting to induce a form of immunity which is quite different to NAI, not only in its narrow antigenic focus, but also in the asexual stage targeted. This has important implications for vaccinologists. Firstly, studies of naturally-acquired anti-merozoite immune responses may be of limited utility for vaccine development: in particular, there is little reason to suppose that the parasite antigens which are immunodominant in a non-protective naturally-acquired response to the merozoite should be the best targets for a protective vaccine. Secondly, the clinical outcome of a highly effective merozoite-targeting BSV could be quite different from the 'phenotype' of NAI, which typically results in chronic asexual and sexual parasitaemia. An effective merozoite-targeting vaccine would be expected to 'short-circuit' the dynamic equilibrium between host acquisition of anti-PfEMP1 responses and parasite PfEMP1 variation. While parasitaemia can rebound from a dip due to an anti-PfEMP1 response by antigenic switching, a merozoite-targeting immune response which reduced the PMR to less than 1 should result in parasite clearance – both protecting the vaccinee against disease and blocking onward transmission from that individual.

1.4. Merozoite invasion of erythrocytes

The merozoite is essentially a cell specialised in the invasion of erythrocytes. Because this is one of the stages of the parasite life-cycle exposed to the extracellular environment, the merozoite has long been recognised as a major target for vaccines and other antimalarial agents. The dynamic process of erythrocyte invasion is thus one of the most intensively studied host-pathogen interactions, and yet on-going research into the complex molecular machinery involved continues to yield surprises. Understanding of the invasion process is central to the selection of merozoite-targeting-vaccine candidate antigens: the following section will therefore review current understanding of events from the morphogenesis of the mature merozoite until the completion of erythrocyte invasion.

1.4.1. Events prior to erythrocyte egress

At least two distinct apical organelles are involved in invasion – the micronemes and the rhoptries. Morphogenesis of each has been characterised by a series of electron micrograph studies. Each merozoite contains tens of micronemes which originate near the nucleus and are transported anteriorly upon subpellicular microtubules to their ultimate position, where they form ducts in connection with the cell surface (Bannister, Hopkins et al. 2003). The rhoptries are larger, pear-shaped paired organelles, opening via ducts onto the apex of the merozoite. They are partitioned into two compartments: a duct-like electron-lucent neck containing the rhoptry neck proteins (RONs), and a spherical electron-dense body containing the rhoptry-associated proteins (RAPs) (Bannister, Hopkins et al. 2000). It has been speculated that the electron-lucency of the neck region may reflect the presence of lipids (extracted during the fixation process), while the electron-dense rhoptry body may contain dehydrated proteinaceous material (Bannister, Hopkins et al. 2000). RAPs are trafficked to the rhoptries by interaction with a protein known as RAMA (Richard, Kats et al. 2009).

Following merozoite maturation, schizonts rupture. Video microscopy has demonstrated that this is a rapid, almost explosive process which is completed within approximately a minute from the first visible evidence of impending rupture (Glushakova, Yin et al. 2005). The process appears to be

triggered by the release of a protease, PfSUB1, from a further class of organelle (the exonemes) into the parasitophorous vacuole(Yeoh, O'Donnell et al. 2007). Activities of PfSUB1 include the processing of the MSP1/6/7 complex, and the activation of SERA/papain-like cysteine proteases which are believed to break down the parasitophorous vacuole membrane (PVM) (Koussis, Withers-Martinez et al. 2009). Intriguingly, antibodies may be able to gain access to parasites, perhaps through partially damaged membranes, before rupture is complete: antibodies to SERA5 have been reported to block schizont rupture(Pang, Mitamura et al. 1999).

1.4.2. From egress to tight junction formation

Exposure of merozoites to the low potassium concentration of extracellular fluid appears to be sufficient to trigger a signalling cascade which results in microneme exocytosis, via phospholipase C activation and a rise in intra-merozoite calcium concentration(Singh, Alam et al. 2010). This exocytosis exposes the vaccine-candidate antigens AMA1 and EBA175 (see below) on the merozoite surface. The rise in Ca^{2+} also appears, via calmodulin and PfPKB, to result in phosphorylation of the protein GAP45, which may prime the actin-myosin motor complex for invasion(Vaid, Thomas et al. 2008).

In vitro, the median time from erythrocyte rupture to contact with a red cell is less than one minute (Gilson and Crabb 2009). Many such contacts appear to be low affinity, and result only in transient, non-committed merozoite attachment rather than successful invasion. Some merozoites, however, re-orient to bring their apical tip into contact with the erythrocyte surface. It is unclear whether this re-orientation is mediated by a specific parasite adhesin, and to my knowledge, there are no reports of specific inhibitors of either the initial low affinity interaction or re-orientation (as opposed to inhibition of subsequent stages).

Successful re-orientation results in formation of high affinity interactions between parasite adhesins and erythrocyte receptors. The Duffy-binding-like (DBL) domain-containing erythrocyte binding antigen family (EBA175, EBA140, EBL1 and EBA181) are important adhesins thought to play a role in

this stage; the first three among these have been shown to interact with the glycophorin family of erythrocyte receptors (Tham, Healer et al. 2012). As well as their adhesive role, they appear to have an important function in signalling the engagement of the merozoite with the erythrocyte: it has been demonstrated that the interaction of EBA175 with glycophorin A is sufficient to trigger a fall in intra-merozoite calcium and the release of rhoptry-neck proteins to the merozoite surface(Singh, Alam et al. 2010).

The five known members of the reticulocyte-binding-protein homologue (RH) family are believed to comprise a second group of adhesins for erythrocyte receptors, although specific receptors have only been identified for PfRH4 and PfRH5 (complement receptor 1 and basigin respectively) (Tham, Wilson et al. 2010; Crosnier, Bustamante et al. 2011; Tham, Healer et al. 2012). The precise function of the RHs as distinct from the EBAs is unclear. The observation that up-regulation of the RH family member PfRH4 can compensate for the loss of the PfEBA175-glycophorin A interaction (either due to PfEBA175 deletion, or neuraminidase treatment of erythrocytes) has resulted in a view that the EBA and RH proteins play closely related, redundant and perhaps interchangeable roles (Stubbs, Simpson et al. 2005). This is, however, at odds with the observations that these proteins have distinct subcellular localisations, that all *Plasmodium* spp. appear to have at least one member of each family, and that *P. vivax* appears to be unable to invade cells lacking the Duffy antigen which is the receptor for that parasite's solitary EBA protein, Duffy binding protein (DBP).

Following re-orientation, a complex of proteins originating in the rhoptry neck (RON2, RON4 and RON5) translocate from the posterior part of the rhoptry neck to the cytosolic face of the erythrocyte membrane (Richard, MacRaild et al. 2010). The process by which this translocation occurs is unknown. RON2 possesses a transmembrane domain and a loop which remains external to the erythrocyte. Engagement of this loop with a hydrophobic trough in AMA1 completes the tight junction (TJ) which can be visualised as an AMA1-RON4 ring by immunofluorescence (Riglar, Richard et al. 2011). Blockade of the AMA1-RON2 interaction by AMA1-binding mAbs or peptides (such as

the R1 peptide which binds the AMA1 trough (Harris, Casey et al. 2005)) inhibits invasion, resulting in failure of parasitophorous vacuole formation and the aberrant discharge of RAP1 onto the erythrocyte surface (Richard, MacRaild et al. 2010; Riglar, Richard et al. 2011; Srinivasan, Beatty et al. 2011). Completion of the TJ does not appear to be required for high affinity attachment, which can occur in the presence of AMA1-RON2 interaction blocking agents (Srinivasan, Beatty et al. 2011). There is some uncertainty over whether the AMA1-RON2 interaction results in signalling within the merozoite, for instance to initiate parasite motor complex activation: R1-inhibited parasites are seen by video microscopy to 'pull' vigorously against the erythrocyte membrane, whilst a mAb which blocks this interaction also seems to block motility (Richard, MacRaild et al. 2010; Srinivasan, Beatty et al. 2011).

1.4.3. Motile invasion and parasitophorous vacuole formation

Invasion of the erythrocyte is driven by the merozoite's actin-myosin motor, linked via intracellular adapters and transmembrane proteins/domains to the extracellular adhesin domains which interact with host cell receptors (Gilberger, Thompson et al. 2003; Baum, Gilberger et al. 2008). This process is conserved across invasive life-cycle stages of *Plasmodium* spp. and other apicomplexan parasites (Baum, Gilberger et al. 2008; Angrisano, Riglar et al. 2012).

As invasion proceeds, the ectodomains of multiple merozoite surface proteins are shed into solution as a result of cleavage by parasite proteases present at or near the tight junction, including the micronemal protease PfSUB2 (Harris, Yeoh et al. 2005; Olivieri, Collins et al. 2011). Meanwhile, the rhoptry-derived protein RAP1 is ejected into the nascent parasitophorous vacuole, and can be seen to spread posteriorly over the invading merozoite, eventually enveloping it (Riglar, Richard et al. 2011). The function of this protein, and the RAP2 and RAP3 proteins with which it heterodimerises, is unclear. It has been reported that each of these proteins are non-essential in the blood-stage *in vitro* on the basis that each can either be genetically deleted, or rendered functionally null (truncations of RAP1 prevent normal subcellular localisation of RAP2 and RAP3) (Baldi, Andrews et al. 2000; Baldi, Good et al. 2002). However it seems highly likely that they do serve important

functions *in vivo* and probably also in the *in vitro* asexual cycle: all sequenced plasmodial genomes include RAP complexes, RAP1 has only ever been truncated rather than fully deleted (and achieving even this was 'challenging'), and deletion of the RAP2 gene itself did not result in a viable parasite (Baldi, Andrews et al. 2000; Baldi, Good et al. 2002; Sterkers, Scheidig et al. 2007). The fact that antibodies to the RAP1/RAP2 complex are among the most potent inhibitors of erythrocyte invasion yet described, and that immunisation with RAP1 and/or RAP2 has repeatedly been shown to protect non-human primates against *P. falciparum* challenge, further supports the notion that these proteins have an important and hitherto uncharacterised function (Schofield, Bushell et al. 1986; Ridley, Takacs et al. 1990; Collins, Walduck et al. 2000).

The composition of the parasitophorous vacuole (in particular, whether it is composed of parasite-derived or host-derived lipid) has been a source of considerable controversy over a number of years. A role for parasite-derived lipids has been supported by visualisation of the transfer of fluorescent lipids from the parasite apex to the erythrocyte membrane and parasitophorous vacuole membrane, and by the absence of the decrease in erythrocyte size which would be expected to accompany invagination of a sufficient area of host-derived membrane to form the PVM (Mikkelsen, Kamber et al. 1988; Dluzewski, Zicha et al. 1995). If parasite derived lipids are inserted into the host membrane, the processes driving this membrane fusion are unknown. Studies of the capacitance of cells being invaded by the related parasite *Toxoplasma gondii*, however, suggested that the PVM was largely host derived (Suss-Toby, Zimmerberg et al. 1996). The PVM has been demonstrated to contain certain host-derived proteins, such as aquaporin 3, but not others, such as band 3, raising the possibility of some form of selective mechanism functioning at the tight junction (Bietz, Montilla et al. 2009). Conversely, some rhoptry-derived merozoite proteins are found in the external RBC membrane, such as the CLAG3 nutrient channel (Nguitragool, Bokhari et al. 2011).

Invasion is completed by the sealing of a PVM 'fission pore', an event which can be visualised by tracking the constriction and then dispersal of the RON4 ring marking the TJ (Suss-Toby, Zimmerberg

et al. 1996; Riglar, Richard et al. 2011). After this, dense granules containing the protein RESA are released into the PV, and an extensive remodelling of the RBC cytosol and surface takes place, enabled by protein export through the PTEX pore in the PVM (de Koning-Ward, Gilson et al. 2009).

Although it is not immediately apparent how antibodies could inhibit intra-erythrocytic development of the parasite, it has been reported that anti-$MSP1_{19}$ antibodies which do not block invasion of RBCs can sometimes block parasite growth at a later stage, perhaps by means of being carried into the PVM during invasion (Bergmann-Leitner, Duncan et al. 2006 ; Moss, Remarque et al. 2011).

The entire re-invasion process from disruption of the parental schizont membrane to the sealing of the nascent ring-stage parasite inside the newly infected cell thus comprises a complex and co-ordinated molecular chain of events. The complexity of the process and the involvement of multiple parasite proteins present numerous opportunities for vaccine-induced antibody to act against the parasite, thus breaking the chain. Whether such antibody can overcome the twin hurdles of antigenic diversity and the brief merozoite exposure window remains a critical unknown.

1.5. Project aims

The starting points for this project were the observed lack of efficacy of candidate blood-stage vaccines to date (section 1.3.2) and the belief that increasing understanding of the wide variety of merozoite proteins involved in erythrocyte invasion (section 1.4) offered opportunities for the exploration and development of novel potential vaccine antigens.

Although sceptical about whether vaccine developers should attempt to emulate NAI or draw inferences from it to guide the selection of candidate antigens (section 1.3), I felt that the contrast between the successful multi-specificity immune response involved in NAI and the lack of efficacy of single-subunit candidates BSVs was an interesting one. In particular, I felt that the complexity of the 'molecular machine' involved in the invasion process might be susceptible to the synergistic action of antibodies with two or more specificities: antigens such as EBA175 which had been proposed as

vaccine candidates but were individually non-essential for invasion might well be more successful as ingredients in a multi-component vaccine. However, construction of multi-component vaccines is expensive and carries risks of immunological competition between the antigens. I therefore felt that it would be of critical importance to empirically demonstrate true synergy between candidate components, rather than simply adopting a 'mix and hope' approach.

More broadly, I felt that there were a number of technical issues hindering the development of BSV candidates. These included a lack of quantitative precision in methods used to measure antigen-specific antibody concentration, parasite neutralisation, and the *in vivo* efficacy of BSVs. Uncertainty regarding the validity of the assay of GIA as a predictor of *in vivo* protection has been a further major contributor to a lack of clarity regarding appropriate methods of pre-clinical prioritisation of BSV candidates. I therefore wished to address these 'strategic' issues in parallel with efforts to develop a candidate vaccine.

Aims of this project were therefore as follows:

- Identification of a vaccine candidate antigen which might out-perform AMA1 and MSP1
- Development of methods to guide rational design of two-antigen combination vaccines
- Improvement of methods for assessment of blood-stage vaccine candidates.

2. Methods

Each Chapter includes a description of methods specific to that work contained within it. The following methodological descriptions relate to techniques and reagents used repeatedly across multiple chapters.

2.1. Viral vectors

P. falciparum antigen genes were codon-optimized for human expression and synthesized by GeneArt GmbH (Regensburg, Germany). Unless otherwise stated, antigens were based on the 3D7 strain coding sequence. PfEBA175, PfRH1, PfRH2, and PfRH4 constructs were based upon fragments known to include erythrocyte binding domains (Triglia, Thompson et al. 2001; Pandey, Singh et al. 2002; Gao, Yeo et al. 2008; Tham, Wilson et al. 2009). Remaining constructs encoded full-length proteins, omitting signal peptides and transmembrane domains where applicable. In some cases predicted N-glycosylation sites were removed by N—Q or S—A substitution.

The following antigens were used (in each case, the GeneDB reference number for the 3D7-strain gene is given, with additional Genbank/NCBI references where antigens were designed based upon sequences downloaded from elsewhere):

- PfEBA175, PF3D7_0731500, Genbank X52524 from Camp strain, amino acid residues 447-795, ELRE...RDDD, the 'F2' erythrocyte binding region (Pandey, Singh et al. 2002);
- PfMSP2 3D7 mono-allelic construct , PF3D7_0206800, amino acid residues 20-244 (truncated to remove GPI anchor attachment site at N246), IKNE...TSLL, with substitution N36Q.
- PfMSP2 biallelic 3D7-FC27 construct, using FC27 allele sequence based upon Genbank sequence J03828. See chapter 3 for further details.
- PfMSP9, PF3D7_1228600, NCBI XM_001350647.1, amino acid residues 25-719, KNDK…EESK, with substitutions N529Q, N580Q, N621Q;

- Pf38, PF3D7_0508000, NCBI XM_001351602.1, amino acid residues 23-327, VENK…REEI, with substitutions S166A, N294Q, S297A, N301Q;
- PfRAP2, PF3D7_0501600, amino acid residues 22-398, DKCE...LNVL, with substitution N281Q.
- PfRAP3, PF3D7_0501500, NCBI XM_001351538.1, amino acid residues 23-399, NKCK…NIFK, with substitutions N50Q, N246Q;
- PfRH1, PF3D7_0402300, NCBI XM_002808591.1, amino acid residues 500-833, LQIV…LTN, with substitutions N685Q, N830Q;
- PfRH2, PF3D7_1335300/PF3D7_1335400, from the PfRH2a sequence NCBI XM_001350047.1, amino acid residues 2030-2531, ELRE…MLLN, a sequence shared between PfRH2a and PfRH2b and previously termed PfRH2A9 (Triglia, Thompson et al. 2001);
- PfRH4, PF3D7_0424200, relatively N-terminal fragment previously termed PfRH4.9 (Tham, Wilson et al. 2009) and known to interact with complement receptor 1, NCBI XM_001351509, amino acid residues 28-766, PSKE…MQNI;
- PfRH4, PF3D7_0424200, fragment previously produced by Kaneko *et al* (Kaneko, Mu et al. 2002) and referred to here as PfRH4K, NCBI XM_001351509, amino acid residues 1329-1607, NHIK...NAYY, the most C-terminal region prior to the transmembrane domain
- PfRH5 fragment (PfRH5frag), PF3D7_0424100, NCBI XM_001351508.1, amino acid residues 191-359, NSIY…IRYH, as previously expressed in *Escherichia coli* (Baum, Chen et al. 2009);
- PfRH5 full-length (PfRH5FL), PF3D7_0424100, NCBI XM_001351508.1, amino acid residues 26-526, ENAI…PLTQ, with substitutions N38Q and N214Q.

Antigens were cloned into replication-deficient adenovirus human serotype 5 (AdHu5) and poxvirus (modified vaccinia virus Ankara, MVA) genomes downstream of a mammalian secretory signal (from bovine tissue plasminogen activator), and viruses prepared using previously described techniques for

MVA (Draper, Moore et al. 2008) and AdHu5 (Alcock, Cottingham et al.). AdHu5 was chosen as a model adenovirus without intellectual property restrictions and suitable for antigen screening.

AdHu5 viruses expressed antigen under the control of the intron-containing native cytomegalovirus immediate-early promoter, modified in the case of PfMSP9, Pf38, PfRAP3, PfRH1, PfRH4, and PfRH5FL expressing viruses to include tandem tetracycline operators in proximity to the TATA box by ligation of a fragment containing these into the SacI restriction site (Sridhar, Reyes-Sandoval et al. 2008; Stanton, McSharry et al. 2008). Such 'tet repressed' viruses were cultured on Trex293 cells (Invitrogen, UK). The production of mono-allelic (3D7) and bi-allelic (3D7 and FVO) adenoviral- and MVA-vectored vaccines against PfMSP1 (previously termed "PfM128") and PfAMA1 has been described elsewhere (Draper, Biswas et al. 2010; Goodman, Epp et al. 2010; Biswas, Dicks et al. 2011). Viral vectored vaccines which did not express malaria antigens were used as negative controls (unless otherwise stated, an AdHu5 virus without an antigen insert, and an MVA virus expressing an influenza antigen) (Draper, Goodman et al. 2009; Forbes, Biswas et al. 2011).

Adenoviruses were titred by immunostaining, carried out by infection of Trex293 cells with serial dilutions of virus. Forty-eight hours post-infection, cells were stained with antibody to the adenovirus hexon protein (Cambridge Bioscience, UK) and detected with HRP-conjugated secondary antibody (Cambridge Bioscience, UK) and ImmPact DAB reagent (Vector Labs, UK).

2.2. Animals and immunization regimes

Mouse and rabbit work was approved by the University of Oxford Animal Care and Ethical Review Committee (in its review of the application for Home Office project license PPL 30/2414), and performed in accordance with all applicable regulations.

Unless otherwise stated, immunisations were intramuscular, with an 8 week prime boost interval, and sera were collected 14 days after the boost immunisation.

6-week old Balb/c female mice were housed under specified-pathogen-free (SPF) conditions. immunised with $1x10^8$ IU AdHu5 PfRH5FL, and boosted with $1x10^7$ PFU MVA PfRH5FL. Rabbit work was conducted by Agrobio, France, and Biogenes, Germany.

Female New Zealand white rabbits (2-4 per group) housed under non-SPF conditions were immunized with $7x10^7$ - $4.5x10^8$ infectious units (IU) of recombinant AdHu5 on day 0, $5x10^7$ - $1x10^8$ plaque forming units (PFU) MVA on day 56. Rabbits immunized with the same negative control vaccines and positive control vaccines (bivalent PfAMA1) were included in each study.

2.3. Enzyme-linked Immunosorbent Assays (ELISA)

Generally, ELISA was performed either by coating NUNC Maxisorp plates overnight at room temperature with 100 ng/well of purified recombinant protein antigen in PBS, or by coating streptavidin-coated NUNC Immobilizer plates for 15 minutes with mammalian cell-culture supernatant containing enzymatically mono-biotinylated antigen (for further details of antigens, see individual chapters) (Crosnier, Bustamante et al. 2011).

Subsequently, plates were washed 6x in PBS containing 0.05% Tween 20 (PBS/T). Plates were blocked with 10% skimmed milk in PBS/T for 1h. Dilution series of serum samples (3-fold from 1:300)

were added for 2h, before the plates were washed again. Alkaline-phosphatase-conjugated goat anti-rabbit IgG or anti-mouse IgG (both from Sigma) were used for detection of the appropriate species' IgG. Plates were washed again and bound antibodies were detected by adding *p*-nitrophenylphosphate substrate (pNPP, Sigma) diluted in diethanolamine buffer (Fisher Scientific, UK). OD_{405} was read 20 minutes after addition of substrate using an ELx800 microplate reader (BioTek, UK). Endpoint titres were taken as the x-axis intercept of the dilution curve at an absorbance value three standard deviations greater than the OD_{405} for naïve rabbit serum.

2.4. Parasite culture and assay of growth inhibitory activity

3D7 and FVO strain parasites were provided to the Jenner Institute by the PATH MVI GIA Reference Center. Dd2 parasites were provided by Bob Pinches (University of Oxford, UK). GB4, Camp and 7G8 parasites were provided by MR4 (reagents MRA-925, MRA-328, and MRA-152 respectively; MR4, ATCC, Manassas, Virginia). All assays of GIA were performed at the Jenner Institute, Oxford University using the method of the PATH-MVI GIA Reference Center (Miura, Zhou et al. 2009), unless otherwise stated.

Culture of parasites was performed using standard methods (Doolan 2002). Unless otherwise stated, culture medium contained 10% pooled human serum. In some cases, magnetic cell separation (MACS) was used to purify late-stage parasites; otherwise, parasites were synchronised using sorbitol osmotic lysis and Percoll density separation (Doolan 2002).

Total IgG was purified using Protein G (Pierce). Briefly, each test IgG (at the concentration specified on each figure) was incubated with synchronized *P. falciparum* late trophozoites and relative parasitemia levels were quantified by colorimetric determination of parasite lactate dehydrogenase after one complete life-cycle (40-42 hours for 3D7; 48 hours for all other parasite strains). Results were calculated relative to growth in the presence of 10 mg/ml IgG from a rabbit immunized with non-malaria control vaccines.

2.5. Indirect immunofluorescence assay

Parasite cultures containing mainly schizonts were smeared onto slides, fixed in 4% paraformaldehyde, permeabilized with 0.1% Triton X100 and quenched with 0.01% sodium borohydride. Slides were then blocked for 1h in 10% goat serum, 1% BSA in PBS before the addition of purified rabbit IgG (see below). Bound IgG was detected with goat anti-rabbit IgG-Alexa 488 conjugate (Invitrogen). Nuclear DNA was counterstained with DAPI. Slides were viewed under a Leica DMI3000 microscope. 3D7 strain parasites were used for all IFA except for PfRH1, for which the FVO strain was used as this antigen is known to be poorly expressed in 3D7(Gao, Yeo et al. 2008).

3. An antigen screen identifies PfRH5 as a promising vaccine candidate

3.1. AUTHORSHIP STATEMENT

This chapter is based upon a manuscript published in *Nature Communications* in December 2011 (Douglas, Williams et al. 2011), with some additional unpublished data. ADD was first author and led the writing of the manuscript. Andrew Williams and Simon Draper contributed to the figures and reviewing the manuscript.

ADD conceived the antigen screen reported in this chapter, selected the antigens, designed the transgene constructs, carried out all DNA cloning, carried out all mouse work, designed and organised externally-contracted rabbit studies, carried out all mouse and rabbit ELISA and LIPS assays, established *P. falciparum* culture and growth inhibition assay (GIA) protocols in the Jenner Institute, and designed the GIA experiments.

Viral vectors were produced by the Jenner Institute Viral Vector Core Facility.

Andrew Williams and Joe Illingworth performed the GIA and IFA experiments.

Simon Draper, Prateek Choudhary, Gathoni Kamuyu and Faith Osier performed the human ELISA studies.

3.2. INTRODUCTION

Two *P. falciparum* blood-stage antigens, merozoite surface protein 1 (MSP1) (Holder 2009) and apical membrane antigen 1 (AMA1) (Remarque, Faber et al. 2008), have dominated blood-stage vaccine development, but appear to require high antibody concentrations to induce protection and suffer antigenic diversity rendering vaccine-induced antibodies strain-specific (Lyon, Angov et al. 2008; Dutta, Sullivan et al. 2009; Miura, Zhou et al. 2009; Thera, Doumbo et al. 2011). There has never been a systematic head-to-head comparison of these and other candidate antigens delivered

using the same human-compatible vaccine platform. More broadly, malaria vaccine development has been hampered by the difficulty of expressing recombinant plasmodial proteins, and by the need for potentially reactogenic chemical adjuvants to induce high-titre antibody responses in humans (Goodman and Draper 2010).

There is thus a pressing need for validation of novel and recently identified antigens using technologies which allow rapid translation into clinical trials. Viral vectored vaccines have recently been shown to induce antibody responses in mice (Draper, Moore et al. 2008; Douglas, de Cassan et al. 2010; Forbes, Biswas et al. 2011), rabbits (Goodman, Epp et al. 2010; Biswas, Dicks et al. 2011), rhesus macaques (Draper, Biswas et al. 2010) and humans (Sheehy, Duncan et al. 2011; Sheehy, Duncan et al. 2012) which compare favourably with leading protein-adjuvant formulations. Unlike recombinant protein vaccines, these vectors benefit from standard manufacturing processes which do not vary between antigens: multiple vectors can therefore be produced for moderate-throughput pre-clinical antigen screening, and the costs and risks associated with production of clinical-grade viral vectors are relatively low. Moreover, viral vectors do not require additional chemical adjuvants, circumventing, to some extent, the problems of reactogenicity and commercially-restricted access to adjuvants which have dogged clinical translation of recombinant protein vaccines. I therefore set out to use adenovirus and poxvirus vectors to screen a literature-selected panel of relatively poorly-characterised *P. falciparum* antigens for their ability to induce merozoite-neutralising antibodies.

3.3. METHODS

3.3.1. Recombinant proteins

Proteins used for human ELISA were as follows. GST-tagged PfRH2A9 (referred to in the ELISA data as PfRH2) was produced as described previously for the 3D7 ("ETSR") allele of the 19 kDa region of PfMSP1 ($PfMSP1_{19}$) (Goodman, Epp et al. 2010). The latter is referred to as PfMSP1 in the ELISA data. An N-terminally His_6-tagged PfRH4K fragment (amino acid residues 1329-1607, NHIK...NAYY, as for the RH4K vaccine antigen (Kaneko, Mu et al. 2002)) was produced by cloning the fragment into the

pTrcHisC plasmid (Invitrogen), transforming Rosetta-strain *E. coli*, inducing expression and purifying protein according to the instructions of the Qiagen Ni-NTA fast-start kit (Qiagen, UK). Recombinant PfEBA175_F2 (referred to in the ELISA data as PfEBA175) and 3D7 strain PfAMA1 (used to generate the data in Figure 3.4.5.1A-B) were produced as previously described and were a kind gift from Dr Chetan E Chitnis (ICGEB, New Delhi, India) (Pandey, Singh et al. 2002; Draper, Biswas et al. 2010; Biswas, Dicks et al. 2011).

PfAMA1 (used for the ELISA in Figure 3.4.5.1C), PfMSP2, PfMSP9, Pf38 and PfRH5 proteins were produced as enzymatically monobiotinylated soluble recombinant proteins by transient transfection of HEK293E cells, essentially as described(Bushell, Sollner et al. 2008); further details of the method will be described elsewhere (CC and GJW, unpublished observations). Supernatants were extensively dialysed against PBS, expression levels normalized, and captured on streptavidin-coated microtitre plates for ELISAs. The PfRH5 protein produced in this manner was confirmed to bind to its erythrocyte receptor, basigin, by surface plasmon resonance (Crosnier, Bustamante et al. 2011).

3.3.2. Animal work

Methods for animal work were as stated in Chapter 2, with the exception that, in the case of the PfRH2 and PfEBA175 groups, rabbits received a third immunization on day 114 with 100µg of either PfRH2 or PfEBA175 recombinant protein mixed with 20µL (18µg) Abisco adjuvant (ISCOM Matrix M, Isconova, Sweden) (Douglas, de Cassan et al. 2010; Draper, Biswas et al. 2010; de Cassan, Forbes et al. 2011).

3.3.3. Human serum samples

UK Adult sera (Figure 3.4.5.1A-B) were obtained from pre-vaccination samples taken from healthy malaria-naïve adult volunteers enrolled in a Phase I/IIa malaria vaccine clinical trial with appropriate

ethical approval (EudraCT number 2008-006804-46, OXREC-A reference 09/H0604/9) (Sheehy, Duncan et al. 2011).

Kenyan adult sera (Figure 3.4.5.1A-B) were collected during adult cross-sectional surveys between 2006 and 2008 from the villages surrounding the Chonyi area in Kilifi, Kenya which experiences moderate malaria transmission with an entomological inoculation rate of 10-100 infective bites/person/year; these adults are considered to have substantial naturally acquired immunity as evidenced by the decline in clinical episodes of malaria with age (Marsh and Kinyanjui 2006). Scientific and ethical approvals for the Kenyan serum samples were granted by the Kenya National Scientific and Research Ethics Committees respectively, SSC No. 1131.

Kenyan Child sera (Figure 3.4.5.1C) samples were obtained from a cohort which has been extensively used to analyze naturally-acquired antibodies against leading blood-stage malaria vaccine candidate antigens (Osier, Fegan et al. 2008). The present work focused on children aged up to ten years of age because they accounted for nearly 90% of all the malaria episodes and thus are in the process of actively acquiring immunity.

3.3.4. ELISA

To generate the rabbit ELISA data in Figure 1C, PfRH2, PfRH4 and PfEBA175 proteins (described above) were coated on Nunc Maxisorp plates at 100 ng/well, or wells of streptavidin-coated plates (Nunc Immobilizer) were saturated with biotinylated Pf38, PfMSP2, PfMSP9, or PfRH5 in PBS and left overnight. The remainder of the ELISA procedure was as described in section 2.3.

To generate the human ELISA data in Figure 3.4.5.1A-B, GST-PfMSP1$_{19}$ (ETSR/3D7/Mad20 allele) or 3D7 AMA1 (see section 3.2.1) protein was coated onto 96 well Nunc-Immuno Maxisorp plates at a concentration of 2µg/mL in PBS and left overnight. The next day plates were washed 6x in PBS containing 0.05% Tween 20 (PBS/T) and blocked for 1h with Casein block solution (Pierce, UK). Plates

were washed again, and then a standard, test sera, internal control and blank samples all diluted in Casein block solution were added to each plate for 2h according to published methodology (Miura, Orcutt et al. 2008; Sheehy, Duncan et al. 2011). The standard was prepared from adult Kenyan immune serum and was serially diluted on every plate to make a standard curve. Plates were washed again, followed by addition for 1h of alkaline phosphatase-conjugated goat anti-human IgG (γ-chain) (Sigma) diluted 1:1000 in Casein block solution. Plates were washed and developed as above. The ELISA unit value of the standard was assigned as the reciprocal of the dilution giving an OD_{405} of 1.0 in the standardized assay. The OD_{405} of individual test samples was converted into ELISA units by using the standard curve and Gen5 ELISA software v1.10 (BioTek, UK). All sera tested against the GST control protein were less than the minimal detection level of the assay.

Alternatively, PfRH2, PfRH4 and PfEBA175 proteins were coated on Nunc Maxisorp plates at 100 ng/well, or wells of streptavidin-coated plates (Nunc Immobilizer) were saturated with biotinylated Pf38, PfMSP2, PfMSP9, or PfRH5 in PBS and left overnight. All test sera were diluted 1:300 in Casein block solution. Washing, blocking, and detection were as for PfMSP1 and PfAMA1. OD 405nm was measured 35 minutes after substrate addition using an ELx800 microplate reader (BioTek, UK).

To generate the human ELISA data in Figure 3.4.5.1C, streptavidin coated plates (NUNC Immobilizer Streptavidin, Thermo Fisher Scientific Inc) were washed three times with PBS-Tween (PBS-0.1% Tween 20). Individual wells were coated with 100µL of antigen and incubated for 45min at room temperature (RT). Plates were then washed four times with Hepes-buffered saline-Tween (HBS-Tween:0.14M NaCl, 5mM KCl, 2mM $CaCl_2$, 1mM $MgCl_2$, 10mM HEPES, 0.1% Tween 20) before incubation with 100µL of test serum sample at a 1/1000 dilution (in HBS-Tween) for 1h at RT. Wells were then washed four times, with HBS replacing HBS-Tween in the final wash. Plates were then incubated for 1h at RT with 100µL of horseradish peroxidase-conjugated rabbit anti-human IgG (Dako Ltd.) at a 1/5000 dilution in HBS-Tween before the final wash and detection with H_2O_2 and *o*-phenylenediamine (Sigma). The reaction was stopped with 25µL of 2M H_2SO_4 per well, and

absorbance was read at 492 nm. Identical positive controls (hyperimmune sera) were run in duplicate on each day of the experiment, on each plate, to allow for standardization of day-to-day and plate-to-plate variations. Twenty sera from UK residents, never exposed to malaria, were used as negative controls.

3.3.5. Luciferase Immunoprecipitation System (LIPS)

The luciferase immunoprecipitation system (LIPS) is a technique which can be used to quantitatively assay antigen-specific antibodies when purified protein antigens are not available (Burbelo, Ching et al. 2009). Briefly, antigen is generated with a luciferase tag (which will emit light in the presence of the appropriate substrate) by transient transfection of mammalian cells. Cells are subsequently lysed, and the quantity of labelled antigen which is immuno-precipitated by test antibodies bound to agarose beads, and hence retained in a filter plate, is assayed using a luminometer.

Details of the LIPS method are lengthy, have previously been described (Burbelo, Ching et al. 2009) and are available in Jenner Institute protocol J211 (written by ADD).

The LIPS method was used for some work reported in this chapter, undertaken early in the project. The development of the collaboration between the Jenner Institute blood-stage vaccine group made available a range of mammalian cell culture supernatants containing enzymatically mono-biotinylated blood-stage antigens. As was the case for LIPS, the tag on this antigen was such that antibody assays could be conducted without prior purification of the protein. Unlike for the luciferase-tagged LIPS antigen, this biotinylated antigen enabled considerably more versatile ELISA-format assays; the LIPS method was therefore not further developed.

3.3.6. GIA

GIA methods were as described in Section 2.4. Experiments depicted in figure 3.4.3.1B were performed using IgG purified from pooled serum of two PfRH5FL-vaccinated rabbits and single rabbits vaccinated with each PfAMA1 vaccine. The selection of these rabbits was performed in a manner designed to underestimate the differences between PfRH5FL and PfAMA1 vaccines: PfRH5FL-vaccinated rabbits chosen exhibited GIA activity at or below the median of the PfRH5FL-vaccinated rabbits illustrated in Figure 3.4.3.1A, while the PfAMA1-bivalent vaccinated rabbit exhibited GIA activity exceeding the median of the PfAMA1-vaccinated rabbits illustrated in Figure 3.4.3.1A. The GIA assays performed at NIH (figure 3) used IgG from the same sera as the experiments in figure 3.4.3.1B, with the exception that IgG from the two PfRH5FL-vaccinated rabbits was not pooled.

3.3.7. Data analysis and statistics

Estimation of the concentration of total IgG necessary to induce 50% GIA (EC_{50}) was performed using non-linear least squares regression in Prism 5 software (GraphPad Software, USA). For each vaccine-parasite strain combination, a four-parameter sigmoidal dose-response curve was fitted to the relationship between $\log_{10}$[total IgG] and percentage GIA, constraining the bottom of the curve to 0% GIA, and the top of the curve to 100% GIA. For each parasite strain, an extra sum-of-squares F-test was used to test a null hypothesis of equal EC_{50} for the tested IgG samples.

3.4. RESULTS

3.4.1. Vaccine design and production

Viral vectored vaccines expressing ten different *P. falciparum* (Pf) blood-stage antigens were designed (Figure 3.4.1.1). These ten antigens were as follows:

- Rhoptry-associated protein 2 (RAP2), selected on the basis that this antigen has previously achieved protection in a non-human primate *P. falciparum* challenge model (Collins, Walduck et al. 2000);
- Rhoptry-associated protein 3 (RAP3), selected on the basis that it is a close homologue of RAP2;
- Merozoite surface protein 2 (MSP2), selected on the basis that a vaccine including MSP2 has previously been suggested to have achieved strain-specific efficacy in a field study (Genton, Betuela et al. 2002);
- Merozoite surface protein 9 (MSP9) which was selected on the basis of evidence that that it can induce growth inhibitory antibodies (Kushwaha, Rao et al. 2001) and that its *P. berghei* orthologue is capable of protecting mice against this stringent blood-stage challenge (Lopera-Mesa, Kushwaha et al. 2008);
- Pf38 which is a recently identified but untested potential vaccine antigen, which has been challenging to express as a recombinant protein and which may be expressed by multiple life-cycle stages (Cowman and Crabb 2006; Gilson, Nebl et al. 2006);
- Five members of the erythrocyte binding-like (EBL) and reticulocyte binding-like (RBL or *P. falciparum* reticulocyte-binding homologue (RH)) protein families (EBA175, RH1, RH2, RH4, and RH5) which have been implicated as important targets of the committed attachment process during red blood cell (RBC) invasion by *P. falciparum* merozoites (Jiang, Gaur et al. 2011; Lopaticki, Maier et al. 2011; Riglar, Richard et al. 2011).

Previously produced vectors expressing the leading vaccine candidates MSP1 (Holder 2009; Goodman, Epp et al. 2010) and AMA1 (Remarque, Faber et al. 2008; Biswas, Dicks et al. 2011) were used as comparators. All of the tested antigens are known to be expressed by *P. falciparum* 3D7 strain parasites with the exception of RH1 (Florens, Washburn et al. 2002; Duraisingh, Triglia et al. 2003; Gilson, Nebl et al. 2006; Gao, Yeo et al. 2008; Baum, Chen et al. 2009; Tham, Wilson et al.

2009), and were based upon the 3D7 strain sequence with the exception of *P. falciparum* erythrocyte binding antigen 175 (PfEBA175) F2 domain from the Camp strain (Pandey, Singh et al. 2002). All antigens were codon-optimised for mammalian expression (Geneart, Germany); further transgene modifications are described in Chapter 2.

Cloning of the antigens into viral-vector progenitor plasmids was accomplished using standard restriction cloning methods (see Chapter 2). Successful cloning was confirmed by PCR amplification of products of appropriate length using two primer pairs to amplify both the entire transgene cassette (flank-to-flank PCR) and a transgene-specific product (identity PCR). Viral vectors were generated by the Jenner Institute Viral Vector Core Facility using published methods (Douglas, Williams et al. 2011). In some cases, such as with MSP9, it was noted that growth of recombinant adenoviruses required repression of expression of the transgene insert. This was achieved by incorporating the tet-operator element within the transgene promoter and producing the vectors in 293Trex cells (Invitrogen) (Douglas, Williams et al. 2011).

For certain antigens, more than one adenovirus-poxvirus vector pair was produced.

In the case of RH4, vectors expressing two different fragments were constructed: one adenovirus-MVA pair expressed the N-terminal region (previously termed RH4.9) which has been shown to interact with the red cell surface protein complement receptor 1 (CR1)(Tham, Wilson et al. 2010); a second vector pair expressed a C-terminal region which had previously been expressed in *E. coli* (here, termed RH4K)(Kaneko, Mu et al. 2002).

Similarly, two pairs of vectors expressing RH5-based antigens were constructed. One pair expressed the full length RH5 protein (here, termed RH5FL); a second pair expressed only a fragment from the central region of RH5 which had previously been expressed in *E. coli* (previously termed 'RH5-2', here termed 'RH5 frag') (Baum, Chen et al. 2009).

Again similarly, vectors expressing both the full-length MSP9 antigen (MSP9FL) and a previously-expressed N-terminal fragment (MSP9P) (Kushwaha, Rao et al. 2001) were produced.

In the case of MSP2, two pairs of vectors were designed in an attempt to elicit antibody capable of recognising both forms of this dimorphic protein. One pair expressed the 3D7-strain antigen. A second pair expressed both the 3D7-strain antigen and the FC27 antigen. The adenovirus in this pair was designed using a strategy which has previously been used in the gene therapy field to permit the expression of more than one protein from a monocistronic (single-promoter, single translation-initiation-site) gene construct, namely the use of a picornaviral 2A peptide, which causes the ribosome to omit a peptide bond from the nascent polypeptide chain (Szymczak, Workman et al. 2004). This insert comprised the full-length codon optimised FC27 allele of MSP2 (Genbank J03828, with a mouse IL12 secretory peptide (MCPLRSLLLISTLVLLHHLPHLSLG)), followed by a picornavirus 2A peptide (GGGSGGGAVKQLNFDLLKLAGDVESNPGP) (Szymczak, Workman et al. 2004), followed by a tPA secretory peptide and the full length 3D7-strain MSP2 sequence.

Production of MVA with this biallelic MSP2 insert failed due to genetic instability of the insert (A Turner, personal communication). An alternate insert was therefore designed for the MVA, with the intention of eliminating the potential for recombination due to duplication of the N-terminal and C-terminal regions. This consisted of a mammalian secretory signal (tPA), the N-terminal (shared) region of MSP2, the 3D7 variable region in tandem with the FC27 variable region (linked only by an MluI restriction site), and finally the shared C-terminal region. Production of MVA with this insert was successful.

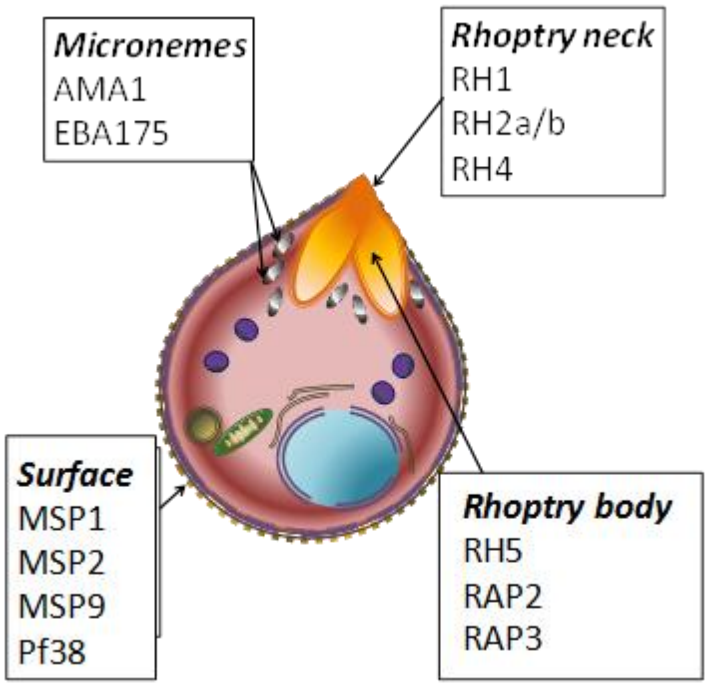

Figure 3.4.1.1: Subcellular localization of vaccine-targeted merozoite antigens.

3.4.2. Vector immunogenicity

All novel antigens were shown to be immunogenic in BALB/c mice, with the exception of RAP2. Antibody induction by vaccination was confirmed by ELISA when recombinant protein antigen was available. ELISA demonstrated immunogenicity of PfEBA175, RH2, RH4K, MSP2 (3D7 and biallelic), MSP9 and Pf38 antigens (Figure 3.4.2.1). ELISA and other data demonstrating the immunogenicity of the MSP1 and AMA1 vaccines used here has been published elsewhere (Goodman, Epp et al. 2010; Biswas, Dicks et al. 2011).

In the case of the RH4.9 and RAP3 antigens, no recombinant protein was available for ELISA. Induction of antigen-specific antibody by vectors expressing antigens was confirmed using the luciferase immunoprecipitation system (LIPS) assay (Burbelo, Ching et al. 2009) (Figure 3.4.2.2).

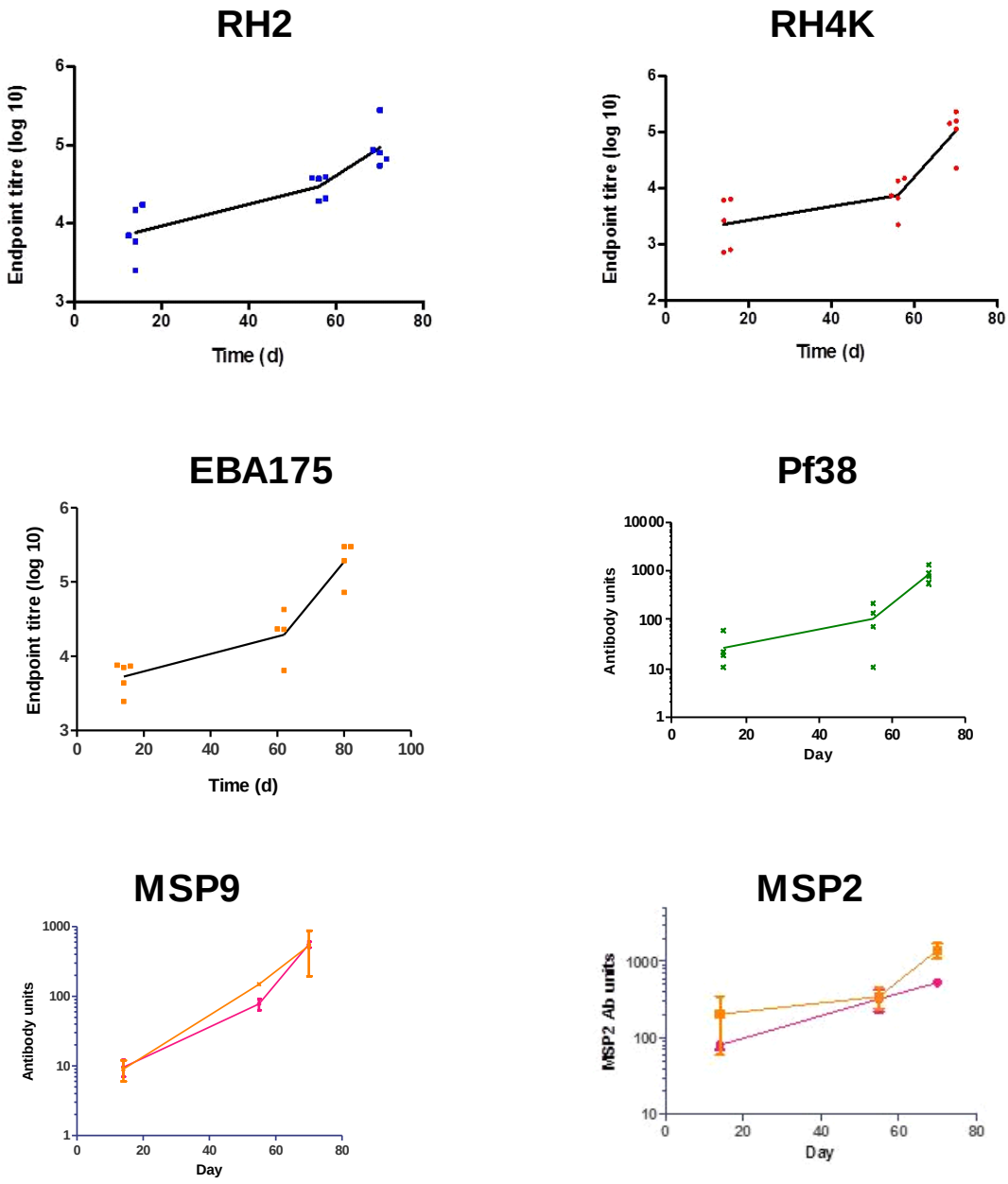

Figure 3.4.2.1 Immunogenicity of vaccines in mice.
Mice were immunized with 1x10^{8} IU AdHu5 followed by 1x10^{7} PFU MVA after an 8 week interval, and ELISA conducted using the appropriate recombinant antigen, as per Methods chapter, with serum from day 14 (post-prime), day 56 (pre-boost) and day 70 (post-boost) samples. n=4-5 per group. Graphs indicate ELISA titres or arbitrary antibody units (after the method of Miura [Miura, Orcutt et al, 2008]). Although not tested here, post-adenovirus antibody titres have typically reached a plateau by day 56; antibody titre rises between day 56 and day 70 are therefore attributable to boosting.

In the case of MSP9, orange line indicates results with full-length antigen while pink line indicates result with previously-expressed MSP9P fragment (aka MSP9NM)(Kushwaha, Rao et al. 2001). The MSP9 coating antigen was full-length 3D7-strain MSP9. In the case of MSP2, orange line indicates 3D7-only vaccine; pink line indicates bi-allelic (3D7 + FC27 bi-allelic) vaccine; the MSP2 ELISA antigen was based upon the 3D7 strain. The MSP2 coating antigen was full-length 3D7-strain MSP2.

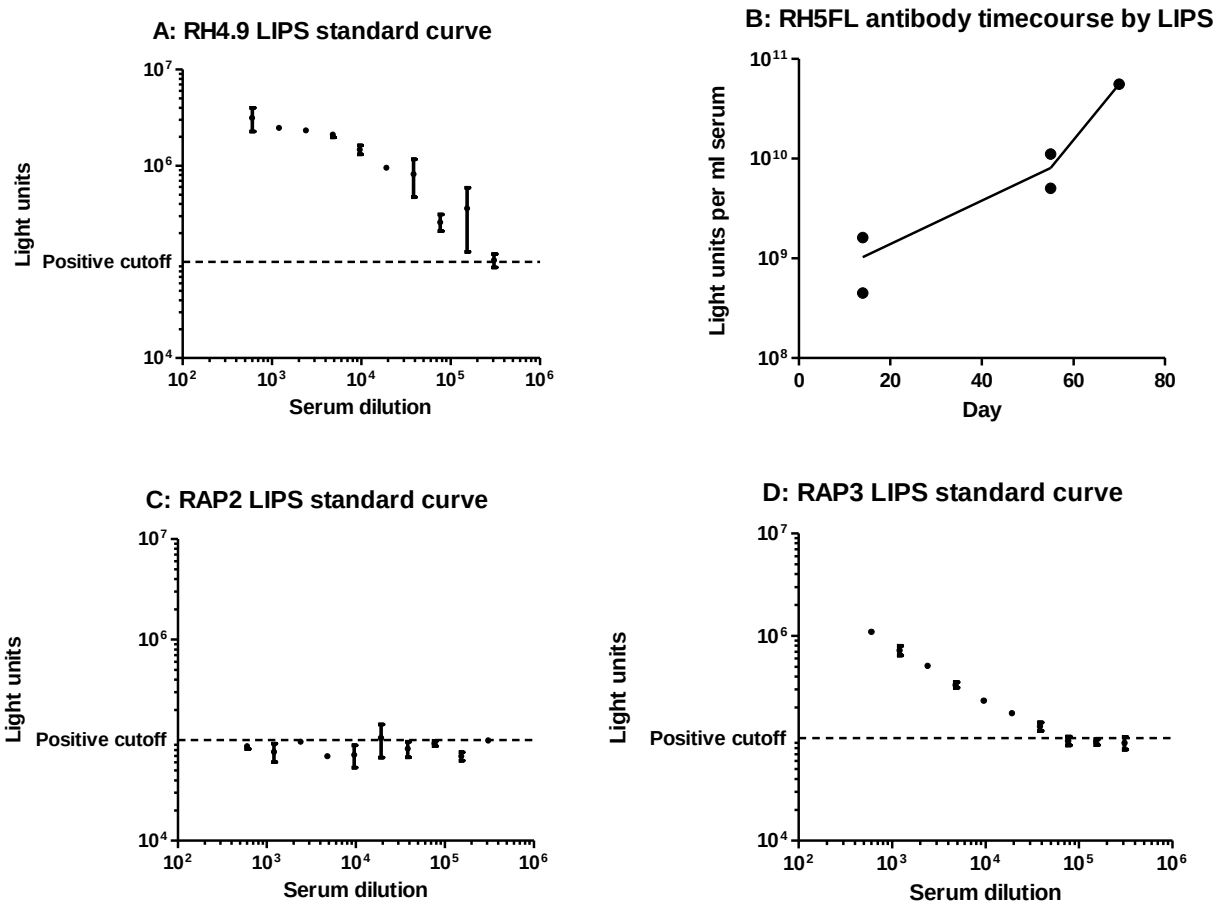

Figure 3.4.2.2 LIPS for RH4.9, RH5, RAP2 and RAP3-specific antibodies
LIPS was conducted using lysate from cells transfected with plasmids encoding renilla luciferase-tagged RH4.9, RH5FL, RAP2 or RAP3 genes. Dilution series of serum from RH4.9, RAP2 or RAP3-immunised mice (after AdHu5-MVA prime-boost immunization) were used in panels A,C and D respectively. Y-axis indicates light units emitted by bead-captured antibody-antigen complexes. Horizontal dotted lines indicate background level of response with naïve mouse serum and cell lysate. A clear response above background level is apparent with RH4.9 and RAP3 but not RAP2.

In the case of RH5FL (panel B), 1:1000 serum dilutions from 2 mice at post-prime, pre-boost and post-boost timepoints were tested. Y-axis plots light unit response.

LIPS was also used to demonstrate the induction of allele-specific responses by the 3D7-strain and bi-allelic 3D7/FC27 MSP2 vaccines (data not shown).

In rabbits, ELISA and LIPS again demonstrated the immunogenicity of PfEBA175, RAP3, RH1, RH2, RH4K, RH4.9, RH5FL, RH5 frag, MSP9 and Pf38 antigens (Figure 3.4.2.3). These results were confirmed by indirect immunofluorescence assay (IFA), demonstrating that the induced IgG antibodies were able to recognize native malaria parasites (experiment conducted in conjunction with Andrew Williams) (Figure 3.4.2.4).

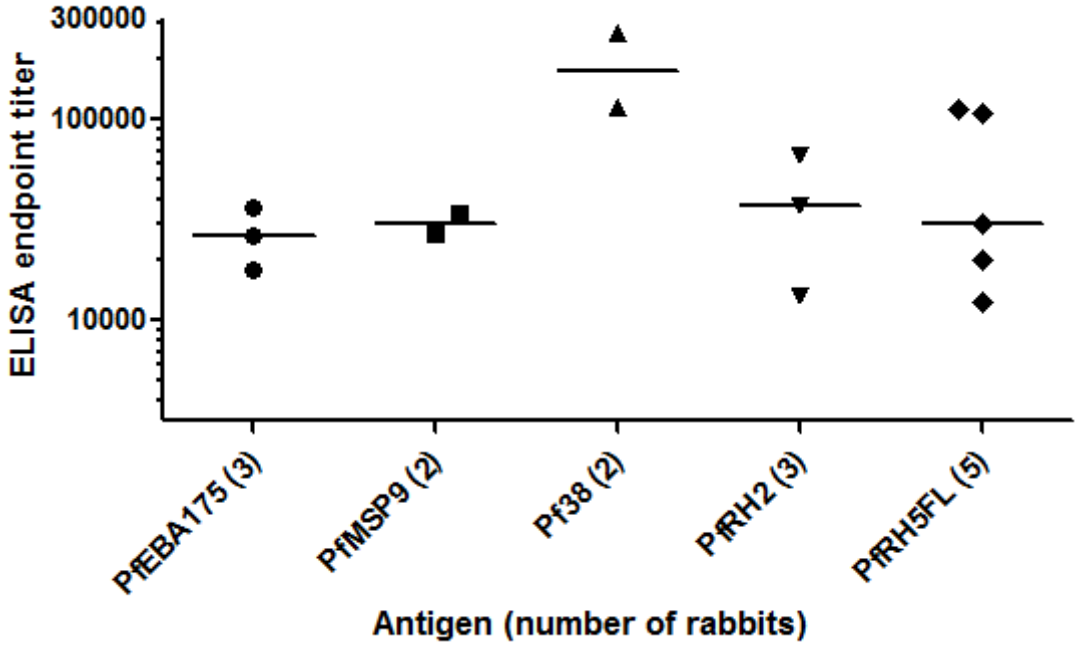

Figure 3.4.2.3 Immunogenicity of vaccines in rabbits
Rabbit sera taken two weeks after final immunisation with PfEBA175, MSP9FL, Pf38, RH2 and RH5FL vaccines contain IgG antibodies which recognize the corresponding recombinant proteins by ELISA at serum dilutions exceeding 1:10,000. Each point is the mean of two replicate wells for an individual rabbit. Line indicates group median.

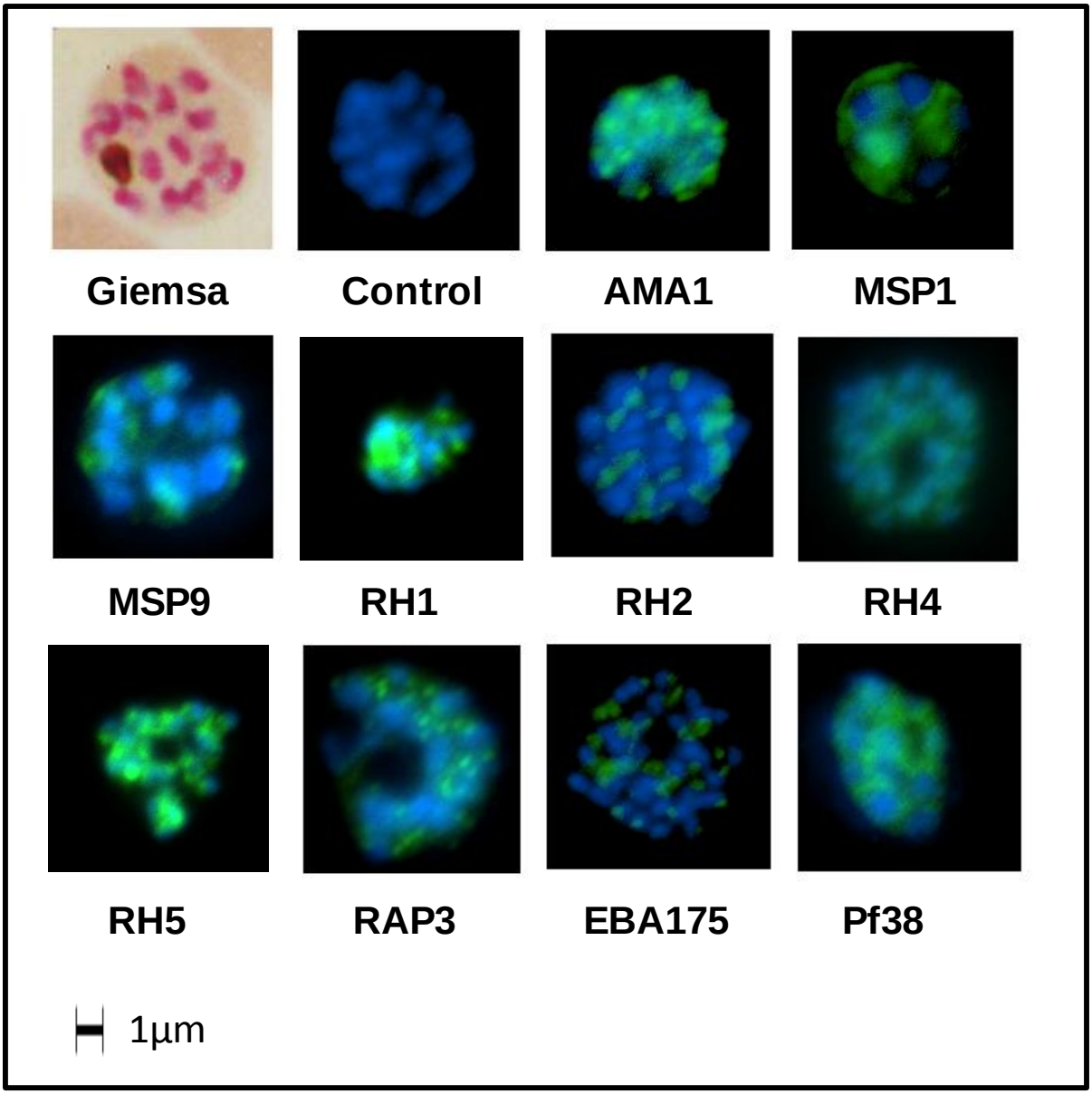

Figure 3.4.2.4 IFA recognition of parasite antigens by vaccine-induced antisera
Indirect immunofluorescence images of P. falciparum schizonts stained with rabbit IgG (green) induced by 10 viral vectored vaccines expressing malaria antigens, and negative control vectors lacking a malaria antigen. Nuclei are counterstained with DAPI (blue). All sera were tested against 3D7 strain parasites, with the exception of anti-RH1 for which FVO strain parasites were used. All images to same scale as Giemsa-stained image (top left).

The RAP2 vaccine was not immunogenic in mice or rabbits, as judged by negative IFA and LIPS assays, although the level of background signal on the LIPS assay was substantial (data not shown). Western blotting of supernatants and cell lysates following transfection of HEK293 cells with plasmids expressing the RAP2 gene (with and without a C-terminal StrepII tag; blots performed using

anti-RAP2 mAb 3A9/48 [Schofield, Bushell et al, 1986] or commercial anti-StrepII mAb [Qiagen]) suggested that the antigen was expressed intracellularly, but that soluble RAP2 was not present in the culture supernatant at detectable levels (data not shown). In contrast, supernatants from cells transfected with EBA175, RAP3, RH2, RH4K, RH5 frag, or RH5FL all contained antigen which was detectable by Western blotting (data not shown; using vaccine-induced polyclonal antibody). Although the primary structure of the RAP2 antigen does not reveal unusual hydrophobicity, it has been noted that the protein accumulates in insoluble inclusion bodies in *E. coli*, and production of soluble RAP2 has proven extremely challenging (Stowers, Prescott et al. 1995) (and L Bird, Oxford Protein Production Facility, Harwell, personal communication). It is possible that RAP2 does not fold correctly and hence accumulates or is degraded in the mammalian secretory pathway. The lack of immunogenicity of this vaccine is somewhat suggestive that the release of soluble protein into the extracellular environment may be necessary for the induction of antibodies by viral vectors.

Neither the 3D7-strain nor the biallelic MSP2 vaccine elicited ELISA or IFA-detectable antibody in rabbits, for reasons which remain unclear. Viral vectors from the same batches were immunogenic in mice both before and after the rabbit immunisation study. It seems unlikely that both rabbits vaccinated with each of two MSP2 vaccines should have received technically inadequate immunisations, or that both MSP2 vaccines should have been the two vaccines among several in the same shipment to have suffered a problem in transit to the rabbit immunisation facility. An immunological rather than technical explanation for this lack of immunogenicity thus seems more plausible. Variable immuno-reactivity of different mouse and rabbit strains to MSP2 antigens has previously been noted, possibly associated with MHC (Pye, Vandenberg et al. 1997). It is possible that the rabbits employed may have lacked MHC capable of presenting the CD4 epitopes present within either MSP2 antigen: the MSP2 gene has short N- and C-terminal regions which are similar between the 3D7 and FC27 alleles (43aa and 74aa respectively), and a central core composed of repetitive amino acid residues(Smythe, Peterson et al. 1990). This structure, somewhat reminiscent of that of CSP, may present a limited array of potential $CD4^+$ helper T cell epitopes.

3.4.3. 3D7 parasite neutralization by vaccine-induced antibodies

The ability of vaccine-induced rabbit IgG to neutralize parasites was tested in the widely-used assay of growth inhibitory activity (GIA) (Miura, Zhou et al. 2009) against 3D7 clone *P. falciparum* parasites. This assay employs total purified IgG (of which only a fraction will be vaccine-induced and antigen-specific). IgG induced by vectors expressing the antigen RH5FL was potently growth inhibitory; more modest degrees of inhibition (though statistically significant by comparison to control rabbit IgG) were found with Pf38, RH4.9, and RH5frag (Figure 3.4.3.1A).

Unlike any other reported antigen to date, anti-RH5FL IgG was more effective than antibodies to the leading antigens AMA1 and MSP1 when tested against vaccine-homologous 3D7 parasites (the clone used for most controlled human malaria infection vaccine-efficacy trials (Sauerwein, Roestenberg et al. 2011), and upon which the vaccine antigen was based).

Data generated using a two-fold serial dilution of total IgG allows for a more accurate comparison of the effect of anti-RH5FL IgG with that of anti-AMA1 IgG. This shows that the effective concentration of total IgG from RH5FL immunized rabbits required to give 50% GIA (EC_{50}) against 3D7 strain parasites was 2-fold lower than that observed with AMA1 (Figure 3.4.3.1A, Table 3.4.3.T1).

FIGURE 3.4.3.1 Growth inhibitory activity of vaccine-induced rabbit IgG (overleaf)

Panel A: *GIA of rabbit IgG tested against 3D7 strain parasites at various concentrations. IgG from all rabbits immunized with each antigen was pooled, with the exception of AMA1 and RH5FL, for which GIA was performed with IgG purified from individual rabbits. Values are mean of two independent experiments, typically with three replicate wells. Error bars indicate inter-well SD, with the exception of AMA1 and RH5FL, for which bars indicate inter-rabbit SD.*

Panel B: *Comparison of effects of RH5FL-induced IgG (blue), IgG induced by vaccination with 3D7-strain AMA1 (green), and IgG induced by vaccination with a bivalent AMA1 (3D7+FVO) vaccine (red) in assays of GIA against laboratory parasite lines 3D7, FVO, Dd2, GB4, Camp and 7G8. Lines indicate dose-response curves fitted by non-linear least squares regression as described in methods section. All assays were performed using IgG purified from pooled serum of two RH5FL-vaccinated rabbits and single rabbits vaccinated with each AMA1 vaccine (see methods for further details). Values are mean of two independent experiments with three replicate wells, with the exception of assays against 7G8 and Camp strains and mono-allelic AMA1 versus FVO (for which results are mean of three wells in a single experiment). Error bars indicate inter-well SD.*

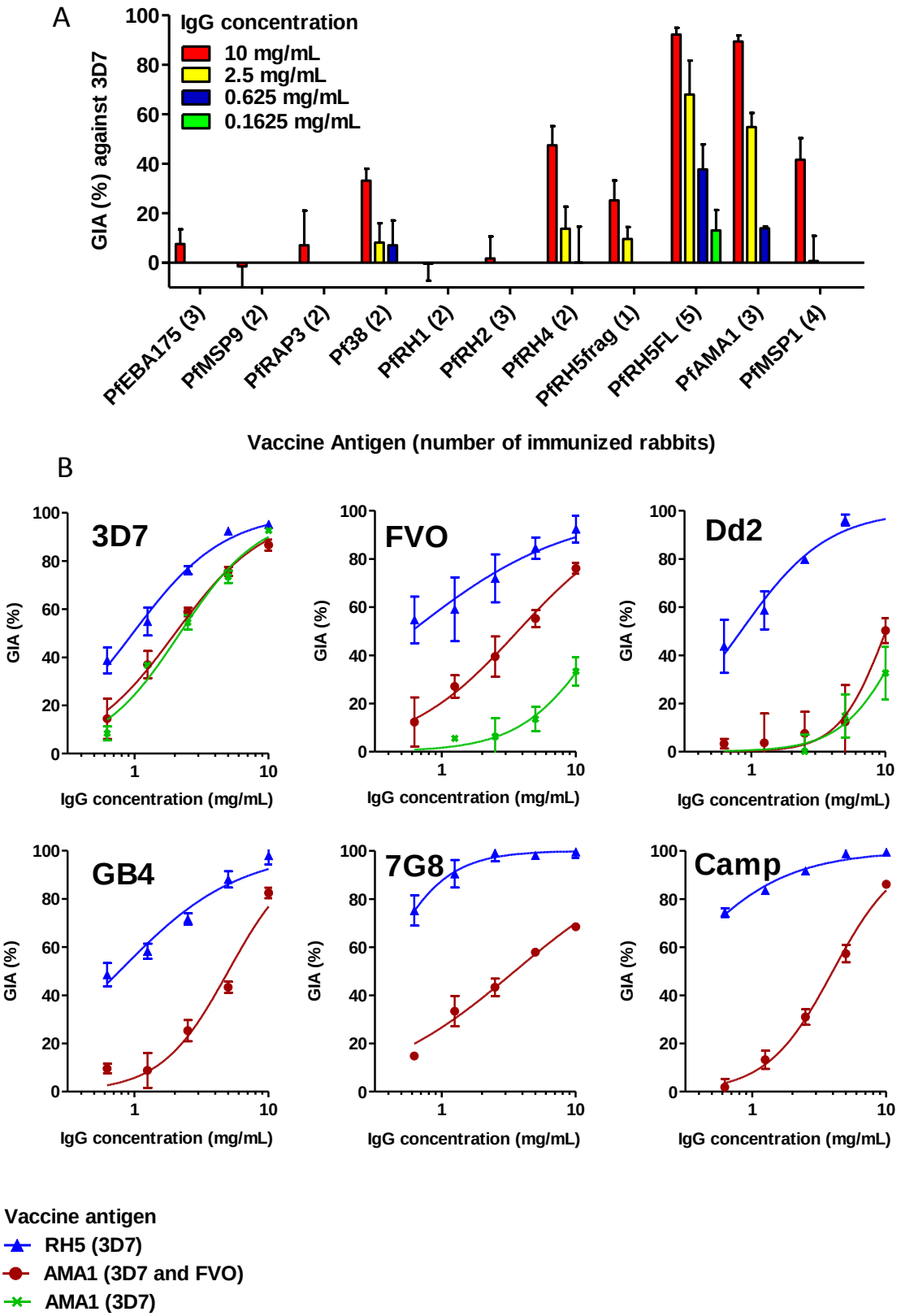

Figure 3.4.3.1 Growth inhibitory activity of vaccine-induced rabbit IgG

	Vaccine antigen (strain of antigen sequence)		
Parasite Strain	RH5FL (3D7)	AMA1 bivalent (3D7 + FVO)	AMA1 mono-allelic (3D7)
3D7	1.11	2.14	2.18
FVO	[<0.625]	3.68	[>10]
Dd2	0.84	[10.1]	[>10]
GB4	0.77	5.02	ND
Camp	[<0.625]	3.99	ND
7G8	[<0.625]	3.50	ND

Table 3.4.3.T1. EC_{50} values for various parasite line / vaccine antigen combinations.
Estimation of the concentration of total IgG (in mg/mL) necessary to induce 50% GIA (EC_{50}) was performed using non-linear least squares regression (as described in methods) and the data presented in Figure 3.4.3.1B. Square brackets indicate estimated EC_{50} values falling outside the range of tested IgG concentrations. ND - not done. For all lines, there was a statistically significant difference between the EC_{50} values of the tested RH5FL and bivalent AMA1 samples ($P < 0.001$ by extra sum-of-squares F-test).

3.4.4. Neutralization of vaccine-heterologous parasites

The anti-RH5FL-induced rabbit IgG was further tested in assays of GIA against vaccine heterologous parasite laboratory lines. Sequencing of the RH5 gene in 18 laboratory parasite lines has previously revealed limited polymorphism (10 amino acid sites) (Hayton, Gaur et al. 2008). Five vaccine-heterologous parasite lines (FVO, Dd2, GB4, Camp and 7G8) were therefore selected on the basis of their genetic divergence from 3D7's RH5 sequence, and their differing patterns of ligand-receptor invasion 'pathway' usage (Lobo, Rodriguez et al. 2006; Hayton, Gaur et al. 2008). Together, these lines included amino acid changes at every polymorphic locus previously identified. Additionally, FVO, Dd2, Camp and GB4 parasites are known to vary substantially from 3D7 parasites in their ability to invade *Aotus nancymaae* erythrocytes – a phenotype believed to be associated with RH5 polymorphisms which may affect receptor recognition (Hayton, Gaur et al. 2008). Of 18 laboratory lines for which the RH5 gene has been sequenced and *Aotus* RBC invasion efficiency quantified, FVO was most divergent from the 3D7 clone upon which the vaccine was based (Hayton, Gaur et al. 2008).

Strikingly, antibodies against RH5FL remained highly effective against all five additional parasite strains tested, in marked contrast to antibodies induced by both mono-allelic (3D7) and bivalent (3D7 and FVO) AMA1 vaccines (Figure 3.4.3.1B). Using the same data, EC_{50} values for the GIA effect of anti-RH5FL and anti-AMA1 IgG against the various parasite strains were estimated (Table 3.4.3.T1). The EC_{50} of anti-RH5FL was even lower against vaccine-heterologous parasite strains than against 3D7 parasites. Taken together with the higher EC_{50} values for anti-AMA1 against vaccine-heterologous parasites, this resulted in a >5-fold reduction in EC_{50} for anti-RH5FL relative to anti-AMA1 against all vaccine-heterologous parasite strains.

The key GIA observations above were independently confirmed, with a notable degree of similarity, by the GIA Reference Center funded by the PATH Malaria Vaccine Initiative (MVI) (Figure 3.4.4.1), as recommended by other studies of invasion-ligand candidate vaccines (Jiang, Gaur et al. 2011). Given the lack of RH1 expression by 3D7 parasites, anti-RH1 IgG was additionally tested against FVO

parasites, which do express this antigen (Rayner, Vargas-Serrato et al. 2001; Gao, Yeo et al. 2008): no GIA was detectable at 10 mg/ml total IgG.

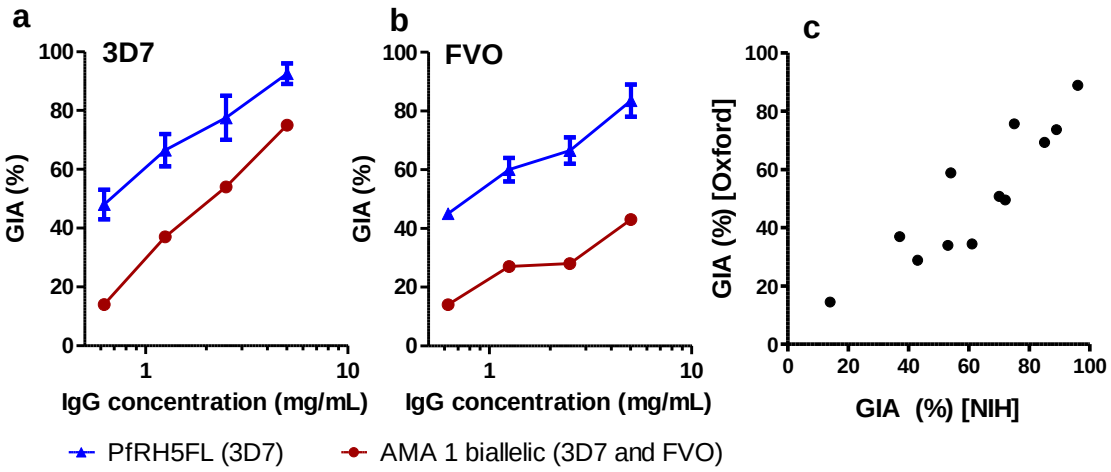

Figure 3.4.4.1 GIA at reference laboratory
Panel A-B: *GIA performed at the PATH MVI funded GIA reference laboratory at NIH, USA against 3D7 strain parasites and FVO parasites. Error bars indicate range of results for the two RH5FL-vaccinated rabbits. Blue, RH5FL (3D7) and red, AMA1 biallelic (3D7 and FVO).*

Panel C: *Comparison of GIA results obtained in Oxford and at NIH. Each point represents the result obtained for a single rabbit at a single IgG concentration. Pearson r = 0.90.*

3.4.5. Assessment of naturally-acquired RH5 antibody responses

Given the low level of sequence diversity in the RH5 gene, it was hypothesized that, despite being vulnerable to antibody, RH5 may not be under substantial immune selection pressure. Consistent with this, it was found that malaria-experienced Kenyans have little or no antibody against RH5, in contrast to all other antigens for which recombinant protein was available as an ELISA coating antigen (Figure 3.4.5.1A-C)(experiments conducted by Simon Draper, Prateek Choudhary, Faith Osier and Gathoni Kamuyu).

Mammals may be tolerant to proteins with extensive primary amino acid homology with mammalian proteins, but this is not the case for RH5: a Protein BLAST search yielded no match with an E-value<1 between RH5 and any mouse or human protein; the closest match for both species was a SLIT-ROBO

RhoGTPase, with limited similarity to residues 160-303 of RH5 (within this limited stretch, RH5 had 26% sequence identity with the human GTPase and 27% identity with the mouse homologue). Indeed, antibodies to RH5FL are readily inducible by vaccination of mice (geometric mean endpoint titre 85000, range 35000 to 216000, n=5) and rabbits (Figure 3.4.1.3), confirming the antigen is not inherently non-immunogenic in mammals.

FIGURE 3.4.5.1 Antibody responses to multiple merozoite antigens in malaria-exposed humans (overleaf)

Panel A: *Semi-quantitative comparison of levels of IgG (as indicated by optical density, OD 405nm, in ELISA) against multiple antigens in 24 Kenyan adult sera relative to background in six malaria-naïve healthy UK adults. Boxes enclose interquartile range, central lines represents median, whiskers indicate 10th and 90th centile. Blue, Kenyan and red, UK.*

Panel B: *Prevalence of antigen-specific IgG among 24 Kenyan adult sera (samples from 3A). The threshold for positivity was defined as the mean OD 405nm plus 3 standard deviations of results for six malaria-naïve UK adults.*

Panel C: *Age-related acquisition of IgG antibodies to blood-stage antigens, such as AMA1 is commonly observed in children in malaria-endemic areas. The data compare acquisition of anti-AMA1 and anti-RH5 IgG in 55-60 children from each of five age groups; acquisition of antigen-specific IgG is minimal for RH5. Boxes enclose interquartile range, central lines represents median, whiskers indicate 10th and 90th centile. Blue, AMA1 and red, RH5.*

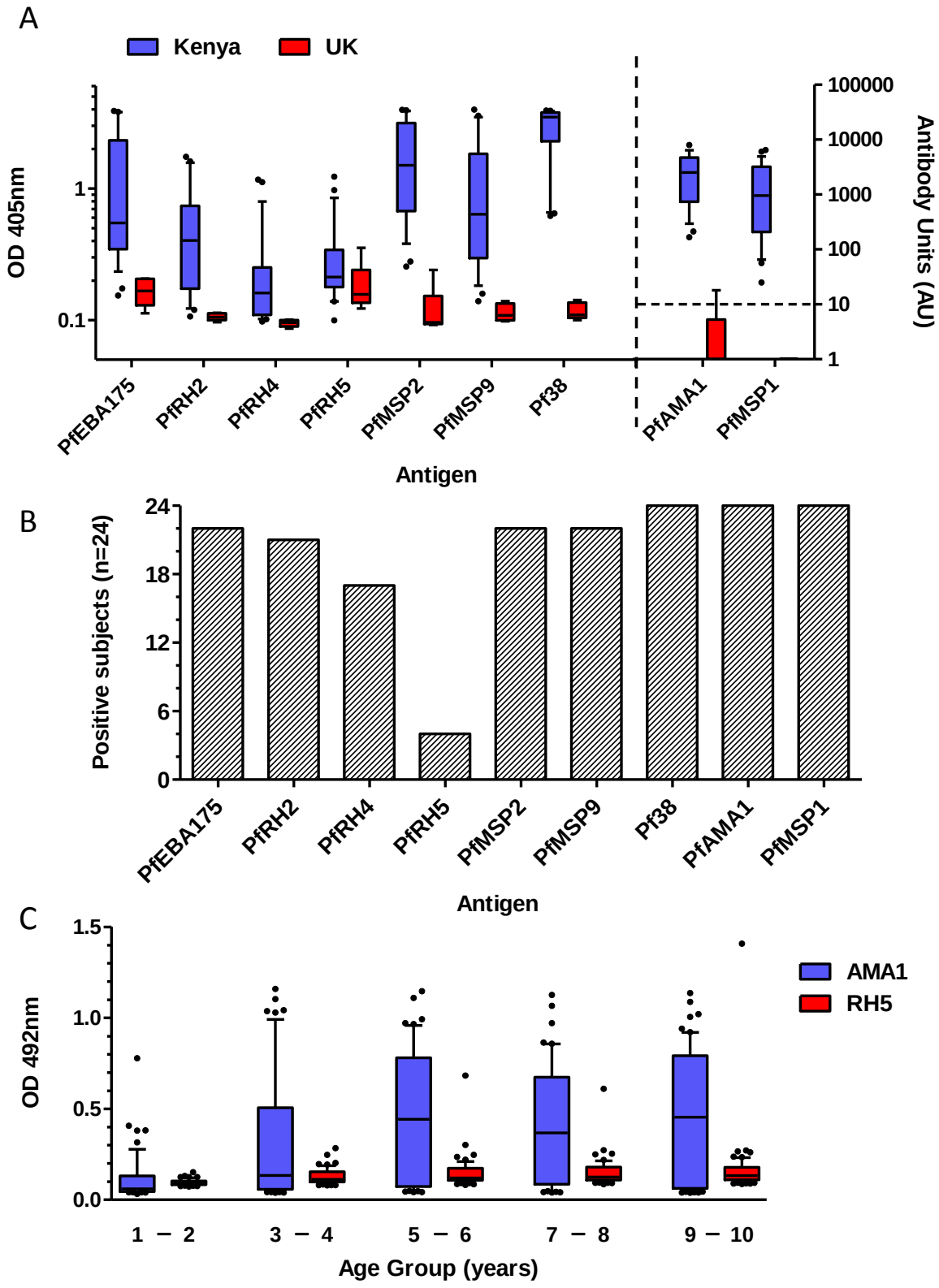

Figure 3.4.5.1 Antibody responses to multiple merozoite antigens in malaria-exposed humans

3.5. DISCUSSION

The work reported in this chapter aimed to use viral vector vaccines as a platform to test the ability of various merozoite antigens to induce parasite-neutralizing antibody, and to compare the potency of GIA induced by such antibodies to that achieved by antibodies to the leading antigens MSP1 and AMA1. Most strikingly, antibodies to the full-length RH5 construct proved highly effective in the assay of GIA.

The potent inhibition shown by anti-RH5FL IgG contrasted with modest inhibition by antibodies induced by RH5frag vectors. When previously tested as a bacterially-expressed immunogen, RH5frag induced antibodies which did not achieve significant GIA against invasion of intact, non-enzyme-treated, human RBCs (Baum, Chen et al. 2009). Another vaccination study utilizing a different bacterially expressed fragment of the RH5 antigen also reported a failure to show GIA *in vitro* (Rodriguez, Lustigman et al. 2008). The conformational accuracy of these bacterially-expressed fragments is unknown: for now, the full-length RH5 immunogen appears to be required to induce functional growth inhibitory antibodies following immunization.

The reason for the lack of anti-RH5 antibody in naturally exposed Kenyans is unclear. The facts that anti-RH5FL IgG induced in animals by these viral vectored vaccines binds both the ELISA antigen and native parasites by IFA (Figure 3.4.1.4), and that the RH5 ELISA coating antigen has been confirmed to bind its host RBC receptor (Crosnier, Bustamante et al. 2011), indicate that incorrect conformation of RH5 ELISA coating antigen is highly unlikely to account for poor detection of anti-RH5 IgG in humans. RH5 mRNA has also been shown to be expressed in field isolates cultured *ex-vivo* both from The Gambia in West Africa (Gomez-Escobar, Amambua-Ngwa et al. 2010), and Kenya in East Africa (Mackinnon, Li et al. 2009), suggesting this inherent lack of immune recognition is not due to the absence of RH5 expression by parasites circulating in endemic areas. Selective down-regulation of RH5 in parasites infecting malaria-experienced individuals who control parasitemia (as suggested by Gomez-Escobar *et al*. (Gomez-Escobar, Amambua-Ngwa et al. 2010)) might lead anti-RH5 IgG titres to be higher in children than in adults. However, additional ELISA assays conducted

using serum from Kenyan children (Figure 3.4.5.1C) yielded results comparable to those observed in adults (Figure 3.4.5.1A-B). The mechanism by which this crucial antigen escapes immune recognition in both adults and children thus requires further investigation.

The breadth of cross-strain parasite-neutralizing activity induced by the RH5FL antigen may represent an intriguing gap in *P. falciparum*'s highly-evolved immune evasion strategies and is unique to date among mono-allelic blood-stage vaccine candidates. A previous study of 18 laboratory strains reported polymorphisms in 10 out of RH5's 526 amino acid residues (Hayton, Gaur et al. 2008). This density of polymorphisms is 3.3-fold lower than in the well-characterized 19 kDa C-terminus of MSP1 ($MSP1_{19}$) (6 out of 96 amino acid residues) (Takala, Smith et al. 2007), which in itself is widely regarded as a highly conserved vaccine target. Data from non-human primate models demonstrate that the amino acid polymorphism in MSP1 can result in strain-specific efficacy of vaccine-induced anti-MSP1 antibody responses (Lyon, Angov et al. 2008). There may thus be a contrast in the immunological effect of the polymorphism in MSP1 versus that in RH5. It is possible that non-immune mechanisms such as adaptation to host erythrocyte variability could drive the apparent excess of non-synonymous relative to synonymous mutations in RH5 (Jeffares, Pain et al. 2007; Volkman, Sabeti et al. 2007; Hayton, Gaur et al. 2008).

Attempts to disrupt the RH5 gene have failed repeatedly, suggesting it is essential for parasite viability (Hayton, Gaur et al. 2008; Baum, Chen et al. 2009), and immunization against rodent malaria homologues of the RH family provides protection in a mouse challenge model (Freeman, Trejdosiewicz et al. 1980) – a finding first reported in 1980, but not translated into a human-compatible vaccine formulation against *P. falciparum* until now. Complementing these data obtained using RH5FL as a vaccine target, an erythrocyte receptor for RH5, and a critical role for this receptor-ligand interaction were recently demonstrated (Crosnier, Bustamante et al. 2011). In contrast to the prevailing views that erythrocyte invasion by *P. falciparum* is a degenerate process

mediated by multiple ligand-receptor pairs and that any merozoite antigen susceptible to antibody is highly polymorphic, RH5-mediated invasion appears to be both essential and vulnerable to blockade.

Multiple strands of evidence now suggest that RH5FL is the best candidate for blood-stage malaria vaccine development to emerge from the *P. falciparum* genome to date. The traditional immuno-epidemiological approach to antigen identification may have focussed vaccine-development efforts more upon immunogenic but polymorphic 'decoy antigens' than 'Achilles' heels' (Crompton, Kayala et al. 2010; Fowkes, Richards et al. 2010). Assaying parasite growth inhibition by vaccine-induced antibodies has, instead, focussed attention upon an antigen which would not have appeared to be an important target of naturally-acquired responses. In this study, anti-RH5FL IgG out-performed anti-AMA1 IgG against homologous 3D7 clone parasites when induced by the same vaccine delivery platform, and importantly for clinical significance, also showed strain-transcending neutralization against other strains. Recently a 3D7 strain AMA1 protein-in-adjuvant vaccine has demonstrated significant strain-specific efficacy in a pre-specified secondary analysis of a Phase IIb study in Malian children (Thera, Doumbo et al. 2011). This result emphasises that antigenic polymorphism is a central problem for the field: the findings reported here suggest that the RH5FL antigen may offer a solution to this problem.

One problem for the blood-stage vaccine field has been the fact that novel antigens have been identified by several separate laboratories, with the potency of the induced antibody tested using differing and non-comparable assay methods. Frequently the vaccine delivery platforms used are not clinically translatable (for example, six-immunisation regimes including complete Freund's adjuvant (Lopaticki, Maier et al. 2011)). This study represented the first effort to compare several blood-stage antigens head-to-head using the same human-compatible vaccine platform and a standard assay technique, comparable to that used by the international reference laboratory. Use of the viral-vector vaccine platform was an important pre-requisite for this study, due to the lack of a recombinant protein-expression technology capable of reasonable-throughput expression of diverse

Plasmodial antigens. An important limitation of this approach is that there is, presumably, some relationship between the quantity of antigen produced and secreted by viral vector-infected cells, the immunogenicity of that particular antigen, and the potency of the antibodies in GIA. Without being able to measure the concentration of antigen-specific antibodies induced by each vaccine, some caution must be exercised in drawing the conclusion that a lack of GIA induced by a viral vector vaccine necessarily rules out the candidacy of that antigen. Conversely, a high level of GIA induced by a particular viral vector vaccine may reflect high levels of antigen expression and immunogenicity of that vaccine, rather than an inherent property of the antigen. Nonetheless, some prioritisation of antigens on the basis of these results does seem reasonable.

The promising results obtained here with anti-RH5FL antibodies suggested that further work was necessary to elucidate their mechanism of action, and to further verify their potency and strain-transcending activity. Such work will be the subject of the following two chapters.

4. Measuring polyclonal antigen-specific antibody concentration by surface plasmon resonance

4.1. AUTHORSHIP STATEMENT

ADD designed and performed all surface plasmon resonance (SPR) assays reported in this chapter.

RH5 and AMA1 protein antigens were supplied by Gavin Wright and Cecile Crosnier.

Human ELISA measurements (used as a comparator for the SPR measurements) were made by Prateek Choudhary, using serum from clinical trials of AMA1 vaccines led by Susanne Sheehy, Chris Duncan, Ruth Ellis, Yimin Wu, Sumi Biswas and Simon Draper(Duncan, Sheehy et al. 2011; Sheehy, Duncan et al. 2012).

The author is grateful for the kind assistance and advice of Geoff Hale, David Staunton, Dirk Aarts, Julia Schollick and Julie Furze.

4.2. INTRODUCTION

Having established that anti-RH5 antibodies were capable of potent neutralisation of merozoites, I wished to establish the quantitative relationship between antibody concentration and efficiency of neutralisation. This chapter describes the development and validation of a novel method to permit this quantitation. The quantitative relationship itself will be described in the following chapter.

Levels of antigen-specific antibody are usually reported as enzyme-linked immunosorbent assay (ELISA) endpoint titres. Such titres are influenced both by antibody concentration and avidity, and are usually not comparable between laboratories, antigens, or species. Carefully standardised ELISA assays are increasingly used to enable inter-laboratory comparability. Referencing of ELISA titres to absolute units (i.e. µg/mL antigen-specific antibody) typically requires the preparation of a standard of known concentration, such as antigen-specific antibody purified on an antigen-affinity column. Such standards are rarely available in the early stages of characterisation of an antigen-specific antibody response. For this reason, quantitative relationships between absolute antigen-specific antibody concentration and biological activity are frequently challenging to elucidate.

In the context of vaccine design, questions sometimes arise which cannot readily be answered without knowledge of absolute antibody concentrations. Examples include the following:

- "Do vaccine-induced antibodies against antigen A or antigen B neutralise the pathogen more potently?" (Williams & Douglas, PLoS Pathogens, in press & Chapter 5) (Miura, Zhou et al. 2009);
- "Do human antibodies against antigen X neutralise the pathogen as effectively as rabbit antibodies?" (Miura, Zhou et al. 2009)
- "In an antigen screening programme, antiserum raised using antigen Y did not achieve pathogen neutralisation although it did contain Y-specific antibodies by ELISA – was the concentration of Y-specific antibodies therefore sufficient to rule Y out as a vaccine target, or might a more immunogenic vaccine succeed?"

- "How potent is adjuvant A relative to adjuvant B which was reported in a different study?"

A straightforward method to measure absolute antibody concentrations without the requirement for a calibration standard of known concentration would therefore be of considerable value to vaccinologists and other researchers working with polyclonal antisera.

Biosensors, such as the Biacore range of SPR devices (GE Healthcare) can monitor the progress of an antibody-antigen binding reaction in 'real time'. These kinetic data are most frequently used to establish the association and dissociation rate constants of the interaction. However reactant concentration is also a key determinant of reaction rate. By designing a biosensor experiment in such a way that the extent to which concentration is rate-limiting can be established, absolute reagent concentration can be measured, independent of association and dissociation rates. This is the basis of a technique which Biacore's manufacturers term 'Calibration Free Concentration Analysis' (CFCA).

A detailed theoretical discussion of this method has previously been published(Christensen 1997). In brief, SPR measures the rate of a binding reaction between a reagent in solution ('analyte') and an immobilised partner ('ligand') (Figure 4.2.1). Successful analyte binding requires two processes: delivery of analyte to the chip surface by a combination of flow and diffusion, and then the analyte-ligand interaction itself. In addition to concentration (the desired unknown), the rate of analyte delivery to the chip will be influenced by temperature, molecular weight of the analyte, diffusion coefficient of the analyte, rate of solution flow and dimensions of the flow cell (all of which are known in the case of an antibody-antigen interaction). The rate of the analyte-ligand interaction at the chip, on the other hand, will be influenced by association rate, dissociation rate, and the density of ligand at the chip surface, none of which are accurately known prior to a CFCA experiment (Figure 4.2.2).

CFCA experiments are designed to maximise the extent to which the rate of reaction is limited by diffusion (and hence by analyte concentration), as opposed to by the kinetics of the analyte-ligand interaction at the chip surface. First, ligand is used at a high density on the surface, to minimise (although not necessarily eliminate) the limitation of the reaction rate by ligand density. Second, only the very first period of the interaction is measured (30 seconds), using an analyte dilution such that equilibration of the reaction would require a much longer period; formation of new ligand-analyte complexes during this period will far outweigh dissociation, and hence the reaction dissociation rate will have minimal influence on the reaction rate. Nonetheless, both the association rate and the ligand density will continue to influence the reaction rate.

The CFCA technique overcomes this by measuring binding rates under two conditions, varying the influence of diffusion upon the reaction rate while ligand density and interaction kinetics remain constant. First, binding is measured under conditions of low analyte flow: under these conditions, diffusion of the analyte down a concentration gradient between the bulk solution and the chip surface (where the ligand is immobilised, and analyte is being removed from solution by binding) will play a relatively large role in determining the rate of the reaction. Second, binding is measured with high analyte flow, which will reduce the importance of this concentration gradient by constantly replenishing analyte at the chip surface. Comparison of the rates of binding under these conditions, via a model of binding kinetics, allows calculation of the analyte concentration.

This technique was first reported in 1997, with refinement of the interaction model in 2002 (Christensen 1997; RichaletSecordel, RaufferBruyere et al. 1997; Sigmundsson, Masson et al. 2002). In particular, Richalet-Secordel *et al.* performed an elegant validation of the method's ability to measure the concentration of a set of mAbs with varying antigen-interaction affinities (RichaletSecordel, RaufferBruyere et al. 1997). The technique has not, however, been applied or

validated in the field of vaccinology. There is one report of the use of a CFCA-like method to measure vaccine-induced polyclonal antigen-specific antibody (Pol, Karlsson et al. 2007) – unusually, the antigen itself in this study was IgE – but this report used an older technique reliant upon complete mass transport limitation (Karlsson, Fagerstam et al. 1993).

Although the necessary measurements can be performed with older Biacore devices (the original reports employed the Biacore 2000), the necessary fitting algorithm has only recently been included in the standard Biacore Evaluation software (T100 version 2, and T200 editions of the software): this advance is likely to make CFCA accessible to a wider non-specialist user-base for the first time. Moreover, the relatively recent development of the biotin CAP chip will also facilitate CFCA analysis: this chip permits repetitive and reproducible regeneration of a chip surface with fresh antigen at a desired capture level, without requiring re-use of antigen which has been exposed to potentially denaturing 'regeneration' treatment such as acid to remove bound antibody.

Recent technological advances are therefore poised to enable much wider application of a relatively old technique. The previously published study of SPR-based analysis of polyclonal antibody concentration did not compare the results of this analysis to antibody concentrations determined using another method, and used a relatively simple binding model applicable only to conditions in which mass-transport limitation is total (whereas the recent software assesses binding under partial mass-transport limitation). Here, it is shown that the results of CFCA experiments, conducted under conditions of partial mass-transport limitation, correlate well with measured antigen-specific antibody concentrations for a panel of mAbs and for polyclonal antisera tested using a validated standardised ELISA. As stated above, the following chapter will apply this methodology to elucidate the quantitative relationship between anti-RH5 antibody concentrations and parasite neutralisation.

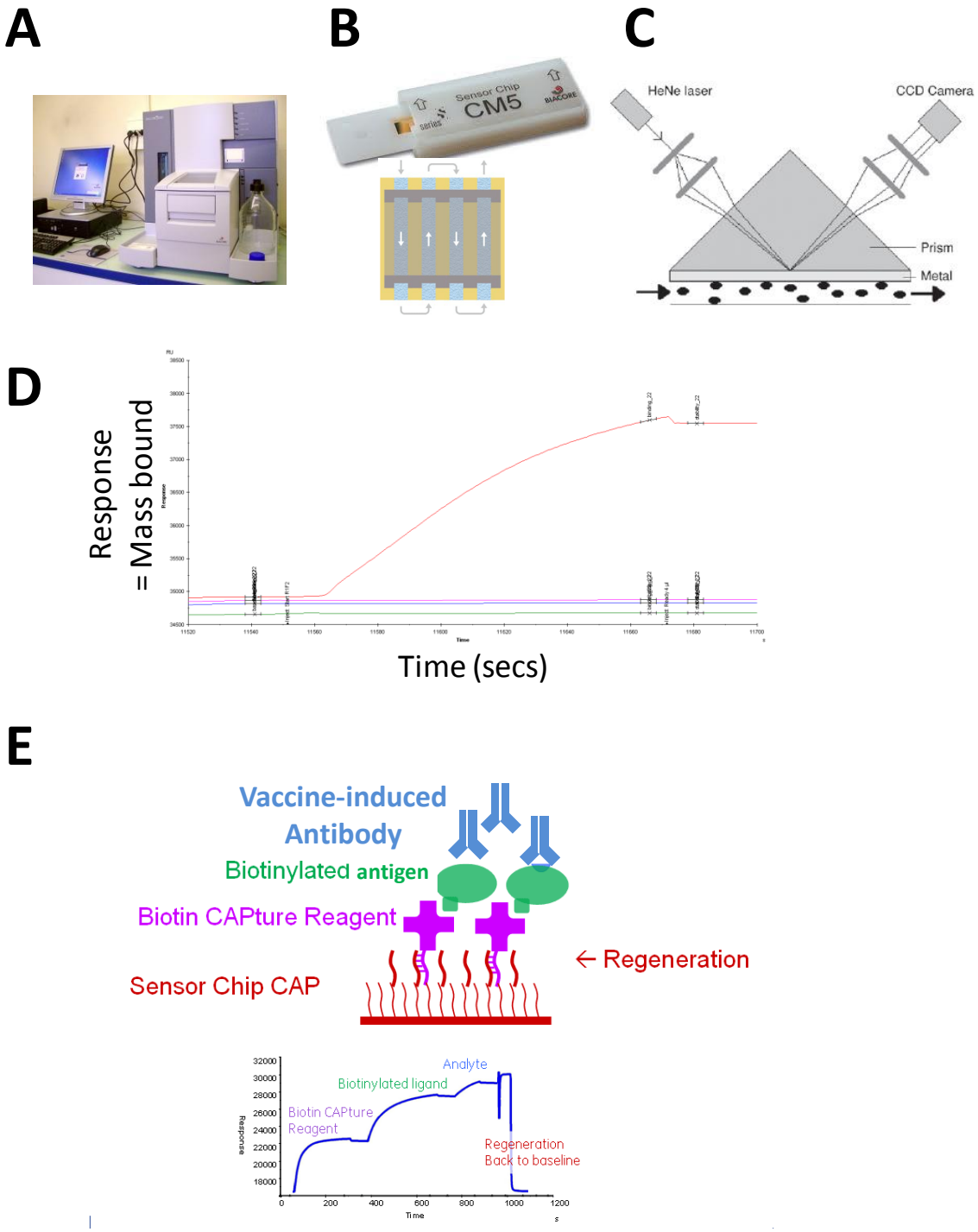

Figure 4.2.1: Principles of SPR

The Biacore instrument (panel A) is programmed to inject a sequence of samples and reagents over a sensor chip (panel B). The binding of molecules to the chip surface gives the response via an interface between a prism and the gold chip surface to laser stimulation (panel C), resulting in a real-time signal proportionate to the mass of material bound to the chip (panel D). The "sensor chip CAP" kit comprises a chip coated with a DNA oligonucleotide, a CAPture reagent (streptavidin attached to the complementary oligonucleotide), and a regeneration reagent capable of dissociating base-pairing. Successive injections of CAPture reagent, a biotinylated antigen 'ligand', and a vaccine-induced antibody 'analyte' allow measurement of antigen-specific binding, followed by regeneration and application of fresh antigen. Panels B,C and E are adapted from the Biacore product literature (GE Healthcare Ltd).

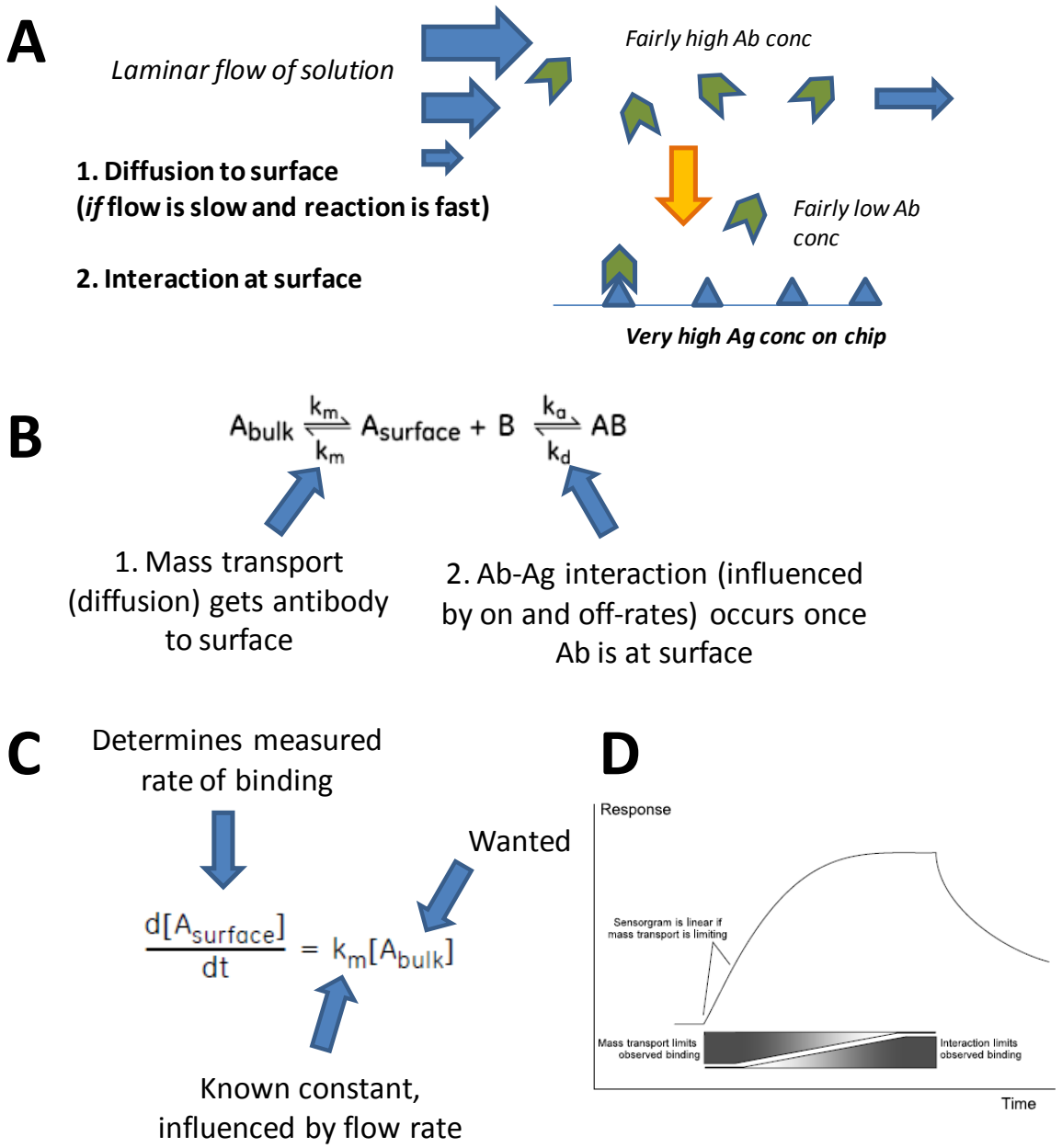

Figure 4.2.2 Principles of Calibration Free Concentration Analysis

Binding of antibody to the chip is influenced by two processes: diffusion down a concentration gradient towards the chip (stage 1), and the antibody-antigen interaction itself (stage 2). These processes are represented graphically in panel A, and in the form of reaction-kinetic equations in panel B. The use of slow flow rates and high antigen density for CFCA maximises the extent to which the reaction is limited by mass transport (stage 1).

*Under conditions of **complete** mass transport limitation, stage 2 is irrelevant and the rate of the binding reaction is proportionate to the concentration of antibody at the surface, which in turn is proportionate to the concentration of antibody in the bulk solution, [A_{bulk}] (panel C).*

*Under conditions of **partial** mass transport limitation, the reaction rate at the surface will be influenced by **both** [A_{bulk}] and the interaction rate at the surface: the measurement of binding at two flow rates allows deconvolution of these factors to estimate concentration. The relative importance of mass transport limitation and interaction-limitation is highest in the early phase of the binding reaction, when unbound antigen is abundant and antibody dissociation is rare (panel D).*

Panels B,C, and D are adapted from Biacore product literature (GE Healthcare Ltd).

4.3. METHODS

4.3.1. Antigen and antibody samples

Generation of anti-PfRH5 murine monoclonal antibodies QA5, 9AD4 and 2AC7 will be described elsewhere (Chapter 6). Briefly, hybridomas were cultured using medium containing ultra-low IgG foetal calf serum (Gibco). mAbs were purified from hybridoma supernatant using Protein G (Pierce), in accordance with the manufacturer's instructions, and buffer exchanged into phosphate-buffered saline using an Amicon device (Millipore). Protein concentrations were established by A_{280} spectrometry (Nanodrop, Thermo Scientific).

Mouse and rabbit anti-PfAMA1 and anti-PfRH5 serum and IgG samples were obtained and prepared as described in Chapter 3. Human serum was obtained from subjects in two previously described clinical trials of PfAMA1-based vaccines (Duncan, Sheehy et al. 2011; Sheehy, Duncan et al. 2012).

Mouse and rabbit work was approved by the University of Oxford Animal Care and Ethical Review Committee (in its review of the application for Home Office project license PPL 30/2414), and performed in accordance with all applicable regulations. Clinical trials were reviewed by the Oxfordshire Research Ethics Committee (OXREC 07/H0604/137) and UK Gene Therapy Advisory Committee (GTAC 142).

Recombinant PfAMA1 and PfRH5 proteins (both 3D7-allele, and enzymatically mono-biotinylated at the C-terminus) were produced by transient transfection of HEK293E cells, as previously described (Bushell, Sollner et al. 2008). Supernatant was extensively dialysed against PBS to remove free biotin.

4.3.2. ELISA

Mouse total IgG endpoint ELISA against recombinant 3D7-strain AMA1 protein was performed as previously described (Biswas, Dicks et al. 2011).

Human total IgG ELISA was performed using a previously validated method, referenced to concentration of an affinity-purified polyclonal human anti-PfAMA1 sample (Miura, Orcutt et al.

2008), using post-vaccination samples from clinical trials of PfAMA1 vaccines, as described above (Duncan, Sheehy et al. 2011; Sheehy, Duncan et al. 2012).

4.3.3. Surface plasmon resonance

CFCA was performed using a Biacore T100 instrument, a Biotin CAP chip, and T100 version 2 control and evaluation software (all from GE Life Sciences, Amersham, UK). Running buffer comprising HBS, 3mM EDTA, and 0.05% Tween-20 ('HBS-EP+'), was prepared and adjusted to pH 7.4, followed by the addition of 1 mg/mL salmon DNA (Sigma) and 2 mg/mL carboxymethyl-dextran (Sigma). The biotin-CAP reagent supplied with the CAP chip was diluted six-fold in HBS-EP+. All experiments were conducted at an analysis temperature of 37°C.

The measured diffusion coefficient of IgG at 20°C in a solution with the viscosity of water, pH 7.4, is 3.9×10^{-11} m^2/s(Jossang, Feder et al. 1988; Pol, Karlsson et al. 2007). The viscosity of the DNA- and dextran-containing buffer at 37°C was 0.754×10^{-3} Pa.s (measured using a TA AR-G2 rheometer [Texas Instruments]). The diffusion coefficient of IgG under given test conditions (D_{test}) can be calculated from that under reference conditions (D_{ref}), given the temperature and viscosity of the test buffer, using the following formula, where T indicates temperature in Kelvin and η indicates dynamic viscosity:

$$D_{test} = D_{ref}\ x\ \frac{T_{test}}{T_{ref}}\ x\ \frac{\eta_{test}}{\eta_{ref}}$$

The diffusion coefficient of IgG under the test conditions (T=310K, η=0.754Pa.s) was therefore calculated to be 5.5×10^{-11} m^2/s. A molecular weight of 150 kDa for IgG was used in the binding model.

Mass-transport limited binding conditions were obtained by capturing a minimum of 800 response units (RU) of antigen. Antigen-specific antibody binding was measured by double reference

subtraction, firstly of the binding of the test sample to a flow cell coated only with the biotin capture reagent, and secondly of the binding of a negative control sample. For monoclonal antibody samples, the control sample was running buffer; for polyclonal samples, the control sample was serum from an unimmunised human, mouse or rabbit, diluted as for the test sample in running buffer.

Initial rates of antigen-specific binding at 5 µL/min and 100 µL/min were measured and compared to permit measurement of concentration and the level of mass-transport limitation (necessary for accuracy of the assay). The chip was regenerated with the manufacturer's supplied regeneration and CAP reagents and fresh antigen prior to each application of antibody; variation in the level of antigen capture between cycles was typically <2%. Unless otherwise stated, all results reported were within the instrument manufacturer's recommended quality control parameters, namely initial binding rates in the range 0.3 RU to 15 RU/second at 5 µL/min flow, and quality control (QC) ratio>0.13.

QC ratios are calculated by the Biacore evaluation software from the measured binding rates at high and low flow rates using the following equation.

$$QC\ ratio = \frac{\sqrt[3]{\frac{1}{flow\ rate\ ratio}}\ x\ (binding\ rate\ ratio - 1)}{1 - \sqrt[3]{\frac{1}{flow\ rate\ ratio}}}$$

Where flow rate ratio = high flow rate / low flow rate = 100/5 = 20
And binding rate ratio = initial binding rate at high flow rate / initial binding rate at low flow rate.

Under completely mass-transport limited conditions, binding rate is proportionate to the cube root of flow rate, resulting in the numerator of the above fraction equalling the denominator, and QC ratio = 1. Under conditions without any mass-transport limitation, binding rate ratio will be 1, resulting in the numerator equalling zero, and hence QC ratio = 0.

4.4. RESULTS

4.4.1. Relationship of CFCA and spectrometric measurements of mAb concentration

To initially validate the CFCA approach using the biotin CAP chip, CFCA measurements were made upon dilution series of three mAbs against the malaria antigen PfRH5. These mAbs recognise different (although overlapping) epitopes, with similar affinities, in the range 2-8x10^9 M^{-1} (Chapter 6).

Figure 4.4.1.1 depicts the observed relationship between CFCA and spectrometrically-determined concentration. A close linear correlation was apparent over the tested range (Pearson r^2>0.99 for all three mAbs; tested range 0.5-4µg/mL for two mAbs, and 0.125 to 16µg/mL for the third). CFCA-measured concentrations were between 50% and 80% of the spectrometer-measured concentrations. Experiments at mAb concentrations above 2µg/mL resulted in QC ratios of less than 0.13, indicating insufficient mass transport limitation for reliable CFCA, although as shown, the results obtained correlated closely with A_{280} measured concentrations.

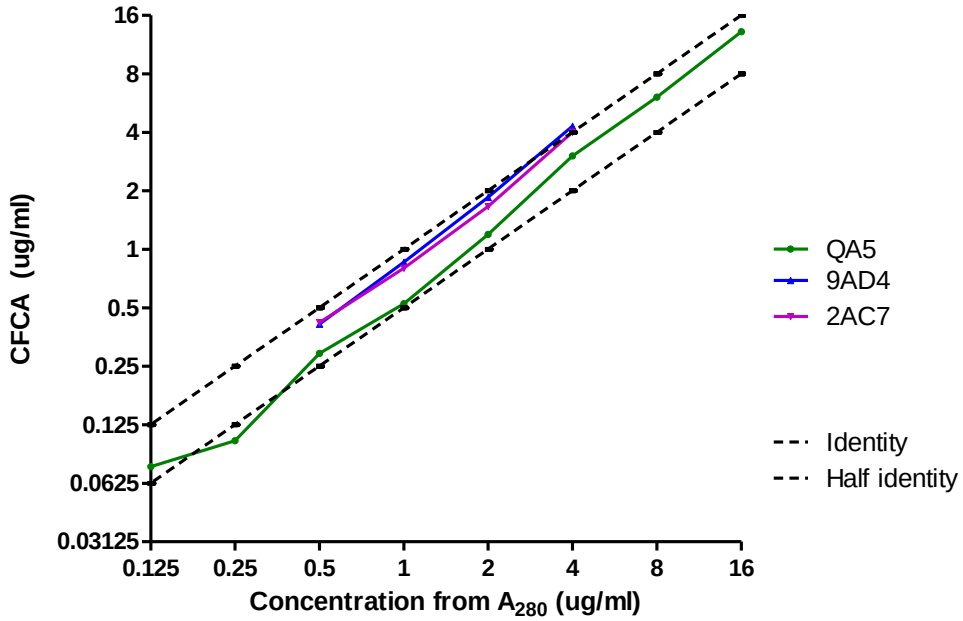

Figure 4.4.1.1 CFCA measurements of concentrations of PfRH5-specific mAb concentrations
Upper dashed line indicates results expected if CFCA results were identical to A_{280}-measured conconcentrations*; lower dashed line indicates CFCA results half the A_{280}-measured concentrations.*

4.4.2. Relationship of CFCA measurements to polyclonal antibody concentrations measured by ELISA

To assess the ability of CFCA to measure antigen-specific antibody concentrations in polyclonal sera, a set of sera from two clinical trials of the malaria vaccine antigen PfAMA1 were studied (Duncan, Sheehy et al. 2011; Sheehy, Duncan et al. 2012). The availability of an affinity-purified antigen-specific anti-PfAMA1 human antibody standard and calibrated ELISA method permitted comparison of the CFCA method to the accepted gold-standard ELISA method.

Figure 4.4.2.1 illustrates the double-referencing procedure used to measure antigen-specific binding, and depicts the effect of partial mass-transport limitation, manifest as more rapid binding under high-flow conditions.

Figure 4.4.2.2 illustrates the observed relationship between CFCA and ELISA measurements: the latter measurements were made using a standardised ELISA, referenced to a purified PfAMA1-specific IgG calibration standard (Miura, Orcutt et al. 2008). Overall, the correlation was close (Pearson r^2=0.96), although the CFCA approach produced concentration estimates around half those from the standardised ELISA.

To further assess the relationship between CFCA and ELISA measurements, results obtained using the two methods with a set of sera from PfAMA1-vaccinated mice were compared (Figure 4.4.2.3); again, the correlation between the two measurements was close (Pearson r^2=0.80).

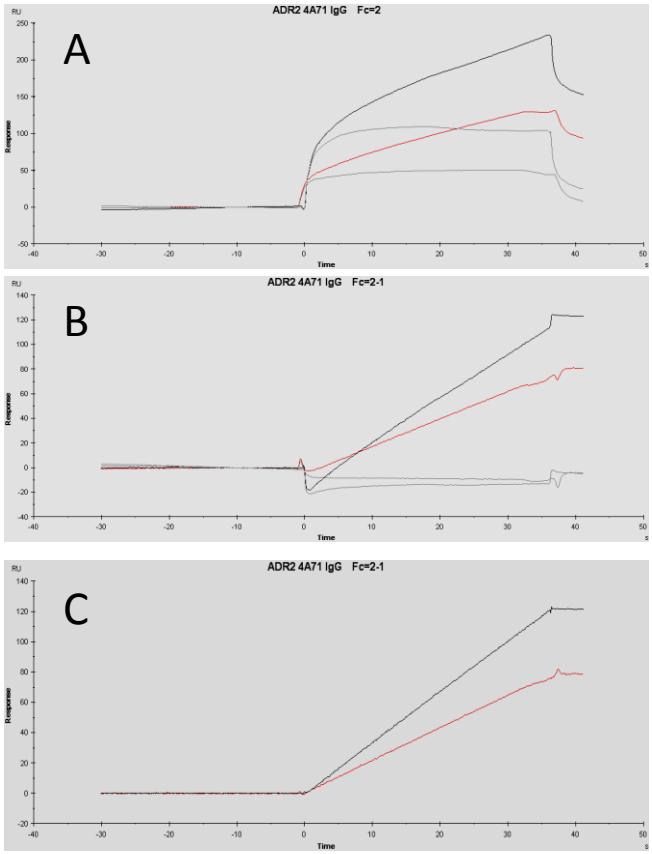

Figure 4.4.2.1 Example of CFCA data processing

CFCA was performed using a sample of Protein G purified polyclonal IgG from an RH5-immunized rabbit. In each panel, the green line represents responses with test sample at flow-rate of 100µL/min, the red line represents responses with test sample at 5µL/min, while grey lines represent equivalent responses with blank samples (IgG from non-immunised rabbits). The x-axis represents time (spanning total of 80 seconds, of which period of sample injection=35 seconds).

Panel A: Responses on PfRH5-coated flow cell

Panel B: Responses after subtraction of non-PfRH5-coated reference cell.

Panel C: Test sample responses after subtraction of blank-sample responses. It can be seen that this early phase of the antibody-binding reaction proceeds at a linear rate. The accelerated rate of the reaction under high-flow conditions indicates that the reaction is partially mass transport limited under slow-flow conditions, permitting accurate extrapolation to rate of reaction under absolute mass transport limitation, and hence to concentration.

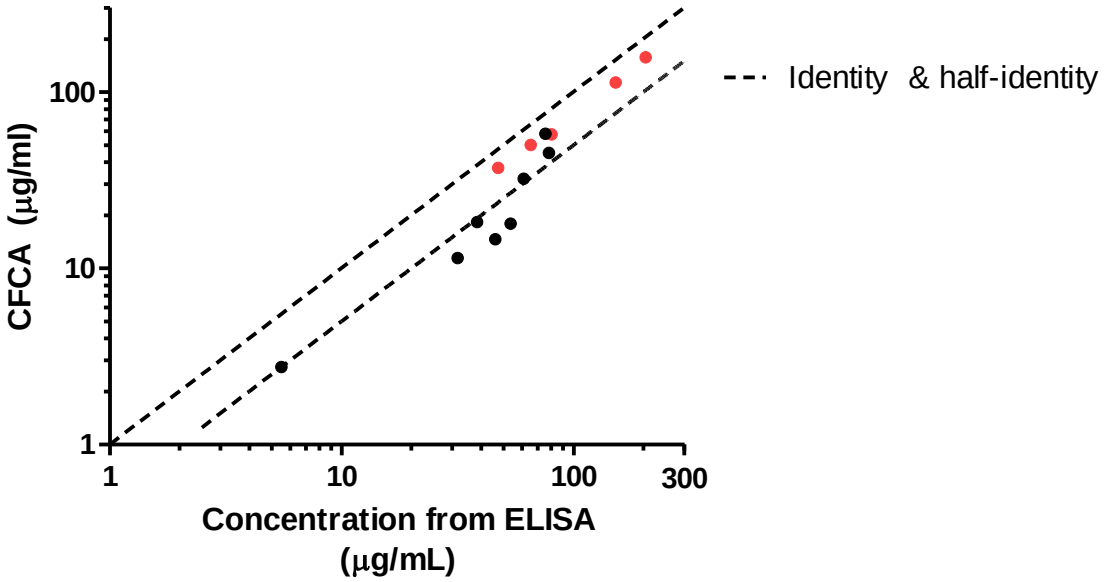

Figure 4.4.2.2 Relationship of CFCA and ELISA measurements of polyclonal antibody concentrations

Human anti-PfAMA1 responses were measured by CFCA and using an ELISA standard curve calibrated by affinity-purified antigen-specific IgG. ELISA responses are the mean from three replicate wells. A single CFCA measurement was made for each sample. Black points indicate results obtained with serum samples from one clinical trial; red points indicate results obtained with plasma samples from a second clinical trial. The initial binding rate of the sample with the lowest concentration (0.17 RU/s) was marginal for reliable CFCA.

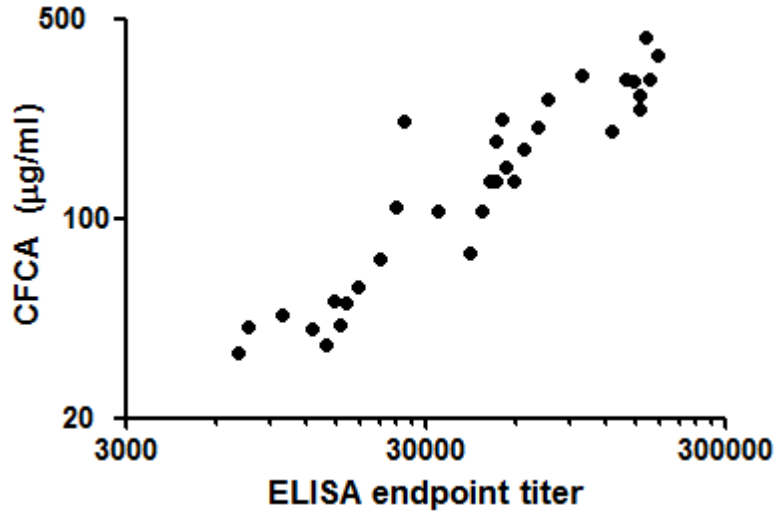

Figure 4.4.2.3 Relationship of CFCA measurements of polyclonal antibody concentration to dilution-series endpoint ELISA titre.

Mouse anti-PfAMA1 responses were measured by both methods, using samples from 12 mice each tested at three dilutions. ELISA responses are mean from two replicate wells. A single CFCA measurement was made for each sample.

4.4.3. Independence of CFCA measurements from antigen capture level

CFCA depends upon the ability to deconvolute the contribution of concentration to the antigen-antibody binding rate from the contribution of other factors, including the density of ligand on the chip surface. To verify that the measured antigen-specific antibody concentrations were indeed independent of ligand density, serial CFCA measurements were performed upon a single sample (total IgG from a PfAMA1-vaccinated rabbit) using a wide range of ligand capture levels (63 - 2600RU).

As shown in figure 4.4.3.1, initial binding rates (at low and high flow rates) increased as capture level increased, indicating that binding was limited to some extent by ligand capture level as well as mass transport. However as the capture level increased, the difference between binding rates at low and high flow rates also increased, resulting in an increasing QC ratio. The QC ratio exceeded the manufacturer's recommended minimum (0.13) for all capture levels above 130RU. Despite the steadily increasing rates of binding as the capture level increased from 130 to 2600RU, the CFCA-calculated concentration was similar across this range (median 261µg/mL, range 230 – 264). Discrepancies of this magnitude are unlikely to be problematic in the field of vaccinology.

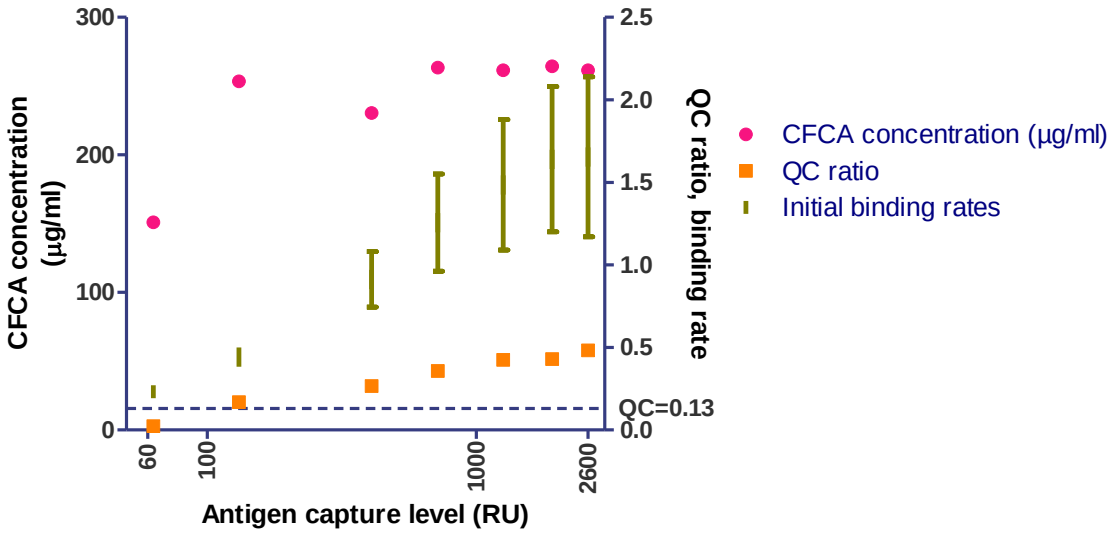

Figure 4.4.3.1 Effect of varying antigen capture level upon CFCA results

See text for interpretation. The same test and blank samples (rabbit serum from PfAMA1-immunised and irrelevant-antigen immunised animals respectively) were applied to chip surfaces with varying levels of captured PfAMA1. The top and bottom of the olive-coloured bars indicate the measured initial binding rate at high and low flow rate respectively (plotted on right-axis in RU/second); the "QC ratios" derived from this are plotted as orange points (right y-axis, no units). CFCA concentration measurements are plotted as pink points (left y-axis).

4.5. DISCUSSION

The key finding of this work has been that results obtained by CFCA correlate closely with the concentrations of polyclonal antigen-specific antibody measured by a carefully-validated ELISA. The same method can readily be applied to antibodies of different species and mAbs.

A tendency was observed for the CFCA measurements of antibody concentration to underestimate the concentrations of mAbs (relative to A_{280}-based quantification), and polyclonal antigen-specific antibody (relative to the standardised ELISA). In both cases, the discrepancy may have arisen from errors in either the CFCA, or in the comparator method: the mAb preparations may have contained some inactive protein, as may the standard used to calibrate the ELISA. Nonetheless, the magnitude of the discrepancy (around 50%) was small relative to the true variability in samples.

One possible source of such an error in the CFCA measurement could be the factor used to convert Biacore RUs into mass of analyte bound to the surface: this relationship varies with distance between the chip surface and the bound molecule, and could conceivably differ between the CM5 chip (for which it has been validated, and on which the antigen would be covalently bound to the chip-surface dextran matrix) and the CAP chip, on which the antigen is separated from the chip surface by a DNA oligomer and streptavidin.

Further potential sources of error arise from heterogeneity of isotypes and binding kinetics among the polyclonal antibody population. Firstly, if a substantial proportion of the measured binding was due to antigen-specific IgM, this could confound measurements, because of the differing molecular weights and diffusion coefficients of IgM and IgG. This was not, however, the case here. All samples were taken after prime-boost immunisation (i.e. not during the primary immune response to the antigen). Additionally, isotype-specific secondary antibodies were used to further confirm the absence of IgM in selected mouse and human samples: there was no detectable binding of an anti-IgM antibody to the antigen-specific antibody, whereas an anti-IgG antibody 'enhanced' the binding response as expected) (data not shown).

Heterogeneity of binding kinetics, however, is inevitable among polyclonal antibody. The estimation of concentration by CFCA involves fitting of a 1:1 binding model with a single association rate term. Such a model does not take account of either heterogeneous association rates or bivalent binding of antibody to the chip. Due to heterogeneity of association rates, the CFCA-measured concentration of antigen-specific antibody will, by necessity, be an estimate based upon the average association rate in the sample. Although imperfect, this is an advance upon ELISA-based methods which assume equal avidity in the calibration standard and the test sample.

The valency of binding is unlikely to be a significant factor here, because the slope of the early phase of the binding curve is determined largely by concentration and the monovalent association rate: progression from univalent to bivalent binding does not in itself affect the SPR signal, and is therefore relevant only to the likelihood of subsequent dissociation – a factor which is negligible at this stage, as discussed above.

Satisfactory results were obtained over a concentration range from 0.1 µg/mL to 16µg/mL with mAb samples, and from 0.05 µg/mL to 1 µg/mL with polyclonal antibody samples. Serum was routinely used at a 1:250 dilution; non-specific binding became problematic with serum less dilute than 1:100, despite the addition of dextran and DNA to the buffer. Non-specific binding of serum proteins to the CAP chip is known to be particularly problematic (manufacturer's documentation). This imposed a lower limit of sensitivity of around 5µg/mL serum antibody concentration – however it may well be possible to improve substantially upon this by capturing higher levels of ligand, using an alternative ligand capture technique less vulnerable to non-specific binding, or using purified IgG rather than serum to reduce non-specific binding.

The CAP chip has the advantage that it permits straightforward, repeated, reproducible and stable regeneration of the surface with fresh antigen prior to each sample application. This avoids any uncertainty regarding destruction of conformational antibody epitopes by the regeneration solution (glycine HCl pH <3 is typically used to dissociate antigen-antibody interactions). The combination of

the CAP chip with enzymatically mono-biotinylated antigen permits the measurement of antigen-specific antibody concentrations without requiring any purified recombinant protein: in this case, the antisera were raised using viral vector vaccines, and raw supernatant containing biotinylated antigen was used as the ligand.

Sample consumption by the technique is minimal (1µL serum per measurement at 1:250 dilution). Availability of a Biacore machine with the most recent software is clearly a pre-requisite with substantial capital cost (although technically adept users may be able to perform measurements using older machines and fit a binding model using other software, as described(Christensen 1997)). Costs per day of Biacore instrument usage in Oxford range from USD150 to USD400; consumables costs are c. $2 per sample (the CAP chip can be extensively re-used – effectively limited only by the quantity of supplied CAP reagent). An advantage of SPR is the automation of the instrument, which requires no user input after loading of samples. Optimisation of the throughput of the CFCA method described here has not yet been attempted. The critical measurements take c. 1 minute per sample; the speed of this method is limited largely by the time taken to capture antigen from a dilute supernatant prior to every sample application. An optimised protocol using purified, high-concentration antigen could analyse 5 to 10 samples per hour.

Further development of SPR-based methods for vaccine-induced antibody characterisation is likely to prove rewarding. As well as concentration, SPR can be used to identify the IgG subclasses contributing to an antigen-specific response (Swanson, Ferbas et al. 2004), and could readily be developed to measure the absolute proportion of a response contributed by each subclass. Moreover, SPR-based methods of antibody affinity/avidity analysis could have substantial advantages over currently used assays. So-called 'avidity ELISA' (for example sodium thiocyanate displacement techniques) typically assesses antibody dissociation only, occurring under highly non-physiological conditions, producing only relative measurements in uninformative units. Recent reports of vaccine-induced antibody affinity measurement by SPR have used high-ligand-density

surfaces on which affinity measurements are likely to be highly influenced by bivalent binding, and have either investigated only dissociation rate (Reddy, Anders et al. 2012), or have used an index based upon total binding and dissociation which would be expected to be strongly associated with antibody concentration (Kasturi, Skountzou et al. 2011; Haynes, Gilbert et al. 2012). The determination of absolute concentration by CFCA on the other hand, permits subsequent measurement of both association and dissociation rates of polyclonal antibodies (Pol, Karlsson et al. 2007), either within the same experiment, or potentially using a low-ligand-density chip surface to minimise the effect of bivalent binding.

Overall, the results presented here suggest that CFCA has the potential to make a useful addition to ELISA in monitoring vaccine-induced antigen-specific antibody concentrations. It is unlikely to supplant ELISA for routine measurements of antibody levels in one sample relative to another. However it is likely to permit reasonably accurate measurements of absolute antibody concentration in polyclonal serum, in cases where affinity-purified antigen-specific antibody standards are unavailable. More frequent reporting of absolute antibody concentration is likely to assist comparisons between laboratories, antigens and species which is simply impossible at present using data reported as ELISA titres: of course, accurate inter-study comparison will still require standardisation of the antigen used for CFCA, and, to some extent, the protocol.

The work reported in this chapter enabled the use of CFCA to elucidate the relationship between anti-PfRH5 antibody concentration and parasite neutralisation, and comparison of the relationship to that with anti-PfAMA1 antibodies. This quantitative comparison will be described in the following chapter.

5. Enhancing blockade of *Plasmodium falciparum* erythrocyte invasion

Assessing combinations of vaccine-induced antibodies against RH5 and other merozoite antigens

5.1. AUTHORSHIP STATEMENT

ADD conceived all experiments reported in this chapter, performed all surface plasmon resonance assays, and developed the strategy and analysis used to assess the possibility of synergy between antibodies in GIA.

GIA was performed by Andrew Williams, Joe Illingworth, Prateek Choudhary, and Linda Murungi in Oxford, and Ababacar Diouf, Kazutoyo Miura and Carole Long at NIH, USA.

RH5 protein was provided by Gavin Wright and Cécile Crosnier.

This chapter is based upon a manuscript which is currently in press at *PLoS Pathogens.* This was co-written by ADD, Andrew Williams and Simon Draper, and on which ADD and AW are co-first authors.

5.2. INTRODUCTION

Despite the promise shown in pre-clinical studies by vaccines encoding full-length RH5 alone, (Douglas, Williams et al. 2011) it remains essential to continue optimizing pre-clinical, next-generation vaccine candidates. One strategy is to assess multi-antigen vaccines for their potential to induce antibodies that act synergistically, in order to achieve higher levels of parasite neutralization for any given level of vaccine-induced antibody. Several studies have investigated the effects of mixing antibodies against multiple merozoite antigens on parasite neutralization. For example, co-immunizing rabbits with EBA175, RH2 and RH4 elicits an antibody repertoire that is more potent in inhibiting parasite growth than antibodies elicited by any single one of these antigens. (Lopaticki, Maier et al. 2011) It has also been reported that antibodies against GPI-anchored micronemal protein (GAMA) and EBA175 additively inhibit parasite growth, while antibodies against GAMA and AMA1 did not produce additive effects (Arumugam, Takeo et al. 2011). Some degree of synergy has been reported between antibodies against RH5 and EBA175 (Region II), but only at low antibody

concentrations (Ord, Rodriguez et al. 2012). Furthermore, antibodies against *P. falciparum* RH5 interacting protein (Ripr), which forms a complex with RH5, inhibit the growth of multiple *P. falciparum* lines additively when combined with antibodies against EBA175, RH2 and RH4 (Chen, Lopaticki et al. 2011). However, none of these studies quantitatively assessed the interactions between antibody specificities in a manner that distinguishes additive from synergistic effects.

Given the inherent difficulties in including more than one antigen in a vaccine (Saul and Fay 2007), a careful and rational assessment of potential combinations is required. Here, parasite neutralization by purified IgG against RH5 in combination with IgG against seven other merozoite antigens was investigated and synergistic antibody interactions were identified. It was also shown that antibodies against full-length RH5 are highly effective in neutralizing short-term-adapted parasite isolates from Cambodian patients with malaria, as well as laboratory-adapted parasite lines (Douglas, Williams et al. 2011). Furthermore, antibodies against RH5 are more potent than those against the leading blood-stage vaccine candidate AMA1, as indicated by a lower concentration of antigen-specific IgG required to give 50% GIA (EC_{50}). These results demonstrate that RH5 plays a critical role in erythrocyte invasion by parasite isolates from a malaria-endemic region, and provide additional evidence for RH5 as a leading blood-stage vaccine candidate.

5.3. METHODS

5.3.1. Vaccine constructs, animals and immunization regimes

Vaccines, rabbit immunization and sampling regimes were as described in Section 2.1.

5.3.2. Parasite culture and growth inhibitory activity (GIA) assays

Parasite culture and GIA methods were generally as described in Section 2.4.

GIA assays involving short-term-adapted *P. falciparum* isolates were conducted at the PATH Malaria Vaccine Initiative (MVI) GIA Reference Center as previously described (Miura, Zhou et al. 2009), using Protein G-purified total IgG from the serum of five rabbits immunized with full-length RH5 vaccines and five rabbits immunized with bivalent (3D7 + FVO) AMA1 vaccines (Douglas, Williams et al. 2011). Cryopreserved stocks of parasite isolates obtained directly from Cambodian patients with uncomplicated malaria in 2009 were adapted to *in vitro* culture for up to 12 weeks. Sequencing and genotyping of RH5 in the Cambodian parasite isolates was as previously described (Manske, Miotto et al. 2012). Cambodian parasite isolates were obtained under a study protocol approved by the Cambodian National Ethics Committee for Health Research and the NIAID Institutional Review Board (ClinicalTrials.gov identifier: NCT00341003).

Where EC_{50} was measured for individual rabbit IgG samples, the concentration of IgG required to give 50% GIA (EC_{50}) was estimated by interpolation on the plot of $\log_{10}$[total IgG] versus % GIA with the measured points connected by straight lines (or extrapolation from the adjacent line segment, in the case of samples for which the EC_{50} value lay outside of the tested IgG concentration range). Very similar results were obtained using non-linear least squares regression, fitting variable slope dose-response curves using the equation %GIA=100/(1+10^(($\log_{10}EC_{50}$-$\log_{10}$[IgG])*HillSlope)) (Prism v5.03, GraphPad Software) although the quantity of data for each rabbit IgG sample was not sufficient for reliable curve-fitting (data not shown). Where a single estimate of antigen-specific EC_{50} was calculated for a *P. falciparum* sample by combining data obtained from multiple rabbit IgG samples, a dose-response curve was fitted to all available data by non-linear least squares regression, as above.

5.3.3. Antigen-specific antibody EC_{50} estimation

The principle and method of calibration-free concentration analysis (CFCA) of antigen-specific antibody by surface plasmon resonance (SPR) has been described previously (Sections 4.2 and 4.3.3). RH5 and AMA1 proteins (enzymatically mono-biotinylated at the C-terminus) were produced by transient transfection of HEK293E cells, as previously described (Bushell, Sollner et al. 2008), and extensively dialysed against PBS to remove free biotin. Purified rabbit IgG samples from five RH5-vaccinated rabbits and five AMA1-vaccinated rabbits were prepared as above.

IgG samples were diluted 20-fold in parasite culture medium, and the total protein concentration measured by spectrometry (Nanodrop, Thermo Scientific). These samples were further diluted 100-fold in running buffer (section 4.3.3), resulting in final total IgG concentrations in the range 12-25 µg/mL in the samples used for CFCA.

Mass-transport limited binding conditions were obtained by capturing a minimum of 800 response units (RU) of antigen. Antigen-specific antibody binding was measured by double reference subtraction, firstly of the binding of antigen-specific antibody to a flow cell coated only with the biotin capture reagent, and secondly of the binding of an equivalent concentration of total IgG from a rabbit immunized with viral vectors lacking a *Plasmodium* antigen. Initial rates of antigen-specific binding at 5 µL/min and 100 µL/min were measured and compared to permit measurement of concentration and the level of mass-transport limitation (necessary for accuracy of the assay). The chip was regenerated with the manufacturer's supplied regeneration and CAP reagents and fresh antigen prior to each application of antibody; variation in the level of antigen capture between cycles was typically <2%. All results reported were within the instrument manufacturer's recommended quality control parameters, namely initial binding rates in the range 0.3 RU to 15 RU/second at 5 µL/min flow, and QC ratio>0.13 (reflecting adequate mass transport limitation for concentration estimation).

The same samples were assayed for GIA against the 3D7 parasite clone, and with the exception of one AMA1-vaccinated rabbit, were from the same sera used for GIA assays involving short-term-

adapted parasite isolates. CFCA data were used to calculate antigen-specific antibody concentrations in the Protein G purified total IgG samples used in GIA assays. By combining this with the GIA EC_{50} in terms of total IgG measured as above, the GIA EC_{50} in terms of antigen-specific antibody was calculated.

5.3.4. Assessment of synergy

Synergy between two agents is defined as an effect greater than would be predicted from the two agents, when mixed, acting independently of each other to produce an additive effect (Greco, Bravo et al. 1995). An effect less than that predicted from two agents acting independently may be termed antagonism, although it may be worth drawing a distinction between a sub-additive combination (in which the effect remains at least as strong as that of the more potent individual component) and a truly antagonistic combination in which the two agents together actually perform worse than the more potent of the agents would have performed alone. Although conceptually relatively straightforward, there is a degree of controversy regarding these definitions, stemming primarily from disagreement regarding the appropriate method of calculation of the expected additive effect of two agents. As has been reviewed elsewhere, there are multiple differing definitions of pharmacological additivity: this work employs two such definitions, each of which have properties which render them useful in some contexts (Greco, Bravo et al. 1995).

Bliss' definition of independent action (henceforth referred to as 'Bliss additivity') is related to probability theory (Bliss 1939). In the context of neutralization of a population of merozoites which would otherwise have invaded erythrocytes, suppose two antisera (A+B) each individually have a probability of neutralizing a given merozoite, and then define the probability of *successful* invasion in the presence of A as $P(Inv_A)$, or in the presence of B as $P(Inv_B)$. If A + B are Bliss additive, the probability of *successful* invasion in the presence of a mixture of *both* A *and* B, $P(Inv_{A+B})$ will be the same as that of the occurrence of *both* of two independent events: $P(Inv_{A+B}) = P(Inv_A \cap Inv_B) = P(Inv_A).P(Inv_B)$.

Malaria vaccinologists conventionally express neutralization in terms of percentage GIA = (1-probability of *successful* invasion)*100, hence $P(Inv_A)=1-\frac{GIA_A}{100}$. Rearranging gives rise to the following equation for Bliss additivity in GIA :

$$GIA_{[A+B]\ Bliss} = \left[1-\left(1-\frac{GIA_A}{100}\right)*\left(1-\frac{GIA_B}{100}\right)\right]*100 \qquad \text{(Equation 1)}$$

I developed, with Andrew Williams and Joe Illingworth, an assay to screen combinations of anti-RH5 IgG ('antibody A') and IgG against each of seven other antigens ('antibody B') for synergistic activity. In this screening assay, the GIA effect of a range of concentrations of antibodies against antigen B was measured with and without the addition of a fixed concentration of anti-RH5 IgG. The observed effect $GIA_{[RH5\ +\ B]\ Obs}$ was compared to the expected effect $GIA_{[RH5+B]\ Bliss}$. Statistically significant deviations between the observed and predicted values indicated non-independence, either synergy (greater GIA effect than the predicted value) or sub-additivity (weaker effect than the predicted value).

Bliss' definition of additivity has the advantage that a prediction of an additive effect only requires knowledge of the level of effect of each individual constituent of a mixture. Although appealingly simple to apply, this does not account for the fact that the shapes of different agents' concentration *vs.* effect curves differ: an agent with a rapidly steepening concentration *vs.* effect curve is said to be positively co-operative. Mixtures of such an agent *with itself* may thus appear to be synergistic according to Bliss' definition (in different circumstances, a misleading apparent antagonistic effect could also arise).

A more complex but more robust definition of additive action, avoiding this problem, is that of Loewe additivity (Greco, Bravo et al. 1995). When an experiment is conducted with an appropriate selection of mixtures of concentrations of agents A and B, it is possible to plot a three-dimensional plot (or contour plot) of [A] versus [B] versus effect. From these 3-dimensional data, a two

dimensional plot on axes of [A] and [B] can be constructed in which a line links points (A,B) at which the mixture [A]+[B] results in the same level of effect (an 'isobologram').

GIA assays were performed with two combinations of antibody (anti-RH5 with either anti-RH4 or AMA1 IgG), using all possible combinations of six concentrations of both antibodies. From these data, three-dimensional contour plots and two-dimensional isobolograms were constructed for anti-RH5 IgG combined with either anti-RH4 or anti-AMA1 IgG. For anti-RH4 alone, the concentration of IgG used in these experiments was insufficient to give 50% GIA. A concentration of 10 mg/mL, which had previously been shown to give 50% GIA using the same purified IgG (Douglas, Williams et al. 2011), was therefore assumed as the EC_{50} value for anti-RH4 IgG.

The axes of such a plot can be labelled either with simple concentrations, or with concentration of each agent as proportion of its EC_{50} (i.e. $\frac{[A]}{EC_{50,A}}$).

Loewe's definition of additivity states that, for such a plot:

$$1 = \frac{[A]}{EC_{50,A}} + \frac{[B]}{EC_{50,B}} \qquad \text{(Equation 2)}$$

In other words, if agents A + B are Loewe additive, a 50% effect will be achieved by a mixture of any percentage of the EC_{50} of A and any percentage of the EC_{50} of B, such that the two percentages sum to 100%. On the isobologram plot, such a combination would result in a straight line between $x=EC_{50,A}$ and $y=EC_{50,B}$. Mixtures which achieve synergistic effects will require lower concentrations to achieve 50% effect, resulting in a concave isobologram.

This approach has the additional benefit of permitting quantification of the strength of synergistic (or antagonistic) action between two agents. Hewlett's synergy index, S (Greco, Bravo et al. 1995) measures the degree of concavity of the isobologram, with the magnitude of S above 1 implying the level of synergy:

$$S = ON/OM \qquad \text{(Equation 3)}$$

where, ON = distance from origin to intersection of the Loewe additivity line and the x=y line, and OM = distance from origin to intersection of 50% isobologram and the x=y line.

5.3.5. Statistical analysis

Differences in EC_{50} values between anti-RH5 and anti-AMA1 IgG were determined by Mann-Whitney U test. Where EC_{50} values were estimated by regression, differences in EC_{50} and the slope of the curve were simultaneously assessed by extra sum-of-squares F-test. Differences between the observed GIA for each combination of antibodies and the predicted GIA based on Bliss independence were determined by repeated measures two-way ANOVA with Bonferroni post-hoc testing. *P* values of <0.05 were considered statistically significant. All analyses were conducted using GraphPad Prism version 5.03 for Windows (GraphPad Software Inc., USA).

5.4. RESULTS

5.4.1. Quantification of EC_{50} of antigen-specific IgG in GIA assays

GIA is routinely assessed with total IgG purified from immunized animals, only a small fraction of which is specific for the immunogen. To quantify the antigen-specific antibody EC_{50} values of both anti-RH5 and anti-AMA1 rabbit IgG, an SPR-based assay using the Calibration Free Concentration Analysis (CFCA) technique was applied. This calculates concentrations of reagents in a solution based upon the kinetics of a binding reaction. It had previously been established that results obtained with this method correlate closely with measurements of antibody concentrations obtained using a standardized ELISA (Miura, Orcutt et al. 2008), and with spectrometer-determined concentrations of a range of anti-RH5 mouse mAbs (see chapter 4).

Antigen-specific antibody concentrations were measured by CFCA in total IgG samples purified from each of ten rabbits, five vaccinated with RH5 and five with AMA1 (Figures 5.4.1.1A). The EC_{50} of antigen-specific antibody from each rabbit in GIA assays conducted with total IgG against the 3D7 *P. falciparum* clone was then independently determined (Figure 5.4.1.1B-D). The median antigen-specific EC_{50} was found to be 88 µg/mL for AMA1 (range 56-124 µg/mL, 95% CI for mean 59-121 µg/mL). This GIA EC_{50} value is close to that previously reported for 3D7 AMA1-specific rabbit

antibody (70 μg/mL [95% CI for mean 50-100 μg/mL], obtained using affinity-purified anti-AMA1 antibody (Miura, Zhou et al. 2009)), further supporting the validity of the CFCA method. The median antigen-specific antibody EC_{50} for RH5 was found to be 50 μg/mL (range 44-90 μg/mL, 95% CI for mean 32-81 μg/mL), around 40% lower than that observed for AMA1, although this did not reach statistical significance (Figure 5.4.1.1D, $P = 0.055$, Mann-Whitney U test).

A second estimate of the antigen-specific antibody EC_{50} for each antigen against the 3D7 parasite clone was obtained by pooling data from all five rabbits and fitting a dose-response curve by non-linear least squares regression (Figure 5.4.1.1E). As expected, these results were similar to those obtained from the individual samples' median EC_{50} values: 90 μg/mL (95% CI 78-105 μg/mL) for AMA1 and 40 μg/mL (95% CI 32-48 μg/mL) for RH5. This analysis shows significant differences in both the EC_{50} (lower with anti-RH5 IgG) and the slope of the curves (steeper with anti-AMA1 IgG) ($P<0.0001$ by extra sum-of-squares F-test). It thus appears that the antigen-specific rabbit antibody EC_{50} for anti-RH5 IgG is approximately half of that observed for anti-AMA1 IgG against the vaccine-homologous 3D7 parasite clone.

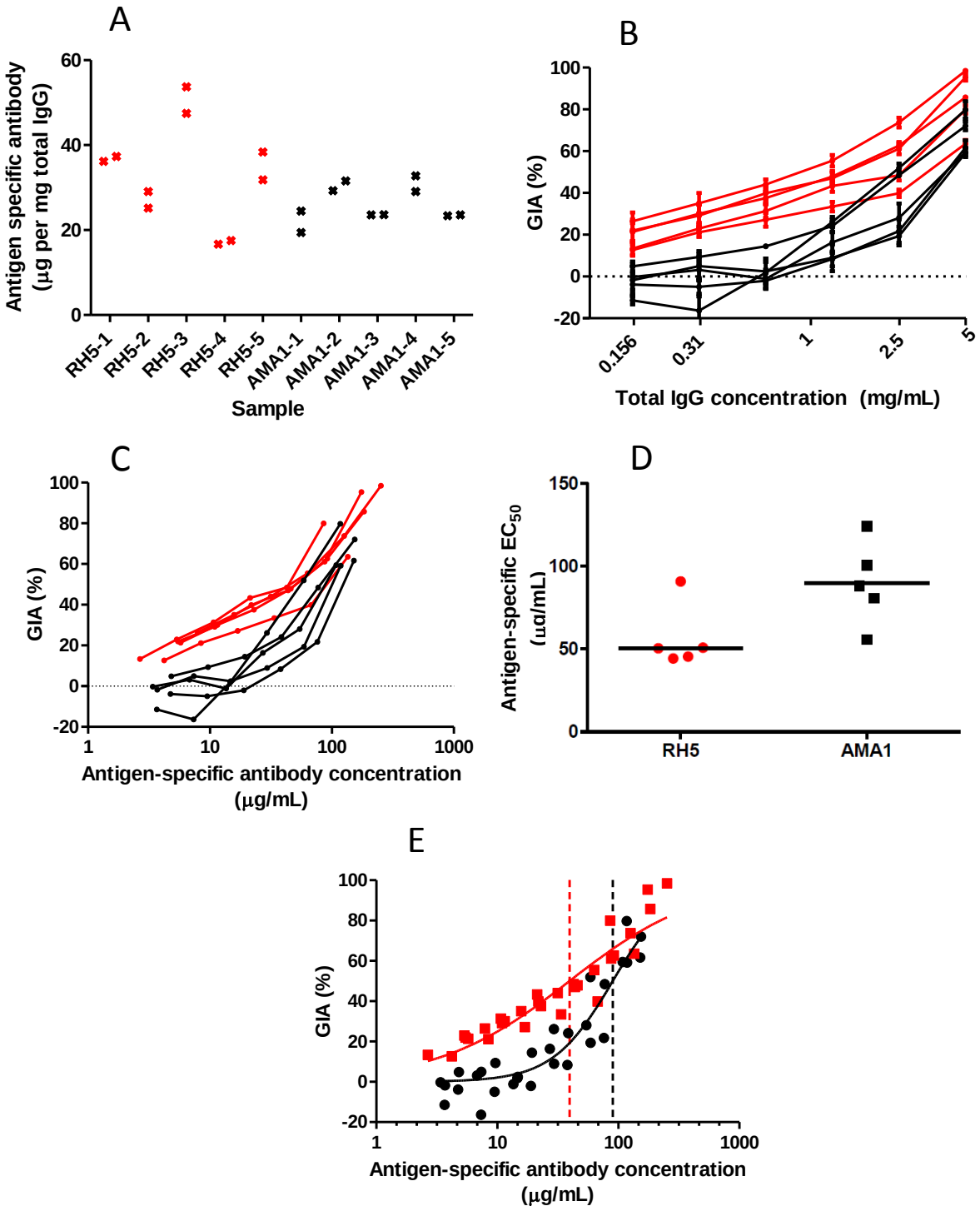

Figure 5.4.1.1: Measurement of EC_{50} of antigen-specific anti-RH5 and anti-AMA1 polyclonal rabbit antibodies

See following page for figure legend.

Figure 5.4.1.1: Measurement of EC_{50} of antigen-specific anti-RH5 and anti-AMA1 polyclonal rabbit antibodies (preceding page)

Panel A *- CFCA-measured antigen-specific antibody as a proportion of total IgG (measured by spectrometry) for each of ten rabbits. Individual points indicate mean of three measurements.*

Panel B *- GIA vs. total IgG concentration, with lines connecting data for each of five RH5-vaccinated rabbits (red) and five AMA1-vaccinated rabbits (black). Each point is the mean of three replicate wells in two independent experiments, i.e. n=6. Error bars indicate SEM.*

Panel C *- GIA (from the experiments depicted in panel **B**) vs. antigen-specific antibody concentration (calculated for each sample using the data in panel **A**), for each of five RH5-vaccinated rabbits (red) and five AMA1-vaccinated rabbits (black). Each point is the mean of triplicate wells in two independent experiments.*

Panel D *- antigen-specific antibody EC_{50} values for RH5 and AMA1, calculated by interpolation from the data in panel **C**. Individual data-points and the median are shown.*

Panel E *- Dose-response curve fitted to all GIA vs. antigen-specific antibody concentration data for the 3D7 parasite clone (multiple IgG dilutions for each of five rabbits for RH5 and AMA1). Dashed vertical lines indicate the fitted EC_{50} value for anti-RH5 (red) or anti-AMA1 (black) IgG. Each GIA value is the mean of triplicate wells in each of two experiments (n=6). Red indicates anti-RH5 samples; black indicates anti-AMA1 samples.*

5.4.2. Antibodies against RH5 are highly effective against *P. falciparum* isolates obtained from Cambodian patients with malaria

In order for RH5 to be a viable vaccine candidate antigen, anti-RH5 antibodies must be effective against naturally-circulating parasite isolates that cause malaria. To investigate this possibility, GIA assays were performed, using rabbit IgG generated in Oxford, by collaborators at the PATH-MVI funded international GIA reference laboratory at NIH, USA. These assays used five *P. falciparum* isolates that were obtained directly from Cambodian patients with malaria. 18-microsatellite analysis of these parasite isolates indicated that CP806, CP830, CP845 and CP887 were clonal (or clone-predominant) and that CP803 was multi-clonal (Rick Fairhurst, personal communication). IgG from rabbits immunized with RH5 was highly effective against all five parasite isolates (Figures 5.4.2.1 and 5.4.2.2A-E). Antigen-specific IgG EC_{50} values were estimated for anti-RH5 and anti-AMA1 IgG samples against each parasite isolate, as performed previously for the 3D7 parasite clone. For each parasite

isolate, these values were significantly lower for anti-RH5 than for anti-AMA1 IgG samples (Figure 5.4.2.1, figure 5.4.2.2F and Table 5.4.2.T1; *P*<0.05 by Mann-Whitney U test).

Sequencing of the RH5 gene in 18 laboratory-adapted parasite lines has previously shown a total of ten non-synonymous mutations (Hayton, Gaur et al. 2008). Polyclonal IgG against RH5 (3D7 clone) remained effective against parasite lines differing from 3D7 at each of these loci (Douglas, Williams et al. 2011).

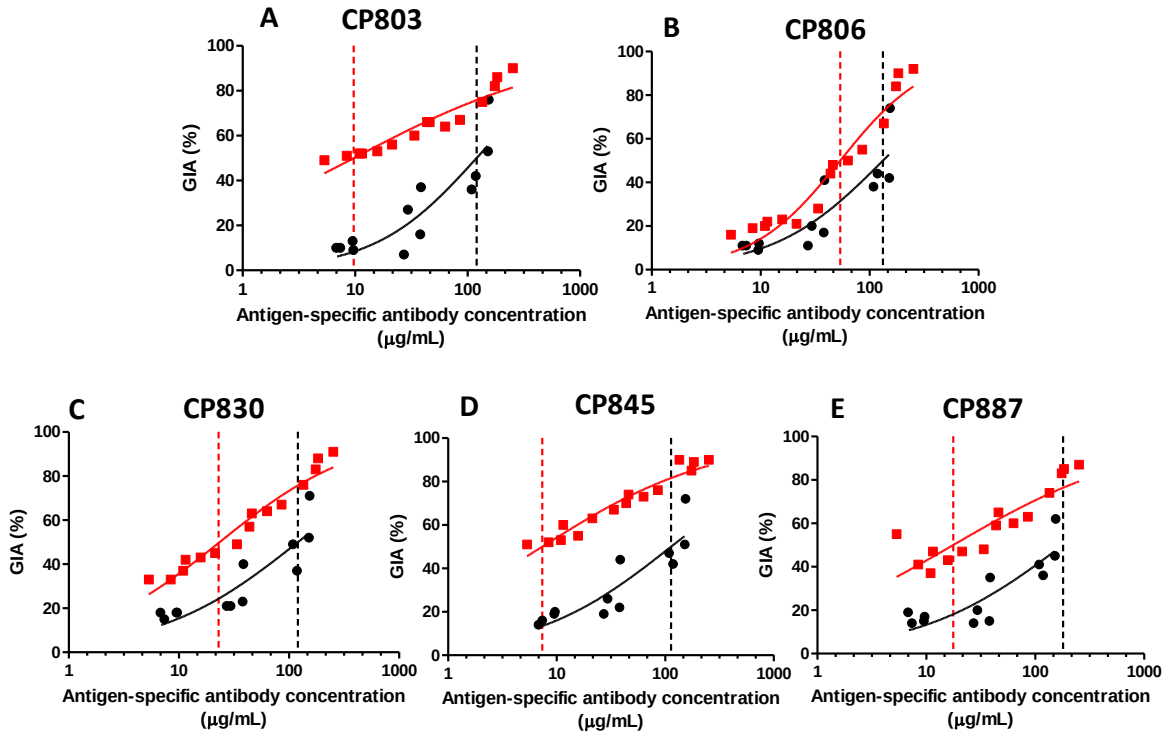

Figure 5.4.2.1 GIA assays using short-term-adapted parasites from Cambodia; EC_{50} analysis based upon pooled data from all rabbits

Dose-response curves were fitted to all GIA versus antigen-specific antibody concentration data for each isolate and antigen combination (multiple IgG dilutions for each of five rabbits for RH5 and each of four rabbits for AMA1). Dashed vertical lines indicate the fitted EC_{50} value for anti-RH5 IgG (red) or anti-AMA1 (black) IgG for that isolate. Each value is the mean of three wells in a single experiment. Red indicates anti-RH5 samples; black indicates anti-AMA1 samples.

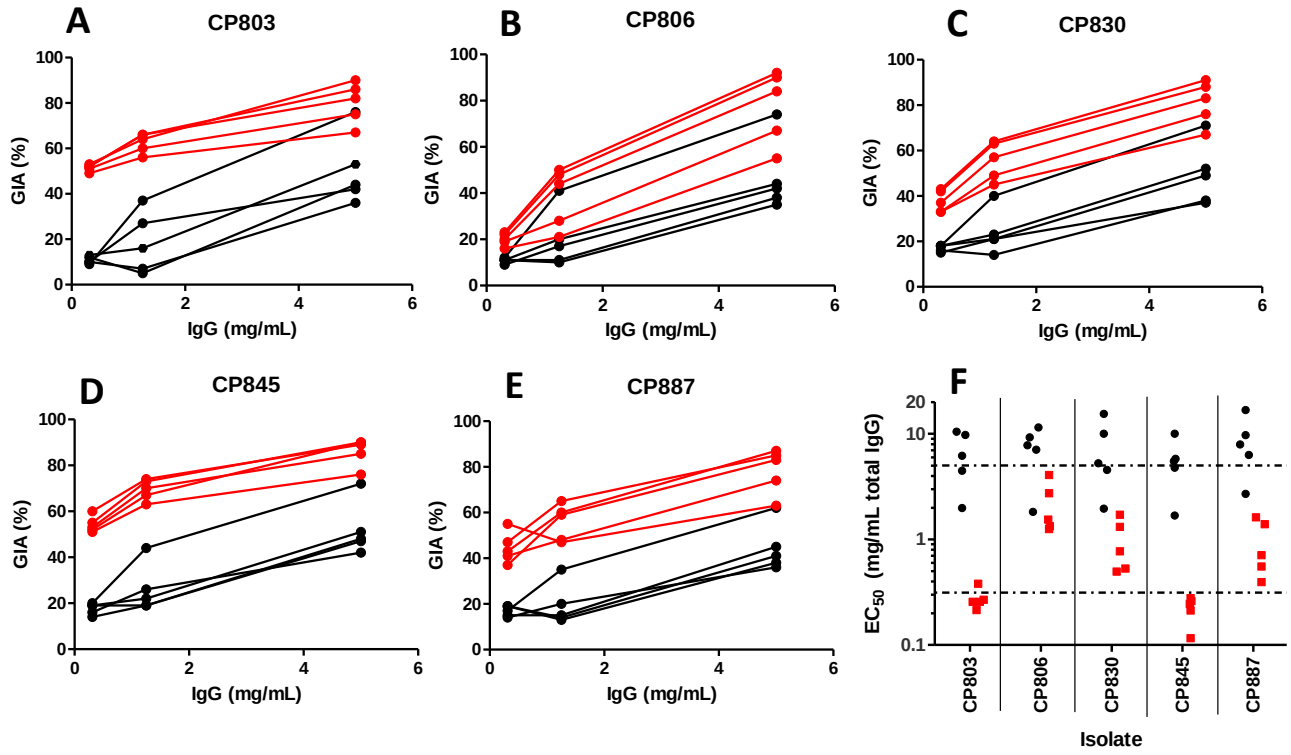

Figure 5.4.2.2 – GIA assays using short-term-adapted parasites from Cambodia; analysis based upon EC_{50} values of samples from individual rabbits

At each concentration tested, anti-RH5 total IgG achieved a greater degree of growth inhibition than total IgG from rabbits vaccinated with bivalent (3D7 + FVO) AMA1.

***Panels A-E** illustrate GIA results obtained against Cambodian parasite isolates CP803, CP806, CP830, CP845 and CP887 respectively, with IgG from each of 10 rabbits. All samples were tested at 0.31, 1.25 and 5 mg/mL. Each point illustrates the mean of triplicate wells; lines link results for a single rabbit. Red lines indicate results for RH5-vaccinated rabbits; black lines indicate results for AMA1-vaccinated rabbits.*

***Panel F** summarizes the data presented in panels **A-E** in terms of EC_{50} values for each sample against each parasite isolate, with each red point indicating a RH5-vaccinated rabbit and each black point indicating an AMA1-vaccinated rabbit. Horizontal dotted lines indicate the upper and lower IgG concentrations tested; median EC_{50} values outside this range were calculated by extrapolation from these data and hence should be regarded as approximations only.*

Table 5.4.2.T1: GIA EC_{50} values of anti-RH5 and anti-AMA1 IgG against various Cambodian parasite isolates and the 3D7 parasite clone

Total IgG EC_{50} value for Cambodian parasite isolates is the median of observed values for five individual rabbits; values in italics are extrapolated from observed values. Antigen-specific antibody EC_{50} values are derived from fitting of a single curve to all available GIA data points for each antigen and each parasite (as depicted in Figure 5.4.2.1). For comparison, estimated EC_{50} values of the total and antigen-specific IgG against the 3D7 parasite clone are also shown. 3D7 antigen-specific IgG values are as calculated in Figure 5.4.1.1E, whereas total IgG values are a mean, with 95% CI in parentheses, from eight independent experiments that have estimated the total IgG EC_{50} of anti-RH5 and anti-AMA1, with a total of five immunized rabbits for each antigen (Figure 5.4.1.2B, Figure 5.4.4.1A-B (Douglas, Williams et al. 2011)).

Parasite	EC_{50} (mg/mL total IgG, anti-AMA1 IgG)	EC_{50} (mg/mL total IgG, anti-RH5 IgG)	EC_{50} (µg/mL AMA1-specific IgG)	EC_{50} (µg/mL RH5-specific IgG)
CP803	*6.2*	*0.3*	172	9.7
CP806	*7.8*	1.5	133	54
CP830	*5.3*	*0.8*	121	23
CP845	*5.5*	*0.2*	113	7.4
CP887	*7.9*	*0.7*	*180*	18
3D7	3.1 (2.27 – 3.81)	1.5 (0.95 – 2.01)	90	40

Whole-genome sequencing of the Cambodian parasite isolates (performed as part of a global genomic epidemiology study (Manske, Miotto et al. 2012)) revealed non-reference alleles at two non-synonymous SNPs in the RH5 gene that were not identified in the sequencing of laboratory-adapted parasite lines (Table 5.4.2.T2). The same study (Manske, Miotto et al. 2012) sequenced a total of 227 isolates from South East Asia, Africa and Papua New Guinea. Across this total data set, these variants were found to be relatively common in South East Asia (allele frequencies of 0.28 and 0.30). However, no significant association was observed between the presence of these novel mutant alleles and the EC_{50} of anti-RH5 IgG against any of the Cambodian parasite isolates. Moreover, there were no other RH5 SNPs with an allele frequency greater than 0.05 in any of the aforementioned geographical regions (5.4.2.T2); since RH5 had sufficient read coverage in most isolates, it is unlikely that any important SNP was overlooked due to poor genotyping (Olivo Miotto and Dominic Kwiatkowski, personal communication). Hence, novel SNP polymorphisms that are not currently catalogued are likely to be at very low frequency in the three geographical areas sampled by the study. The functional importance of RH5 therefore appears to be conserved across both laboratory-adapted parasite lines and parasite isolates from multiple malaria-endemic regions. Crucially, these data suggest that a vaccine against RH5 may be able to induce antibodies that neutralize diverse, naturally-circulating *P. falciparum* parasites.

Table 5.4.2.T2: RH5 genotypes in parasites isolated from Cambodia

Amino acid residues are represented by single letter codes. 'Polymorphism' denotes the reference (3D7) allele, amino acid number and non-reference allele. The presence of two amino acids at a single locus indicates a mixed genotype. '?' indicates unknown. 'Non-3D7 allele frequency' denotes the proportion of sequenced loci with a non-3D7 allele at that locus: Lab=22 laboratory lines previously sequenced (Hayton, Gaur et al. 2008; Baum, Chen et al. 2009; Crosnier, Bustamante et al. 2011). For comparison, allele frequencies estimated by genome sequencing are shown for three major endemic regions (Manske, Miotto et al. 2012), using data provided at http://www.malariagen.net/Alciparum/data. SEA = South East Asia (81 samples from Thailand and Cambodia), AFR = Africa (125 samples from Kenya, Mali and Burkina Faso) and PNG = Papua New Guinea (21 samples).

Grey shading indicates synonymous SNPs; blue shading indicates SNPs with non-reference allele frequency ≤5% in all sequenced populations of parasite isolates; green shading indicates SNPs not previously identified in laboratory-adapted parasite lines and with non-reference allele frequency >5% in at least one population of parasite isolates; and yellow shading indicates SNPs with non-reference allele frequency >5% of laboratory-adapted parasite lines and parasite isolates.

	Field isolates tested in GIA in current study					Non-3D7 allele frequency			
Polymorphism	CP803	CP806	CP830	CP845	CP887	SEA	AFR	PNG	Lab
E48K	E	E	E	E	E	0	0	0	0.09
E69E									
N88D	N	N	N	N	N	0	0.01	0	0.00
Y147H	H	H	Y	Y	H	0.28	0.09	0.05	0.00
H148D	D	D	H	H	D	0.3	0.1	0.05	0.00
S197Y	S&Y	?	S	S&Y	Y	0.54	0	0.38	0.23
C203Y	Y	Y	C	C&Y	Y	0.62	0.79	0.9	0.77
I204K,R	I	I	I	I	I	0	0	0	0.09
A233E	A	A	A	A	A	0	0	0.05	0.00
N347Y,D	N	N	N	N	N	0	0	0	0.09
Y358F	Y	Y	Y	Y	Y	0	0	0	0.09
E362D	E	E	E	E	E	0	0.01	0	0.05
I364I									
H365N	H	H	H	H	H	0	0.01	0	0.00
V371I	V	V	V	V	V	0	0.05	0	0.00
I407V	I	I	I	I	I	0	0.03	0	0.05
I410M	I	I	M	I	I	0.35	0	0.1	0.09
K429N	K	K	K	K	K	0	0	0	0.14
Q477H	Q	Q	Q	Q	Q	0	0.01	0	0.00
I493V	I	I	I	I	I	0	0	0	0.00

The concentration of vaccine-induced antibody required to neutralize parasites will be lower if antibodies against multiple antigens can act synergistically. To explore this possibility, GIA assays were conducted to systematically explore the effects of combinations of purified anti-RH5 rabbit IgG with purified rabbit IgG against seven other merozoite antigens – AMA1, MSP1, EBA175, RH2, RH4, Pf38 and RAP3. Total anti-RH5 IgG was diluted to 0.156 mg/mL, a concentration that induced 20-30%

growth inhibition of the 3D7 parasite clone, and then combined with a range of concentrations of purified total IgG against the other antigens.

There was no evidence of a synergistic effect against the 3D7 parasite clone when IgG against RH5 was combined with IgG against RAP3, MSP1 or AMA1 (Figure 5.4.3.1A-C). Lower concentrations of anti-AMA1 (≤2.5 mg/mL) resulted in less GIA than the predicted additive, reaching statistical significance at 1.25 mg/mL (P<0.05; Figure 5.4.3.1C). While this could be described as an antagonistic interaction, GIA was never lower than that achieved by the more potent individual component; this interaction could perhaps more informatively be termed sub-additive rather than antagonistic.

In contrast, combining anti-RH5 IgG with anti-Pf38 or anti-EBA175 IgG produced synergistic effects at high concentrations of the latter antibodies (Figure 5.4.3.1D,E). The observed GIA was significantly higher than the predicted values at 5 mg/mL of anti-Pf38 IgG (P<0.001, Figure 5.4.3.1D), and at both 2.5 mg/mL (P<0.05) and 5 mg/mL of anti-EBA175 IgG (P<0.001, Figure 5.4.3.1E). Lower concentrations of anti-Pf38 and anti-EBA175 IgG neither achieved detectable GIA when used alone, nor resulted in a significant change in GIA from that achieved by 0.156 mg/mL of anti-RH5 IgG when used in a mixture.

Strikingly, when anti-RH5 IgG was combined with IgG against RH2 and RH4, a clear synergistic effect was observed. Here, every concentration of anti-RH2 or anti-RH4 IgG tested (ranging from 0.156-5 mg/mL) produced a statistically significant synergistic effect when combined with anti-RH5 IgG (P<0.01; Figure 5.4.3.1F,G). These data indicate that the greatest synergistic activity may be achieved when combining anti-RH5 IgG with antibodies against other RH family members.

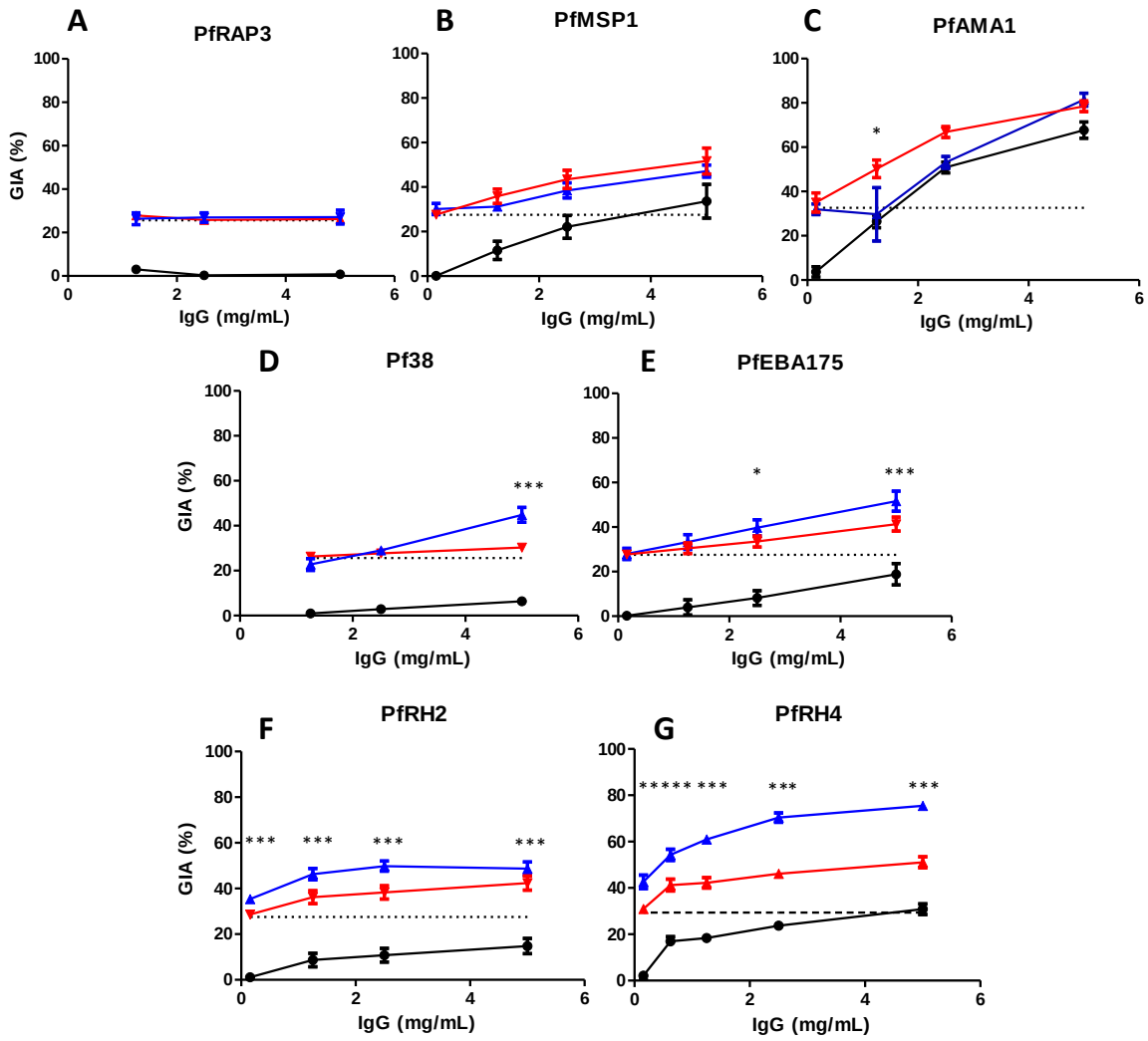

Figure 5.4.3.1: GIA effects of anti-RH5 IgG in combination with polyclonal antibody specific for other merozoite antigens

*Percentage GIA against the 3D7 parasite clone over increasing concentrations of total purified IgG from rabbits immunized with **A)** RAP3, **B)** MSP1, **C)** AMA1, **D)** Pf38, **E)** EBA175, **F)** RH2 and **G)** RH4, with (blue line) or without (solid black line) the addition of a fixed low concentration of RH5-immunized rabbit IgG (0.156 mg/mL) which, when used alone, gives approximately 25% GIA (dashed black line). Predicted additive effects were calculated according to Bliss independence and illustrated as the red line on each graph. Data points represent the mean of triplicates from two independent experiments. Bars indicate SEM for all six replicates over two experiments. Asterisks indicate that the predicted and observed values differed significantly (*P<0.05; **P<0.01; ***P<0.001, 2-way ANOVA with Bonferroni post-hoc testing).*

5.4.4. Quantitative assessment of synergy

3D-surface/contour plots and isobolograms are routinely used to quantify synergy between drugs. This work applied this methodology to antibodies specific for merozoite antigens. GIA assays were performed with all combinations of six concentrations of anti-RH5 IgG together with either anti-RH4 or anti-AMA1 IgG. The constructed plots revealed a concave-rightwards pattern in both the contour plots and isobolograms for the combination of anti-RH5 and anti-RH4 IgG (Figure 5.4.4.1A,C), in contrast to the parallel contour pattern for anti-RH5 and anti-AMA1 IgG (Figure 5.4.4.1B,D). For the anti-RH5/anti-RH4 IgG combination, the 50% isobologram indicates that the concentration of antibody needed to reduce parasite growth by 50% is lower than would be predicted if the antibodies were acting independently and thereby producing a Loewe additive effect (Figure 5.4.4.1C). Hewlett's S (a quantitative index of the extent of synergy) had a value of 2.9 (>1 implies synergy). Under the definition of Loewe additivity, half the EC_{50} concentration of anti-RH5 IgG combined with half the EC_{50} concentration of anti-RH4 IgG would achieve 50% GIA; in this case Hewlett's S value would be 1. The observed Hewlett's S value of 2.9 indicates that the required concentration of each antibody to achieve 50% GIA is approximately 3-fold less than predicted under the assumption of additivity. In contrast, the isobologram for the anti-RH5/anti-AMA1 IgG combination was close to the line of Loewe additivity, with a value of 0.96 for Hewlett's S (Figure 5.4.4.1D). Thus, despite the appearance of Bliss sub-additivity in the earlier experiment (Figure 5.4.3.1C), anti-RH5 and anti-AMA1 IgG appear to act virtually additively in combination when assessed using the Loewe definition which accounts for the self-cooperativity of the mixed antibodies.

Although the isobologram approach provides clear analysis of synergy, it is perhaps more relevant to the *in vivo* situation to consider the effects of mixing equal concentrations of IgG from animals immunized with different antigens. This was examined for the combination of anti-RH5 and anti-RH4 IgG (Figure 5.4.4.1E). The effect of combining an equal amount of anti-RH5 with anti-RH4 IgG was

similar to doubling the concentration of anti-RH5 IgG, i.e. the 50:50 combination of IgG was equivalent to the same total amount of IgG against RH5 IgG alone. However, the GIA of the combination was clearly superior to that achieved by doubling the concentration of anti-RH4 IgG, emphasizing the large differences in potency of the two antibody specificities. Therefore, for very potent antibodies such as anti-RH5 IgG, equivalent increases in GIA may be achieved by either synergistic combination with another component or by relatively modest changes in the concentration of the most potent antibody alone. This clearly has important implications for decision-making regarding potential multi-antigen antibody-inducing vaccines.

Figure 5.4.4.1 (overleaf): Contour plots and isobolograms of GIA achieved by anti-RH5 IgG in combination with either anti-RH4 or anti-AMA1 IgG

***Panel A,B** – Contour plots of GIA versus concentration of total IgG combined from rabbits immunized with either RH5 or RH4 (**A**), or with either RH5 or AMA1 (**B**). Each experiment was conducted independently. GIA assays were performed twice in triplicate for each IgG combination. Total IgG EC_{50} values were 0.625 or 1.25 mg/mL for anti-RH5 IgG alone, and 2.5 mg/mL for anti-AMA1 IgG alone – these were within the range of previously measured values (Table 5.4.2.T1). Black lines are contours linking anti-RH5 and anti-RH4 IgG combinations inducing 25%, 50% and 75% GIA (as labelled), obtained by interpolation between observed GIA values. Blue shaded area indicates 0-25% GIA, green area indicates 25-50% GIA, orange area indicates 50-75% GIA, pink area indicates 75-100% GIA. Thin diagonal dashed line from origin indicates line of equal concentration of IgG from each component.*

***Panel C,D** – 50% GIA isobologram for anti-RH5 and anti-RH4 IgG (**C**) and anti-RH5 and anti-AMA1 IgG (**D**) combinations. Red line links the observed combination of anti-RH5 IgG and either anti-RH4 or anti-AMA1 IgG that induced 50% GIA, plotted on axes of anti-RH5 and anti-RH4/anti-AMA1 IgG concentration expressed as percentage of the EC_{50}. These are the same data as illustrated by the 50% contour in panels **A** and **B**. Dashed line illustrates 50% contour predicted if anti-RH5 IgG and the other antibody are Loewe additive. Diagonal x=y line from origin links points at which anti-RH5 and anti-RH4/AMA1 IgG concentrations (as proportion of EC_{50}) are equal; the letters M and N indicate the line intersections used to calculate Hewlett's synergy index.*

***Panel E** – GIA attained by mixing equal concentrations of anti-RH5 with anti-RH4 IgG (blue line), plotted against the total IgG concentration in the well shown on the lower x-axis (i.e. twice the concentration of each individual component). These data correspond to the points linked by the dashed diagonal line in panel **A**. For comparison, the solid red line indicates the GIA effect when anti-RH5 IgG is used alone at the concentrations on the lower x-axis (i.e. twice the concentration of anti-RH5 IgG in the antibody mixture), and the dashed red line indicates the GIA effect of anti-RH5 IgG alone at the concentration shown on the upper dashed x-axis (i.e. the concentration of anti-RH5 IgG present in the antibody mixture). The solid and dashed black lines indicate the same relationship for anti-RH4 IgG.*

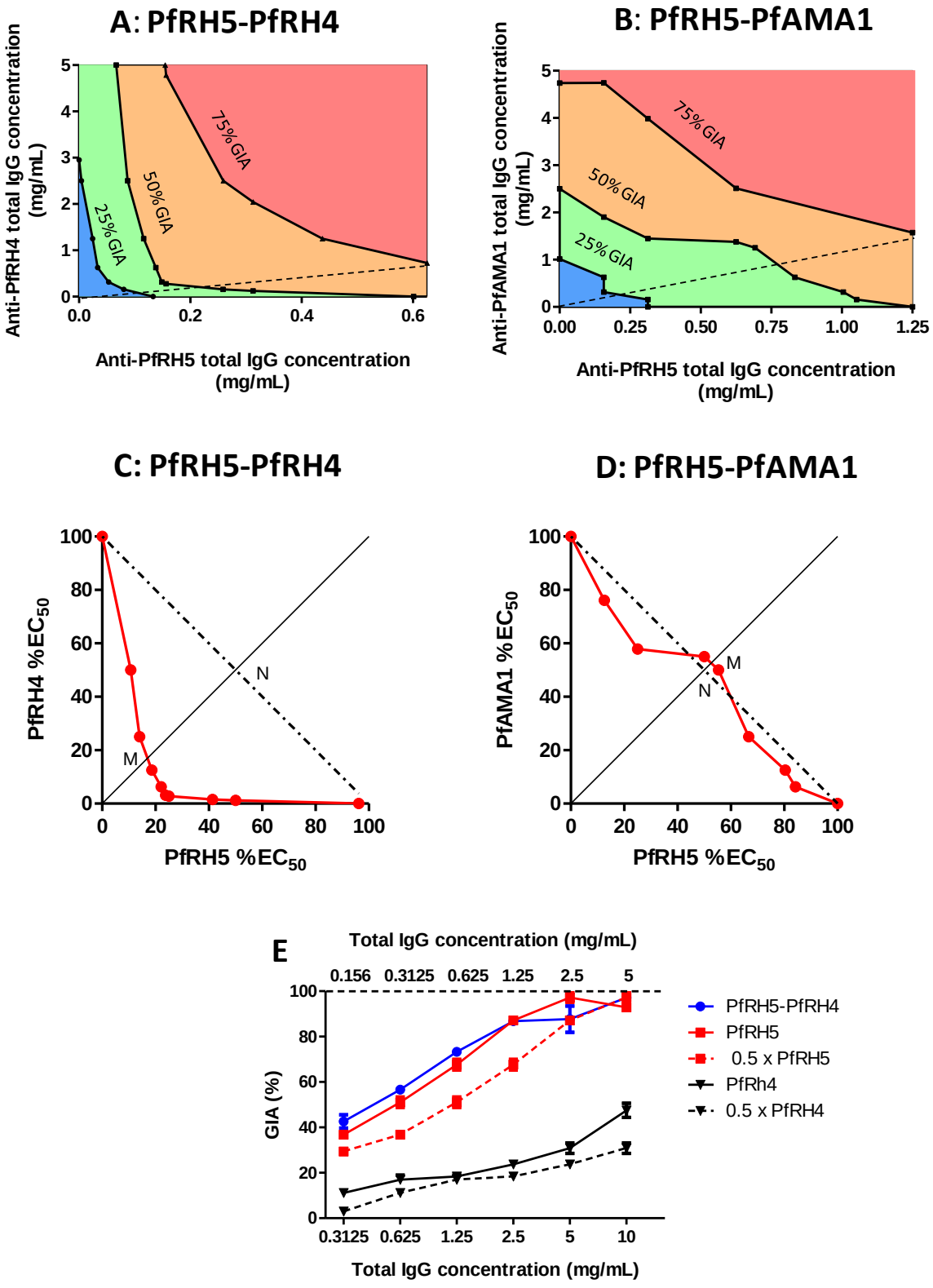

Figure 5.4.4.1: Contour plots and isobolograms of GIA achieved by anti-RH5 IgG in combination with either anti-RH4 or anti-AMA1 IgG

See preceding page for figure legend

4.4.5 Synergy against vaccine-heterologous parasite lines

To determine if the additive and synergistic effects observed against the 3D7 parasite clone are strain-transcending, mixtures of anti-RH5 IgG with anti-EBA175, anti-RH2 or anti-RH4 IgG were tested in GIA assays using the FVO parasite line. Of all the laboratory-adapted parasite lines for which the RH5 gene sequence has been reported, FVO differs from 3D7 at four amino acid positions, the most between any pair of parasite lines (Hayton, Gaur et al. 2008). When anti-RH5 and anti-EBA175 IgG were combined, the modest synergistic effect observed against the 3D7 parasite clone was still apparent (Figure 5.4.5.1A). However, when anti-RH5 and anti-RH2 IgG were combined, only an additive effect was observed (Figure 5.4.5.1B). Moreover, the promising synergy achieved by the combination of anti-RH5 and anti-RH4 IgG was completely absent, consistent with FVO being reliant on sialic-acid (SA) dependent invasion routes (Narum, Haynes et al. 2000) (Figure 5.4.5.1C). Clearly, the rational design of multi-component vaccines that achieve synergistic antibody effects will require assessment of the presence, or absence, of such synergies in the neutralization of multiple parasite lines/isolates.

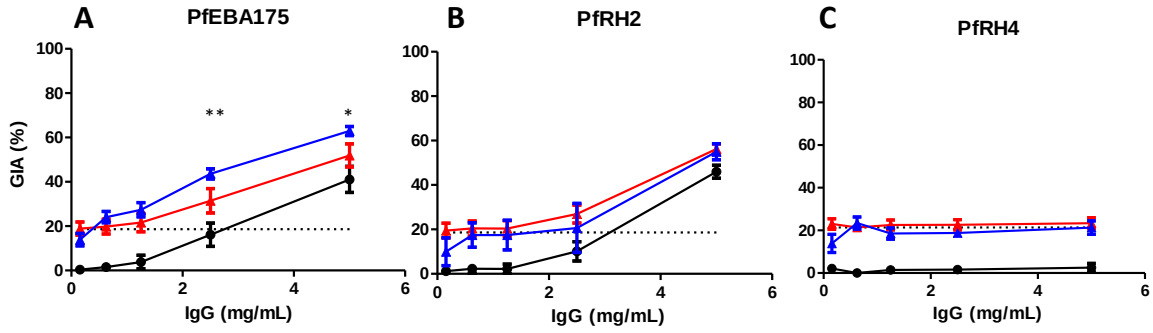

Figure 5.4.5.1: GIA synergies against the vaccine-heterologous FVO parasite clone

*Percentage GIA against the FVO parasite clone over increasing gradients of concentrations of IgG from rabbits immunized with A) EBA175, B) RH2 or C) RH4 with (blue line) or without (solid black line) the addition of a fixed low concentration of RH5-immunized rabbit IgG (0.156 mg/mL) which, when used alone, gives approximately 20% GIA (dashed black line). Predicted additive effects were calculated according to Bliss independence and illustrated as the red line on each graph. Data points represent the mean of triplicates from two independent experiments. Bars indicate SEM for all six replicates over two experiments. Asterisks indicate that the predicted and observed values differed significantly (*P<0.05; ** P<0.01; 2-way ANOVA with Bonferroni post-hoc testing).*

5.5. DISCUSSION

The work reported in this chapter and the preceding chapter has shown that multiple laboratory-adapted parasite lines and naturally-circulating parasite isolates are susceptible to anti-RH5 IgG, which neutralizes parasites at concentrations that are comparable to or, in many cases, lower than anti-AMA1 IgG. Furthermore, it has frequently been suggested that multi-antigen blood-stage vaccines may induce antibodies that act synergistically. Some published data have hinted that such effects may indeed be achievable (Lopaticki, Maier et al. 2011; Ord, Rodriguez et al. 2012). These experiments extended considerably upon this previous work, by identifying synergy between antibody combinations using a quantitative methodology that has not, as far as I am aware, previously been applied to vaccine development.

The extent of known polymorphism in the RH5 gene in laboratory-adapted parasite lines is limited (10 of 526 amino acid residues) (Hayton, Gaur et al. 2008). This work showed that naturally-circulating *P. falciparum* isolates from Cambodia, as well as laboratory-adapted parasite lines (Douglas, Williams et al. 2011), are highly susceptible to anti-RH5 antibody. Sequencing of the RH5 gene in these Cambodian parasite isolates revealed only two non-synonymous SNPs which have not been previously identified in laboratory-adapted parasite lines, and no RH5 SNPs with a minor allele frequency exceeding 5% were identified in sequence data from 227 parasite isolates from diverse geographical areas. Taken together, these data indicate that the parasite isolates used in these assays represent the diversity found in three important malaria endemic regions. Moreover, in addition to the 3D7 parasite clone upon which the RH5 immunogen is based, GIA of anti-RH5 IgG has now been assessed against five laboratory-adapted parasite lines and five short-term-adapted parasite isolates. No apparent relationship between RH5 genotype and the EC_{50} of anti-RH5 IgG has been observed. It seems likely that the extent of polymorphism between 3D7 and other parasite lines (a maximum of four pairwise single amino-acid differences) is insufficient to have a substantial impact upon the binding of polyclonal antibody. The need to interact with basigin (Crosnier,

Bustamante et al. 2011) and other binding partners, such as Ripr (Chen, Lopaticki et al. 2011), could impose functional constraints on the possible extent of mutation in RH5. Therefore, it may prove challenging for *P. falciparum* to evolve resistance to an efficacious RH5 vaccine by means of antigenic drift.

Whilst significantly lower EC_{50} values for anti-RH5 IgG than for anti-AMA1 IgG were observed in the Cambodian parasite isolates (up to a 17-fold difference), the difference in EC_{50} against the vaccine-homologous 3D7 parasite clone was relatively modest (approximately 2-fold). Given the extremely high titres of anti-AMA1 antibodies required to achieve protective effects in non-human primate models of malaria, (Dutta, Sullivan et al. 2009) it seems probable that the design of vaccines with lower *in vitro* EC_{50} values will enhance the likelihood of achieving *in vivo* efficacy. Therefore, there may be distinct advantages in identifying an additional antigen that produces synergistic effects when used in combination with anti-RH5 IgG.

Synergy between antibodies against RH invasion ligands was observed, and to a lesser extent, dynergy between anti-RH5 IgG and antibody to EBA175 (F2 region), another well-characterized invasion ligand. The other antibody combinations tested (notably mixtures of anti-RH5 with either anti-AMA1 or anti-MSP1 IgG) achieved levels of GIA close to those predicted by Bliss additivity (or in the case of AMA1 IgG, Loewe additivity). This is consistent with previous work showing a lack of synergy when antibodies against AMA1 and MSP1 are combined. (Faber, Remarque et al. 2007; Arnot, Cavanagh et al. 2008) Interestingly, we did not identify antibody combinations resulting in truly antagonistic interactions, as implied by a previous study where naturally-exposed individuals were immunized with a candidate AMA1 vaccine (Miura, Zhou et al. 2008). It is thus possible that antibodies specific for other antigens may antagonize anti-AMA1 responses.

Given the multi-stage nature of *P. falciparum* erythrocyte invasion (Baum, Maier et al. 2005; Riglar, Richard et al. 2011), there seem to be two ways in which synergistic antibody action might occur: antibodies of different specificities may act 'in series', cumulatively resulting in neutralization via partial inhibition of successive stages of invasion; alternatively, antibodies may act 'in parallel', inhibiting a number of closely-related and possibly mutually redundant invasion processes. The precise functions of RH5 and other RH family members are yet to be fully elucidated. However, it is known that these proteins all bind specific receptors on the erythrocyte and it has been proposed that the EBA and RH protein families may be involved in tight attachment of the merozoite (Riglar, Richard et al. 2011). RH5 cannot be genetically knocked out, and antibodies against basigin can completely eliminate erythrocyte invasion in the absence of antibodies targeting any other ligand-receptor pathways (Crosnier, Bustamante et al. 2011). Therefore, it is unlikely that RH5 is functionally redundant with other RH proteins, and may instead partner with them to facilitate merozoite invasion of erythrocytes. Further work is necessary to understand how these merozoite ligands interact during erythrocyte invasion, and to elucidate the obviously crucial role of RH5 in this process. For now, our results indicate that multi-antigen blood-stage vaccines will be more efficacious when they induce antibodies against antigens with closely-related or complementary 'parallel' functions.

The inclusion of multiple antigens in a vaccine may incur substantial cost and risk of antigenic competition. It is possible that such effects may well outweigh relatively modest synergistic effects (Saul and Fay 2007). Consequently, rigorous assessment of possible antigen combinations is required prior to clinical trials. In pre-clinical models, factors other than the presence of synergy must also be considered. These include the quantitative extent of the synergy, the extent of strain-transcending efficacy, and the relative immuno-dominance and possible immune interference arising from different antigen combinations *in vivo*. Extrapolating from controlled *in vitro* studies of vaccine-induced rabbit antibodies is more difficult than doing so from studies focusing on drug discovery.

Whereas known quantities of drugs can be administered, the quantity and specificity of human antibodies produced against each component of a multi-antigen vaccine cannot be controlled *in vivo* and may vary substantially between individuals; thus, components that synergize when mixed artificially *in vitro* may prove less efficacious *in vivo* due to antigenic interference. Indeed, it was found that a 2- to 3-fold increase in anti-RH5 IgG could be expected to have the same effect as the combination of anti-RH4 and anti-RH5 IgG without antigenic interference. These data confirm that extremely careful consideration should be given to the prospects for doubling antibody concentrations against a single antigen by improved formulation and/or antigen delivery, rather than attempting to induce consistently high antibody titres against two antigens by co-immunization.

In summary, the work in this Chapter provides further evidence that RH5 will be a more effective single-component vaccine than previously-tested merozoite antigens, and encourages its prompt clinical development as a vaccine. This work has also provided the clearest demonstration to date that rationally designed antigen combinations may achieve truly synergistic effects of polyclonal antibody against a pathogen. These results point the way towards testing of second-generation RH-targeting vaccines, and the identification of additional antigenically-conserved blood-stage antigens that act synergistically with RH5.

Approaches to the identification of such 'second-component' antigens may be bioinformatically-led (for example a screen of all antigens identified in proteomic studies in schizonts which also have signal peptides), or may be functionally led (targeting antigens with a known or suspected role in erythrocyte invasion, and particularly those with functions closely related to RH5). I therefore set out to gather further data regarding the function of RH5, as will be described in the following chapter.

6. Mechanistic basis of Plasmodium falciparum neutralisation by antibodies to PfRH5

6.1. AUTHORSHIP STATEMENT

ADD conceived the experiments performed in this chapter (with valuable input from Simon Draper, Andrew Williams, Tony Holder and Ellen Knuepfer), but much of the data were generated with the assistance of others.

ADD performed all animal work, generated/selected/purified monoclonal antibodies (with the expert assistance of Julie Furze for hybridoma culture and Drew Worth for flow cytometry), performed all AVEXIS and ELISA-format assays and all surface plasmon resonance assays, and prepared Fabs.

RH5 and basigin proteins were kindly supplied by Gavin Wright and Cécile Crosnier.

GIA, merozoite attachment, and IFA experiments using the samples generated by ADD were performed by Andrew Williams, with the assistance of Prateek Choudhary, Linda Murungi, Sara Zakutansky, and Dennis Awuah.

I am very grateful for the input and ideas of Ellen Knuepfer, Tony Holder, and David Ferguson regarding IFA, video microscopy, and EM studies.

The DiSH system was kindly provided by Richard Shimkets, Abeome Corp, under an evaluation license.

6.2. INTRODUCTION

The proposed mechanisms of action of antibodies against important blood-stage *P. falciparum* antigens have proven complex and controversial, despite intensive study over a period of decades. There appear to be at least three possible distinct mechanisms of action of antibody against MSP1: inhibition of proteolytic processing of $MSP1_{42}$, direct inhibition of erythrocyte invasion, and inhibition of parasite development after invasion is completed (Moss, Remarque et al. 2011). A recent study found that two anti-AMA1 mAbs act via blockade of the interaction of AMA1 with rhoptry neck protein 2 (RON2) (Collins, Withers-Martinez et al. 2009; Srinivasan, Beatty et al. 2011), but additional actions of polyclonal anti-AMA1 have also been suggested, including inhibition of proteolytic processing and cross-linking mediated inhibition of AMA1 redistribution on the merozoite surface (Dutta, Haynes et al. 2005).

The interaction of RH5 with the erythrocyte surface protein basigin (BSG) is essential for merozoite invasion into red blood cells (RBCs), and blockade of this interaction by anti-BSG mAbs can inhibit invasion (Crosnier, Bustamante et al. 2011). It therefore seems plausible that blockade of the interaction by anti-RH5 antibodies could have a similar effect. However it is also possible that anti-RH5 antibodies may act via additional mechanisms, such as blockade of the interaction of RH5 with Ripr (Chen, Lopaticki et al. 2011), or simply via steric hindrance of the RH5's proposed role in the formation of the merozoite-erythrocyte tight junction, and the moving junction thereafter (Baum, Chen et al. 2009).

The work reported in this chapter attempted to explore some of these possibilities, and hence to gain further insight into the function of RH5. An important component of this work was the generation and detailed characterisation of RH5-specific mouse mAbs.

6.3. METHODS

6.3.1. Vaccines, animals and polyclonal antibody generation

Vaccines and animal work were as described in Section 2.1 and 2.2 respectively.

6.3.2. Attachment, growth inhibition and indirect immunofluorescence assays

3D7 and FVO parasite maintenance, synchronisation and growth inhibition assays were performed as described in Section 2.4.

Free merozoite preparation and attachment assays were performed as described elsewhere (Boyle, Wilson et al. 2010; Riglar, Richard et al. 2011). Briefly, merozoites isolated by filter-disruption of MACS-purified schizonts were mixed with cytochalasin D and antibody and then with erythrocytes, washed with RPMI, fixed with 0.0075% glutaraldehyde/ 4% paraformaldehyde, and stained with Giemsa. At least 2000 RBCs were counted to enumerate the percentage of RBCs with attached merozoites.

Indirect immunofluorescence assays were carried out as described in Section 2.5, with the exception that, for some assays, free merozoites were used (prepared as above), and, for some assays, Triton X-100 permeabilisation was omitted.

6.3.3. Avidity-based extracellular interaction screen (AVEXIS)

AVEXIS was performed using plate-captured biotinylated recombinant RH5 and pentameric β-lactamase-conjugated basigin, in accordance with a previously published method (Bushell, Sollner et al. 2008; Crosnier, Bustamante et al. 2011) with the exception that, between capture of the RH5 on the plate and the application of the basigin, a sample of serum or monoclonal antibody diluted in PBS was applied for 1 hour, followed by 6 washes with PBS. Where ELISA was performed for comparison with AVEXIS, the method was as described in Section 2.3.

6.3.4. Monoclonal antibodies

Anti-RAP1 mouse mAb 7H8/50 was obtained from MR4 (Schofield, Bushell et al. 1986). Anti-RON4 mouse mAb 24C6 was a kind gift from Jean-Francois Dubremetz (Alexander, Arastu-Kapur et al. 2006).

Monoclonal antibodies against RH5 were raised by vaccinating BALB/c mice with the RH5FL AdHu5-MVA regime as above. Spleens were harvested three days after the MVA boost. Splenocytes from one mouse were fused with Sp2/0 myeloma cells (ECACC, HPA, UK), and plated in semi-solid methylcellulose-based medium (ClonacellHY, Stemcell Technologies, Canada) in accordance with the manufacturer's instructions. Two successive rounds of limiting dilution cloning were performed to select hybridomas which secreted IgG capable of binding recombinant RH5 by ELISA (performed as described in Chapter 3) . A second set of mAbs were generated using the proprietary Direct Selection of Hybridomas (DiSH) system (Abeome Inc, Georgia USA)(Price, McKinney et al. 2009). Briefly, splenocytes from a second mouse were fused with Sp2ab cells, and immediately subcultured into 9 flasks. After 7 days, the resulting B-cell-receptor-overexpressing cells were stained with biotinylated RH5, streptavidin-phycoerythrin, and goat-anti-mouse IgG-allophycocyanin. Single cells staining positively with both fluorophores were selected and deposited singly into culture wells by a MoFlo cytometer with CyClone module (Beckman Coulter). One ELISA-positive clone originating from each subculture flask was selected for further study.

Hybridomas were grown in medium with ultra-low immunoglobulin foetal calf serum (Gibco, UK), using CellLine1000 two-compartment bioreactors for larger preparations (Integra Biosciences, Switzerland). Monoclonal antibody was purified from supernatant by affinity chromatography using Protein G (Pierce). IgG sub-classes of mAbs were confirmed by ELISA, with pre-adsorption of purified monoclonal antibody onto Maxi-Sorp plates (Nunc, UK), followed by detection using biotinylated

mouse subclass-specific antibodies (eBioscience, UK) and alkaline-phosphatase conjugated streptavidin (Sigma Aldrich, UK).

Fabs were prepared using immobilised papain for murine IgG2a (9AD4) and rabbit IgG, and immobilised ficin for murine IgG1 (QA5 and 2AC7), following the manufacturer's protocols (both from Pierce). Undigested IgG and Fc fragments were removed by passing the digest over a Protein A agarose column (Pierce), followed by buffer-exchange of the Fab-containing flow-through into incomplete *P. falciparum* culture medium (for GIA) or PBS (for SPR) using Amicon centrifugal concentrators (Millipore).

6.3.5. Monoclonal antibody epitope mapping

Biotinylated peptides were synthesised by Mimotopes Pty Ltd, Australia. Peptides were resuspended in DMSO at 50 mg/mL, diluted in PBS to a working concentration of 10µg/mL, applied to streptavidin-coated plates and ELISA performed as above. Initial mapping used a set of 20mer peptides based upon the 3D7 RH5 sequence, each offset by 8 amino acid residues from the previous peptide (i.e. overlapping by 12 amino acid residues). Subsequent mapping of minimal linear epitopes for QA5 and 9AD4 used peptides progressively truncated from each terminus of the 20mer recognised by each mAb. Subsequently, ELISA was performed using a third set of peptides based upon the minimal linear epitopes but each with one amino acid mutated to alanine (or glycine, where the original amino acid residue was alanine).

6.3.6. Surface plasmon resonance

SPR equipment, software, buffers and antigens were as described above (section 4.3.3). Antigen-specific antibody binding was measured by subtraction of the binding of antibody to a flow cell coated only with the biotin capture reagent.

Experiments to assess competitive blockade of monoclonal antibody binding employed high concentrations of mAb (20µg/mL) applied at relatively slow flow rates (5µL/min); each injection was continued until saturation binding was reached. Binding of each mAb was measured with preceding injections of either buffer or each other mAb, and compared to the response-unit-change during continued application of that first injection.

Multi-cycle kinetic measurements were performed with fresh RH5 capture prior to each application of antibody. Levels of antigen capture were around 50RU, consistent with those recommended by GE for an 80 kDa ligand and 150 kDa analyte. Three to five serially diluted samples of each antibody were prepared, typically spanning a concentration range of 200nM to 2nM. Binding of each sample was measured during a 120 second association phase and 800 second dissociation phase, each on two occasions with independently prepared samples. Double-referencing was performed by subtraction of responses on the non-RH5-coated flow cell, and responses after injection of buffer. A bivalent analyte binding model was fitted globally for intact IgG samples. A 1:1 binding model was fitted globally for Fab samples.

6.4. RESULTS

6.4.1. RH5 is not localised to the merozoite surface prior to contact with RBCs

Indirect immunofluorescence assays (IFA) have previously localised RH5 to the apical end of the merozoite, possibly within the rhoptry body(Rodriguez, Lustigman et al. 2008; Baum, Chen et al. 2009). Some immuno-electron microscopy (IEM) images have suggested that RH5 may be located on the surface of free merozoites (Chen, Lopaticki et al. 2011).

IFA (performed by Andrew Williams) demonstrated that RH5 does not co-localise with the rhoptry body marker RAP1 (Figure 6.4.1.1A). This result has been confirmed and extended by a collaborator using RH5 antibodies I provided, demonstrating lack of co-localisation of RH5 with markers of the rhoptry body, rhoptry neck or micronemes (RAP1, RON4 and EBA175 respectively), either in schizonts or purified free merozoites (Ellen Knuepfer, personal communication- data not shown). It therefore seems likely that RH5 has a distinct subcellular localisation from these well-characterised markers – perhaps a sub-compartment of the rhoptry. Moreover, RH5 does not appear to be accessible to antibody on the surface of free merozoites: in contrast to anti-AMA1 antibodies, no staining was observed when anti-RH5 antibodies were applied to purified free merozoites without prior permeabilisation (Figure 6.4.1.1B).

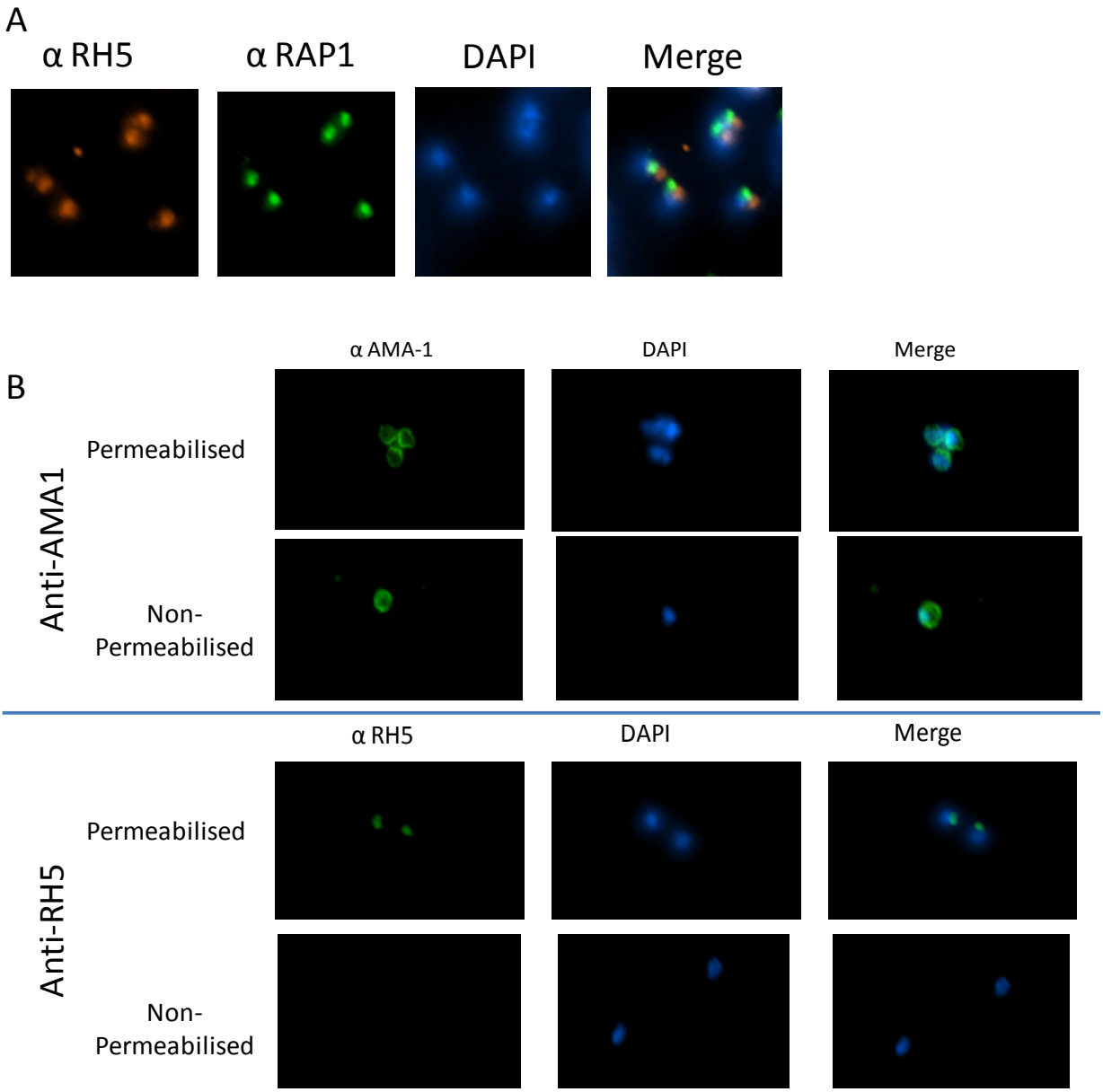

Figure 6.4.1.1 Free merozoite polyclonal anti-RH5 IFA
Panel A: IFA was performed with fixed and permeabilised free merozoites using rabbit polyclonal anti-RH5 (red) and mouse mAb anti-RAP1 (green). RH5 does not co-localise with RAP1.

Panel B: IFA was performed with free merozoites with and without Triton X-100 permeabilisation, using mouse polyclonal anti-RH5 and mouse polyclonal anti-AMA1. Unlike AMA1, anti-RH5 is not detectable on the surface on non-permeabilised free merozoites.

This result is consistent with previously published results, which suggest that exposure of the merozoite to low potassium-concentration medium is sufficient for microneme release, but that rhoptry release requires contact of the merozoite either with the red cell surface or with soluble glycophorins (Singh, Alam et al. 2010). Given that the interaction of RH5 with basigin is essential for RBC invasion, translocation of RH5 to the surface presumably does occur, but requires an additional signal from the extracellular environment. Moreover, it suggests that the time window for the action of vaccine-induced anti-RH5 antibody is likely to be even shorter than total duration of extracellular exposure of the merozoite.

6.4.2. Anti-RH5 polyclonal antibody inhibits tight attachment of merozoites to RBCs

It has previously been shown that inhibition of the function of RH-family members and related proteins can impair the formation of the merozoite-RBC tight junction (TJ): RH4-null W2mef parasites form few tight junctions when in contact with neuraminidase-treated red cells, and antibodies to Ripr inhibit tight attachment of merozoites to erythrocytes(Chen, Lopaticki et al. 2011).

To further clarify the stage of the invasion process inhibited by anti-RH5 antibodies, merozoite attachment assays were performed by Andrew Williams(Riglar, Richard et al. 2011) (Figure 6.4.2.1). These assays demonstrated that rabbit polyclonal anti-RH5 antibodies markedly reduced tight attachment of merozoites to RBCs. As has previously been noted with other invasion-inhibitory treatments such as R1 peptide(Riglar, Richard et al. 2011), the level of attachment inhibition was somewhat less than the level of inhibition measured by the assay of GIA with an equivalent concentration of anti-RH5 antibody; it may be that anti-RH5 is capable of exerting some additional growth inhibitory effect after the stage of reorientation. Transmission electron microscopy is one technique which can resolve whether or not reoriented merozoites have successfully formed tight junctions (Srinivasan, Beatty et al. 2011): such studies will be important future experiments.

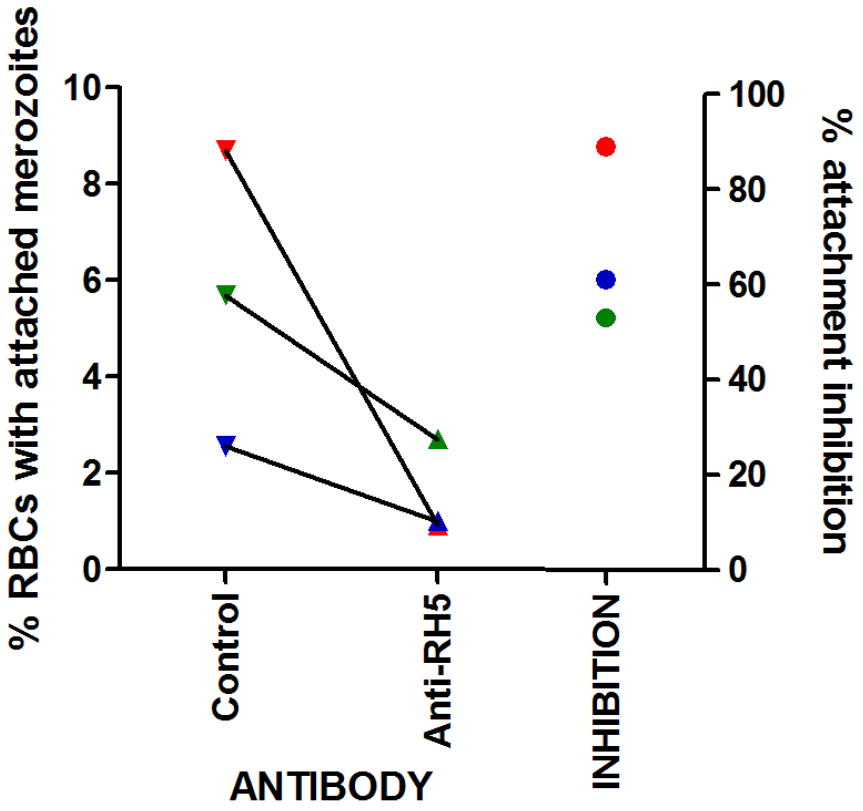

Figure 6.4.2.1: Anti-RH5 antibodies inhibit attachment of merozoites to RBCs

Three independent assays of merozoite attachment to RBCs were conducted, each represented by points of a different colour. Lines link observations from a single assay in the presence of 10 mg/ml IgG from an RH5-immunised rabbit, and in the presence 10 mg/mL IgG from a rabbit immunised with a non-malaria antigen. Right-hand column indicates the percentage reduction in attachment induced by anti-RH5 (calculated from the same data; plotted on right axis).

6.4.3. Anti-RH5 antibodies which block interaction with BSG neutralise merozoites

The identification of basigin as the erythrocyte-surface binding partner of RH5 and the availability of a quantitative *in vitro* assay of RH5 binding to basigin (based upon the AVidity-Based EXtracellular Interaction Screen [AVEXIS]) prompted me to investigate whether RH5-vaccine-induced polyclonal serum was capable of blocking this interaction. I found that sera from mice and rabbits vaccinated with the full-length RH5 antigen, but not those vaccinated with a previously-used fragment of the antigen (Baum, Chen et al. 2009), were capable of complete blockade of this interaction at dilutions up to 1:300 (Figure 6.4.3.1).

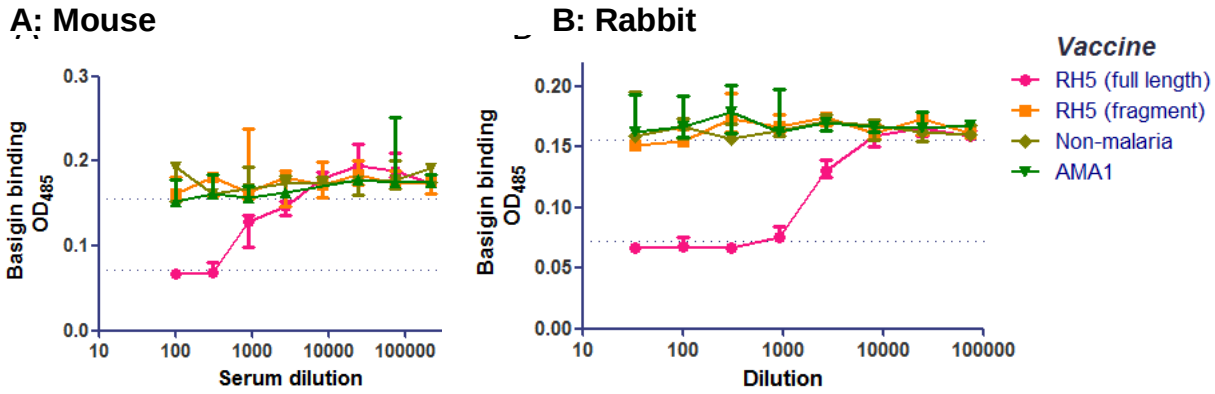

Figure 6.4.3.1: Polyclonal anti-RH5 antiserum blocks the RH5-basigin interaction
AVEXIS was performed with plate-bound RH5 and soluble pentameric basigin. Prior to application of basigin, wells were incubated with serial dilutions of antisera from mice (panel A) or rabbits (panel B) immunised with full-length RH5, a previously described RH5 fragment(Baum, Chen et al. 2009), AMA1, or viral vectors lacking a malaria antigen. Points and error bars indicate median and range of three replicate wells.

To further investigate whether antibodies blocking the RH5-BSG interaction were causally responsible for the neutralisation of merozoites, I generated two panels of mAbs (a total of 8 demonstrably unique mAbs) which were capable of binding RH5 by ELISA. Five of the hybridomas were generated using a proprietary system which enables flow-cytometric sorting of single antigen-specific hybridoma cells (Figure 6.4.3.2A) (Price, McKinney et al. 2009). Basic characteristics of these eight mAbs are summarised in table 6.4.3.T1.

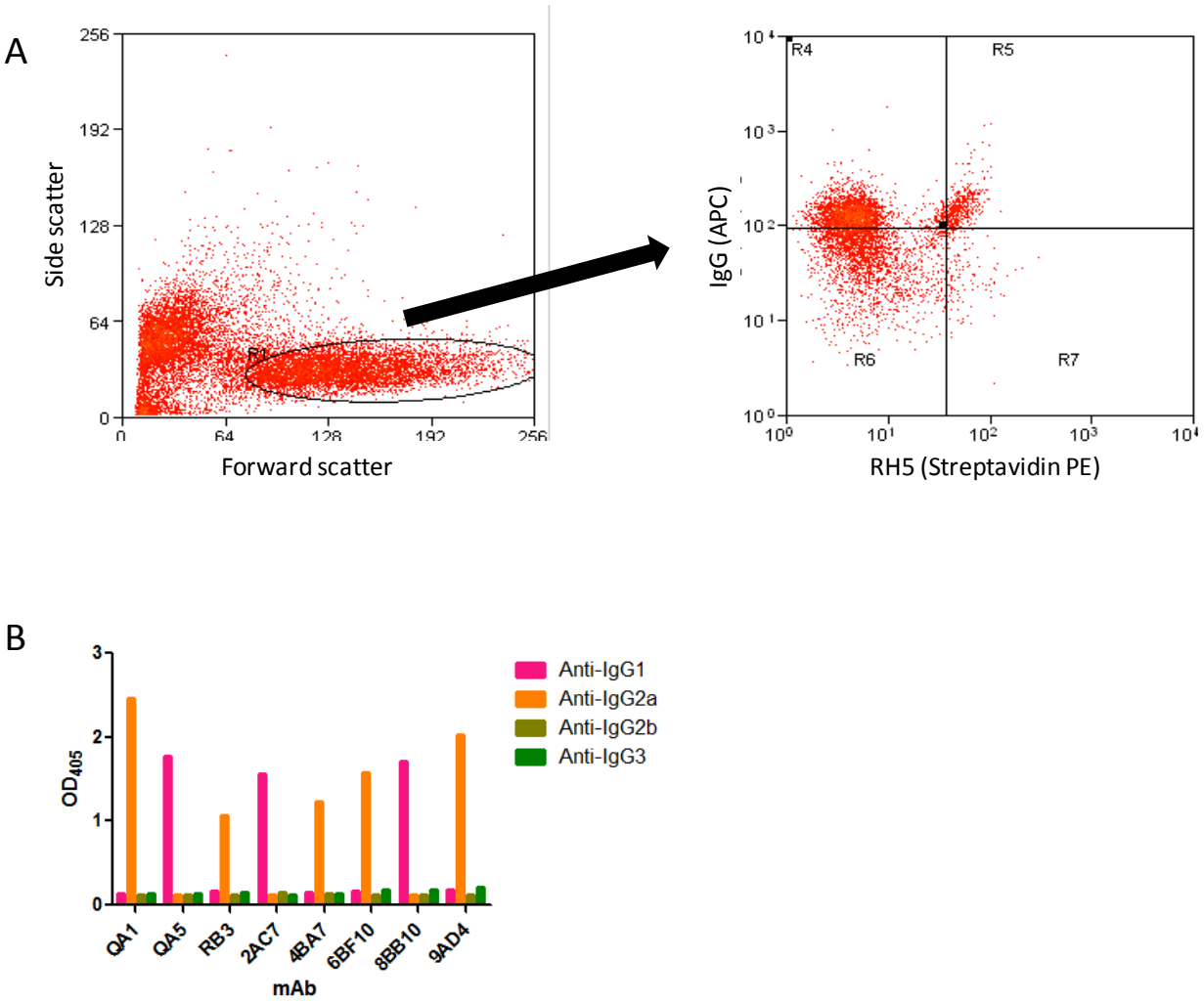

Figure 6.4.3.2 Example of DiSH flow-cytometric sorting of RH5-specific hybridoma cells
Panel A: Viable cells were selected on the basis of light scattering characteristics (left-hand panel), followed by selection of single dual $IgG^{+}RH5^{+}$ cells (right-hand panel, upper-right quadrant).

Panel B shows results of mAb isotyping.

mAb name	Fusion partner cell line	Isotype
QA1	Sp2/0	IgG2a
QA5	Sp2/0	IgG1
RB3	Sp2/0	IgG2a
2AC7	Sp2ab	IgG1
4BA7	Sp2ab	IgG2a
6BF10	Sp2ab	IgG2a
8BB10	Sp2ab	IgG1
9AD4	Sp2ab	IgG2a

Table 6.4.3.T1 Basic characteristics of anti-RH5 mAbs

I proceeded to test the ability of the anti-RH5 mAbs to block the interaction of RH5 with BSG (Figure 6.4.3.3). Because the affinity of the basigin-RH5 interaction is extremely low (K_D ~ 1µM, with a dissociation half-life of ~3 seconds), detection of this interaction in an ELISA-format assay requires the multimerisation of one of the binding partners to enhance the avidity of the interaction – the basis of the AVEXIS assay (Bushell, Sollner et al. 2008). Pre-incubation of plate-bound RH5 with mAbs QA1, QA5 and 6BF10 consistently and completely blocked the binding of pentameric basigin. mAbs 4BA7, 8BB10 and RB3 did not inhibit the interaction. These results were consistent when the assay was kindly repeated in reverse orientation (plate-bound basigin and soluble pentameric RH5-antibody complexes) by Cécile Crosnier (data not shown in thesis).

Results were inconclusive with mAbs 2AC7 and 9AD4. mAb 2AC7 inhibited the interaction, although this inhibition was incomplete and inconsistent when the assay was repeated in reverse orientation. Effects of 9AD4 were markedly dependent upon orientation: this mAb was capable of complete blockade of the interaction when incubated with plate-adsorbed RH5, but had little or no effect when incubated with soluble RH5.

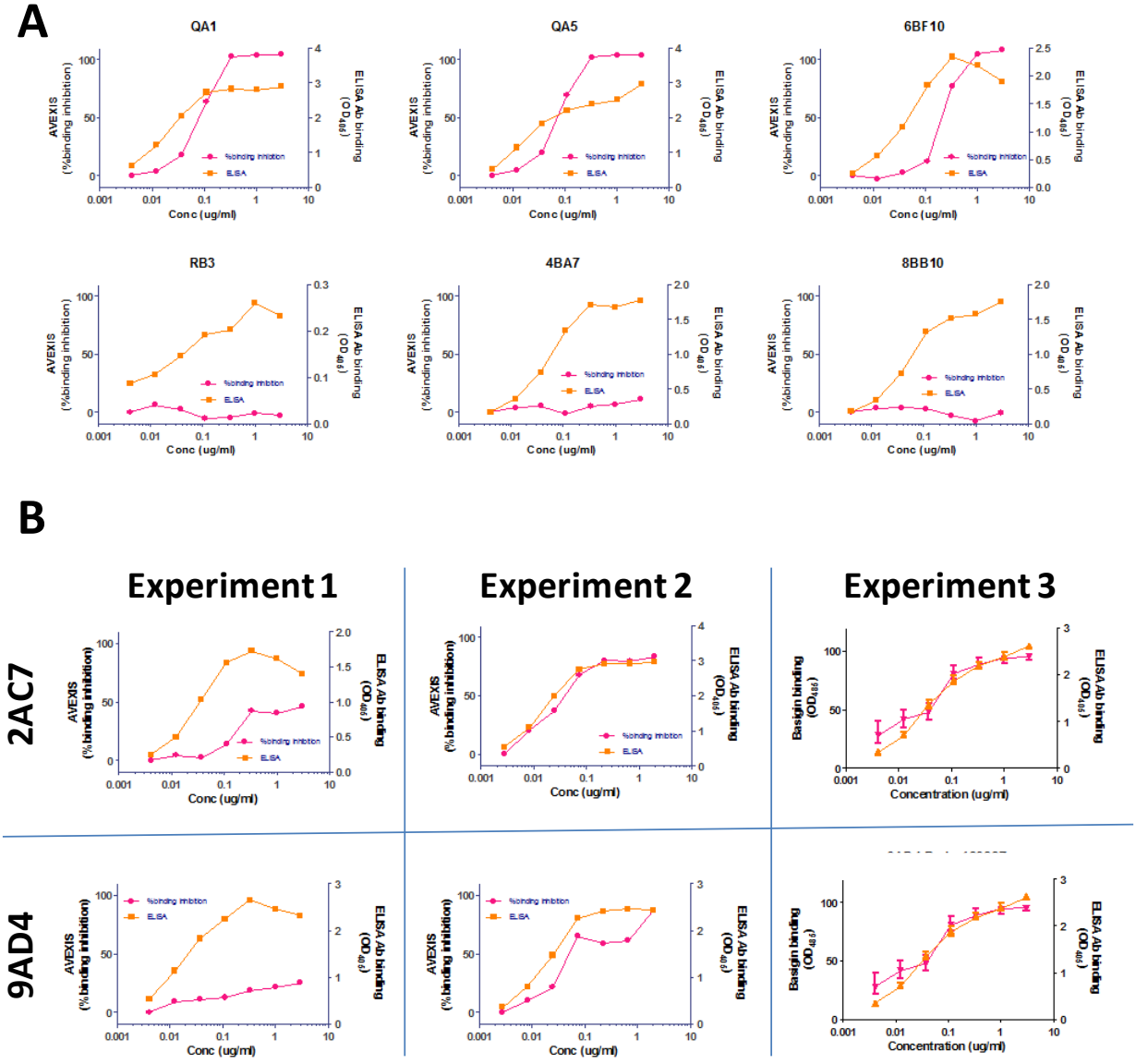

Figure 6.4.3.3: Effect of anti-RH5 mAbs on RH5-BSG interaction

Each sub-panel depicts the effect of an individual mAb tested at a range of concentrations (x-axes) upon the level of binding of basigin (pink line, left-hand axes). 0% binding was defined as the OD_{485} in the absence of BSG; 100% binding was defined as OD_{485} in the presence of RH5 and BSG without any mAb. To permit comparison to levels of binding of mAb, and estimation of the concentration of mAb which achieved saturation binding to RH5, total IgG ELISA was carried out using replicate wells with an identical gradient of concentrations of each mAb (orange line, right-hand axes).

Panel A shows results for mAbs with which consistent results were obtained in these experiments and reverse-orientation AVEXIS (plate-bound basigin; C Crosnier, data not shown). mAbs in the upper row (QA1, QA3, 6BF10) block the RH5-basigin interaction. mAbs in the lower row (RB3, 4BA7, 8BB10) do not block the interaction. Note the lower OD_{405} for ELISA with RB3 – this may reflect heterogeneity of the RH5 ELISA antigen, with some plate-captured molecules lacking the RB3 epitope (see below).

Panel B shows results for mAbs 2AC7 and 9AD4, for which results of reverse-orientation AVEXIS and repeat AVEXIS with plate-captured RH5 were inconsistent.

The ability of each of the mAbs to neutralise 3D7-strain parasites was tested in GIA assays (performed by Andrew Williams). We found that all three mAbs which were capable of complete blockade of the RH5-BSG interaction in the AVEXIS assay (QA1, QA5 and 6BF10) were capable of some degree of parasite neutralisation, although with varying levels of potency (Figure 6.4.3.4A). The three mAbs which had no effect upon the RH5-BSG interaction in AVEXIS neutralised parasites ineffectively, achieving no more than 20% GIA at 500µg/mL. The two mAbs which produced ambiguous results in the AVEXIS assay were highly potent in the assay of GIA, with EC_{50} values of 62µg/mL (9AD4) and <15µg/mL (2AC7). Although some caution must be exercised in comparing the results of different GIA assays, these EC_{50} values appear lower than those reported for the well-characterised anti-AMA1 mAbs 4G2 and 1F9 (Dutta, Haynes et al. 2005; Coley, Parisi et al. 2006). I am aware of only one report of an anti-merozoite mAb with a comparable GIA EC_{50} (directed against the rhoptry-associated protein complex) (Schofield, Bushell et al. 1986), and a further old report of a mAb with a surprisingly low EC_{50} of 50 ng/mL – this report has subsequently been questioned and never replicated (Schmidt-Ullrich, Brown et al. 1986; Saul 1987).

Of 18 laboratory strains for which the PfRH5 gene has previously been sequenced, FVO was most divergent from the 3D7 strain upon which the vaccine antigen used to raise the mAbs was based. Although the FVO and 3D7 RH5 sequences differ at only four amino acid positions(Hayton, Gaur et al. 2008), we proceeded to test the mAbs in GIA against FVO parasites, in light of the possibility that changes to crucially-positioned amino acid residues may affect individual antibody epitopes. mAbs which neutralised 3D7 remained effective against FVO, and in fact tended to be more effective against the heterologous strain (Figure 6.4.3.4B).

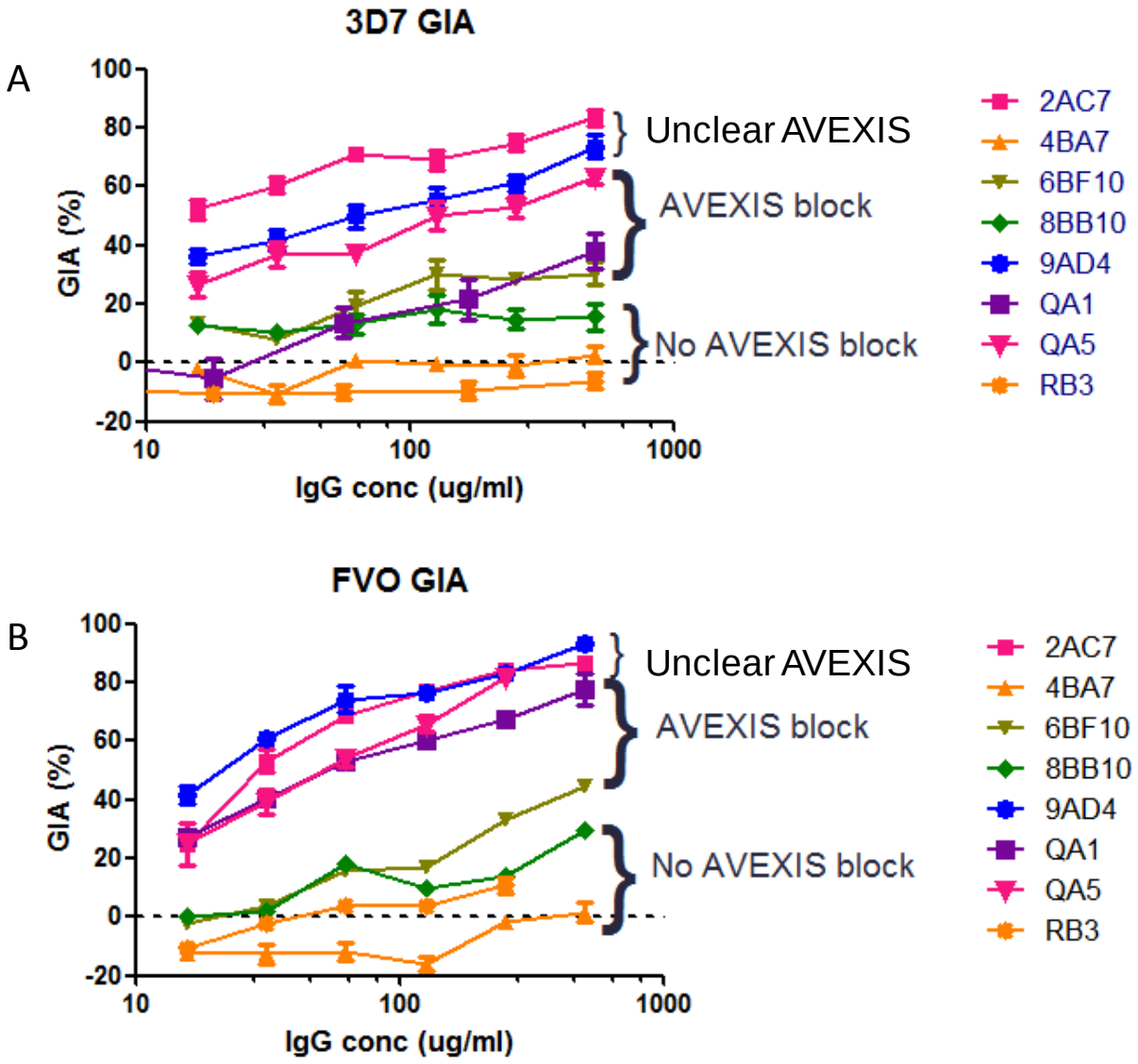

Figure 6.4.3.4 Effects of anti-RH5 mAbs in GIA assays

Anti-RH5 mAbs were tested in GIA assays at a range of concentrations against 3D7 parasites (panel A) and FVO parasites (panel B). Results displayed are the mean of two experiments with triplicate wells for 3D7, or a single experiment with triplicate wells for FVO. Error bars indicate inter-well SEM.

6.4.4. Mapping of inhibitory epitopes

To further explore the mechanism of action of anti-RH5 antibodies, and to shed light upon the regions of RH5 required for BSG binding, I attempted to map the binding sites of all 8 mAbs using a panel of overlapping 20mer peptides (Mimotopes Ltd, UK). The epitopes bound by four of the mAbs were successfully mapped: Figure 6.4.4.1A illustrates that each of these mAbs bound to a distinct linear epitope – either a single peptide, or an overlapping pair of peptides. Of these four antibodies, two had been shown to neutralise parasites in the GIA assay: QA5, and 9AD4.

The minimal linear epitopes bound by these two inhibitory antibodies were further defined using series of truncated peptides (Figure 6.4.4.1 B and D). Interestingly, each of these minimal epitopes contained one of the four amino acid residues which differ between 3D7 and FVO, but the antibodies remained capable of binding to equivalent peptides representing the FVO allele (Figure 6.4.4.1B and D). In order to evaluate which amino acid residues within these minimal peptides were particularly important for antibody binding, I assessed the ability of the mAbs to bind a further series of peptides in which each residue was sequentially mutated to alanine ('alanine walking'; Figure 6.4.4.1C and E).

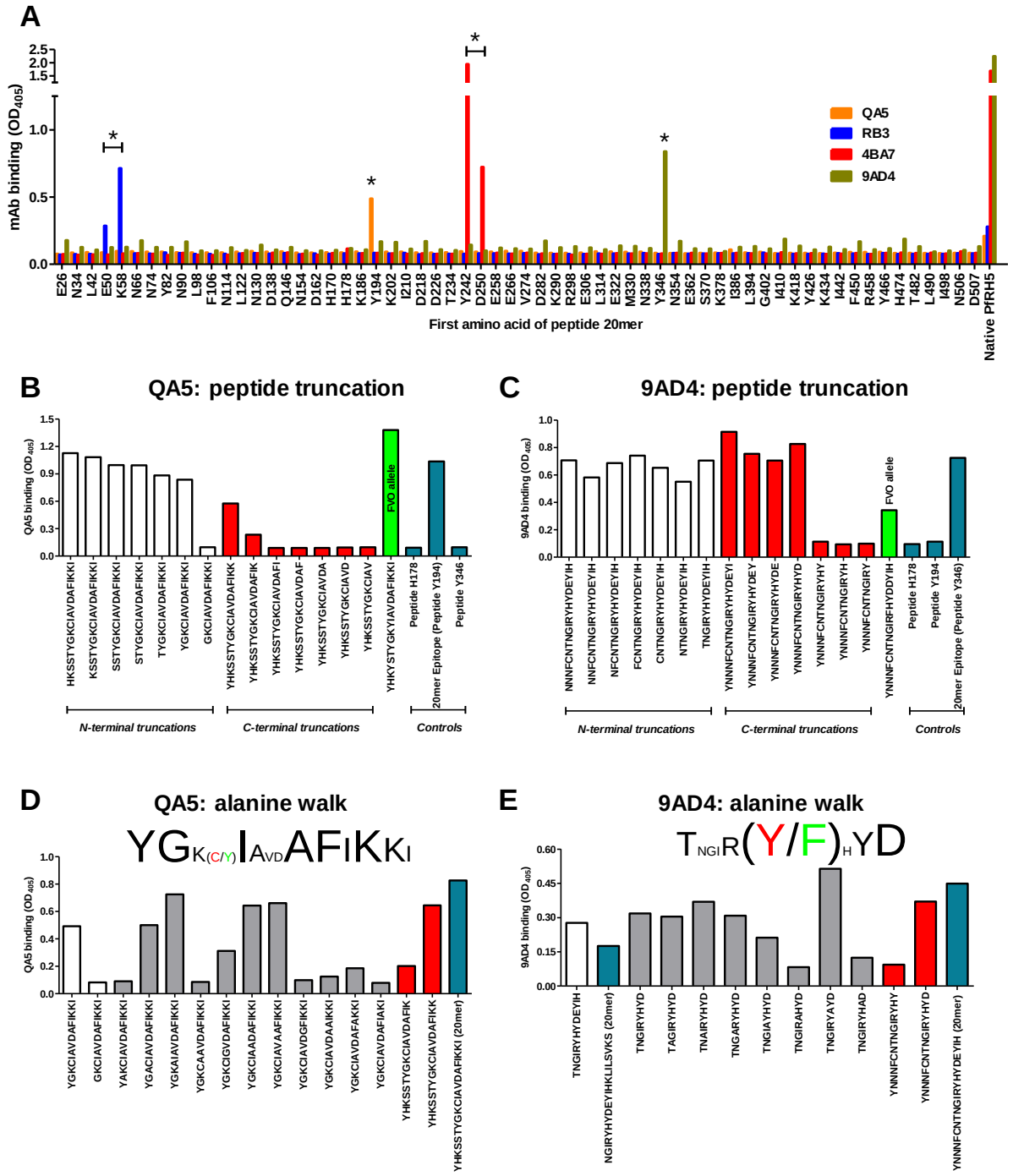

Figure 6.4.4.1 Mapping of linear epitopes for mAb binding
See following page for figure legend

Figure 6.4.4.1 Mapping of linear epitopes for mAb binding (previous page)
A: ELISA assessment of binding of mAbs to overlapping RH5-derived 20mer peptides. Numbering of amino acid residues indicates position within the RH5 antigen without any signal peptide (i.e. a 501 amino acid residue sequence, of which residues 1-5 = ENAIK). Stars indicate significant binding (OD_{405} values greater than 3 standard deviations above the mean for an individual monoclonal). There was no detectable binding of mAbs QA1, 2AC7, 6BF10 or 8BB10 to any peptide (data not shown). RB3 bound two overlapping peptides, EKDDIKNGKDIKKEIDNDKE and KDIKKEIDNDKENIKTNNAK. QA5 bound the peptide YHKSSTYGKCIAVDAFIKKI. 4AC7 bound two overlapping peptides, YDINNKNDDSYRYDISEEID and DSYRYDISEEIDDKSEETDD. 9AD4 bound the peptide YNNNFCNTNGIRYHYDEYIH.

Panel B illustrates binding of mAb QA5 to peptides progressively truncated from the N-terminus (white) and the C-terminus (red) of its 20mer-epitope YHKSSTYGKCIAVDAFIKKI. Results are the mean of two replicate assays. Truncation of the N-terminus beyond Y174 abrogated binding; truncation of the C-terminus beyond I188 progressively reduced binding, which was completely abrogated by truncations beyond K186. Binding to a 20mer with FVO strain sequence (YHKYSTYGKYIAVDAFIKKI; green) was similar to that to the 3D7-strain 20mer (blue).

Panel C illustrates binding of 9AD4 to progressively truncated peptides derived from its 20mer epitope YNNNFCNTNGIRYHYDEYIH, as shown for QA5 in panel B.

Panel D illustrates binding of QA5 to peptides with each of the internal amino acid residues in the sequence YGKCIAVDAFIKK progressively mutated to alanine (or glycine in the case of the two alanines in the native sequence). Results are the mean of two replicate assays; results obtained on the same plates with peptides from the N- and C-terminal truncation set are shown in white and red respectively. The lettering "YGKCIAVDAFIKKI" indicates the inferred linear epitope for QA5, with sizes of lettering proportional to the reduction in binding resulting from mutation of each amino acid; the red C indicates the residue which differs between 3D7 and FVO sequences.

Panel E illustrates binding of 9AD4 to the series of 'alanine walk' peptides within the inferred minimal epitope, as shown for QA5 in panel D.

A further two of the growth-inhibitory mAbS (QA1 and 2AC7) did not bind any of the set of peptides, suggesting that they recognise conformation-sensitive or discontinuous epitopes. To localise the QA1 and 2AC7 binding sites relative to the mapped QA5 and 9AD4 epitopes, and to assess the relationship of the QA5 and 9AD4 epitopes relative to each other on the folded antigen, I performed a competitive binding assay using surface plasmon resonance (SPR; Figures 5.4.4.2 and 5.4.4.3). Most strikingly, prior binding of 9AD4 was capable of complete blockade of subsequent binding of QA1, QA5 or 2AC7. The only pair of antibodies for which no binding competition was evident was QA1 and QA5.

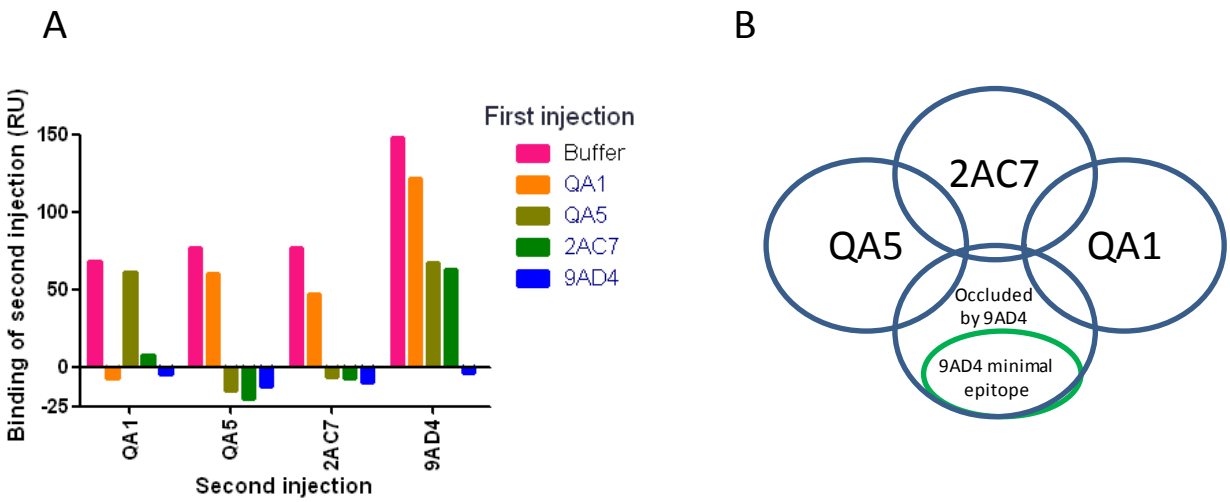

Figure 6.4.4.2: Competitive binding of growth-inhibitory mAbs
An SPR-based assay was used to assess competition between mAbs QA1, QA5, 2AC7 and 9AD4 for binding to chip-immobilized RH5. Panel A shows levels of binding (measured as SPR response units, RU) of each mAb when delivered as a second injection, preceded by a first injection comprising either buffer or another mAb. Reduction in binding when preceded by a particular mAb rather than buffer thus indicates competition between the two mAbs. Further data are shown in figure 6.4.4.3.

Panel B shows a schematic model of the binding sites of the four mAbs on the surface of the RH5 molecule; overlap between the blue circles indicates competition, suggesting overlap of the regions occluded by each mAb. mAb 9AD4 appears to be capable of binding to a minimal epitope which is unaffected by prior binding of any of the other mAbs; this may reflect heterogeneity in the protein coated on the chip (e.g. some chip-bound RH5 molecules may display a 9AD4 epitope but lack the epitopes for other mAbs).

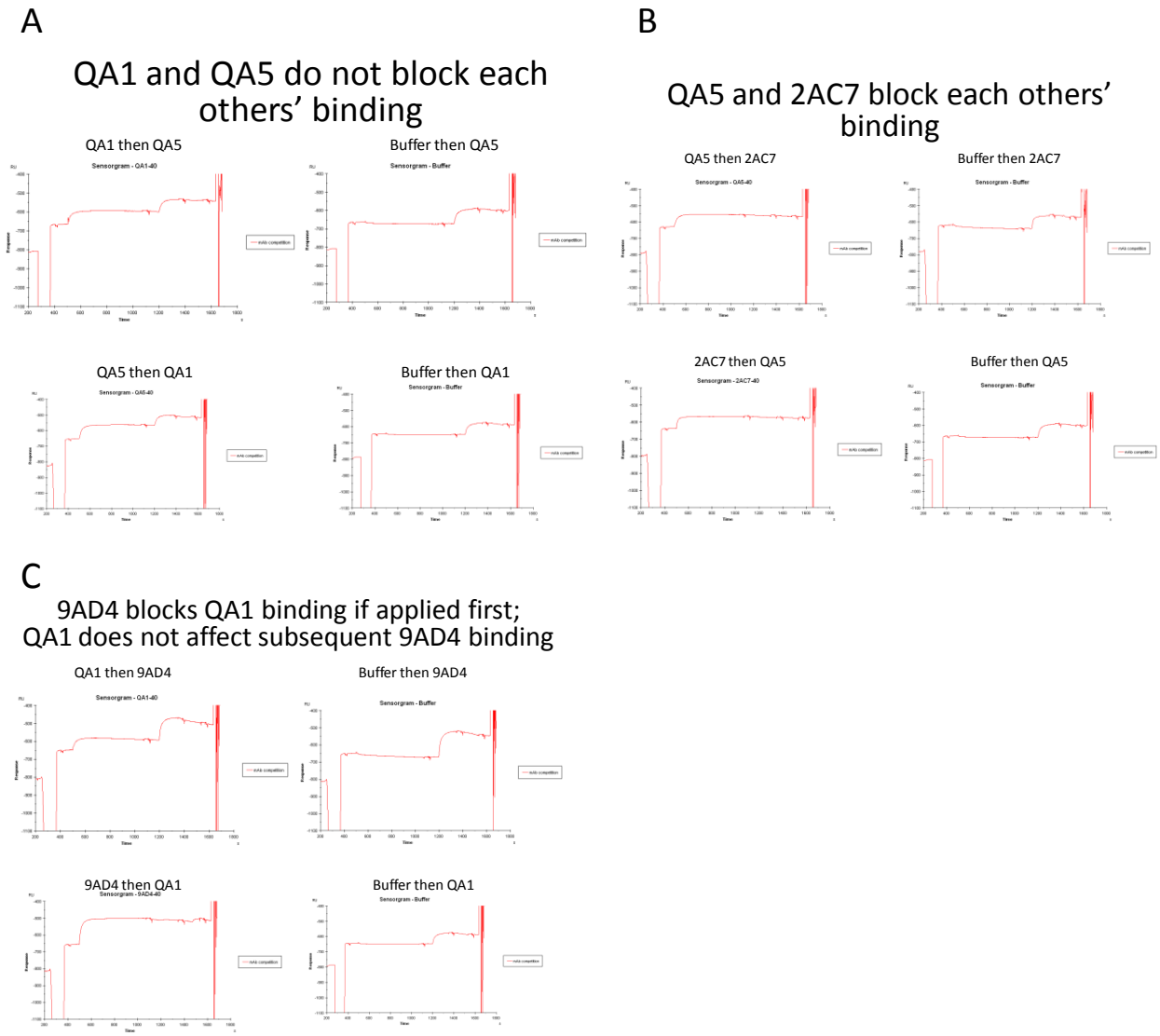

Figure 6.4.4.3 Competition binding by SPR- examples of response v time traces

For summary of results, see Figure 6.4.4.2. This figure illustrates selected results. Each sensorgram depicts four injections, and plots binding to the RH5-coated flow cell (Fc2) after subtraction of binding to the reference flow cell (Fc1). The preliminary injection (up to 400 seconds) is of RH5; approximately 200RU of antigen binds the chip. The next injection (from 500 seconds to 1100 seconds) is of either a mAb or buffer, as labelled (referred to as 'first injection' in Figure 6.4.4.2); in each case, this reaches saturation. The next injection (from 1200 seconds to 1350 seconds) is of a different mAb; binding of this injection is the response plotted in Figure 6.4.4.2. A final injection of the first mAb/buffer is performed from 1400 seconds to 1460 seconds; little or no binding is seen with this injection, confirming that binding of this mAb has remained close to saturation.

Panel A shows the results of competition between QA1 and QA5; these mAbs do not compete.

Panel B shows the results of competition between QA5 and 2AC7; these mAbs block each other's binding, regardless of the order of application.

Panel C shows the results of competition between 9AD4 and QA1. Prior application of 9AD4 completely blocks subsequent binding of QA1; prior application of QA1, however, has a relatively modest effect upon subsequent 9AD4 binding.

I also conducted overlapping-peptide epitope mapping ELISA using polyclonal rabbit and mouse anti-sera (Figure 6.4.4.4). The pattern of binding was similar between individual animals and between mice and rabbits. There was no detectable recognition of the majority of the peptides by either mouse or rabbit sera. Somewhat surprisingly, there was no recognition of the peptides bound by the QA5 and 9AD4 mAbs by any of two mouse and three rabbit serum samples. It is hard to understand why this should be the case when B cells producing antibodies with these specificities were clearly represented in the mouse spleens harvested for mAb generation 3 days after MVA immunisation. The best-recognised peptides were around the N-terminus (amino acid residues 1-20 and 49-93 of the antigen [numbered from the first amino acid after the signal peptide]) and C-terminus (amino acid residues 465-502); these regions may represent relatively unstructured regions of the protein. With both mouse and rabbit sera, recognition of heat-denatured RH5 was substantially weaker than that of unheated protein, emphasising the contribution of conformation-sensitive antibodies to the anti-RH5 response.

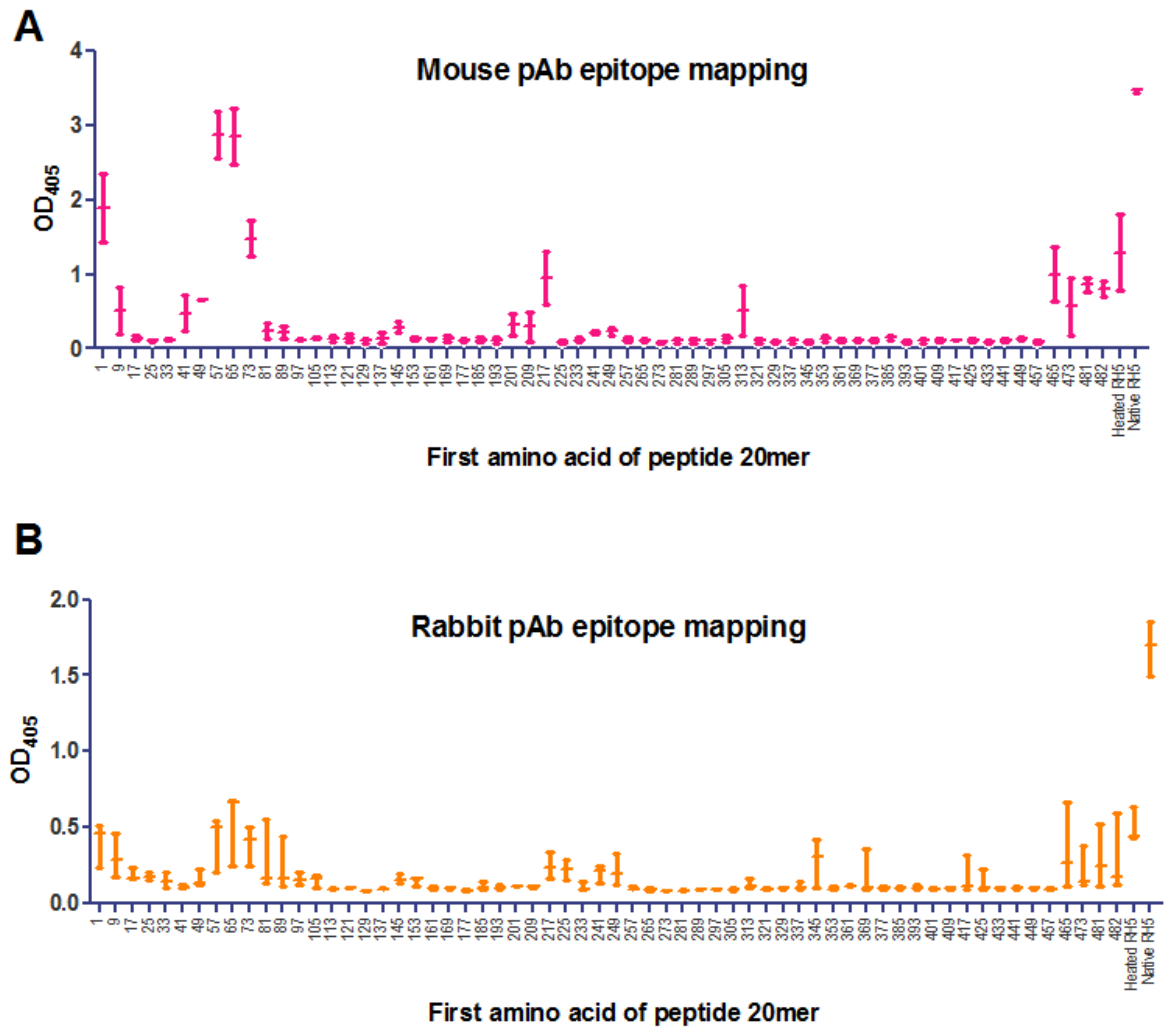

Figure 6.4.4.4 Mapping of linear epitopes recognised by polyclonal antisera

Panel A: Sera from two BALB/c mice immunized with AdHu5 RH5 and MVA RH5 vaccines ($1x10^8$ IU. and $1x10^7$ PFU with an 8 week interval) were collected two weeks after the boost vaccination. ELISA was performed to assess the binding of antisera to overlapping peptide 20mers spanning the RH5 sequence, as well as to RH5 protein and heat-denatured (boiled) RH5 protein. Sera were used at 1:1000 dilution Points / error bars depict median and range of measurements made using serum from two separate animals.

Panel B – results for rabbit antisera, as for panel A with the exception that n=3.

6.4.5. Kinetic characterisation of inhibitory monoclonals

The binding kinetics of selected mAbs were analysed by SPR. Rate constants and overall affinities of these mAbs are summarised in Table 6.4.5.T1; Figure 6.4.5.1 illustrates observed and model-fitted binding curves. Interestingly, on-rates of the most potent antibodies (2AC7 and 9AD4) were relatively high, and substantially higher than the value of $1x10^5$ $M^{-1}s^{-1}$ used to illustrate an influential previous discussion of kinetics of merozoite neutralisation by antibody(Saul 1987). Off-rates were sufficiently slow to result in interaction half-lives well in excess of the likely period of extracellular exposure of a viable merozoite. All four mAbs had K_D values in the range 2-7nM, such that even the lowest concentrations present during the GIA assay (15µg/mL = 100nM) would be >10-fold in excess of those required to achieve 50% binding at equilibrium.

The affinity of mAb QA5 for the 20mer peptide containing its epitope was substantially lower than that of QA5 for RH5 protein, with the difference largely attributable to a 10-fold higher off-rate. This suggests that, although the antibody is capable of binding to a linear epitope, an additional contribution to high-affinity binding is made by the conformation and context of the epitope within the folded protein.

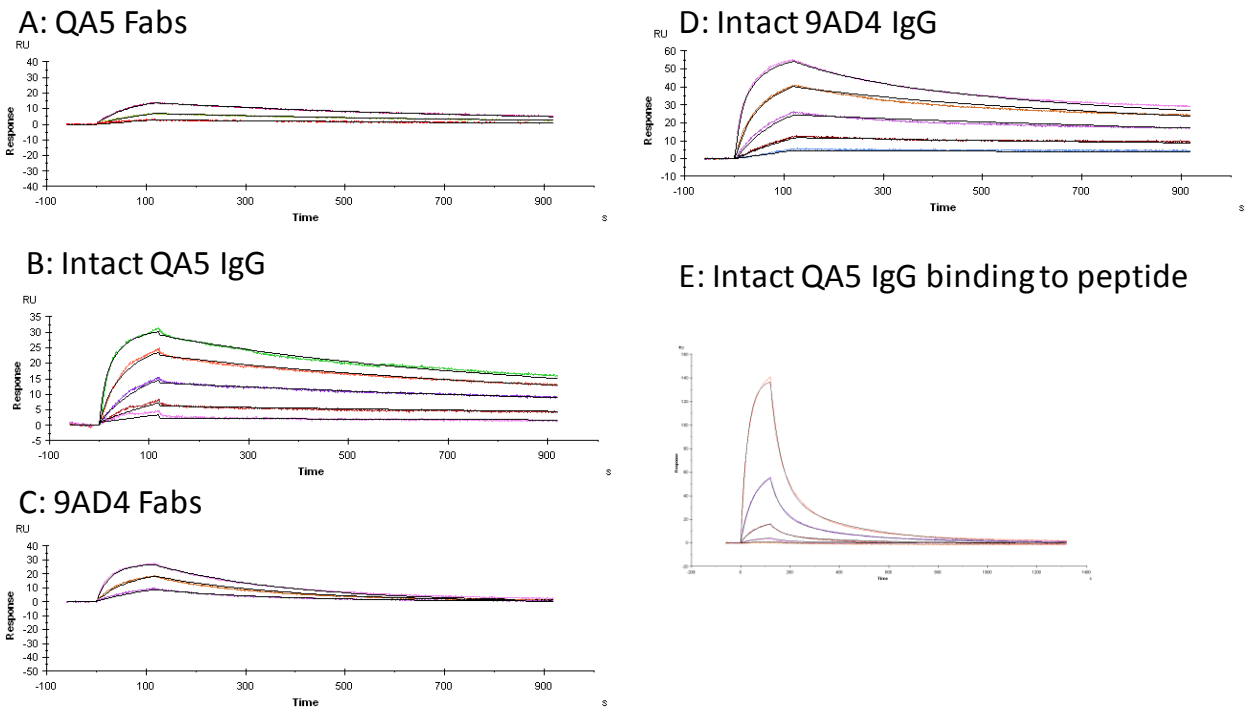

Figure 6.4.5.1: Kinetics of binding of monoclonal antibodies and Fabs.
Panel A depicts observed and 1:1 model-fitted binding of QA5 Fabs to RH5 protein at concentrations of 3, 1, and 0.3µg/mL.

Panel B depicts observed and bivalent model-fitted binding of intact QA5 IgG to RH5 protein at concentrations of 30, 10, 3.3, 1.1 and 0.37µg/mL.

Panel C depicts observed and 1:1 model-fitted binding of 9AD4 Fabs to RH5 protein at concentrations of 3, 1, and 0.3µg/mL.

Panel D depicts observed and bivalent model-fitted binding of intact 9AD4 IgG to RH5 protein at concentrations of 10, 3.3, 1.1, 0.37, and 0.12µg/mL.

Panel E depicts observed and bivalent model-fitted binding of intact QA5 IgG to peptide YHKSSTYGKCIAVDAFIKKI at concentrations of 40, 10, 2.5, 0.625 and 0.156µg/mL. Note that the density of potential mAb binding sites on the chip (and hence the maximal level of binding, R_{max}) was substantially higher in this experiment than for experiments with RH5 protein as the antigen, and that the observed dissociation time was longer. Unlike for QA5 binding to protein (panel B), it is clear that the majority of QA5 dissociates from the peptide within 1 minute of the start of the dissociation phase.

Ligand	Analyte	Replicate	$k_{on}=k_a$ (k_a1 if bivalent) $M^{-1}s^{-1}$	$k_{off}=k_d$ (k_d2 if bivalent) s^{-1}	K_D (or k_d1/k_a1 if bivalent) M	K_D (µg/mL)	Interaction half-life (min)
RH5	**QA1**	1	2.39E+05	0.00173	7.24E-09		
		2	1.06E+05	0.001968	1.86E-08		
		Median	**1.72E+05**	**1.85E-03**	**1.29E-08**	1.9	6
RH5	**QA5**	1	9.87E+04	6.93E-04	7.02E-09		
		2	1.36E+05	0.001162	8.58E-09		
		Median	**1.17E+05**	**9.28E-04**	**7.80E-09**	1.2	12
RH5	**QA5 Fab**	1	2.33E+05	0.001255	5.38E-09		
		2	1.73E+05	0.001287	7.46E-09		
		Median	**2.03E+05**	**1.27E-03**	**6.42E-09**	1.0	9
Peptide	**QA5**	1	3.44E+04	0.0194	5.64E-07	85	0.6
RH5	**2AC7**	1	1.36E+06	6.79E-04	5.01E-10		
		2	4.94E+05	0.00258	5.22E-09		
		Median	**9.26E+05**	**1.63E-03**	**2.86E-09**	0.4	7
RH5	**9AD4**	1	1.21E+06	0.00111	9.17E-10		
		2	6.30E+05	0.002917	4.63E-09		
		Median	**9.20E+05**	**2.01E-03**	**2.78E-09**	0.4	6
RH5	**9AD4 Fab**	1	5.58E+05	0.003755	6.73E-09		
		2	4.33E+05	0.003508	8.10E-09		
		Median	**4.96E+05**	**3.63E-03**	**7.41E-09**	1.1	3

Table 6.4.5.T1: Kinetic characterisation of anti-RH5 mAbs

6.4.6. Anti-RH5 Fabs are capable of merozoite neutralisation

In order to further elucidate the mechanism of parasite neutralisation by anti-RH5 antibody, I wished to compare the effectiveness of monovalent Fabs and intact IgG in the assay of GIA. Previous studies of Fabs derived from polyclonal and monoclonal antibodies against AMA1 have suggested that these neutralise parasites at least as effectively as intact IgG (Dutta, Haynes et al. 2005; Collins, Withers-Martinez et al. 2007). In contrast, Fabs are markedly less potent than intact IgG at neutralising certain viruses (Edwards and Dimmock 2000). Such differences may arise from the enhanced avidity of bivalent binding, cross-linking of antigen by intact IgG, or greater steric hindrance effects by the larger intact IgG molecule.

I generated Fab preparations by digestion using papain (for mouse IgG2a mAbs and rabbit IgG) and ficin (for mouse IgG1 mAbs). Coomassie-stained gels of the Fab preparations demonstrated that the mAb-Fab samples were >90% pure, without substantial contamination by intact IgG, and the rabbit-Fab samples were approximately 70% pure (Figure 6.4.6.1). In GIA experiments performed by Andrew Williams and Dennis Awuah, we observed that Fabs derived from the QA5, 2AC7 and 9AD4 inhibitory mAbs had GIA EC_{50} values approximately 10-fold higher than those obtained with intact IgG (Figure 6.4.6.2). At higher concentrations, however, Fabs proved as effective as intact IgG. Rabbit polyclonal Fab samples were marginally less potent than intact IgG in parasite neutralization at low concentrations, but had similar EC_{50} values.

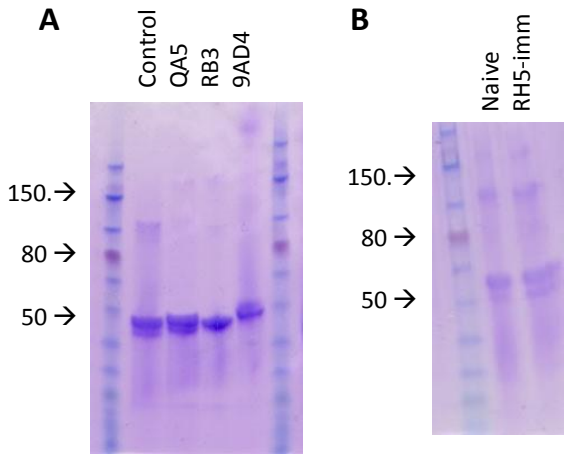

Figure 6.4.6.1 Coomassie-stained non-reducing non-boiled SDS-PAGE gel of Fab preparations

Panel A shows mAbs (control = irrelevant IgG1 isotype control)

Panel B shows rabbit polyclonal antibody derived from malaria-antigen naive and RH5-immunised rabbits.

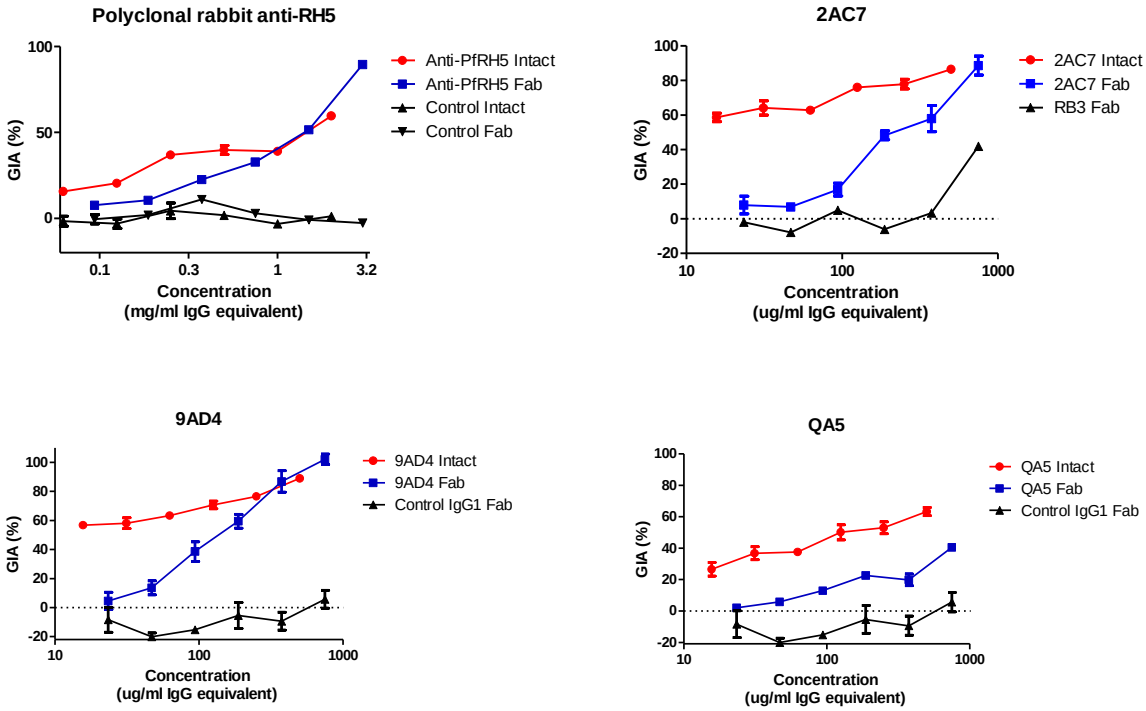

Figure 6.4.6.2: GIA with anti-RH5 Fabs as compared to GIA with intact IgG
Panels A-D show results with total polyclonal rabbit anti-RH5, mAb 2AC7, mAb 9AD4 and mAb QA5 respectively. In each case, GIA with intact IgG is plotted in red, GIA with Fabs is plotted in blue, and controls are plotted in black. Results are mean of two assays, each with three replicate wells; error bars plot inter-well SEM. Irrelevant control rabbit IgG and Fab (black line panel A) and intact/ Fab-digested mAbs (data not shown) did not induce significant GIA.

Concentrations are shown as 'IgG equivalent'. For Fabs, this is the weight/volume concentration of IgG which would have the same molar concentration of antigen-binding sites (i.e.1.5x the w/v Fab concentration). A case could also be made for representing Fab concentrations as the concentration of IgG which would have the same molar concentration of molecules (i.e. 3x the w/v Fab concentration). The latter representation would right-shift the Fab concentration v. GIA curves, increasing the apparent discrepancy between the Fab and intact IgG GIA effects.

To exclude the possibility that the digestion process had reduced the RH5 binding activity of the Fabs, I measured the concentration of bio-active RH5-binding 9AD4 Fab and the on-rate of the interaction using SPR techniques (calibration-free concentration analysis [see Chapter 4] and multi-cycle kinetic analysis respectively). The measured values were 50% lower than those obtained with the intact IgG, a difference insufficient to explain the 10-fold discrepancy in the GIA results.

6.5. DISCUSSION

The work reported in this chapter attempted to begin the important process of understanding the mechanism of *P. falciparum* neutralisation by anti-RH5 antibodies, in the hope that understanding of this process could assist in the design of improved strategies to inhibit erythrocyte invasion. This initial effort has generated reagents and some preliminary data which should help to facilitate and inform future studies; in some respects, however, it has raised more questions than it has answered.

6.5.1. Timing of RH5 action during invasion process

The finding that RH5 does not appear to be localised on the surface of non-permeabilised merozoites suggests that it may only become accessible to vaccine-induced antibody after the merozoite contacts the red cell. If this is the case, the time window in which anti-RH5 must act to block invasion may be shorter than 30 seconds; indeed, if the antibody is acting between red cell contact and reorientation or TJ formation, this period may be as short as 11 seconds(Gilson and Crabb 2009). Such a brief period of antigen exposure will place substantial kinetic constraints upon the binding of antibody, making it all the more surprising that anti-RH5 appears to be so effective (Saul 1987). Work currently under way is attempting to elucidate whether the contact of free merozoites with soluble glycophorin is sufficient to result in RH5 release onto the erythrocyte surface. Such a result would be consistent with previously published data(Singh, Alam et al. 2010). Of note, however, there is some debate in the field about the timing of release of merozoite adhesins, and other laboratories have reportedly been unable to detect EBA-175 on the surface of free merozoites (E Knuepfer, personal communication).

Although one IFA study reported localisation of RH5 to the moving junction around the actively invading merozoite (Baum, Chen et al. 2009), subsequent efforts to study the fine localisation of RH5 by IFA or immuno-electron microscopy have not been particularly successful (Riglar, Richard et al. 2011), largely due to lack of clarity of staining by anti-RH5 antibodies. I had hoped that the high-titre polyclonal antibodies and mAbs generated using the RH5 viral vector vaccines may permit immuno-

EM studies, but preliminary experiments using these reagents were unsuccessful (D Ferguson, personal communication).

The results of the merozoite attachment assay suggest an effect of anti-RH5 antibody upon the reorientation of merozoites and/or subsequent TJ formation. Notably, however, the level of inhibition of attachment with 10 mg/mL polyclonal anti-RH5 IgG was in some assays as low as 50-60%, whereas this antibody concentration would reliably result in >90% GIA against 3D7 strain parasites. This is somewhat suggestive that anti-RH5 antibody may be having some additional effect, i.e. that the invasion of even some of the parasites which had apparently reoriented may yet be blocked by the antibody. Ongoing work will attempt to address this question using a number of approaches. Firstly, planned video microscopy studies may demonstrate whether anti-RH5 does indeed block reorientation. However, it is common for merozoites to contact and then detach from red cells without reorientation even in the absence of antibody (Gilson and Crabb 2009); clear demonstration of antibody-mediated reorientation blockade is therefore likely to require recording of a large number of schizont rupture events – a painstaking process. Secondly, IFA using a marker of TJ formation, for example the assembly of a RON4 ring (Riglar, Richard et al. 2011), may clarify whether merozoites which reorient despite the presence of anti-RH5 antibody have formed TJs, or whether this has been blocked by the antibody. However determining TJ formation by IFA remains somewhat subjective. A final planned approach which may allow more objective scoring of TJ formation is transmission electron microscopy (TEM) of merozoite attachment assay specimens (prepared in the presence of anti-RH5 antibodies, but *without* necessarily using immuno-gold). The formation of TJs is relatively unambiguous under TEM (Srinivasan, Beatty et al. 2011).

6.5.2. Relationship of parasite neutralisation to RH5-BSG binding blockade

Comparison of the effects of the anti-RH5 mAbs in AVEXIS and GIA assays has suggested that there is not a straightforward relationship between the ability of a mAb to block the RH5-BSG interaction and its ability to neutralise parasites. While mAbs which blocked the RH5-BSG interaction did

consistently neutralise parasites, it was striking that some mAbs which potently blocked the interaction as measured by AVEXIS had modest effects in GIA (e.g. QA1), while the two mAbs which were most potent in GIA had inconsistent effects in the AVEXIS assay (9AD4 and 2AC7). It is of considerable interest to establish whether these antibodies truly are capable of blockade of the RH5-BSG interaction or not. The extremely high parasite-neutralising potency strongly suggests that these mAbs are blocking a crucial part of the invasion process. If this is not the RH5-BSG interaction, such antibodies may instead be blocking the interaction of RH5 with another binding partner (with Ripr being a prime candidate). Alternatively, of course, this potency may arise not from a specific block of the interaction of RH5 with a partner, but instead simply from steric and cross-linking effects of the binding of antibodies with high on-rates to a critical and dynamic component of the invasion machinery – 'spanners in the works' – a result supported to some extent by the loss of potency of 2AC7 and 9AD4 Fabs relative to intact IgG.

It is quite plausible that the ability of a mAb to block an interaction in the AVEXIS assay may not be representative of its ability to do so in the context of a GIA assay: it seems worthwhile to give some consideration to possible reasons for such misleading results. Firstly, artefactual results may arise due to the multivalent binding of the pentameric AVEXIS prey to the plate-bound bait, and the bivalent binding of the mAb. Such effects could include antibody-mediated cross-linking of prey (when RH5 is the pentameric prey), potentially resulting in apparent *enhancement* of the binding of RH5 to BSG by mAbs which do not block the interaction – such effects were seen with mAbs 4BA7, 8BB10, and possibly also with 2AC7 and 9AD4 when the assay was performed by Cécile Crosnier. The closely packed molecular context of mAb, pentameric prey and immobilised bait may also result in a particular risk of artefactual steric hindrance of binding by a mAb which would not block the monomeric BSG-RH5 interaction.

Secondly, artefacts may arise due to differing affinities of the mAbs for RH5. Accurate kinetic analysis is prevented by the facts that the concentrations of the RH5 and BSG used in the assay were both

unknown (both are used as labelled but unpurified constituents of culture supernatant), and that mAb binding may have occurred bivalently. However the range of mAb concentrations used in the AVEXIS assays (0.003 - 10 µg/µL = 20pM - 67nM) spanned the measured K_D values for mAbs analysed by SPR, and were lower than the concentrations tested in GIA. The most potent interaction-blocking mAbs (such as QA5) were capable of complete blockade of the interaction at around 1µg/µL (6.7nM) – very close to their measured K_D, and it is perhaps unsurprising that effective blockade would not occur at concentrations beneath the K_D. It is probably more relevant to examine whether blockade occurs at the higher concentrations, in excess of K_D, which are present in GIA wells.

Moreover, when performed with plate-bound RH5 and pentameric BSG, mAb was applied as a separate step (followed by washing) preceding the application of BSG. Dissociation of RH5-mAb complexes may have been occurring during BSG binding; the half-lives of the monovalent mAb RH5 interactions were brief enough that substantial dissociation may have occurred during the hour of incubation with BSG – the extent of such unphysiological dissociation may have varied considerably between mAbs with differing k_{off} values. In retrospect, such unphysiological dissociation could readily be prevented by ensuring that mAb, RH5 and BSG are simultaneously present, as was the case when the assay was performed with plate-immobilized basigin.

Unambiguous demonstration of whether mAbs 2AC7 and 9AD4 do indeed affect the RH5-BSG interaction is clearly a priority. An SPR approach similar to that used for the mAb competition binding experiments may achieve this, minimising the potential for artefactual results due to multimeric interactions and unphysiological kinetic effects: for example assay of whether the binding of monomeric basigin to chip-bound monomeric RH5 can be prevented by an immediately preceding injection of a saturating concentration of Fab. I have not had access to the reagents (e.g. purified basigin and/or RH5) to permit such an experiment, but hope that this may be a possibility in the near future.

In vitro assays of the ability of vaccine-induced polyclonal sera to blockade the interaction of parasite adhesins and their receptors have previously been proposed to be useful readouts of functional antibody induction, and hence potential surrogates of *in vivo* protection (Chitnis and Sharma 2008). The result presented here suggest that, at least for RH5, such an approach will be of limited value: given the possibility of multiple mechanisms of antibody action, it is probably more relevant to study the ability of vaccine-induced antibodies to achieve GIA – a functional readout much more closely related to the *in vivo* situation. Of course, for other parasite species, notably *P vivax,* for which *in vitro* neutralisation assays remain challenging, receptor-ligand binding blockade assays may have a larger role.

6.5.3. Kinetics and valency of antibody binding

As was the case for the assays of antibody-mediated blockade of RH5-BSG interaction, the reagents available for the SPR measurement of the kinetics of mAb-RH5 binding have not been optimal, as reflected by the fairly substantial inter-replicate variability of the measurements. Because of a lack of purified RH5, these experiments were conducted using chip-bound biotinylated RH5 and injections of mAbs. Such experiments are complicated by the potential for bivalent mAb binding and for variations in the concentration of bio-active mAb relative to contaminants such as aggregates in each sample. Such impurities would influence the protein concentration of the sample (as measured by A_{280}), artificially reducing the apparent k_{on} and K_D. The design of the experiments attempted to minimise the effects of bivalent mAb binding by using sparse capture of RH5 on the chip, fitting a bivalent binding model, and replicating observations using Fabs where possible. Nonetheless, it would be preferable to conduct these experiments with chip-immobilised mAb, allowing accurate comparison between mAbs of the kinetics of monovalent mAb binding to a single preparation of gel-filtered, aggregate-free purified RH5.

As the mAb kinetic data currently stand, they raise the possibility that binding on-rate may be an important parameter in determining neutralisation potency. This seems highly plausible, because parasite neutralisation is constrained to occur within a brief window of antigen exposure, and a doubling in on-rate will have the same effect upon the rate of antibody-antigen binding as a doubling in concentration. Such a relationship has previously been demonstrated for anti-viral antibody responses, although the study used rate of virus neutralisation as a proxy for on-rate, rather than direct biophysical measurement (Roost, Bachmann et al. 1995). However unlike for antibody-virion interactions, for which binding kinetics can be studied by immobilising whole virions on the SPR chip and for which neutralisation kinetics can be studied by leaving neutralisation reactions to proceed for varying periods of time before applying virions to cells, study of the kinetics of antibody-merozoite interactions is not currently possible. One cannot assume that the measured on-rate of antibody binding to protein on a chip is directly related to the '*in vivo* on-rate' for antibody in its molecular micro-environment on the merozoite surface. The relationship between duration of antigen exposure and the *in vivo* on-rate as well may be an important factor, alongside an antigen's functional importance and immunogenicity, in determining how sensitive the parasite is to antibody directed against a particular antigen. The on-rates of the mAbs reported in the current study are within the 10^5-10^6 $M^{-1}s^{-1}$ range which has been proposed to represent a biophysical limit, determined by protein diffusion rates rather than the nature of the antibody binding site(Northrup and Erickson 1992; Foote and Eisen 1995). It has been suggested in studies of humans vaccinated with tetanus toxoid that this limit is reached after a single vaccination, and that on-rates are not further enhanced by boost vaccinations (Poulsen, Jensen et al. 2011). mAbs with k_{on} values around 10^6 $M^{-1}s^{-1}$ are, however, regularly described, suggesting that the diffusion limit is at the upper end of the proposed range: changes in the mean k_{on} of vaccine-induced polyclonal antibody *within* the 10^5-10^6 $M^{-1}s^{-1}$ range could have the same effect as a 10-fold increase in antibody concentration. The tetanus toxoid study did not take account of the potential effect of adjuvants upon affinity. It is not clear, therefore, whether antibody on-rate is a parameter which can be enhanced via somatic

hypermutation or clonal selection, and hence which the vaccinologist can or should attempt to influence through vaccine design, such as adjuvant selection. This may well be a question worthy of further investigation.

While mAb on-rates are plausibly related to their neutralisation potency, it is arguably less likely that off-rates are relevant. Modern antibody-inducing vaccine platforms are capable of inducing antigen-specific antibody concentrations well in excess of 15µg/mL (100nM; 10-fold higher than mean antibody k_D values achieved after a single alum-adsorbed tetanus toxoid vaccination (Poulsen, Jensen et al. 2011)). Few blood-stage vaccine developers believe that BSVs will achieve protection without concentrations above this level. In the relevant *in vivo* situation, therefore, antibody concentrations are well in excess of those required to bind the majority of antigen at equilibrium, and the time taken for a merozoite to complete invasion is likely to be far shorter than the dissociation half-life of an antigen-antibody complex which has formed (Gilson and Crabb 2009). Antibody binding is therefore close to being irreversible within the relevant timescale: the rate at which antigen is complexed, largely determined by the on-rate and concentration, is therefore likely to be more relevant than off-rate (Saul 1987) (see also section 9.2.4). Although an association between antibody off-rate and risk of disease was recently reported in an immuno-epidemiological study of natural immunity to malaria, such evidence is far from establishing a causal link (Reddy, Anders et al. 2012): it seems quite likely that off-rate could be simply a marker of another immune response induced by repeated exposure. Indeed, the same study demonstrated that off-rate decreased with increasing age (and hence, presumably, increasing prior malaria exposure) (Reddy, Anders et al. 2012).

The experiments conducted here with anti-RH5 Fab suggested a significant reduction in the potency of parasite neutralisation by Fabs as compared to intact IgG. This contrasts with the lack of effect of digestion of anti-AMA1 antibodies upon their neutralising potency (Dutta, Haynes et al. 2005; Collins, Withers-Martinez et al. 2007), and is suggestive that there is some additional neutralising

action of intact anti-RH5 IgG beyond simple occlusion of RH5's BSG-binding sites. Given the slow-off rates of the monovalent mAb-RH5 interactions and the high molar concentrations of antibody present in the GIA assays relative to the K_D, avidity of the bivalent interaction seems relatively unlikely to be a major factor in this context. It is possible that antibody-induced impedance of the movement of RH5 molecules relative to each other, and relative to other proteins, may be enhanced by cross-linking of RH5 molecules and the presence of the bulkier intact IgG molecule.

A further and intriguing possibility is that bivalent anti-RH5 IgG binding may have an 'active' or 'gain-of-function' effect upon the parasite, rather than resulting in a simple 'loss-of-function' of RH5 in BSG binding. There is increasing understanding of the cascade of signalling events involved in co-ordinating the events occurring at the extracellular RBC-merozoite interface and the intracellular invasion machinery. Although RH5, lacking a transmembrane domain, is not the most obvious candidate for a signalling molecule, it is possible that the binding of certain anti-RH5 antibodies could mimic the engagement of parasites with the RBC, triggering premature activation of downstream invasion events. Such a 'gain-of-function' effect could potentially achieve parasite killing with a low level of antigen-antibody occupancy, lowering the antibody concentration required for neutralisation: for this reason, discovery of an antigen vulnerable to such an effect could have considerable value in reducing the quantity of vaccine-induced antibody required to achieve protection against disease.

Overall, however, the reduction in potency of anti-RH5 Fabs is relatively modest compared to the potency changes observed when some virus-neutralizing mAbs are digested, which may exceed 100-fold(Edwards and Dimmock 2000). Despite this potency reduction, it is clear that monovalent binding of anti-RH5 Fabs can achieve high levels of GIA, an observation consistent with the hypothesis that simple blockade of the interaction of RH5 with its binding partners is a major contributor to parasite neutralisation.

6.5.4. Value of epitope mapping

Perhaps the clearest data provided by this work has been the identification of linear epitopes recognised by the growth inhibitory mAbs QA5 and 9AD4. This epitope mapping suggests two regions of the protein which are likely to be surface-exposed, and at least in the case of the QA5 epitope, likely to be closely related to the basigin binding site. The competition binding experiments have suggested that the inhibitory mAb epitopes are likely to be fairly closely clustered together.

It has previously been found that accessible surface area (A, in square angstroms, $Å^2$) of globular proteins, is approximately related to mass (M, in daltons), according to equation 5.5.1(Janin 1979):

$$A \approx 11.1M^{2/3} \qquad \textit{Equation 5.5.1}$$

This would suggest that the 63 kDa RH5 molecule has a surface area of approximately 18000 $Å^2$ (or 14000 $Å^2$ in the case of its 45 kDa processed form (Baum, Chen et al. 2009)). Crystallographic studies of antibody-antigen complexes have suggested contact areas of 200-800$Å^2$ (Newman, Mainhart et al. 1992; MacCallum, Martin et al. 1996). The overlapping epitopes recognised by the growth inhibitory mAbs QA5, 2AC7, 9AD4 and QA1 are therefore likely to occupy only a small fraction of the molecule's surface. The fact that a substantial proportion of the mAbs raised bind this region suggests that it is at least strongly immunogenic, if not immuno-dominant. It is possible however that the hybridoma screening ELISA, which employed RH5 with a C-terminal CD4d3+4 tag and bound to the plate via a C-terminal biotin moiety, may have skewed the distribution of selected antibodies towards those for which the epitopes were accessible with the antigen in this format. It will be of interest in future work to establish whether the epitopes bound by non-inhibitory mAbs cluster in distinct areas from those bound by inhibitory mAbs (as assessed by competition binding).

One reason for mapping the epitopes bound by neutralising mAbs is the belief that improved understanding of such epitopes may facilitate the design of improved immunogens, and such efforts have played major roles in efforts to design immunogens capable of inducing broadly-neutralising

antibodies against influenza and HIV. In the case of these pathogens, such mAbs are extremely rare when the immune system is presented with the intact protein; in the case of RH5, the situation appears to be somewhat different. Potent anti-RH5 responses do not appear to be induced in the context of natural infection, but nor do strong responses to non-neutralising RH5 epitopes; when the immune system is presented with RH5 in the form of subunit vaccine, a substantial proportion of the induced Abs appear to be capable of strain-transcending neutralisation. It is therefore questionable whether reduction of the RH5 immunogen to a 'minimal inhibitory region' is desirable: any such reduction would have to be conducted with great care to avoid reducing the immunogenicity of the molecule by removing $CD4^+$ T cell epitopes, and to avoid affecting the conformation of the neutralising epitopes. The 100-fold reduction in affinity of QA5 for its linear epitope as compared to for RH5 protein illustrates that even where 'linear neutralising epitopes' can be identified, they may be poor mimics of the protein immunogen. It seems optimistic to suppose that a peptide or misfolded protein vaccine would induce a particularly effective antibody response against the antigen as presented by the parasite. Rather than assisting vaccine development by leading to development of a reduced RH5 immunogen, identification of inhibitory epitopes on the RH5 surface may instead help to ensure that future vaccine formulations, which may include particulate or multimeric RH5 antigens, do indeed present these epitopes rather than burying them internally.

6.5.5. Concluding remarks

Each of the groups of experiments described in this chapter has provided some information regarding the mechanism of action of anti-RH5 antibody, and each has posed further questions. The experimental tools now available to address these questions – notably imaging, interaction analysis by surface plasmon resonance, and genetic manipulation of parasites – are considerably more powerful than were available to facilitate studies of the mechanism of action of anti-AMA1 antibodies over the past 10-20 years. It seems likely that this will be an area of interest for a number of groups for some time to come, but that data may be generated quite rapidly over the coming months and years. Hopefully the mAbs generated here will play an important role in this effort.

Clearly better understanding of the invasion process, and in particular the parts of it which are closely related to RH5, may highlight promising novel antigens for future blood-stage vaccines. Almost as a separate issue, it is important to consider whether these mAbs can contribute more directly to efforts to develop RH5-targeting vaccines and therapeutics.

The idea of developing antimalarial drugs targeting merozoite invasion is frequently proposed. Although the superficial logic for such drugs seems attractive – parasites must invade to cause disease – the rationale may not withstand closer scrutiny. Firstly, the kinetic constraints imposed by the brief window of merozoite exposure would apply to non-membrane-penetrant drugs as well as to vaccine-induced-antibodies, requiring a high drug dose to be effective: this would be a particular issue for drugs with relatively high manufacturing costs, such as mAbs. Secondly, speed of action of drugs is a key factor when treating severely ill patients. One of the reasons proposed for the superior efficacy of artemisinins relative to other antimalarials is their unique activity throughout the asexual cycle, contributing to a rapid onset of action (within minutes of administration) (O'Neill, Barton et al. 2010). Severe malaria is thought to be caused mostly by mature parasites, for example via sequestration in the microvasculature (Miller, Good et al. 1994), but invasion-targeting drugs would have no impact on the density of such mature parasites for around 24 hours after administration. It

therefore seems highly questionable whether such drugs could ever be front-line antimalarials, although an adjunct role (e.g. as a 2nd component in a combination with a faster-acting drug) is perhaps conceivable. These anti- RH5 mAbs are thus unlikely to have direct therapeutic value. However the original motivation for the development of these reagents was indeed to use them *in vivo* – not as therapeutics or to probe basic parasitology, but instead as translational tools, for passive transfer studies to clearly demonstrate a causal link between parasite-neutralising antibody and protection against *P. falciparum.* This remains an important and viable possibility, and will be discussed further in Chapter 9.

7. Analysis of subpatent parasite density data following experimental human malaria infection

Use of mathematical models to infer vaccine efficacy from quantitative PCR data

7.1. AUTHORSHIP STATEMENT

ADD performed all numerical analysis reported in this Chapter. qPCR analysis was performed by Nick Edwards and Laura Andrews. I am grateful for the input and advice of Philip Bejon.

The data analysed here were obtained during clinical trials led by Susanne Sheehy, Chris Duncan, Geraldine O'Hara, David Porter, Susie Dunachie, Michael Walther, Dan Webster, Fiona Thompson and others.

7.2. INTRODUCTION

Preliminary efficacy screening of candidate malaria vaccines using controlled human malaria infection (CHMI) with the bites of *Plasmodium falciparum*-infected mosquitoes is a well established procedure, allowing relatively quick and cost-effective prioritisation and optimisation of vaccines prior to expensive and time-consuming efficacy trials in the field (Andrews, Andersen et al. 2005).

Following such challenges, quantitative PCR (qPCR) monitoring of volunteers' sub-patent parasite density is routine (Hermsen, Telgt et al. 2001; Andrews, Andersen et al. 2005).

A substantial problem for blood-stage vaccine development has been uncertainty regarding whether a vaccine effect could be detected in the pre-patent period, and hence detected in a CHMI trial, or whether such effects might become apparent only after microscopic patency. This uncertainty, compounded by the fact that even quite large changes in blood-stage parasite multiplication rate (PMR) would be expected to have minimal effects upon the time to microscopic patency after mosquito-bite challenge (Sanderson, Andrews et al. 2008) has led to a belief that blood-stage vaccine candidates may not be adequately assessed by CHMI trials, but instead may require expensive field efficacy trials. I recently published an analysis illustrating that the effects of natural immunity are indeed apparent as a reduction in PMR in the pre-patent period (Douglas, Andrews et al. 2011). Uncertainty remains regarding whether PMR can be accurately measured after sporozoite-challenge CHMI.

A variety of mathematical models have been used to analyse qPCR data to estimate vaccine effects upon the liver-to-blood parasite inoculum (LBI) and upon PMR (Cheng, Lawrence et al. 1997; Hermsen, de Vlas et al. 2004; Bejon, Andrews et al. 2005; Roestenberg, de Vlas et al. 2012). The reliability and comparability of these methods are unknown, despite the fact that they may have a critical role in evaluating vaccine efficacy.

Pre-erythrocytic vaccines may produce non-sterile partial protection, reflected by a reduction in LBI in vaccinees relative to controls. Asexual blood-stage vaccines (BSVs) may reduce the blood-stage parasite multiplication rate (PMR) in vaccinees relative to controls, and may also result in pre-erythrocytic efficacy, due to expression of blood-stage antigens during the late liver stage. The ability to measure and distinguish these two types of vaccine effect may thus be of considerable importance.

Moreover, mathematically-measured PMR is likely to be a more sensitive measure of partial BSV efficacy than time to microscopic patency. It has previously been noted that reductions in PMR of <50% are unlikely to likely to result in a detectable effect upon time to patency after mosquito-bite CHMI (Hermsen, de Vlas et al. 2004; Sanderson, Andrews et al. 2008). Although a recent report suggested that BSV vaccine efficacy could readily be assessed in such trials (Roestenberg, de Vlas et al. 2012), the authors assumed very substantial vaccine effects upon PMR (>70% reductions).

The main types of models which have been used for this purpose are as follows: simple exponential growth (Cheng, Lawrence et al. 1997); sine-wave based functions (Simpson, Aarons et al. 2002; Bejon, Andrews et al. 2005); and a waveform based upon the cumulative density function of the normal distribution ('normal-CDF based') (Hermsen, de Vlas et al. 2004). A recent WHO meeting to discuss challenge trial endpoints highlighted the lack of consensus regarding which modelling method should be used and recommended that both sine-wave and normal-CDF based models should be used until this controversy can be resolved (Moorthy, Diggs et al. 2009).

qPCR data covering at least one full parasite lifecycle has now been collected from 273 subjects who have undergone sporozoite challenge in Oxford. This chapter describes the use of this large data set to compare approaches to analysis of these data. Because estimation of PMR for individuals is a primary purpose of parasitemia monitoring for asexual blood-stage vaccines (to permit, for example, correlation of immune parameters with PMR), the analysis was restricted to models capable of providing individual-level estimates of both LBI and PMR. More complex models designed to address variation in the parasite population or host responses over periods of microscopically patent growth were not included (Molineaux, Diebner et al. 2001; Dietz, Raddatz et al. 2006; Recker, Buckee et al. 2011). The reproducibility of LBI and PMR estimates produced by different methods is compared, and the ability of the models to predict out-of-sample observations is assessed.

7.3. METHODS

7.3.1. Volunteers, qPCR, software, models

Data was drawn from all qPCR-monitored sporozoite challenge trials conducted in Oxford up to December 2011- a total of 14 challenges including 301 volunteers, of whom 6 were re-challenged on a subsequent occasion. 18 volunteers were infected using cryopreserved sporozoites administered intramuscularly or intradermally (Sheehy et al, manuscript in preparation); all other volunteers were infected by the bites of five mosquitoes. For the 183 volunteers in the first nine trials (McConkey, Reece et al. 2003; Walther, Dunachie et al. 2005; Webster, Dunachie et al. 2005; Dunachie, Walther et al. 2006; Dunachie, Walther et al. 2006; Walther, Thompson et al. 2006; Thompson, Porter et al. 2008; Porter, Thompson et al. 2011) the qPCR method of Andrews was used (Andrews, Andersen et al. 2005). For the 118 volunteers in the four most recent challenge trials, a second qPCR method was used, as described elsewhere (Ewer et al submitted, Sheehy et al submitted). Briefly, this method involves filtration to remove leucocytes, using a Whatman VFE multi-well filter plate, followed by DNA extraction using a QiaAmp kit (Qiagen), and a Taqman-probe based real-time quantitative PCR assay (Hermsen, Telgt et al. 2001).

The absolute minimum quantity of data for modelling was considered to be 2 positive PCR data points separated by 48hrs, leaving data from a total of 274 volunteers for analysis (108 with the current PCR method; 166 with the previous method). Modelling was conducted using Stata version 11 (StataCorp, Texas); graphs were produced using Stata and Prism 5 (Graphpad Software).

The following methods of LBI and PMR estimation were compared. Further details of the models, including parameter definitions, are described in table 7.3.1.T1. Phrases in parentheses and quotes indicate shorthand subsequently used to refer to each method.

1. Direct qPCR quantification of LBI ('first cycle peak'). Regarding the maximum measured parasite density during the first bloodstage generation (up to day 8.25) as a measure of the LBI.

2. Exponential model ('linear')

$\log_{10}(PCR) = m(day - 7.5) + c$

3. Sine-wave model ('sine') (Simpson, Aarons et al. 2002)*:*

$\log_{10}(PCR) = c + m(day-6.5) + a[\sin [\pi*(day-6.5) + k]$

4. Normal CDF model ('**N-CDF**') (Hermsen, de Vlas et al. 2004)*:*

$$\mathrm{PCR} = \beta_1 x * \sum_{g=1}^{10}\left(\beta_2{}^{g-1} * \left(F\left(\frac{(day-[\mu_1+\mu_2(g-1)+\mu_3(g-1)])}{\sqrt{(\sigma_1+(g-1)(\sigma_2+\sigma_3))}}\right) - F\left(\frac{(day-[\mu_1+\mu_2 g+\mu_3(g-1)])}{\sqrt{(\sigma_1+\sigma_2 g+\sigma_3(g-1))}}\right)\right)\right)$$

(Where g represents parasite generations since leaving the liver, F(x)=CDF of standard normal distribution). As has previously been described, μ_1 μ_2, σ_1, σ_2, and σ_3 were regarded as constants, estimated using data from previous studies (Hermsen, de Vlas et al. 2004).

5. Ratios of geometric mean parasitemia in first and second blood-stage parasite lifecycles ('cycle means') (Roestenberg, de Vlas et al. 2012). For this purpose, a 40-hour parasite lifecycle was assumed (see supplementary figure 1B-C), with the first lifecycle extending from day 7.0 to day 8.25, and the second cycle from day 8.25 to day 9.90; data from each cycle was only analysed if the time of diagnosis for that volunteer was more than half-way through the cycle. This model was fitted to a subset of volunteers who were qPCR positive at all timepoints during this period.

For each subject, results prior to the first point >20p/ml were treated as missing. All subsequent points <20p/ml or negative were replaced with 10p/ml.

Table 7.3.1.T1: Parasitemia model comparisons

Model	Vaccine-relevant estimated parameters		Additional parameters			
	LBI (parasites/ml)	**PMR (fold/48hr)**	**Constant**	**Gradient**	**Lifecycle time intervals**	**Synchronicity**
Exponential	Fitted value on day 7.5	10^{2m}	c	m	n/a	n/a
Sine wave	$10^{(\|a\|+c)}$	10^{2m}	c	m	2 day lifecycle duration; k shifts phase of sine wave and could be considered to adjust for variable time of liver release.	a (determines sine wave amplitude)
Normal CDF	$\beta_1 x$	β_2 Per (mu2+3) days. (Corrected to fold per 48hrs for comparison with other models)	$\beta 1x$	β_2	μ_1 time to liver release μ_2 period a ring remains unsequestered μ_3 period between sequestration and re-invasion	$\sigma_1^2, \sigma_2^2, \sigma_3^2$ Variances in μ_1, μ_2, μ_3 respectively.

7.3.2. Comparison of predictive accuracy of models

For the three approaches which fit a model (linear, sine and N-CDF), the capacity of models to predict future parasite density was assessed by fitting each model to each individual's data, omitting the final two PCR points. An out-of-sample forward prediction was then made for the final recorded PCR point prior to treatment, and the error in this prediction (relative to the actual recorded PCR value) calculated. Further assessment of predictive capacity was performed using leave-one-out-cross-validation (LOOCV), in which each model was successively re-fitted to an individual's data with each single data point omitted in turn. The root mean square error (RMSE) of the LOOCV prediction was calculated for each individual.

7.4. RESULTS

7.4.1. Clinical trial qPCR data

Figure 7.4.1.1A demonstrates that the Taqman-based qPCR method is highly accurate, with a coefficient of variation (%CV) less than 10% for parasite densities exceeding 40p/ml, and in the range 10-100% for parasite densities of 10-40p/ml. The accuracy of the previous (SybrGreen-based) qPCR assay has previously been reported(Andrews, Andersen et al. 2005).

The periodicity of parasitemia over the first 96 hours of blood-stage growth is illustrated by figure 7.3.1.1B-C. Troughs in parasitemia are separated by approximately 40 hours (i.e. at days 8.3, 9.9 and 11.6), similar to the *in vitro* lifecycle duration of 3D7.

22/94 mosquito-bite challenge subjects studied using the Taqman assay were positive at levels above 20p/ml. Figure 7.4.1.2A demonstrates that the maximum PCR value on day 7 is predictive of time of subsequent diagnosis, and that this relationship was stronger when the Taqman qPCR assay was used. Figures 7.4.1.2B-C demonstrate that the majority of volunteers are qPCR positive during the first cycle using the Taqman assay, while a number of subjects studied with the SybrGreen assay became qPCR positive later, sometimes with high levels of parasitemia; such results may reflect false-negative results with the SybrGreen assay at earlier timepoints.

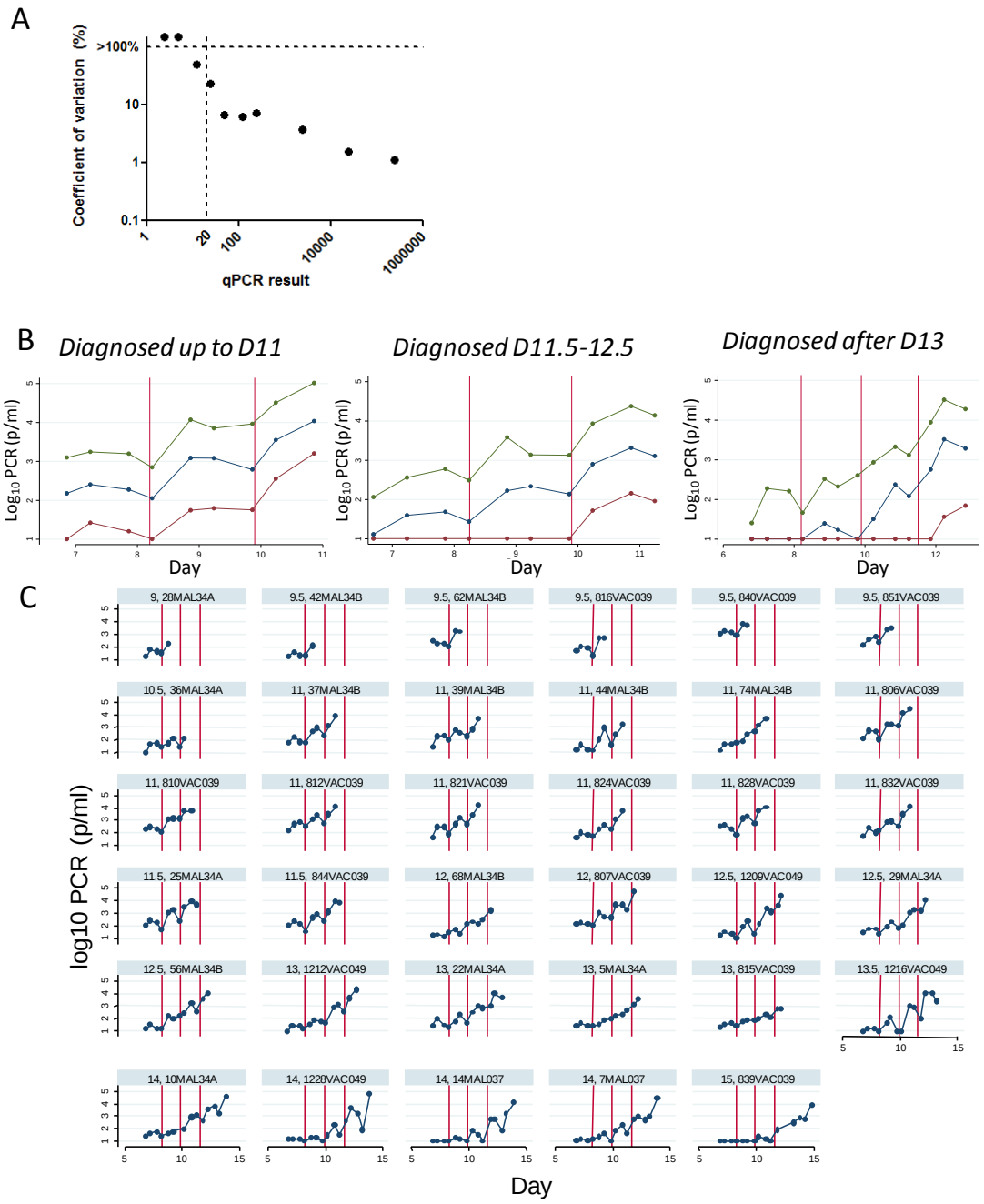

Figure 7.4.1.1 Accuracy of Taqman qPCR assay and timecourses of qPCR results

Panel A: Accuracy of Taqman qPCR assay. Sorbitol-synchronised ring-stage 3D7 parasites were cultured and counted using a haemocytometer and Giemsa-stained thin film microscopy. A dilution series of parasites was spiked into 2ml whole blood-samples, producing parasite densities ranging from 240,000 to 2.4p/ml. 8 replicate DNA extractions and PCR assays were performed (each PCR assay included 3 replicate wells). Figure illustrates coefficient of variation (ie inter-DNA-extraction standard deviation as a percentage of result) versus parasite density.

Panel B: Timecourse of parasitemia for subjects in Taqman-assayed trials, grouped by time of diagnosis as indicated in sub-panel captions. Blue line indicates median parasitemia for each group, with red and green lines indicating 10th and 90th centiles respectively. Red vertical lines at day 8.2, 9.9 and 11.6 highlight 'troughs' of parasitemia, separated by 40 hours. qPCR-negative points are plotted at log_{10}(PCR)=1.

Panel C: Parasitemia timecourses for 35 randomly selected individuals, ordered by time of diagnosis. Red vertical lines as in panel B.

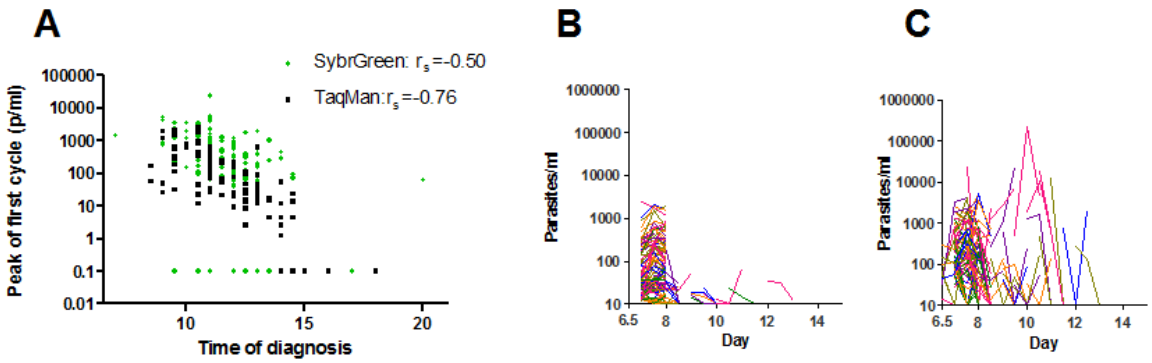

Figure 7.4.1.2 First peaks of parasitaemia measured with Taqman and SybrGreen qPCR assays
Panel A: Relationship between time of diagnosis and peak parasitemia during first generation after liver egress, comparing results obtained with SybrGreen and Taqman assays. r_s= Spearman rank correlation coefficient; p<0.001 for both assays, but strength of correlation is greater with Taqman assay.

Panel B: First quantified peak of parasitemia using Taqman assay. Graph illustrates the first PCR-positive data point and the two following points for each of 108 subjects in trials for which Taqman assay was used, plotted versus time of sampling.

Panel C: First quantified peak of parasitemia using SybrGreen method. As for panel B; 166 subjects.

7.4.2. Models fits similar lines and produce similar parameter estimates

Figure 7.4.2.1 illustrates the lines fitted by the different models to a subset of volunteers.

Figure 7.4.2.2 demonstrates the close relationship between LBI and PMR estimates produced by linear, sine and normal-CDF models (and, for the LBI estimates the qPCR-measured peak parasite density during the first blood-stage parasite lifecycle). For subjects studied using the Taqman-based PCR method, Pearson correlation coefficients exceeded 0.92 for all comparisons between LBI-estimation methods, and exceeded 0.75 for all comparisons between PMR-estimation methods.

As has recently been proposed (Roestenberg, de Vlas et al. 2012), PMR was also estimated using the geometric mean parasitemia in the first and second lifecycles for a subset of volunteers without any negative data points over this period. Figure 7.4.2.3 demonstrates the results of this approach, which correlated reasonably with the linear model (Pearson r=0.45).

Unexpectedly, it was found that PMR estimates produced by all methods correlated negatively with the peak first-cycle parasite density (Figure 7.4.2.4). Although these relationships were relatively weak, they were highly statistically significant (r_s=-0.32, -0.25 and -0.31 for linear, sine and N-CDF PMR estimates respectively; p<0.0001 for all three). Similar relationships were apparent between PMR estimates and model-estimated LBI values (data not shown).

Figure 7.4.2.1 Comparison of lines fitted by different models using qPCR data from a random subset of 20 volunteers (overleaf)
Throughout, blue dots indicate qPCR measurements, plotted at $log_{10}2$=0.3 if negative; red vertical lines indicate approximate divisions between parasite lifecycles at days 8.2, 9.9 and 10.6 (as per supplementary figure 2). Volunteers are ordered by time of blood-film diagnosis.

Panel A depicts lines fitted by linear model (red).
Panel B depicts lines fitted by sine-wave model (red).
Panel C depicts lines fitted by normal-CDF model (red).

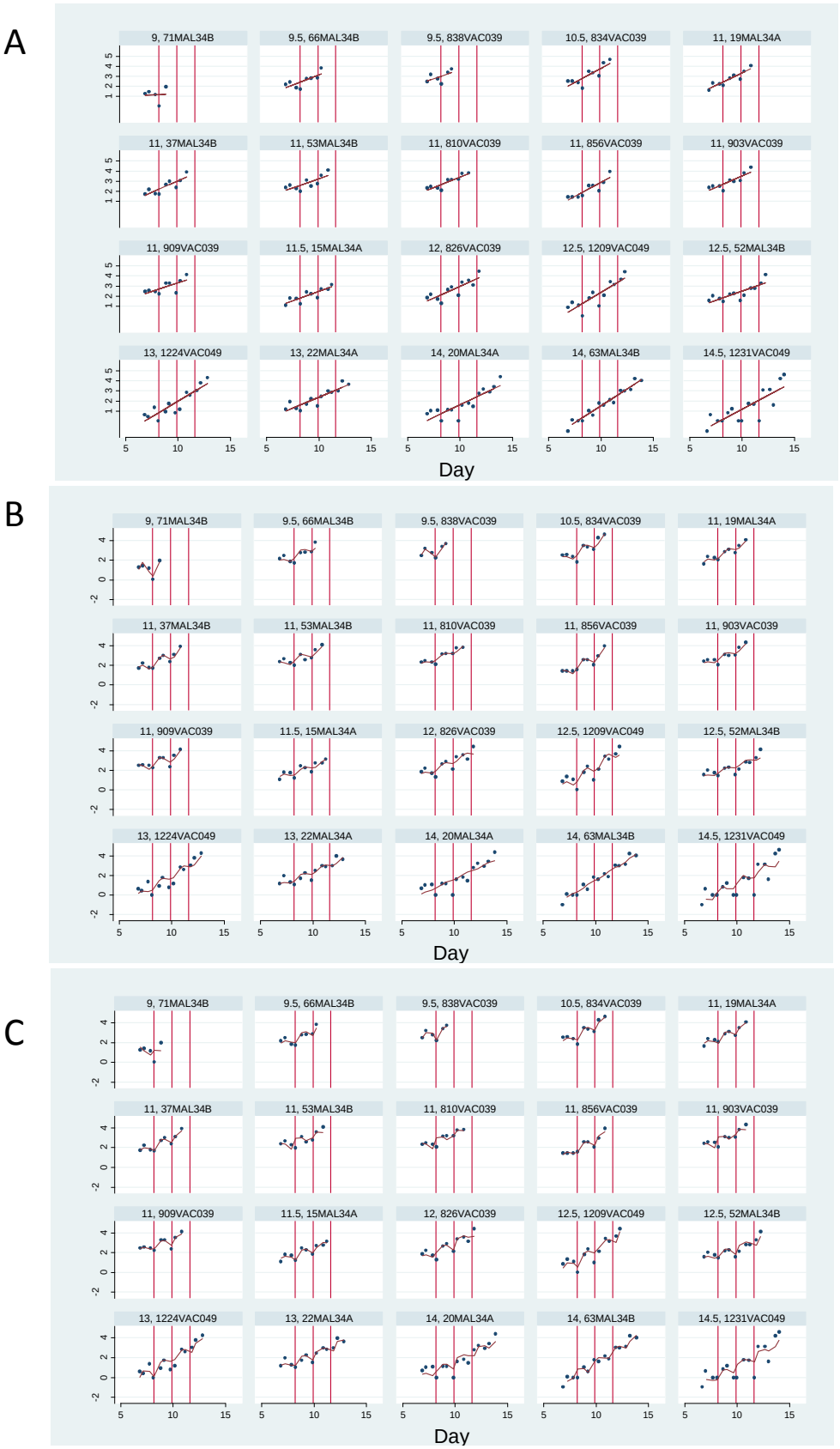

Figure 7.4.2.1 Comparison of lines fitted by different models using qPCR data from a random subset of 20 volunteers

See previous page for figure legend

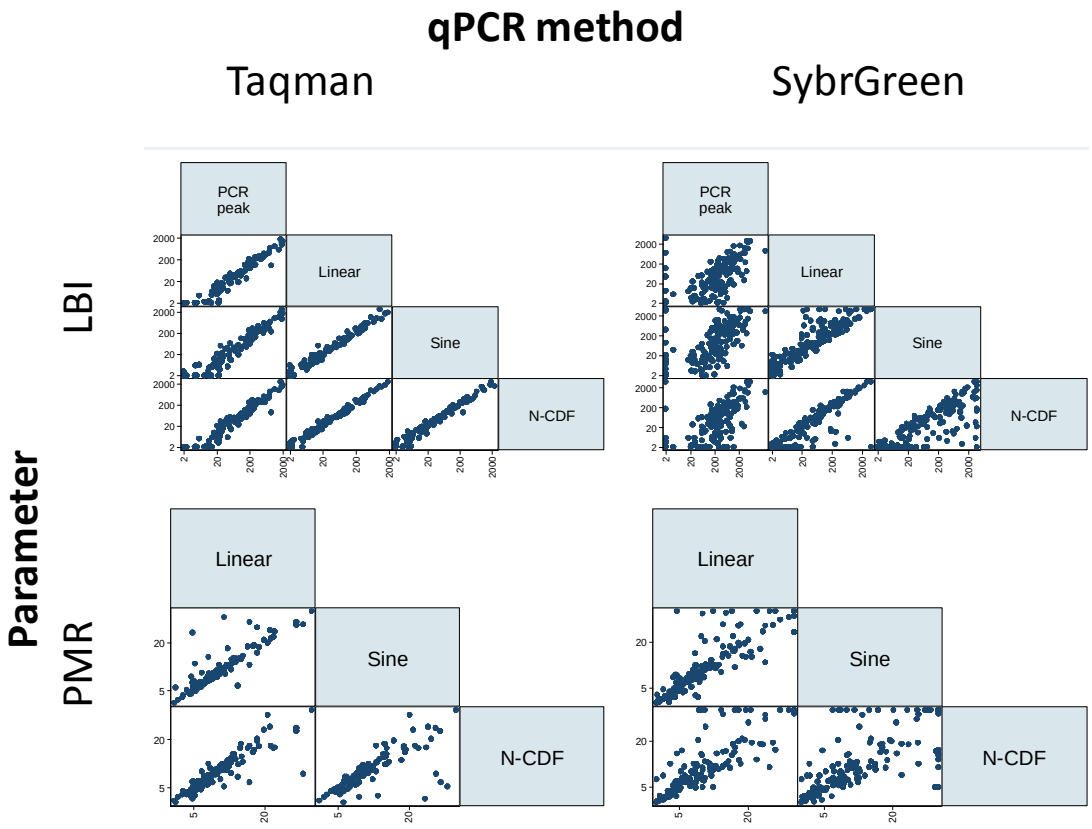

Figure 7.4.2.2 LBI and PMR estimates from different models

Upper left: Matrix scatterplot illustrating close correlations of LBI estimates from linear, sine-wave and normal-CDF (N-CDF) models with each other and with the peak measured parasitemia in the first blood-stage life-cycle, for studies conducted using Taqman assay. LBI estimates <2p/ml are plotted at 2, and >2000 at 2000.

Upper right: Matrix scatterplot illustrating close correlations of LBI estimates from linear, sine-wave and normal-CDF (N-CDF) models with each other and with the peak measured parasitemia in the first blood-stage life-cycle, for studies conducted using SybrGreen assay. LBI estimates <2p/ml are plotted at 2, and >2000 at 2000.

Lower left: Matrix scatterplot illustrating correlations of PMR estimates from linear, sine-wave and normal-CDF (N-CDF) models, for studies conducted using Taqman assay. PMR estimates >30-fold per 48hrs are plotted at 30.

Lower right: Matrix scatterplot illustrating correlations of PMR estimates from linear, sine-wave and normal-CDF (N-CDF) models, for studies conducted using SybrGreen assay. PMR estimates >30-fold per 48hrs are plotted at 30.

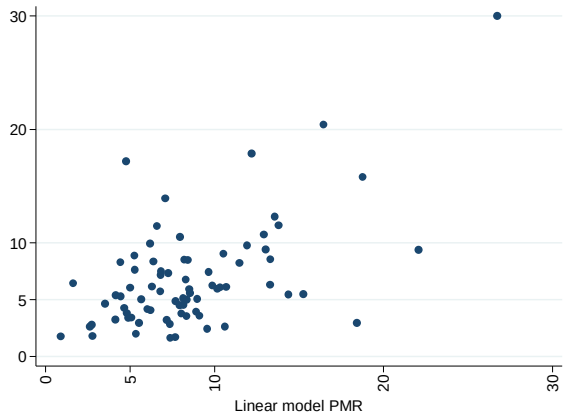

Figure 7.4.2.3 PMR estimates obtained using linear model and using ratio of geometric mean parasitemia in first and second asexual cycle.
Analysis was restricted to subjects with qPCR-positive data points throughout these cycles.

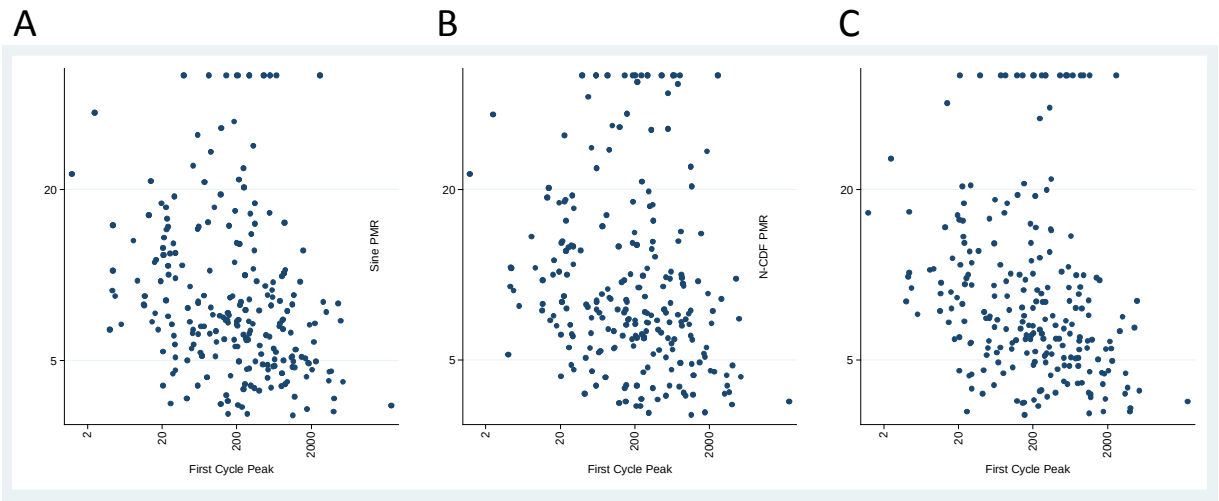

Figure 7.4.2.4 Relationship between PMR estimates and peak PCR result in first asexual cycle.
Panel A shows linear model PMRs; panel B shows sine model PMRs; panel C shows N-CDF model PMRs.

7.4.3. Predictive accuracy of models

Cross-validation approaches assess the capacity of a model to make an accurate prediction of the outcome (dependent) variable for an observation which is omitted from the data set used to fit the model. Such approaches are useful for comparing models with different structures. Two such

approaches were used to compare the linear, sine-wave and normal-CDF models' ability to predict forward or within the time period of the data used to fit each model.

The accuracy of forward and LOOCV predictions are depicted in figure 7.4.3.1. Accuracy of predictions was compared by Kruskal-Wallis test with Dunn's post-test. There was no significant difference ($p>0.05$) between the forward predictive accuracy of the models. The normal-CDF model was slightly but statistically significantly less accurate than the linear model for LOOCV prediction ($p<0.0001$).

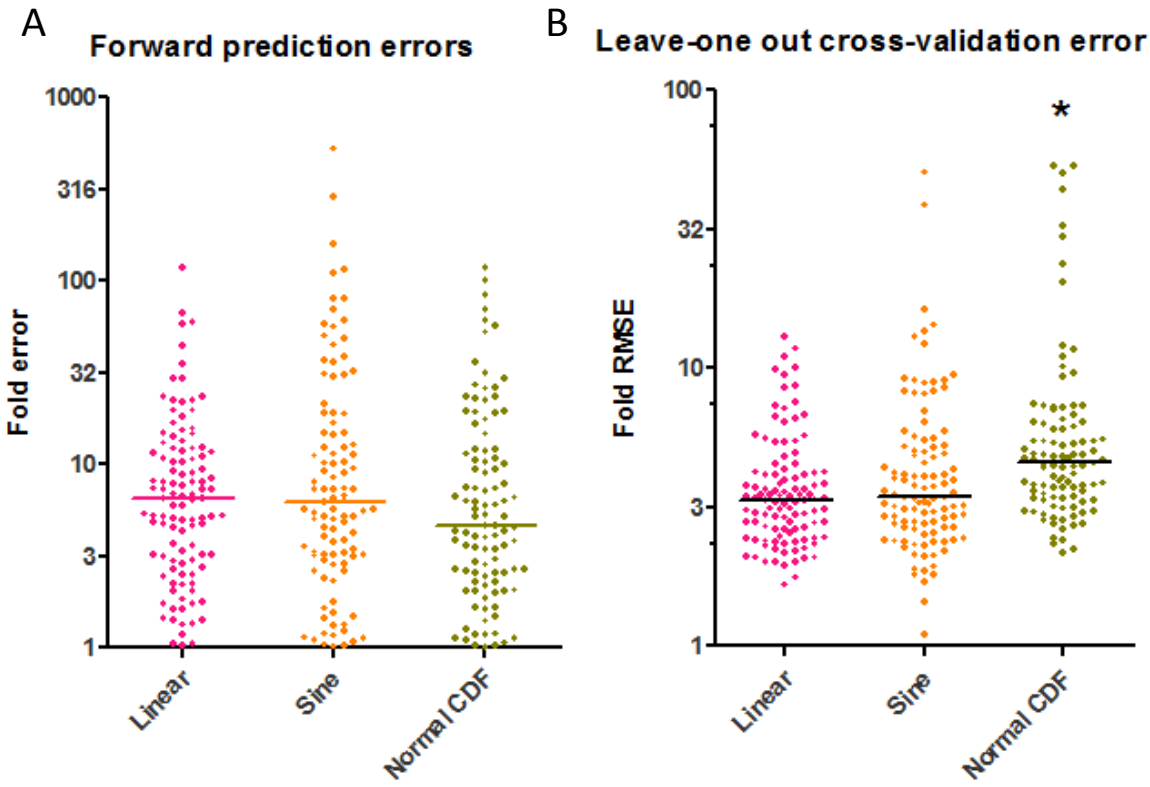

Figure 7.4.3.1 Comparison of predictive accuracy of models.
Panel A: Comparison of forward-predictive accuracy of linear, sine and normal-CDF models: fold error in prediction of time-of-diagnosis PCR using data lacking final 2 points
Panel B: Leave-one-out cross-validation. For each volunteer, each individual qPCR data point was serially omitted from the model-fitting data set, and errors in the prediction of point were calculated. Root mean square of individual-point errors was calculated for each volunteer, and anti-logged to produce fold-RMSE-error.

7.5. DISCUSSION

For the purposes of clinical trial outcome reporting, where the primary objective is to estimate LBI and PMR, the outputs of these models compared appear to be very similar. The more complex sine and normal CDF models did not achieve improved predictive accuracy relative to the linear model.

To maximise the reliability of LBI and PMR estimation, the quality of the data which is input to the modelling process may be more important than the use of complex models. Simple steps would include the recording of time of venepuncture in hours rather than days, at least twice-daily PCR, and use of individuals' weight to estimate blood volume for calculation of total LBIs.

Non-model-based estimation of LBI is possible. The first peak of parasitaemia occurs between days 7 and 8, is probably a good approximation to the true LBI, and correlates closely with model-derived outputs. Model-based estimation of LBI is probably only necessary for those subjects for whom parasites are undetectable by PCR at this stage. Efforts to enhance the sensitivity of PCR towards 1 or 2p/ml at this timepoint would be highly worthwhile and could entirely eliminate the need for model-based LBI estimation. Such increases are possible by extracting DNA from larger blood sample volumes (my unpublished observations).

This work has demonstrated that the output of two previously published models (Hermsen, de Vlas et al. 2004; Bejon, Andrews et al. 2005) correlate closely. Interestingly a far simpler linear model provides estimates of LBI and PMR that closely correlate with both methods. This model also correlates with an alternative method of PMR estimation based upon mean parasitemia in each asexual lifecycle cycle, and is simpler than this 'cycle means' method to apply to subjects with qPCR negative data-points and widely varying times of diagnosis. This information will be useful both for investigators applying parasite lifecycle modelling to assess vaccine efficacy in malaria challenge trials, and for funders and regulatory agencies attempting to judge the outcome of such trials.

A rough 'rule of thumb' for the power of phase IIa CHMI studies is that the magnitude of the 'signal' (change in parasite dynamics due to vaccine efficacy) must be approximately equal to the 'noise' (within-group inter-individual standard deviation). 80% power to detect an inter-group difference equal to the inter-subject standard deviation by a two-sample t-test at the 5% significance level requires 16 subjects per group- slightly larger than a typical phase IIa CHMI study, but not entirely impractical.

Existing pre-erythrocytic vaccines are capable of substantially greater than 10-fold reductions in LBI, and it is likely that reductions larger than this (perhaps reduction to zero) are required to achieve any clinically significant effect(Hill 2006). The ratio of vaccine-efficacy 'signal' to control-group 'noise' is thus highly favourable under mosquito-bite challenge.

Estimation of PMR is considerably more challenging and inevitably requires some mathematical analyis of qPCR data. Whichever model is used, the inter-individual standard-deviation of estimated PMR among vaccine-naïve subjects is of the order of 20-60% of the PMR. In contrast to the situation for pre-erythrocytic vaccines, the magnitude of PMR reduction required to achieve an effect upon clinical disease is unknown, and it is plausible that PMR changes of the same magnitude as (or even smaller than) the inter-individual SD in PMR estimates could result in clinical efficacy. Moreover, given that no BSV has yet demonstrated a statistically significant effect upon PMR, the most sensitive possible detection of smaller PMR changes is likely to be valuable in guiding vaccine development.

The difficulty of detecting an effect of a BSV upon PMR in a mosquito-bite CHMI trial is further compounded by the relationship between PMR and LBI observed here. It is unclear whether this correlation represents a genuine biological phenomenon (ie that PMR in the subpatent period genuinely decreases rapidly with increasing LBI) or whether it represents an artefact of the PCR or modelling process. Plausible biological explanations for this phenomenon might include the possibility that the longer period of subpatent BS growth in low-LBI subjects favours the emergence

of more-rapidly replicating parasite sub-clones, such as those expressing well host-adapted PfEMP1 variants. Regardless of the explanation, this relationship somewhat confounds efforts to measure PMR independently of LBI, a principal aim of the analysis.

The signal:noise ratio in PMR following mosquito-bite CHMI is thus relatively unfavourable for all but the largest vaccine-induced changes. Nonetheless, the current study shows that estimates of individuals' PMR after mosquito-bite CHMI are reasonably consistent regardless of the model used. Blood-stage *P falciparum* CHMI, however, permits simpler and more accurate measurement of PMR during a longer period of blood-stage growth, without the complication of inter-individual variation in the inoculum (Sanderson, Andrews et al. 2008). For this reason, it is likely that future RH5 vaccine clinical trials will be conducted using BS challenge.

8. Protective efficacy of PfRH5 vaccines in *Aotus nancymaae*

8.1. AUTHORSHIP STATEMENT

ADD proposed the *Aotus* study, contributed to securing funding, designed the study and wrote the protocol, travelled to Peru for the prime and boost vaccinations and the challenge period, formulated the vaccines, conducted the ELISA assays, designed and supervised the ELISPOT assays, and analysed all data.

The study could not have been conducted without the contributions of the following individuals:

Carmen Lucas, Luis Lugo-Roman, Lynn E Lambert, Jeromy Moorhead, Jorge Nuñez, Meddly Santolalla, Lorena Tapia: animal care, procedures and monitoring.

G Christian Baldeviano, Kimberly Edgel, Andres G Lescano, Julio Ventocilla: supervision of study at NAMRU6 and conduct of immunological assays.

Cécile Crosnier and Gavin Wright: supply of recombinant PfRH5 protein vaccine.

Yimin Wu: supply of recombinant FVO protein vaccine.

Ali Turner and Jenner Institute Viral Vector Core Facility: production of viral vector vaccines.

8.2. INTRODUCTION

Initial proof-of-concept for RH-family targeting vaccines was provided by the early observation that active or passive immunisation against a Py235 family member was capable of protecting mice against *P. yoelii* (Freeman, Trejdosiewicz et al. 1980; Holder and Freeman 1981). Despite considerable interest in *P. falciparum* RH-family members as vaccine candidates, however, no test of the *in vivo* efficacy of such vaccines has been conducted. Only humans, great apes, and certain New World monkey species are susceptible to *P. falciparum. In vivo* testing of the efficacy of candidate vaccines against *P. falciparum* thus requires either clinical trials (with the attendant costs of GMP-compliant vaccine manufacture), or trial in non-human primates. Only non-human primate testing permits the study of untreated microscopically-patent blood-stage infections, and the way in which these can be modified by vaccine-induced immunity.

Two New World monkey genera have been used for testing of vaccines against blood-stage *P. falciparum: Aotus* and *Saimiri.* In recent years, *Aotus nancymaae* have been the preferred model, largely due to the availability of colonies of captive-bred animals in the USA and Latin America, and the reproducibility of infection in this species. No *Aotus* colonies are currently maintained in Europe.

Infection of vaccine-naïve *Aotus nancymaae* with the FVO strain of *P. falciparum* results in virulent and rapidly progressive parasitaemia. Review of ten previously published vaccine studies indicates that, of a total of 90 malaria-antigen naïve control animals, 86 required treatment for either uncontrolled parasitaemia or anaemia (Kumar, Yadava et al. 1995; Kumar, Collins et al. 2000; Stowers, Cioce et al. 2001; Hisaeda, Saul et al. 2002; Stowers, Chen Lh et al. 2002; Collins, Galland et al. 2005; Darko, Angov et al. 2005; Lyon, Angov et al. 2008; Dutta, Sullivan et al. 2009; Tsai, Duggan et al. 2009). Antigens based upon PfAMA1 and PfMSP1 have proven reproducibly protective in these trials, with possible protection demonstrated by PfMSP3 and PfEBA175 antigens. However this protection has been strain-specific, and robust protection has only been achieved by the formulation

of antigens with complete Freund's adjuvant. Lesser degrees of protection have been achieved by regimes including Montanide ISA720 (Seppic) (Jones, Narum et al. 2001; Lyon, Angov et al. 2008), which is no longer thought to be tolerable for human use(Roestenberg, Remarque et al. 2008). No human-compatible vaccine formulation has achieved clinically meaningful protection in this model (when animals were immunised with a a PfAMA1 antigen formulated with AS02 then challenged with the less stringent FCH4 strain of *P. falciparum,* a statistically significant effect upon parasite density was achieved, but there was not a significant effect upon the outcome of infection (Dutta, Sullivan et al. 2009)).

One concern in efficacy testing of a vaccine based upon an invasion ligand is that the relative importance of different invasion ligands may differ with regard to invasion of different species' erythrocytes. While FVO and certain other parasite lines are able to infect *Aotus,* many *P. falciparum* lines are unable to invade *Aotus* erythrocytes (Collins, Galland et al. 1994; Hayton, Gaur et al. 2008). PfRH5 was originally identified from genetic linkage study of the progeny of a cross between parasites able and unable to invade *Aotus* erythrocytes, which demonstrated that this phenotype was related to a single amino acid polymorphism in the PfRH5 gene, determining the ability of PfRH5 to bind to *Aotus* red cells (Hayton, Gaur et al. 2008). Moreover, collaborators kindly established that IgG from PfRH5-vaccinated rabbits was capable of blocking invasion of FVO parasites into *Aotus* red cells (A Diouf, K Miura and C Long, unpublished observations). It thus appears that PfRH5 is essential for *Aotus* erythrocyte invasion by *P. falciparum*, as it is for human erythrocyte invasion.

This chapter describes an *Aotus nancymaae* challenge trial conducted in collaboration with the US Naval Medical Research Unit 6 (NAMRU6) in Peru. The study aimed to test the hypothesis that PfRH5-based vaccines could achieve *in vivo* protection against *P. falciparum*.

8.3 METHODS

8.3.1 Animals, immunisations and challenge

The production of PfRH5-expressing adenovirus and modified vaccinia virus Ankara (MVA) vectored vaccines has previously been described (Douglas, Williams et al. 2011). For the *Aotus* study, a ChAd63 adenovirus expressing the same PfRH5 transgene was produced by the Jenner Institute Viral Vector Core Facility, using standard methods (Goodman, Epp et al. 2010; Douglas, Williams et al. 2011). Recombinant PfRH5 protein with C-terminal hexa-His and rat CD4d3+4 tags (kindly provided by G Wright and C Crosnier) was produced and purified from transiently transfected HEK293E cells, essentially as described(Crosnier, Bustamante et al. 2011). All PfRH5 vaccines were based upon the 3D7 strain sequence. The production of the bi-allelic (3D7 + FVO) ChAd63 PfAMA1 vaccine and of PfAMA1 protein based upon the FVO allele (a kind gift of Y Wu) have been reported elsewhere (Kennedy, Wang et al. 2002; Biswas, Dicks et al. 2011). ChAd63 expressing renilla luciferase was used as a non-malaria-antigen control adenovirus (a kind gift of Matthew Dicks).

Captive-bred *Aotus nancymaae* were housed at the US Naval Medical Research Unit 6 (NAMRU6) Laboratory Animal Facility. Randomisation to groups was stratified by pre-trial weight. Immunisations were performed by the intramuscular (IM) route on days 0 and 54, with the exception of those containing Freund's adjuvant, which were given subcutaneously (SC) on days 0 (complete), 26 (incomplete) and 54 (incomplete). Doses used were $5x10^9$ infectious units (IU) for adenoviruses, $2x10^8$ plaque-forming units (PFU) for MVA, 50µg for protein, 250µL for complete and incomplete Freund's adjuvant (Sigma), and 48µg for Abisco-100 (Isconova). Groups were as set out in Table 8.3.1. The study was approved by the NAMRU6 Institutional Animal Care and Use Committee, the US Navy Bureau of Medicine, and the University of Oxford Animal Care and Ethical Review panel.

	PRIME Day 0	Day 26	BOOST Day 54	Day 69
A ***Control***	Non-malaria adenovirus (ChAd63-luc, 5e9 IU, IM)	N/A	PBS + Abisco-100 48ug, IM	**FVO-strain challenge**
B ***RH5 Freund's***	RH5-CD4-3D7 protein 50ug + CFA, SC	RH5-CD4-3D7 protein 50ug + IFA, SC	RH5-CD4-3D7 protein 50ug + IFA, SC	
C ***RH5 Ad-Prot***	RH5-3D7 adenovirus (ChAd63-RH5FL, 5e9 IU, IM)	N/A	RH5-CD4-3D7 protein 50ug + Abisco-100 48ug, IM	
D ***RH5 Ad-MVA***	RH5 adenovirus (ChAd63-RH5FL, 5e9 IU, IM)	N/A	RH5 poxvirus (MVA RH5FL, 2e8 PFU, IM)	
E ***AMA1 Ad-Prot***	AMA1-3D7/FVO adenovirus (ChAd63-AMA1biallelic, 5e9 IU, IM)	N/A	AMA1-FVO protein 50ug + Abisco-100 48ug, IM	

Table 0.1.T1 Groups and vaccine regimes in *Aotus nancymaae* challenge study

Fifteen days after the final vaccination (i.e. study day 69), animals were challenged intravenously with 10^4 FVO-strain *P. falciparum* infected red cells taken from a donor monkey, as described (Stowers, Cioce et al. 2001). From day 72, daily thin-film parasitaemia quantification and alternate-day hematocrit measurements were conducted. Animals were treated when parasite density reached 200,000/µL or hematocrit fell to 25%; or upon reaching study day 28 if no parasites had been seen in the preceding week; or upon reaching study day 38. Laboratory staff were blinded to animals' treatment allocation.

8.3.2 Analysis of efficacy

The study protocol included a pre-specified method of analysis of trial data for efficacy, as follows:

The following vaccine efficacy endpoints were recorded, as used in a previous *Aotus – P. falciparum* challenge study (Lyon, Angov et al. 2008) and a recent study of *P. knowlesi* infection of rhesus macaques (Mahdi Abdel Hamid, Remarque et al. 2011).

1. Ordinally-ranked treatment status (treatment for parasitemia [TxP]; treatment for anaemia [TxA]; no treatment).

2. As a continuous variable, $\log_{10}$(Cumulative parasitaemia) up to day 10, the day on which the first animal in the study required treatment.

3. As a secondary continuous variable, *in vivo* growth inhibition, calculated in the manner of Mahdi Abdel Hamid *et al* (Mahdi Abdel Hamid, Remarque et al. 2011).

For group B (Freund's adjuvant), no adjuvant-matched control group was included in the study, but historical control data were available from seven previously-published studies in which *Aotus nancymaae* were subjected to FVO-strain challenge after receiving Freund's adjuvant without a blood-stage antigen (Kumar, Yadava et al. 1995; Kumar, Collins et al. 2000; Stowers, Cioce et al. 2001; Hisaeda, Saul et al. 2002; Stowers, Chen Lh et al. 2002; Darko, Angov et al. 2005; Tsai, Duggan et al. 2009). Of a total of 45 such animals, 40 required treatment for uncontrolled parasitaemia, while 5 required treatment for anaemia. Kendall's tau-b was used to test a null hypothesis of equivalent outcome between group B and historical Freund's control animals. As a secondary efficacy outcome measure for this group, $\log_{10}$(cumulative parasitaemia to day 10) was compared between groups B and A, bearing in mind that group A will not have received Freund's adjuvant.

For groups C and E, group A is an adjuvant-matched control group. No direct negative control group was included for group D, and there is no direct historical control available for these animals. Experience from rodent and clinical trials suggests that MVA does not confer any non-specific inhibitory effect upon blood-stage parasite growth (Draper, Goodman et al. 2009) (SJ Draper and others, manuscript in preparation). Group A was thus the most relevant available comparator for group D. The primary analysis of efficacy in groups C, D and E was therefore comparison of $\log_{10}$(cumulative parasitaemia to day 10) in each group to group A by Mann-Whitney test.

8.3.3 ELISA

Preliminary ELISA using *Aotus* plasma samples was conducted as described for rabbit anti-PfRH5 responses (Section 2.3), using enzymatically biotinylated CD4-tagged PfRH5, but with the following modifications. Firstly, casein (Pierce) was used as a blocking reagent and for the dilution of primary and secondary antibodies. Secondly, a custom-made anti-*Aotus*-IgG secondary antibody conjugated to horseradish peroxidase was used (Lampire, USA; a kind gift of H Tilley). Thirdly, *o*-phenylenediamine dihydrochloride (OPD) substrate solution was used (Sigma). Finally, results were calculated by interpolation from a standard curve prepared using serial dilutions of a pool of pre-challenge sera from group D animals, as previously described (Miura, Orcutt et al. 2008).

ELISA for anti-PfAMA1 responses was performed similarly, with the exception that non-streptavidin-coated plates (Maxisorp, Nunc) were coated overnight with 2µg/mL recombinant PfAMA1-FVO (the same protein used for immunisation).

8.3.4 ELISPOT

Ex-vivo interferon-γ (IFN-γ) ELISPOT was performed essentially as previously described(Draper, Biswas et al. 2010), with the following modifications.

PfRH5 peptides (20mers overlapping by 10 amino acid residues (αα) spanning the PfRH5 antigen sequence) were synthesised by Mimotopes Ltd, resuspended in DMSO to 100 mg/ml, pooled, and diluted in R10 medium. PfAMA1 peptides (20mers overlapping by 10 αα spanning the biallelic PfAMA1 antigen sequence found in the adenovirus) have previously been described(Sheehy, Duncan et al. 2012). Peptides were used at a final in-well concentration of 5µg/mL of each peptide with no more than 0.5% v/v DMSO). Wells containing 10µg/mL phytohaemagglutinin (PHA) and 20 ng/mL staphylococcal enterotoxin B (SEB) (both from Sigma) were used as positive controls; negative control wells contained R10 with 0.25% v/v DMSO only.

Anti-human IFN-γ antibodies were used, as in previous *Aotus* ELISPOT experiments (Jordan-Villegas, Perdomo et al. 2011): mAb 1-D1-K for capture, and biotinylated mAb 7-B6-1 as secondary (both from Mabtech).

Assays were performed with 100,000 PBMCs per well, using cells which had been frozen in FCS with 10% DMSO. Cells from each animal were tested in PfRH5 and PfAMA1 peptide-containing wells and negative control wells (each in duplicate), and in a single positive control well.

8.4 RESULTS

8.4.1 Vaccine-induced protection

Figure 8.4.1.1 shows timecourses of parasitaemia over time in each group. Figure 8.4.1.2 shows timecourses of haematocrits over time in each group. Figure 8.4.1.3 shows summary efficacy measures: cumulative parasitaemia to day 10 post-challenge (day 10 was the day on which the first animal required treatment) and a Kaplan-Meier plot of untreated survival.

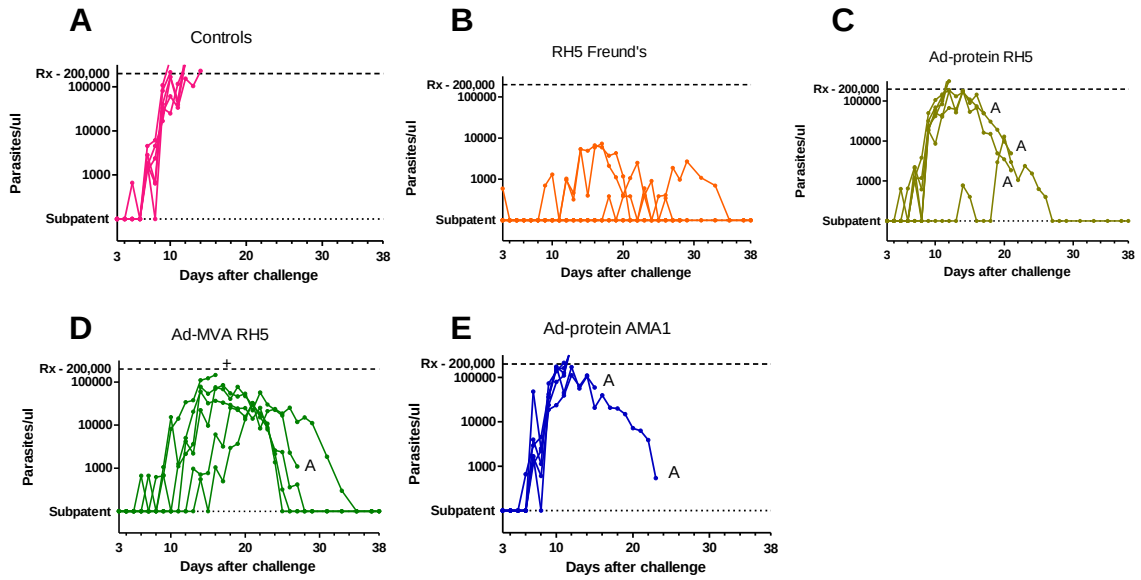

Figure 8.4.1.1 Timecourses of parasitaemia in each group of *Aotus nancymaae*
Panels A-E depict timecourses of parasitaemia for individual animals in groups A-E respectively. Upper horizontal dotted line indicates the 200,000 parasites/μL threshold for initiation of antimalarial treatment because of hyperparasitaemia; lower horizontal dotted line indicates absence of thin-film detectable parasites. 'A' indicates treatment due to anaemia; '+' indicates death.

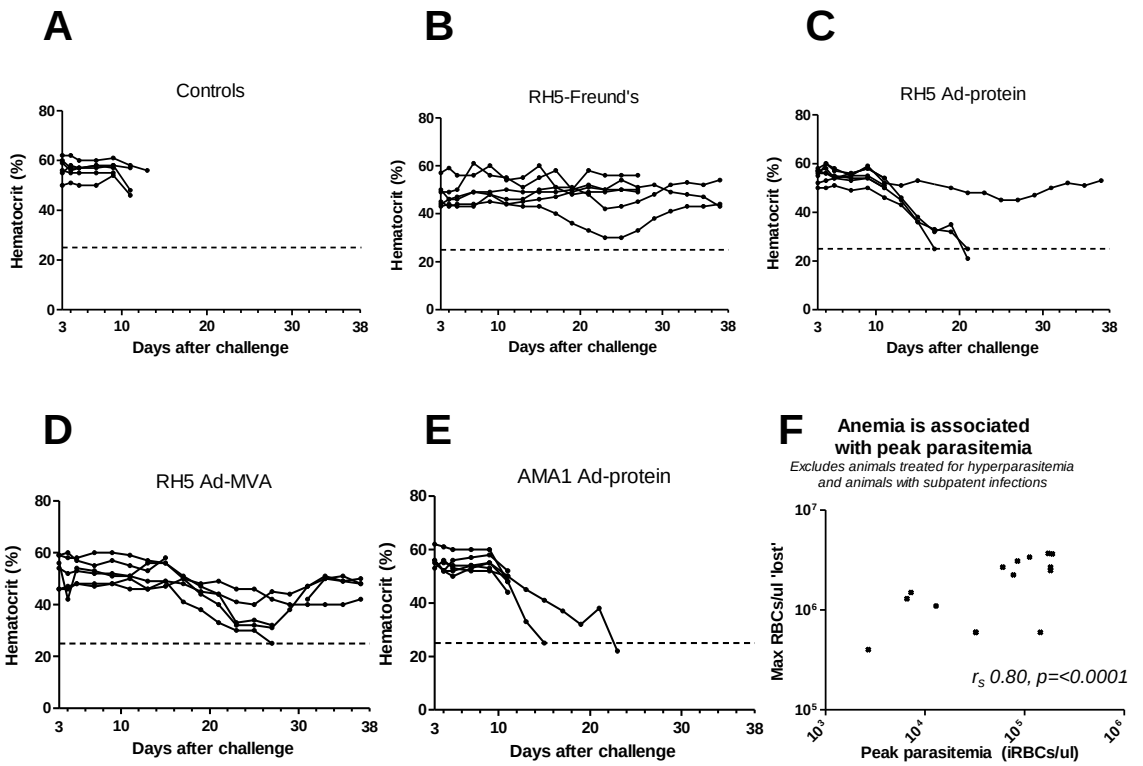

Figure 8.4.1.2 Anaemia during *Aotus nancymaae* challenge infection

Panels A-E depict timecourses of haematocrits for individual animals in groups A-E respectively. Horizontal dotted line indicates 25% Hct threshold for initiation of antimalarial treatment because of anaemia. Panel F depicts relationship between peak parasitaemia and number of red cells per microliter 'lost' due to malaria (10^5 cells per percentage point fall in Hct from baseline to nadir).

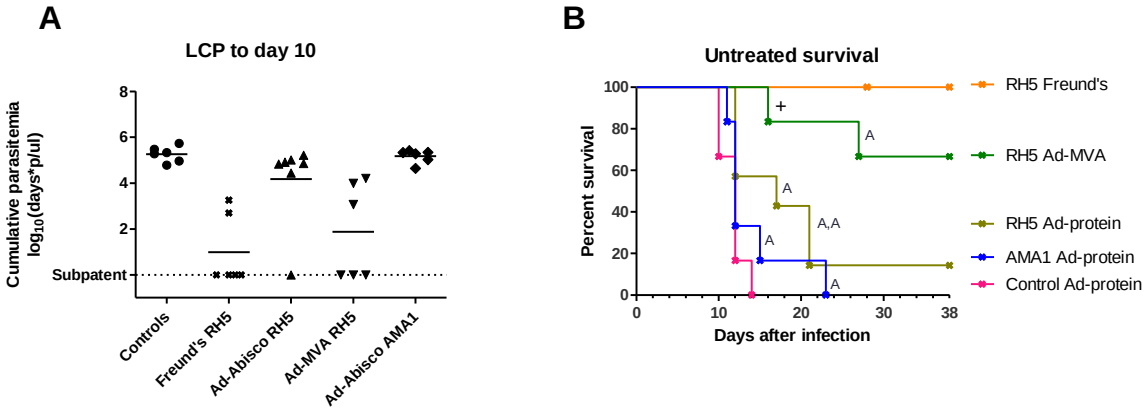

Figure 8.4.1.3 Summary measures of vaccine efficacy in *Aotus nancymaae*

Panel A depicts log cumulative parasitaemia to day 10. Panel B is a Kaplan-Meier plot of duration of untreated survival. 'A' indicates treatment for anaemia; + indicates death. For statistical interpretation, see text.

None of the animals immunized with PfRH5 protein in Freund's adjuvant (group B) required treatment. Comparison against historical controls yielded a value of Kendall's tau-b of -0.758, with asymptotic standard error of 0.092. The z-value for a tau-b significance value (tau-b/ASE) was therefore -8.24; for samples with n>30, this value approximately follows a standard normal distribution, implying p<0.001 for no association between PfRH5 immunisation and outcome. On the secondary outcome measure for this group, $\log_{10}$(cumulative parasitaemia to day 10), the vaccine effect was also highly significant (p=0.002 by Mann-Whitney test comparing to group A). No parasites were seen by thin-film microscopy at any point in two of the group B animals, with only a single parasite seen on one occasion in a third animal; the remaining three animals self-cured after periods of microscopically-patent parasitaemia.

Significant vaccine efficacy was also seen in the adenovirus-MVA group (group D; p=0.002 by Mann-Whitney test of $\log_{10}$(cumulative parasitaemia to day 10) versus group A). Four out of six of the animals in this group self-cured, with one animal requiring treatment due to anaemia and one death due to pericardial effusion in an animal with relatively high parasitaemia. Death due to natural cardiac causes is not uncommon in captive *Aotus* (LE Lambert, personal communication) but, for the sake of analysis, this animal was considered to have succumbed to uncontrolled parasitaemia.

Vaccine efficacy, as assessed by the primary outcome measure of $\log_{10}$(cumulative parasitaemia to day 10), was not statistically significant in the adenovirus-protein PfRH5 or adenovirus-protein PfAMA1 groups (groups C + E respectively). There was, however, a strong trend towards reduced $\log_{10}$(cumulative parasitaemia to day 10) in group C (p=0.052 by Mann-Whitney test versus group A), while 3/7 animals in this group required treatment for anaemia (after controlling parasitaemia), and a further animal self-cured. All six animals in group E required treatment for uncontrolled parasitaemia.

As has been previously described, anaemia appeared in this study to be an intermediate outcome of infection (between self-cure and uncontrolled parasitaemia) (Figure 8.4.2). Minimal haematocrits

occurred several days *after* the peak of parasitaemia. By the time that animals required treatment for anaemia, parasite densities had typically fallen 10-100-fold from their peak value. Some animals experienced rapid falls in hematocrit with parasitaemias of <0.1%. The fall in hematocrit from baseline to trough correlated with peak parasitaemia, and corresponded to loss of approximately 25-fold more red cells than had been infected at the peak of parasitaemia. Given the long half-life of red cells (>100 days for human RBCs), such loss is strongly suggestive of abnormal destruction of non-infected red cells; the timing of this loss, coinciding with clearance of infected red cells, raises the possibility of a contribution of immune responses to this destruction. It has previously been noted that merozoite proteins may adhere to the surface of non-infected red cells(Layez, Nogueira et al. 2005); immune responses to such proteins may underlie the anaemia seen in partially protected *Aotus.*

Blood-stage vaccine developers have faced uncertainty regarding appropriate methods for assessing vaccine efficacy in early phase clinical trials. It has been unclear whether efficacy of such vaccines could be detected in controlled human malaria infection (CHMI) trials, in which the subjects must be treated at the time of microscopic patency, or whether vaccine efficacy must be evaluated in large, prolonged, and expensive field trials. In the current study, the density of the blood-stage parasite inoculum (approximately 140 parasites per mL of blood) and the duration of pre-patent asexual growth were similar to those observed in mosquito-bite CHMI trials. Figure 8.4.1.4A demonstrates that the effect of the PfRH5 vaccines was apparent as a delay in time to microscopic patency. This effect was of marginal statistical significance (p=0.04 for group B v group A, and p=0.06 for group D v group A by log-rank test) but the trend was clear; a similar effect size would have reached statistical significance with the larger sample sizes of c. 12/group as used in CHMI trials. Figures 8.4.1.4B-C demonstrate that pre-patent period was predictive of outcome, and that large changes in *in vivo* parasite multiplication rate, likely to be detectable after CHMI, are required in order to achieve self-cure. These results support the view that blood-stage vaccines can and should demonstrate *in vivo* biological effects in CHMI trials prior to field trials.

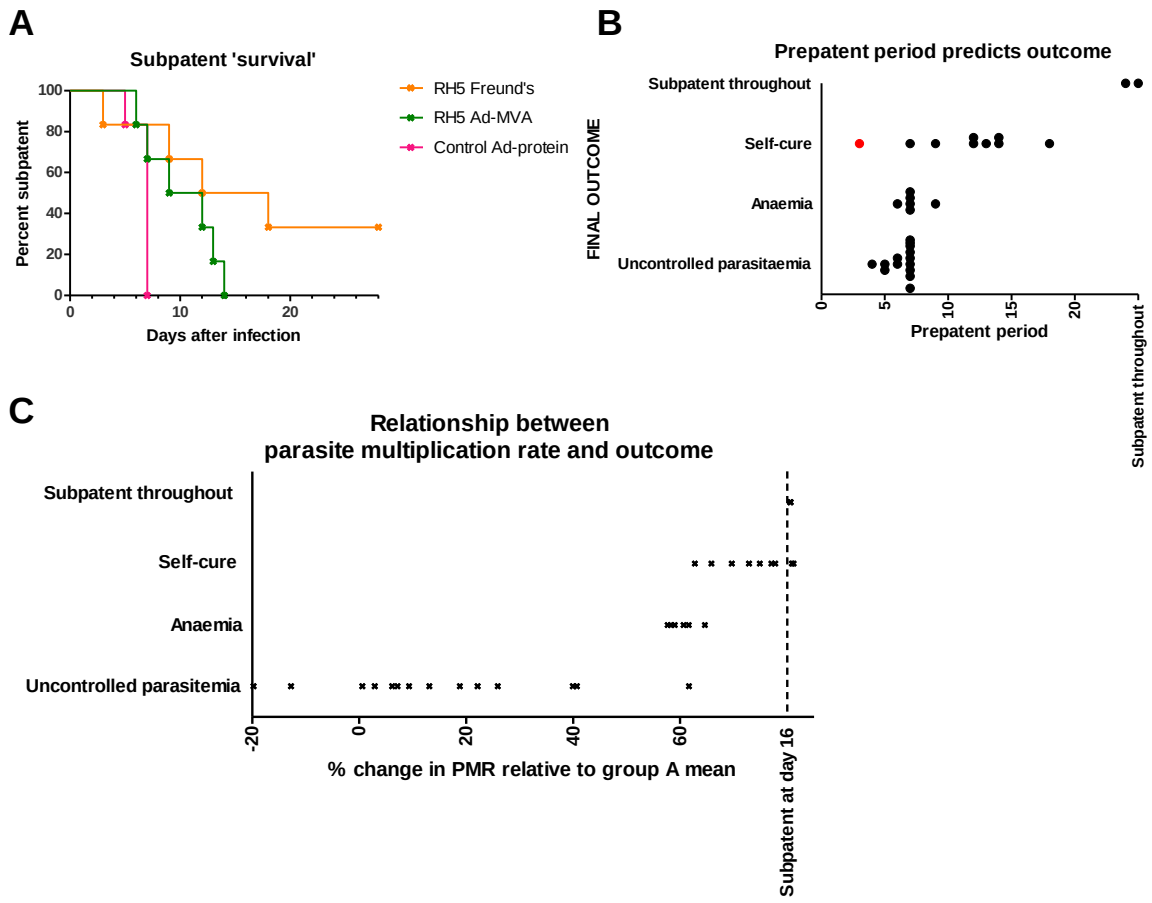

Figure 8.4.1.4 Effect of PfRH5 vaccines upon endpoints potentially measurable prior to microscopic patency in clinical trials

Effect of PfRH5 vaccines was apparent as prolonged time to microscopic patency and >60% change in *in vivo* parasite multiplication rate (PMR) in animals which ultimately self-cured.

Panel A shows that pre-patent periods for the two vaccine-protected groups differed from those of the controls.

Panel B shows that pre-patent periods are predictive of final outcome of challenge. Red point indicates one animal which had a single parasite seen by thin-film microscopy on day 3, and no further parasites seen at any point.

Panel C illustrates that large changes in parasite multiplication rates appear to be required to permit animals to self-cure; changes of such magnitude could readily be detected in CHMI trials(Sanderson, Andrews et al. 2008). PMR was calculated as % reduction in fold-increase/48hrs of parasitaemia up to day 16, relative to the mean in group A, similar to a previously described approach (Mahdi Abdel Hamid, Remarque et al. 2011); this calculation essentially involved linear regression of all parasite density data up to day 16 . Day 16 was chosen on the basis that inspection of parasitaemia curves suggested that parasite growth was exponential up to this point, with no obvious change in PMR as might be expected due to challenge-induced adaptive immune responses.

8.4.2 Immunogenicity of vaccines

The vaccines induced PfRH5- and PfAMA1- specific antibody responses, as measured by ELISA (Figure 8.4.2.1), and T cell responses, as measured by IFN-γ ELISPOT (Figure 8.4.2.2).

Mainly PfRH5-specific ELISPOT responses were seen in animals in groups C and D, while PfAMA1-specific responses were seen in group E (Figure 8.4.2.2A). Cells from all animals produced >1000 spots/million PBMCs in response to positive control SEB/PHA stimulation. High levels of non-peptide-specific responses were seen in animals from groups B and C (Figure 8.4.2.2B); Freund's adjuvant-induced innate cell activation may underlie the responses in group B but it is unclear why such responses should have been seen in group C, but not in the adjuvant-matched groups A or E. Unexpectedly some animals in groups C and D appeared to have AMA1-specific responses; again, the reason for this is unclear, but it is possible it may reflect previous exposure of these animals to environmental apicomplexa.

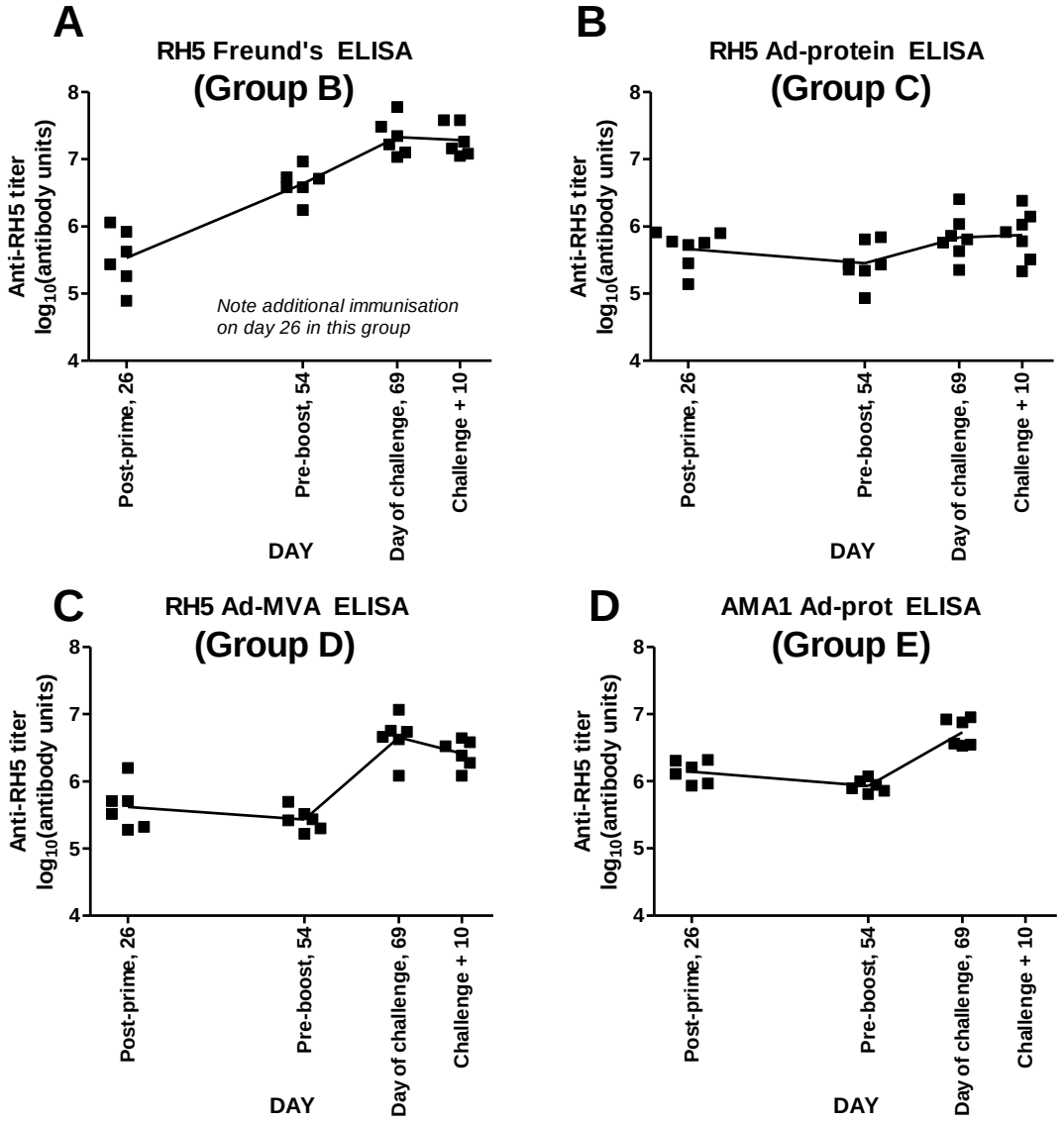

Figure 8.4.2.1 Anti-PfRH5 and anti-PfAMA1 ELISA timecourses in *Aotus nancymaae*.
Panel A depicts results for group B (PfRH5 protein-Freund's adjuvant);

Panel B depicts results for group C (PfRH5 adenovirus - protein with Abisco-100);

Panel C depicts results for group D (PfRH5 adenovirus-MVA);

Panel D depicts results for group E (PfAMA1 adenovirus - protein with Abisco-100).

Y-axis units are arbitrary and not comparable between PfRH5 and PfAMA1, defined in the manner of Miura et al(Miura, Orcutt et al. 2008). Lines link group means. All animals were ELISA-negative on day 0 (no OD_{490} values in excess of 0.1 at 1:300 serum dilution were recorded).Note that these preliminary ELISA results were obtained with the same CD4d3+4 tagged PfRH5 protein which was used for immunisation of group B, and boosting of group C: hence some of the measured response in these groups may be directed to the tag. Work is ongoing to repeat these assays with untagged PfRH5.

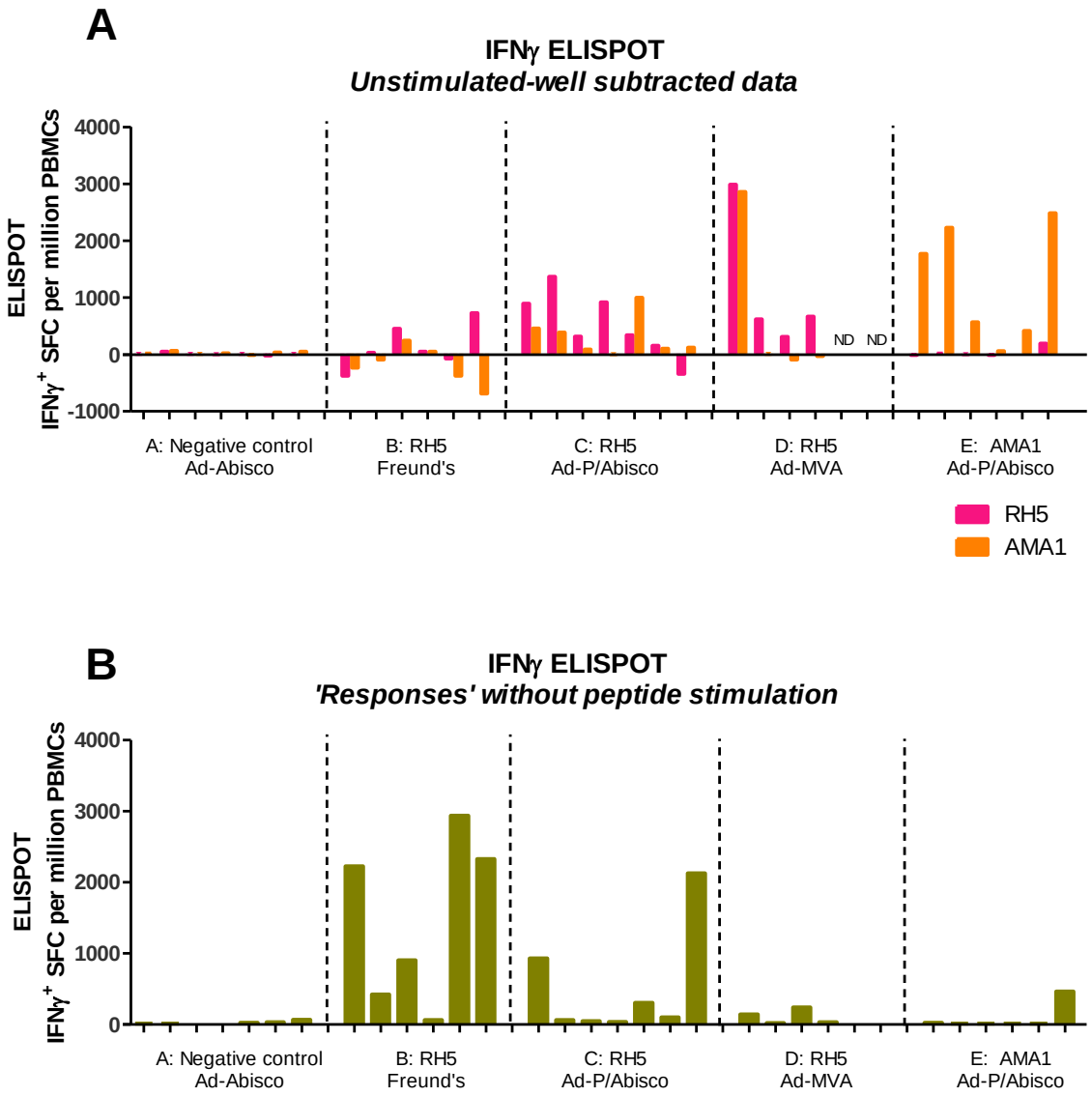

Figure 8.4.2.2 *Aotus nancymaae* IFN-γ ELISPOT.
Ex-vivo ELISPOT was conducted using frozen cells collected on the day of challenge.

Panel A depicts mean of duplicate PfRH5-stimulated and PfAMA1-stimulated wells after subtraction of responses in negative control wells.

Panel B depicts levels of non-peptide-specific responses.

There was a strong association between day-of-challenge anti-PfRH5 antibody responses and outcome of challenge infection (Figure 8.4.2.3). This relationship was consistent across animals immunised with different vaccine-adjuvant formulations/platforms. Anti-PfRH5 antibody responses

in excess of $3x10^6$ antibody units appeared to result in a >50% probability of untreated survival. There was no significant relationship between ELISPOT-measured IFN-γ responses and protection (Spearman's r=-0.09, p=0.71).

The protocol-specified primary analysis for an immunological correlate of protection was an examination of the relationship between PMR and GIA. GIA assays are currently ongoing in the international reference laboratory at NIH.

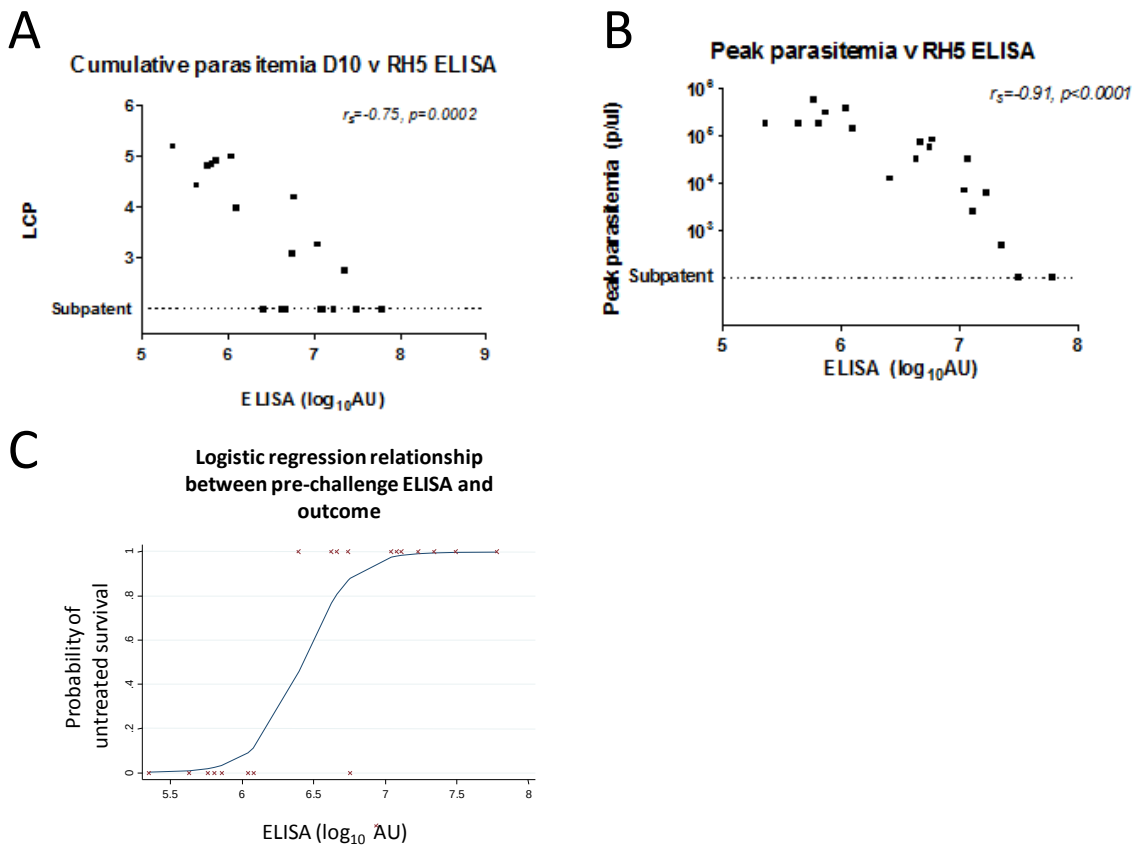

Figure 8.4.3.3 Relationship between anti-PfRH5 antibody responses and vaccine efficacy.
Each subpanel depicts the same ELISA data plotted against a different outcome measure: log_{10}(cumulative parasitaemia to day 10) (LCP) in panel A, peak parasitaemia in panel B, and categorical outcome (untreated survival) in panel C.

Spearman rank correlation coefficients and p values are shown in panels A and B. Logistic regression analysis was performed using Stata version 11. For the logistic regression relationship, McFadden's Pseudo-R^2 was 0.70, p<0.001. All analyses included only PfRH5-vaccinated animals (i.e. groups B, C, D).

8.5 DISCUSSION

The protection achieved by the adenovirus-MVA and protein-Freund's PfRH5 vaccine regimes in this *Aotus* challenge study is highly encouraging. Such robust protection has not been observed after vaccine-homologous challenge of *Aotus* monkeys immunised with PfAMA1, PfMSP1 or PfMSP3 antigens formulated with Freund's adjuvant (Stowers, Cioce et al. 2001; Hisaeda, Saul et al. 2002; Stowers, Kennedy et al. 2002), even when the vaccine antigen was matched to the FVO challenge strain. Although it achieved a lesser degree of protection than the Freund's regime, the result obtained with the adenovirus-MVA regime was most encouraging, as this is the first demonstration of clinically meaningful protection in this model with a human-compatible regime. The viral vector doses used were similar to human doses.

The PfRH5 antigen of the challenge strain, FVO, differed at four amino acid loci from the 3D7 strain upon which the vaccines were based (Hayton, Gaur et al. 2008) (note that the vaccine antigens contained additional amino acid substitutions to remove N-linked glycosylation sites, as described in sections 2.1 and 8.3.1) . No greater level of divergence was identified among the PfRH5 genes of 227 field parasite isolates which were recently sequenced (Manske, Miotto et al. 2012) (Williams & Douglas *et al.*, PLoS Pathogens in press), suggesting that pre-existing antigenic polymorphism is unlikely to pose a substantial obstacle to efficacy of PfRH5-based vaccines.

Given that no blood-stage vaccine has yet proven unambiguously protective in either CHMI or field trials, the ability of *Aotus* trial results to predict clinical efficacy is as yet unknown, and has been controversial in the past (Heppner, Cummings et al. 2001; Stowers and Miller 2001). In the case of vaccines which target invasion ligands such as PfRH5, there must be particular caution regarding the use of animal models, in case the ligand is more important in the model than in humans: however the data appear clear that PfRH5 is essential for invasion of both human and Aotus red cells (Hayton, Gaur et al. 2008; Crosnier, Bustamante et al. 2011). Nonetheless, there does appear to be a spectrum of sensitivity to anti-PfRH5 antibody among *P. falciparum* lines, which does not appear to

correlate with PfRH5 genotype and may instead reflect the relative functionality of non-PfRH5 invasion ligands in each strain (Douglas, Williams et al. 2011) (Williams & Douglas *et al.*, PLoS Pathogens, in press). FVO is around the median of this distribution among laboratory lines; the most 'anti-PfRH5 resistant' line we have identified is the 3D7 clone, with an *in vitro* GIA EC_{50} (determined using anti-PfRH5 rabbit IgG) of approximately twice that of FVO. It is therefore possible that some strains of *P. falciparum* invading human erythrocytes may be less vulnerable to anti-PfRH5 antibodies than FVO invading *Aotus* erythrocytes. Ongoing work will aim to address this by comparing the capacity of anti-PfRH5 IgG to inhibit parasite growth *in vitro* in human and *Aotus* erythrocytes.

The relationship between anti-PfRH5 antibody responses and protection is simply an association rather than proof of causation. However the relationship is strong, and suggests that there will also prove to be a relationship between GIA and protection (the protocol-specified primary analysis for an immunological correlate of protection). It seems highly plausible that merozoite-neutralising antibodies, as measured by the GIA assay, can be a causal mechanism of vaccine-induced protection. Formal demonstration of such causation remains important and will require passive transfer studies, but the results of the current study go some way towards validation of the strategy of selection of antigens on the basis of their ability to induce parasite-neutralising antibody in the assay of GIA. The demonstration of this relationship should therefore assist not only in the development of future PfRH5-based vaccines, but also in the future selection of further promising candidate antigens.

The animals in the current study were challenged two weeks after the final vaccination, at a time when the vaccine-induced antibody responses are likely to have been close to maximal. The duration of the protection induced by these vaccines is thus a key unknown, with obvious relevance to the likelihood of a PfRH5-based vaccine achieving protection in field efficacy trials. The clarity of the relationship between anti-PfRH5 antibodies and protection should allow some extrapolation of the duration of protection from serological follow-up of this cohort of animals, with the caveat that their

antibody titres may have been influenced by exposure to *P. falciparum.* Given the low level of immunogenicity of PfRH5 in the context of natural human infection, it will be of particular interest to see whether vaccine-induced anti-PfRH5 responses are boosted by exposure to parasites. We have considered re-challenge of this cohort of animals, possibly with a second (non-FVO) parasite strain, but on balance we feel that the results of such re-challenge are likely to be confounded to some extent by varying levels of prior exposure to *P. falciparum,* and hence we do not view this as a priority. It is likely to be more informative to establish whether the vaccine achieves protection in humans, and if so, progress to explore duration of protection.

If and when a causal relationship between anti-PfRH5 antibodies and protection is established, optimisation of the PfRH5 vaccine regime to enhance the induction and maintenance of antibody responses will clearly be a priority. The hierarchy of antibody responses in the current study was somewhat surprising, with adenovirus-MVA outperforming an adenovirus prime – protein boost regime. This was at odds with our previous experience with other antigens in mice, macaques and humans (Douglas, de Cassan et al. 2010; Draper, Biswas et al. 2010; de Cassan, Forbes et al. 2011) (and SJ Draper *et al.*, unpublished observations), in which antibody induction by adenovirus-protein regimes has consistently exceeded that achieved by viral-vector only regimes. Notably we have found that adenovirus-protein PfRH5 regimes have performed equivalently to adenovirus-MVA regimes in mice and rabbits, but not outperformed them (data not shown). There are a variety of possible explanations for the disappointing performance of the adenovirus-protein regime. Firstly, the Abisco-100 adjuvant may not be potent in *Aotus* at the dose used (the lower end of the manufacturer's recommended range for rhesus macaques, which have approximately 5-fold higher body mass); there are, as far as we are aware, no previous data on the performance of this adjuvant in New World monkeys. Other adjuvants which are excellent inducers of antibody responses in humans, such as AS02A, have previously performed relatively disappointingly in New World monkeys (Dutta, Sullivan et al. 2009). PfAMA1 protein in Abisco-100 boosted the pre-existing adenovirus-induced antibody response by a median of 8-fold (day 69 relative to day 54), as

compared to the weak 2.6-fold boost achieved by PfRH5 in Abisco-100, suggesting that the adenovirus-protein regime performed particularly poorly with PfRH5. PfRH5-expressing MVA, by comparison, achieved a median 20-fold boost in titres. It is possible that the PfRH5 protein may, in some respect, be sub-optimal in a manner that can be overcome by repeated immunisations in Freund's, but not by adenovirus-protein immunisation. In particular the substantial (c. 100 amino acid) CD4d3+4 tag attached to it is immunogenic, and may provide immunological competition, distracting the response from protective epitopes.

Our belief remains that an optimised protein-adjuvant vaccine, possibly with adenoviral priming, is likely to achieve the highest antibody titres in humans. The development of an improved, rat CD4 tag-free PfRH5 protein vaccine is ongoing as a priority, and future studies with this antigen will explore a variety of alternative clinically-applicable adjuvants.

9. Concluding remarks and future directions

9.1. SUMMARY OF FINDINGS

9.1.1. RH5-based vaccines

As reported in chapter 3, this project's principal finding has been that vaccination with the novel blood-stage antigen RH5 induces antibodies which are capable of strain-transcending parasite neutralisation. In assays of GIA against vaccine-homologous 3D7 parasites, anti-RH5 antibodies are more potent than antibodies to the leading candidate AMA1, whether the comparison is made on the basis of total IgG concentration (which will be influenced by vaccine immunogenicity) or antigen-specific IgG concentration. The magnitude of this potency difference is, however, relatively modest (approximately two-fold), suggesting that a RH5-based vaccine would still need to induce and maintain a high antibody concentration to achieve *in vivo* protection. Given the results of previous clinical trials of AMA1 vaccines, which have not conclusively demonstrated protection despite mean antigen-specific antibody concentrations of around 200µg/mL (Spring, Cummings et al. 2009), it seems likely that a single-component RH5 vaccine would have to achieve antigen-specific antibody concentrations in excess of 100µg/mL: a challenging, though maybe not impossible, task.

One possible means of reducing the total quantity of antigen-specific antibody which must be induced by a blood-stage vaccine would be to incorporate two or more components with synergistic actions. The hope that two antigens may act synergistically is frequently expressed by vaccinologists: achieving and demonstrating genuine synergy, as distinct from an additive or sub-additive effect, is considerably more challenging. The work reported here has clearly and quantitatively demonstrated synergistic parasite neutralisation by antibodies to RH5 and RH4. When mixed in equal parts, the magnitude of the synergistic effect was comparable to a doubling in the concentration of anti-RH5; the synergy was apparent against 3D7 but not FVO strain parasites. The methodology developed to

identify this synergy is likely to be of use in future studies; the value of the RH5-RH4 synergy for a field-deployed blood-stage vaccine is open to question, and will depend both upon the extent of antigenic competition when the two antigens are co-administered, and upon the receptor-ligand usage profiles of parasites in the field.

Further work is required to fully elucidate the mechanism of parasite neutralisation by anti-RH5 antibodies. It seems clear, however, that antibodies that block the RH5-BSG interaction are capable of parasite neutralisation; that certain regions of the RH5 molecule comprise neutralising epitopes; and that binding of bivalent intact IgG molecules contributes to but is not absolutely necessary for parasite neutralisation.

Most encouragingly, the work reported here has clearly demonstrated that human-compatible RH5 vaccines can protect *Aotus nancymaae* against a heterologous-strain *P. falciparum* blood-stage challenge, and that this protection correlates strongly with antibody titre. It is likely that the protection will also correlate with GIA (assays are currently ongoing). This work will be an important stepping stone towards clinical trials, and may permit further studies of anti-RH5 mediated protection in the *Aotus* model.

9.1.2. Vaccine-evaluation methodology

The work reported in Chapter 7 attempted to improve the methods used to assess blood-stage (BS) vaccines in Phase IIa clinical trials, with a view to refining the analysis of a future clinical trial of RH5-based vaccines. The analysis of measurement of blood-stage parasite growth dynamics in Phase IIa clinical trials has demonstrated that a variety of techniques for estimation of LBI and PMR produce fairly closely correlated outputs. This should inspire confidence in PMR estimates for future mosquito-bite CHMI trials of BS vaccines.

Routine reporting of antibody levels as ELISA titres has been widespread in the field for many years. The application of SPR technology, as described in Chapter 4, to measure absolute antibody

concentrations may help researchers to present results in a manner which facilitates comparison between laboratories, antigens, and species.

9.2. FUTURE DIRECTIONS

9.2.1. RH5 viral vector vaccine clinical trial

The Jenner Institute has recently obtained funding for Good Manufacturing Practice (GMP) compliant manufacture and clinical trial of RH5-based viral vector vaccines. A period of manufacturing process development is therefore commencing for the ChAd63 and MVA RH5 vaccines (as tested in *Aotus*). Manufacturing itself is likely to commence in early 2013, with a view to Phase Ia trials in healthy UK adults in early 2014. Initial aims will be to study the safety and antibody immunogenicity of the vaccines; this will be followed by a Phase IIa blood-stage *P. falciparum* challenge to assess the ability of the vaccines to exert an *in vivo* effect.

9.2.2. RH5 protein vaccine development

Although viral vector RH5 vaccines achieved protection in *Aotus*, it seems likely that a protein-adjuvant vaccine component will be required to achieve the highest possible antibody levels, possibly by administering such a component in an adenovirus prime / protein-adjuvant boost regime. Production and purification of full-length RH5 protein without the CD4d3+4 tag has not proven possible in mammalian cells (C Crosnier [Sanger Centre] and J Illingworth [Jenner Institute], personal communication); nor has expression in *Pichia pastoris* (AD Douglas, unpublished observations) or expression of a variety of RH5 constructs in *E. coli* (M Higgins [U. of Oxford], personal communication). Expression of RH5 with a reasonable yield (10-20µg/mL) has, however, been possible in a proprietary *Drosophila* S2 stable cell-line-based system (W de Jongh, ExpreS^{2}ion Biotechnologies, Denmark, personal communication). Efforts are currently ongoing to optimise the process for purification of this protein, characterise its immunogenicity, and secure funding for GMP-compliant manufacture.

9.2.3. Medium-term RH5 vaccine regime optimisations

The details of the first generation of RH5 vaccines to enter clinical trial are already close to being finalised (ChAd63 and MVA RH5 as described in this thesis, and a Hexa-His-tagged monomeric RH5 protein produced from S2 cells), but refinement of these immunogens to generate second-generation RH5 vaccines will be a priority. Given the lengthy lead-times for GMP manufacture of novel immunogens, exploration of such refinements should probably start immediately. Relatively small improvements in RH5 vaccine immunogenicity – for example doubling of induced antibody titres – could have a substantial clinical impact.

9.2.3.1. Viral vectors

It seems likely that small improvements to the RH5 viral vectors may be possible. Possible improvements to the RH5 transgene cassette may include optimisation of the secretory peptide (synthetic secretory peptides may enhance the efficiency of secretion and hence antibody induction relative to the currect tPA peptide (Barash, Wang et al. 2002)), and inclusion of expression-enhancing elements, such as hepadnavirus post-transcriptional regulatory elements (Garg, Oran et al. 2004; Sun, Li et al. 2009).

There appears to be a hierarchy of immunogenicity among different adenovirus serotypes in small animals and macaques (Colloca, Barnes et al. 2012). Species E adenoviruses, such as ChAd63, appear to be somewhat less immunogenic than species C vectors, such as human adenovirus serotype 5. Clinical development of species C vectors has been hampered by safety concerns following Merck's STEP trial of an AdHu5 HIV vaccine (Buchbinder, Mehrotra et al. 2008) and efficacy concerns due to the high level of pre-existing anti-AdHu5 immunity in target populations (Dudareva, Andrews et al. 2009), which is associated with reduced vaccine immunogenicity (Buchbinder, Mehrotra et al. 2008). These challenges may be circumvented by novel species C viruses – either simian viruses (Colloca, Barnes et al. 2012), or human viruses engineered to evade pre-existing responses via expression of heterologous hypervariable regions (Roberts, Nanda et al. 2006). Such approaches have not yet reached clinical trial, but should probably be explored for RH5, particularly in view of evidence that

adenoviruses may achieve superior antibody-priming compared to protein-adjuvant formulations (de Cassan, Forbes et al. 2011).

9.2.3.2. Protein immunogens

The likely availability of a high-yielding recombinant RH5 expression platform will enable studies of a variety of modified RH5 protein immunogens.

Initial studies are likely to compare RH5 protein variants with varying mutations to putative N-glycosylation sites, as the effect of such mutations upon functional antibody induction are unpredictable (Stowers, Chen Lh et al. 2002; Bruder, Stefaniak et al. 2010).

Longer-term studies may include investigation of the potential to enhance antibody responses through formulation of RH5 as a multimeric or particulate antigen. A variety of such approaches have been proposed to enhance vaccine immunogenicity (Chackerian, Lowy et al. 2001; Kubler-Kielb, Majadly et al. 2007; Ogun, Dumon -Seignovert et al. 2008; Bachmann and Jennings 2010; Tissot, Renhofa et al. 2010), and the RTS,S malaria vaccine antigen is a virus-like particle based upon a hepatitis B virus surface antigen core (Rutgers, Gordon et al. 1988; Gordon, McGovern et al. 1995). The effectiveness of such approaches seems, however, to be inconsistent: published data frequently do not allow the separation of the effects of multimerisation *per se* from the effects of varying dose, adjuvant, and the addition of $CD4^+$ T cell epitopes within the multimerisation/particle-forming domain. The evidence for this approach is, perhaps, weakest in the case of relatively large protein immunogens such as RH5, which unlike peptide immunogens tend to be immunogenic in monomeric soluble form. Careful thought will need to be given to whether and how to explore such strategies with RH5, and ideally how to use such efforts to draw more general conclusions regarding the utility of this approach.

9.2.3.3. Adjuvants

The most important factor in determining the success or failure of an RH5 vaccine in clinical trials is likely to be the concentration of antibody induced by the vaccine. The adjuvant used to formulate an

RH5 protein vaccine will thus play an absolutely critical role. Leading adjuvants for antibody induction currently include Matrix M (Isconova, Sweden), AS01 (GSK), CoVaccineHT (British Technology Group), Carbopol/MF59 mixtures (Novartis), and liposomal/nanoparticle approaches, including interlamellar cross-linked multilayer vesicles (Spring, Cummings et al. 2009; de Cassan, Forbes et al. 2011; Lai, Seaman et al. 2012; Moon, Suh et al. 2012). Commercial / intellectual property restrictions on the use of these adjuvants are problematic, although 'generic' versions of some are available.

Head-to-head comparison of antibody induction by RH5 protein co-formulated with these adjuvants in mice, rabbits and Old World primates is a priority. Long-term maintenance of antibody concentrations is likely to be a particularly important area for study: there is at present relatively little understanding of whether certain adjuvant properties can promote the generation and survival of long-lived plasma cells capable of maintaining vaccine-induced antibody concentrations for months and years.

9.2.4. Relationship between *in vitro* GIA and protection

The ability of the GIA assay to predict *in vivo* protection is frequently questioned. Resolving this uncertainty is important to clarify whether pre-clinical selection of vaccine candidates on the basis of GIA is appropriate. On balance, the existing evidence supports the notion that very high levels of vaccine-induced GIA are capable of achieving protection against *P. falciparum*: the hypothesis is mechanistically plausible, and associations between GIA and protection have been demonstrated in non-human primates and possibly in humans (Singh, Miura et al. 2006; Duncan, Sheehy et al. 2011; Thera, Doumbo et al. 2011)(Thera, ASTMH conference abstract, 2011). The evidence reported in this thesis of non-human primate protection by an antigen selected largely on the basis of its ability to induce antibodies capable of *in vitro* GIA will lend further support to this belief. Levels of GIA exceeding 60% at 6 mg/ml IgG in the reference laboratory's assay are rare in studies of children from endemic area populations (Crompton, Miura et al. 2010). GIA-inducing vaccines can already achieve more potent parasite neutralisation than this (Spring, Cummings et al. 2009): the relevance of such

immuno-epidemiological studies to assessing likelihood of protection at a vaccine-induced non-natural level of GIA is therefore unclear.

Conclusive demonstration of a causal role for GIA-inducing antibodies would be possible with a passive transfer study of GIA-inducing and non-GIA-inducing anti-RH5 mAbs in *Aotus nancymaae.* A pilot study to assess this possibility was conducted alongside the *Aotus* active immunisation study reported in this thesis. Results are depicted in Figure 9.2.4.1. Clearly these results are promising, but require replication with an appropriate group size and the control of a non-GIA-inducing RH5 mAb.

The QA5 mAb used in this pilot study has an *in vitro* GIA EC_{50} of around 50µg/mL against invasion of human erythrocytes by FVO-strain parasites. Results of ELISA and GIA measurements to establish the concentration of mAb achieved in the pilot study animal are awaited. However the half-life of mouse mAbs in primates and humans is around one day, substantially lower than that of human mAbs (Wang, Wang et al. 2008). Crude pharmacokinetic calculations suggest that even the large mAb dose administered (120mg to a 1kg monkey) would only have been sufficient to achieve a plasma concentration in excess of the *in vitro* EC_{50} for 3-4 days (i.e. around two parasite lifecycles). The magnitude of the observed effect – a greater-than ten-fold reduction in cumulative parasitaemia with respect to control animals – is thus probably as substantial as could be expected.

A future study would probably use the mAb 9AD4, which is somewhat more potent than QA5 in GIA. Maintaining a higher level of mAb (and hence GIA) for a longer period in a future study would be desirable and may be achievable by chimerisation of the 9AD4 Fab regions with a human Fc region.

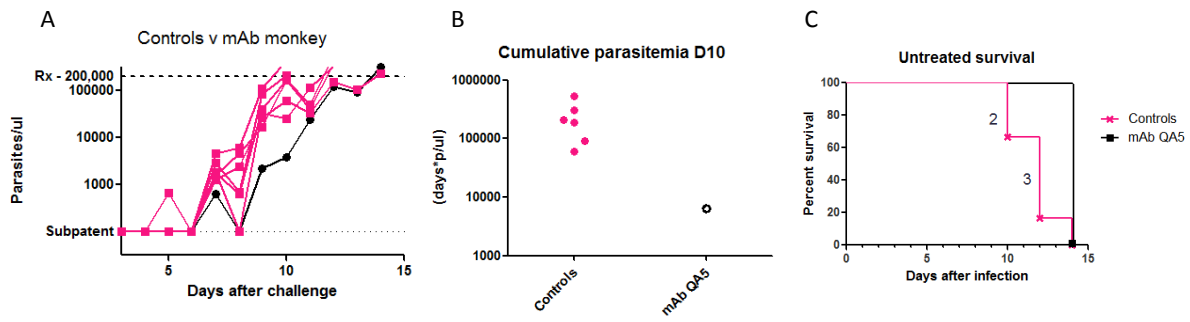

Figure 9.2.4.1 Pilot study of protection by anti-RH5 mAb in Aotus nancymaae
120mg of anti-RH5 mAb QA5 was administered to a single Aotus in divided doses 24 and 48 h after challenge with 10^4 FVO-strain infected Aotus RBCs. Plots show control monkeys (pink, as for the active immunisation trial) and passively immunised monkey (black). Progression of parasitemia was delayed (panel A), cumulative parasitemia to day 10 was reduced approximately 10-fold (panel B) and microscopic patency delayed by 2 days (panel C) with respect to the control group median.

9.2.5. A model for antibody-mediated parasite neutralisation

As discussed above, particularly in the chapter dealing with mechanism of parasite neutralisation by anti-RH5 antibodies, the speed of merozoite invasion into erythrocytes is likely to impose kinetic constraints upon the binding of anti-merozoite antibody. Understanding of these constraints may be important to design of blood-stage vaccines. Figure 9.2.4.2 depicts an attempt to describe the possible effects and interplay of merozoite invasion kinetics, antibody kinetics, and susceptibility of an antigen (or antigen combination) to antibody in determining the efficacy of parasite neutralisation.

As highlighted by Figure 9.2.4.2F, the speed of merozoite invasion *in vivo* is a key unknown. It is quite possible that the speed of invasion may differ between the *in vitro* assay, usually performed in static plates, and the *in vivo* situation of re-invasion, occurring in the context of blood flow and/or parasite sequestration. Differences in invasion speed may well underlie differences between *in vitro* GIA measurements and the impact of an equivalent antibody concentration upon *in vivo* parasite multiplication rate. It is clear that the attainment of 90% *in vitro* GIA at physiological antibody concentrations does not correspond to 90% *in vivo* growth reduction (Spring, Cummings et al. 2009). This suggests that the *in vivo* period of merozoite exposure may well be somewhat shorter than *in*

vitro. Although the quantitative relationship between antibody concentration and neutralisation is likely to differ *in vitro* and *in vivo* (a phenomenon well known to vaccinologists working on other pathogens), there is likely to be a limit on the extent to which these values can differ: for instance it would be quite surprising if invasion *in vivo* were to occur six times more rapidly than *in vitro*. If this were the case, *in vivo* growth inhibition would be expected to correspond to GIA at an approximately six-fold serum dilution. The belief that *in vivo* growth inhibition may be more closely related to *in vitro* GIA at a (currently unknown) sub-physiological IgG dilution is one reason that GIA has been reported throughout this work principally in terms of an EC_{50} value, rather than an absolute value at a particular concentration.

Attainment of high levels of GIA by human vaccinee antibody at such dilutions may well be achievable, but every effort is clearly going to be necessary to identify antigens, and synergistic antigen combinations, which reduce the vaccine-induced antibody concentration necessary to achieve such effects.

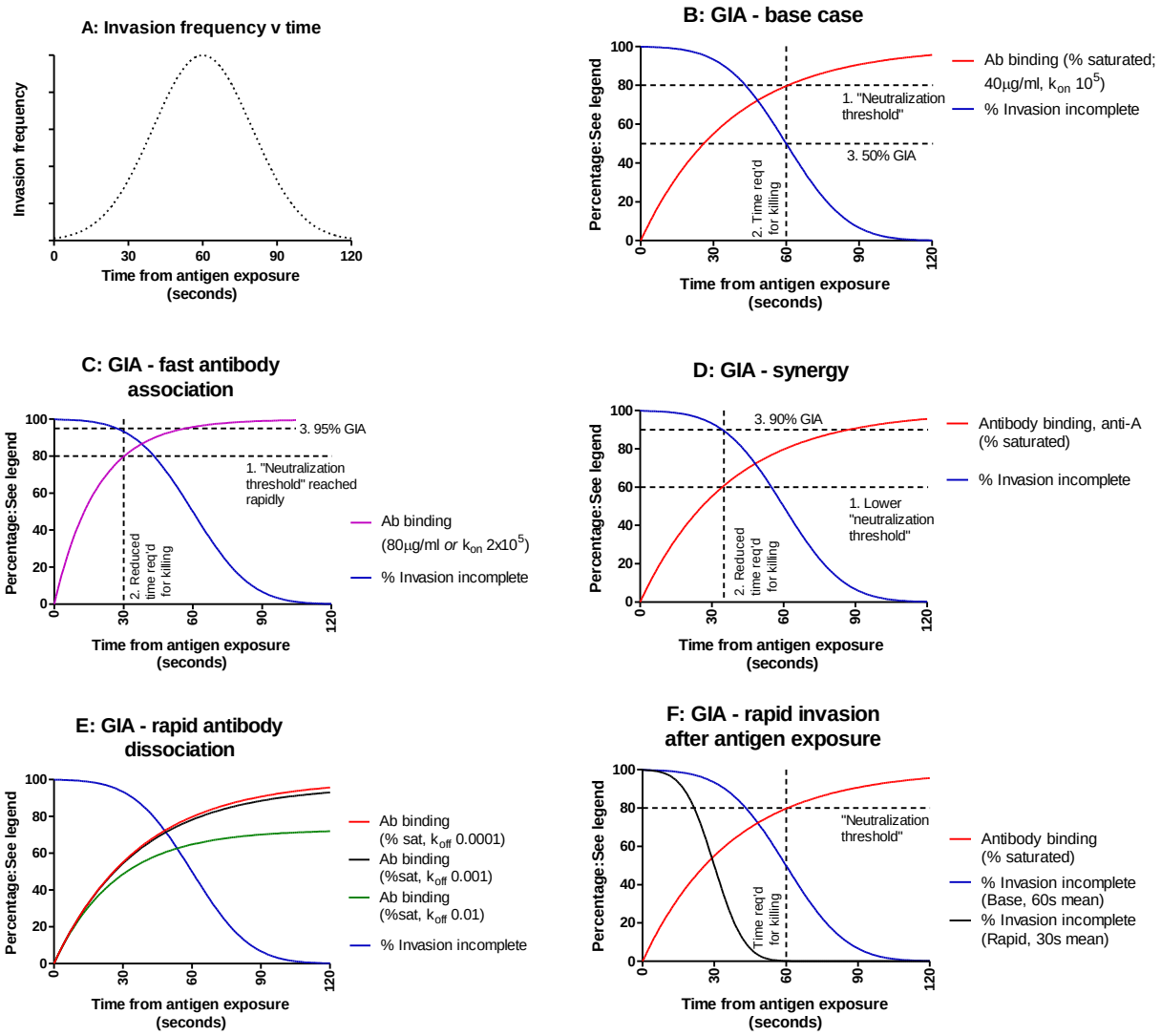

Figure 9.2.4.2 A model for antibody-mediated parasite neutralisation

Panel A illustrates a hypothetical frequency distribution of the period between exposure of a merozoite antigen and completion of invasion (the distribution is normal, with a mean of 60 seconds similar to the in vitro duration of merozoite exposure (Gilson and Crabb 2009), and standard deviation [SD] 20 seconds).

Panel B illustrates a possible relationship between the distribution shown in panel A and GIA. The blue line represents percentage of merozoites which have not yet completed invasion, and thus remain 'available' for neutralisation (this is the inverse cumulative density function [CDF] of the distribution shown in panel A).

Figure 9.2.4.2 continued

The red line in panel B illustrates percentage saturation of an antigen by an antibody which is present at 40µg/mL, with k_{on} of 10^5 $M^{-1}s^{-1}$ and k_{off} of 10^{-4} s^{-1}, and hence overall monovalent affinity (K_D) of 1nM. This concentration is similar to the in vitro EC_{50} of anti-RH5 antibody, and the k_{on} and k_{off} values are similar to measured values for anti-RH5 mAbs (Chapter 6). The concentration is similar to that which can be achieved in vivo in humans by modern subunit vaccine platforms, including viral vectors (Sheehy, Duncan et al. 2012), and the k_{on} value is the same as that assumed in a previous discussion of antibody kinetics and merozoite neutralisation (Saul 1987). Curves were simulated using the 1:1 binding kinetics model incorporated in Prism 5 (GraphPad Software); consideration of the possibility of bivalent binding would be expected to result in, if anything, slightly more rapid antigen saturation due to reduced antibody dissociation. If 80% antigen-antibody saturation is required to achieve neutralisation (the "neutralisation threshold", this will occur at around 60 seconds, and 50% of the merozoites will be neutralised.

Panels C-F show variations upon the scenario depicted in panel B. In each case, the blue and red lines, where present, are identical to those in panel B; lines of different colours indicate kinetics of invasion/binding after one or more variable has changed from the base case in panel B.

Panel C depicts the effect of a doubling of the rate of antibody binding, such as may arise either from a doubling of antibody concentration to 80µg/mL, or from a doubling of antibody on-rate to $2x10^5$ $M^{-1}s^{-1}$. This halves the time required to reach the "neutralisation threshold" and hence results in a substantial increase in GIA, to 95%. Antibody on-rates are rarely measured by vaccinologists; this panel suggests that small uncertainties in the true on-rate could result in substantial errors in previous analyses of kinetic constraints upon merozoite neutralisation (Saul 1987).

Panel D depicts a possible mechanism by which synergy between two antibody specificities could arise. For simplicity, only the binding of one antibody specificity is shown. The effect of the presence of the other antibody is to lower the "neutralisation threshold" slightly, from 80% to 60% saturation. This reduces the time required for antibody binding to ~35 seconds, and hence increases GIA to 90%.

Panel E depicts effects upon antibody binding of changes in the dissociation rate, k_{off}. k_{off} is only likely to be an important parameter affecting the shape of the antibody binding curve if a) concentration is similar to K_D (hence equilibrium will be reached with a substantial proportion of unbound antigen) ***and*** *b) the antibody-antigen association is approaching equilibrium within the period of exposure of the antigen (hence antibody-antigen dissociation becomes almost as frequent as association). These conditions are unlikely to be met for vaccine-induced antibody inhibition of merozoite invasion because a 40µg/mL concentration of antibody (267nM) is high relative to the typical affinity of an antigen-antibody interaction; few in the field would expect antibody to be effective at blocking merozoite invasion at, say, 10-fold lower concentrations which might be closer to the K_D. Panel E illustrates that very large changes (100-fold) in the dissociation rate (relative to those illustrated in panel B) are required to have a substantial effect upon the percentage of antigen saturated by antibody within 60 seconds.*

Panel F depicts the effect of a reduced period of exposure of merozoites (or individual antigens) to antibody, resulting in a change in the invasion versus time frequency distribution shown in panel A. The black line depicts a modified inverse normal CDF, reflecting a mean duration of exposure of 30 seconds, with SD 10 seconds. Under these conditions, neutralisation of parasites is effectively abolished. Importantly however, it would be restored to 50% by a doubling of antibody concentration or association rate, as discussed in panel C. Duration of in vivo merozoite exposure to antibody is thus an important unknown in assessing the likely relationship between neutralising antibody concentration, in vitro GIA, and in vivo protection against malaria.

9.2.6. Towards a synergistic two-component blood-stage vaccine

The work reported here has clearly shown that vaccine-induced antibodies of different specificities can act synergistically to neutralise parasites.

The best chance of truly clinically useful synergy is likely to come from the combination of two antigens which are individually capable of achieving high-level GIA when acting alone: only two of the antibody specificities tested thus far (anti-RH5 and anti-AMA1) would meet this criterion. Detailed study of invasion mechanisms has highlighted certain antigens which are functionally closely related to RH5, e.g. Ripr: such antigens may be capable of inducing high-level GIA alone, and synergising with RH5 (Chen, Lopaticki et al. 2011). Assessment of GIA by anti-Ripr / anti-RH5 combinations will be of considerable interest.

Recombinant antigen expression systems are now capable of expressing the majority of tested *Plasmodial* antigens. Such technologies are likely to permit large-scale screens of the ability of uncharacterised antigens to induce functionally-active antibodies (G Wright [Sanger Centre] and W de Jongh {ExpreS^{2}ion Biotechnologies], personal communication). Such systematic screening approaches may be of considerable value in moving the malaria vaccine field away from its long-standing dependence upon a small group of intensively studied antigens.

9.3. FINAL REMARKS

The identification of RH5 as a promising blood-stage vaccine candidate involved a fortuitous coming-together of emerging data to suggest the role of RH proteins in erythrocyte invasion with a platform capable of expressing the antigen (mammalian cells, via viral vectors) and the infrastructure and translational mind-set of the Jenner Institute. This combination has allowed rapid evaluation and progression of RH5 vaccines from mice, into rabbit and *Aotus* studies.

Now, as RH5 vaccines move towards clinical trials based upon sound pre-clinical rationale, it is surely more important than ever to continue to invest time and effort in the pre-clinical development of optimised RH5 formulations and novel blood-stage antigens.

BIBLIOGRAPHY

Alcock, R., M. G. Cottingham, C. S. Rollier, J. Furze, S. D. De Costa, M. Hanlon, A. J. Spencer, J. D. Honeycutt, D. H. Wyllie, S. C. Gilbert, M. Bregu and A. V. S. Hill (2010). "Long-Term Thermostabilization of Live Poxviral and Adenoviral Vaccine Vectors at Supraphysiological Temperatures in Carbohydrate Glass." Science Translational Medicine **2**(19).

Alexander, D. L., S. Arastu-Kapur, J. F. Dubremetz and J. C. Boothroyd (2006). "Plasmodium falciparum AMA1 binds a rhoptry neck protein homologous to TgRON4, a component of the moving junction in Toxoplasma gondii." Eukaryot Cell **5**(7): 1169-1173.

Andrews, L., R. F. Andersen, D. Webster, S. Dunachie, R. M. Walther, P. Bejon, A. Hunt-Cooke, G. Bergson, F. Sanderson, A. V. Hill and S. C. Gilbert (2005). "Quantitative real-time polymerase chain reaction for malaria diagnosis and its use in malaria vaccine clinical trials." Am J Trop.Med Hyg. **73**(1): 191-198.

Angrisano, F., D. T. Riglar, A. Sturm, J. C. Volz, M. J. Delves, E. S. Zuccala, L. Turnbull, C. Dekiwadia, M. A. Olshina, D. S. Marapana, W. Wong, V. Mollard, C. H. Bradin, C. J. Tonkin, P. W. Gunning, S. A. Ralph, C. B. Whitchurch, R. E. Sinden, A. F. Cowman, G. I. McFadden and J. Baum (2012). "Spatial Localisation of Actin Filaments across Developmental Stages of the Malaria Parasite." Plos One **7**(2): e32188.

Arnot, D. E., D. R. Cavanagh, E. J. Remarque, A. M. Creasey, M. P. K. Sowa, W. D. Morgan, A. A. Holder, S. Longacre and A. W. Thomas (2008). "Comparative testing of six antigen-based malaria vaccine candidates directed toward merozoite-stage Plasmodium falciparum." Clinical and Vaccine Immunology **15**(9): 1345-1355.

Arumugam, T. U., S. Takeo, T. Yamasaki, A. Thonkukiatkul, K. Miura, H. Otsuki, H. Zhou, C. A. Long, J. Sattabongkot, J. Thompson, D. W. Wilson, J. G. Beeson, J. Healer, B. S. Crabb, A. F. Cowman, M. Torii and T. Tsuboi (2011). "Discovery of GAMA, a Plasmodium falciparum merozoite micronemal protein, as a novel blood-stage vaccine candidate antigen." Infect Immun **79**(11): 4523-4532.

Bachmann, M. F. and G. T. Jennings (2010). "Vaccine delivery: a matter of size, geometry, kinetics and molecular patterns." Nature Reviews Immunology **10**(11): 787-796.

Baldi, D. L., K. T. Andrews, R. F. Waller, D. S. Roos, R. F. Howard, B. S. Crabb and A. F. Cowman (2000). "RAP1 controls rhoptry targeting of RAP2 in the malaria parasite Plasmodium falciparum." EMBO J **19**(11): 2435-2443.

Baldi, D. L., R. Good, M. T. Duraisingh, B. S. Crabb and A. F. Cowman (2002). "Identification and disruption of the gene encoding the third member of the low-molecular-mass rhoptry complex in Plasmodium falciparum." Infect Immun **70**(9): 5236-5245.

Bannister, L. H., J. M. Hopkins, A. R. Dluzewski, G. Margos, I. T. Williams, M. J. Blackman, C. H. Kocken, A. W. Thomas and G. H. Mitchell (2003). "Plasmodium falciparum apical membrane antigen 1 (PfAMA-1) is translocated within micronemes along subpellicular microtubules during merozoite development." J Cell Sci **116**(Pt 18): 3825-3834.

Bannister, L. H., J. M. Hopkins, R. E. Fowler, S. Krishna and G. H. Mitchell (2000). "Ultrastructure of rhoptry development in Plasmodium falciparum erythrocytic schizonts." Parasitology **121 (Pt 3)**: 273-287.

Barash, S., W. Wang and Y. Shi (2002). "Human secretory signal peptide description by hidden Markov model and generation of a strong artificial signal peptide for secreted protein expression." Biochem Biophys Res Commun **294**(4): 835-842.

Baum, J., L. Chen, J. Healer, S. Lopaticki, M. Boyle, T. Triglia, F. Ehlgen, S. A. Ralph, J. G. Beeson and A. F. Cowman (2009). "Reticulocyte-binding protein homologue 5 - An essential adhesin involved in invasion of human erythrocytes by Plasmodium falciparum." International Journal for Parasitology **39**(3): 371-380.

Baum, J., T. W. Gilberger, F. Frischknecht and M. Meissner (2008). "Host-cell invasion by malaria parasites: insights from Plasmodium and Toxoplasma." Trends in Parasitology **24**(12): 557-563.

Baum, J., A. G. Maier, R. T. Good, K. M. Simpson and A. F. Cowman (2005). "Invasion by P. falciparum merozoites suggests a hierarchy of molecular interactions." PLoS.Pathog. **1**(4): e37.

Bejon, P., L. Andrews, R. F. Andersen, S. Dunachie, D. Webster, M. Walther, S. C. Gilbert, T. Peto and A. V. Hill (2005). "Calculation of liver-to-blood inocula, parasite growth rates, and preerythrocytic vaccine efficacy, from serial quantitative polymerase chain reaction studies of volunteers challenged with malaria sporozoites." J Infect.Dis. **191**(4): 619-626.

Bergmann-Leitner, E. S., E. H. Duncan, G. E. Mullen, J. R. Burge, F. Khan, C. A. Long, E. Angov and J. A. Lyon (2006). "Critical evaluation of different methods for measuring the functional activity of antibodies against malaria blood stage antigens." Am J Trop.Med Hyg. **75**(3): 437-442.

Bietz, S., I. Montilla, S. Kulzer, J. M. Przyborski and K. Lingelbach (2009). "Recruitment of human aquaporin 3 to internal membranes in the Plasmodium falciparum infected erythrocyte." Mol Biochem Parasitol **167**(1): 48-53.

Biswas, S., M. D. Dicks, C. A. Long, E. J. Remarque, L. Siani, S. Colloca, M. G. Cottingham, A. A. Holder, S. C. Gilbert, A. V. Hill and S. J. Draper (2011). "Transgene Optimization, Immunogenicity and In Vitro Efficacy of Viral Vectored Vaccines Expressing Two Alleles of Plasmodium falciparum AMA1." PLoS ONE **6**(6): e20977.

Bliss, C. I. (1939). "The Toxicity of Poisons Applied Jointly." Annals of Applied Biology **26**(3): 585-615.

Bottius, E., A. Guanzirolli, J. F. Trape, C. Rogier, L. Konate and P. Druilhe (1996). "Malaria: even more chronic in nature than previously thought; evidence for subpatent parasitaemia detectable by the polymerase chain reaction." Trans.R.Soc.Trop.Med Hyg. **90**(1): 15-19.

Boyle, M. J., D. W. Wilson, J. S. Richards, D. T. Riglar, K. K. Tetteh, D. J. Conway, S. A. Ralph, J. Baum and J. G. Beeson (2010). "Isolation of viable Plasmodium falciparum merozoites to define erythrocyte invasion events and advance vaccine and drug development." Proc.Natl.Acad.Sci.U.S.A **107**(32): 14378-14383.

Brooks, A., O. J. Briet, D. Hardy, R. Steketee and T. A. Smith (2012). "Simulated Impact of RTS,S/AS01 Vaccination Programs in the Context of Changing Malaria Transmission." Plos One **7**(3): e32587.

Bruder, J. T., M. E. Stefaniak, N. B. Patterson, P. Chen, S. Konovalova, K. Limbach, J. J. Campo, D. Ettyreddy, S. Li, F. Dubovsky, T. L. Richie, C. R. King, C. A. Long and D. L. Doolan (2010). "Adenovectors induce functional antibodies capable of potent inhibition of blood stage malaria parasite growth." Vaccine **28**(18): 3201-3210.

Buchbinder, S. P., D. V. Mehrotra, A. Duerr, D. W. Fitzgerald, R. Mogg, D. Li, P. B. Gilbert, J. R. Lama, M. Marmor, C. Del Rio, M. J. McElrath, D. R. Casimiro, K. M. Gottesdiener, J. A. Chodakewitz, L. Corey and M. N. Robertson (2008). "Efficacy assessment of a cell-mediated immunity HIV-1 vaccine (the Step Study): a double-blind, randomised, placebo-controlled, test-of-concept trial." Lancet **372**(9653): 1881-1893.

Bull, P. C., B. S. Lowe, M. Kortok, C. S. Molyneux, C. I. Newbold and K. Marsh (1998). "Parasite antigens on the infected red cell surface are targets for naturally acquired immunity to malaria." Nature Medicine **4**(3): 358-360.

Burbelo, P. D., K. H. Ching, C. M. Klimavicz and M. J. Iadarola (2009). "Antibody profiling by Luciferase Immunoprecipitation Systems (LIPS)." J Vis Exp(32).

Bushell, K. M., C. Sollner, B. Schuster-Boeckler, A. Bateman and G. J. Wright (2008). "Large-scale screening for novel low-affinity extracellular protein interactions." Genome Res **18**(4): 622-630.

Carter, R. (2001). "Transmission blocking malaria vaccines." Vaccine **19**(17-19): 2309-2314.

Carter, R. and K. N. Mendis (2002). "Evolutionary and historical aspects of the burden of malaria." Clinical Microbiology Reviews **15**(4): 564-+.

Casares, S., T. D. Brumeanu and T. L. Richie (2010). "The RTS,S malaria vaccine." Vaccine **28**(31): 4880-4894.

Chackerian, B., D. R. Lowy and J. T. Schiller (2001). "Conjugation of a self-antigen to papillomavirus-like particles allows for efficient induction of protective autoantibodies." Journal of Clinical Investigation **108**(3): 415-423.

Chen, L., S. Lopaticki, D. T. Riglar, C. Dekiwadia, A. D. Uboldi, W. H. Tham, M. T. O'Neill, D. Richard, J. Baum, S. A. Ralph and A. F. Cowman (2011). "An EGF-like protein forms a complex with PfRh5 and is required for invasion of human erythrocytes by Plasmodium falciparum." PLoS Pathog **7**(9): e1002199.

Cheng, Q., G. Lawrence, C. Reed, A. Stowers, L. Ranford-Cartwright, A. Creasey, R. Carter and A. Saul (1997). "Measurement of Plasmodium falciparum growth rates in vivo: a test of malaria vaccines." Am J Trop.Med Hyg. **57**(4): 495-500.

Chitnis, C. E. and A. Sharma (2008). "Targeting the Plasmodium vivax Duffy-binding protein." Trends Parasitol. **24**(1): 29-34.

Christensen, L. L. H. (1997). "Theoretical analysis of protein concentration determination using biosensor technology under conditions of partial mass transport limitation." Analytical Biochemistry **249**(2): 153-164.

Cohen, S., I. A. McGregor and S. Carrington (1961). "Gamma-globulin and acquired immunity to human malaria." Nature **192**: 733-737.

Coley, A. M., K. Parisi, R. Masciantonio, J. Hoeck, J. L. Casey, V. J. Murphy, K. S. Harris, A. H. Batchelor, R. F. Anders and M. Foley (2006). "The most polymorphic residue on Plasmodium falciparum apical membrane antigen 1 determines binding of an invasion-inhibitory antibody." Infect Immun **74**(5): 2628-2636.

Collins, C. R., C. Withers-Martinez, G. A. Bentley, A. H. Batchelor, A. W. Thomas and M. J. Blackman (2007). "Fine mapping of an epitope recognized by an invasion-inhibitory monoclonal antibody on the malaria vaccine candidate apical membrane antigen 1." J Biol Chem **282**(10): 7431-7441.

Collins, C. R., C. Withers-Martinez, F. Hackett and M. J. Blackman (2009). "An inhibitory antibody blocks interactions between components of the malarial invasion machinery." PLoS Pathog **5**(1): e1000273.

Collins, W. E., G. G. Galland, J. W. Barnwell, V. Udhayakumar, J. S. Sullivan, D. Nace, J. E. Tongren, T. Williams, J. Roberts, Y. P. Shi and A. A. Lal (2005). "Preliminary observations on the efficacy of a recombinant multistage Plasmodium falciparum vaccine in Aotus nancymai monkeys." Am J Trop Med Hyg **73**(4): 686-693.

Collins, W. E., G. G. Galland, J. S. Sullivan and C. L. Morris (1994). "Selection of different strains of Plasmodium falciparum for testing blood-stage vaccines in Aotus nancymai monkeys." Am J Trop Med Hyg **51**(2): 224-232.

Collins, W. E. and G. M. Jeffery (1999). "A retrospective examination of secondary sporozoite- and trophozoite-induced infections with Plasmodium falciparum: Development of parasitologic and clinical immunity following secondary infection." American Journal of Tropical Medicine and Hygiene **61**(1): 20-35.

Collins, W. E. and G. M. Jeffery (1999). "A retrospective examination of sporozoite- and trophozoite-induced infections with Plasmodium falciparum: Development of parasitologic and clinical immunity during primary infection." American Journal of Tropical Medicine and Hygiene **61**(1): 4-19.

Collins, W. E. and G. M. Jeffery (1999). "A retrospective examination of the patterns of recrudescence in patients infected with Plasmodium falciparum." Am J Trop Med Hyg **61**(1 Suppl): 44-48.

Collins, W. E., A. Walduck, J. S. Sullivan, K. Andrews, A. Stowers, C. L. Morris, V. Jennings, C. Yang, J. Kendall, Q. Lin, L. B. Martin, C. Diggs and A. Saul (2000). "Efficacy of vaccines containing

rhoptry-associated proteins RAP1 and RAP2 of Plasmodium falciparum in Saimiri boliviensis monkeys." Am J Trop Med Hyg **62**(4): 466-479.

Colloca, S., E. Barnes, A. Folgori, V. Ammendola, S. Capone, A. Cirillo, L. Siani, M. Naddeo, F. Grazioli, M. L. Esposito, M. Ambrosio, A. Sparacino, M. Bartiromo, A. Meola, K. Smith, A. Kurioka, G. A. O'Hara, K. J. Ewer, N. Anagnostou, C. Bliss, A. V. Hill, C. Traboni, P. Klenerman, R. Cortese and A. Nicosia (2012). "Vaccine vectors derived from a large collection of simian adenoviruses induce potent cellular immunity across multiple species." Sci Transl Med **4**(115): 115ra112.

Cowman, A. F. and B. S. Crabb (2006). "Invasion of red blood cells by malaria parasites." Cell **124**(4): 755-766.

Crompton, P. D., M. A. Kayala, B. Traore, K. Kayentao, A. Ongoiba, G. E. Weiss, D. M. Molina, C. R. Burk, M. Waisberg, A. Jasinskas, X. Tan, S. Doumbo, D. Doumtabe, Y. Kone, D. L. Narum, X. Liang, O. K. Doumbo, L. H. Miller, D. L. Doolan, P. Baldi, P. L. Felgner and S. K. Pierce (2010). "A prospective analysis of the Ab response to Plasmodium falciparum before and after a malaria season by protein microarray." Proc.Natl.Acad.Sci.U.S.A **107**(15): 6958-6963.

Crompton, P. D., K. Miura, B. Traore, K. Kayentao, A. Ongoiba, G. Weiss, S. Doumbo, D. Doumtabe, Y. Kone, C. Y. Huang, O. K. Doumbo, L. H. Miller, C. A. Long and S. K. Pierce (2010). "In Vitro Growth-Inhibitory Activity and Malaria Risk in a Cohort Study in Mali." Infection and Immunity **78**(2): 737-745.

Crosnier, C., L. Y. Bustamante, S. J. Bartholdson, A. K. Bei, M. Theron, M. Uchikawa, S. Mboup, O. Ndir, D. P. Kwiatkowski, M. T. Duraisingh, J. C. Rayner and G. J. Wright (2011). "Basigin is a receptor essential for erythrocyte invasion by Plasmodium falciparum." Nature.

Dame, J. B., J. L. Williams, T. F. McCutchan, J. L. Weber, R. A. Wirtz, W. T. Hockmeyer, W. L. Maloy, J. D. Haynes, I. Schneider, D. Roberts, G. S. Sanders, E. P. Reddy, C. L. Diggs and L. H. Miller (1984). "STRUCTURE OF THE GENE ENCODING THE IMMUNODOMINANT SURFACE-ANTIGEN ON THE SPOROZOITE OF THE HUMAN MALARIA PARASITE PLASMODIUM-FALCIPARUM." Science **225**(4662): 593-599.

Darko, C. A., E. Angov, W. E. Collins, E. S. Bergmann-Leitner, A. S. Girouard, S. L. Hitt, J. S. McBride, C. L. Diggs, A. A. Holder, C. A. Long, J. W. Barnwell and J. A. Lyon (2005). "The clinical-grade 42-kilodalton fragment of merozoite surface protein 1 of Plasmodium falciparum strain FVO expressed in Escherichia coli protects Aotus nancymai against challenge with homologous erythrocytic-stage parasites." Infect.Immun. **73**(1): 287-297.

de Cassan, S. C., E. K. Forbes, A. D. Douglas, A. Milicic, B. Singh, P. Gupta, V. S. Chauhan, C. E. Chitnis, S. C. Gilbert, A. V. Hill and S. J. Draper (2011). "The requirement for potent adjuvants to enhance the immunogenicity and protective efficacy of protein vaccines can be overcome by prior immunization with a recombinant adenovirus." J Immunol **187**(5): 2602-2616.

de Koning-Ward, T. F., P. R. Gilson, J. A. Boddey, M. Rug, B. J. Smith, A. T. Papenfuss, P. R. Sanders, R. J. Lundie, A. G. Maier, A. F. Cowman and B. S. Crabb (2009). "A newly discovered protein export machine in malaria parasites." Nature **459**(7249): 945-949.

Dietz, K., G. Raddatz and L. Molineaux (2006). "Mathematical model of the first wave of Plasmodium falciparum asexual parasitemia in non-immune and vaccinated individuals." Am J Trop Med Hyg **75**(2 Suppl): 46-55.

Dluzewski, A. R., D. Zicha, G. A. Dunn and W. B. Gratzer (1995). "Origins of the parasitophorous vacuole membrane of the malaria parasite: surface area of the parasitized red cell." Eur J Cell Biol **68**(4): 446-449.

Doolan, D. L. (2002). Malaria methods and protocols. Totowa, N.J. ; [Great Britain], Humana.

Douglas, A. D., L. Andrews, S. J. Draper, K. Bojang, P. Milligan, S. C. Gilbert, E. B. Imoukhuede and A. V. Hill (2011). "Substantially reduced pre-patent parasite multiplication rates are associated with naturally acquired immunity to Plasmodium falciparum." J Infect Dis **203**(9): 1337-1340.

Douglas, A. D., S. C. de Cassan, M. D. Dicks, S. C. Gilbert, A. V. Hill and S. J. Draper (2010). "Tailoring subunit vaccine immunogenicity: maximizing antibody and T cell responses by using

combinations of adenovirus, poxvirus and protein-adjuvant vaccines against Plasmodium falciparum MSP1." Vaccine **28**(44): 7167-7178.

Douglas, A. D., A. R. Williams, J. J. Illingworth, G. Kamuyu, S. Biswas, A. L. Goodman, D. H. Wyllie, C. Crosnier, K. Miura, G. J. Wright, C. A. Long, F. H. Osier, K. Marsh, A. V. Turner, A. V. Hill and S. J. Draper (2011). "The blood-stage malaria antigen PfRH5 is susceptible to vaccine-inducible cross-strain neutralizing antibody." Nat Commun **2**: 601.

Draper, S. J., S. Biswas, A. J. Spencer, E. J. Remarque, S. Capone, M. Naddeo, M. D. Dicks, B. W. Faber, S. C. de Cassan, A. Folgori, A. Nicosia, S. C. Gilbert and A. V. Hill (2010). "Enhancing Blood-Stage Malaria Subunit Vaccine Immunogenicity in Rhesus Macaques by Combining Adenovirus, Poxvirus, and Protein-in-Adjuvant Vaccines." J.Immunol.

Draper, S. J., S. Biswas, A. J. Spencer, E. J. Remarque, S. Capone, M. Naddeo, M. D. J. Dicks, B. W. Faber, S. C. de Cassan, A. Folgori, A. Nicosia, S. C. Gilbert and A. V. S. Hill (2010). "Enhancing blood-stage malaria subunit vaccine immunogenicity in rhesus macaques by combining adenovirus, poxvirus, and protein-in-adjuvant vaccines." J Immunol **185**(12): 7583-7595.

Draper, S. J., A. L. Goodman, S. Biswas, E. K. Forbes, A. C. Moore, S. C. Gilbert and A. V. Hill (2009). "Recombinant viral vaccines expressing merozoite surface protein-1 induce antibody- and T cell-mediated multistage protection against malaria." Cell Host Microbe **5**(1): 95-105.

Draper, S. J., A. C. Moore, A. L. Goodman, C. A. Long, A. A. Holder, S. C. Gilbert, F. Hill and A. V. Hill (2008). "Effective induction of high-titer antibodies by viral vector vaccines." Nat.Med **14**(8): 819-821.

Druilhe, P. and J. L. Perignon (1997). "A hypothesis about the chronicity of malaria infection." Parasitol.Today **13**(9): 353-357.

Dudareva, M., L. Andrews, S. C. Gilbert, P. Bejon, K. Marsh, J. Mwacharo, O. Kai, A. Nicosia and A. V. Hill (2009). "Prevalence of serum neutralizing antibodies against chimpanzee adenovirus 63 and human adenovirus 5 in Kenyan children, in the context of vaccine vector efficacy." Vaccine **27**(27): 3501-3504.

Dunachie, S. J., M. Walther, J. E. Epstein, S. Keating, T. Berthoud, L. Andrews, R. F. Andersen, P. Bejon, N. Goonetilleke, I. Poulton, D. P. Webster, G. Butcher, K. Watkins, R. E. Sinden, G. L. Levine, T. L. Richie, J. Schneider, D. Kaslow, S. C. Gilbert, D. J. Carucci and A. V. Hill (2006). "A DNA prime-modified vaccinia virus ankara boost vaccine encoding thrombospondin-related adhesion protein but not circumsporozoite protein partially protects healthy malaria-naive adults against Plasmodium falciparum sporozoite challenge." Infect.Immun. **74**(10): 5933-5942.

Dunachie, S. J., M. Walther, J. M. Vuola, D. P. Webster, S. M. Keating, T. Berthoud, L. Andrews, P. Bejon, I. Poulton, G. Butcher, K. Watkins, R. E. Sinden, A. Leach, P. Moris, N. Tornieporth, J. Schneider, F. Dubovsky, E. Tierney, J. Williams, D. G. Heppner, S. C. Gilbert, J. Cohen and A. V. S. Hill (2006). "A clinical trial of prime-boost immunisation with the candidate malaria vaccines RTS,S/AS02A and MVA-CS." Vaccine **24**(15): 2850-2859.

Duncan, C. J., S. H. Sheehy, K. J. Ewer, A. D. Douglas, K. A. Collins, F. D. Halstead, S. C. Elias, P. J. Lillie, K. Rausch, J. Aebig, K. Miura, N. J. Edwards, I. D. Poulton, A. Hunt-Cooke, D. W. Porter, F. M. Thompson, R. Rowland, S. J. Draper, S. C. Gilbert, M. P. Fay, C. A. Long, D. Zhu, Y. Wu, L. B. Martin, C. F. Anderson, A. M. Lawrie, A. V. Hill and R. D. Ellis (2011). "Impact on Malaria Parasite Multiplication Rates in Infected Volunteers of the Protein-in-Adjuvant Vaccine AMA1-C1/Alhydrogel+CPG 7909." Plos One **6**(7): e22271.

Duraisingh, M. T., T. Triglia, S. A. Ralph, J. C. Rayner, J. W. Barnwell, G. I. McFadden and A. F. Cowman (2003). "Phenotypic variation of Plasmodium falciparum merozoite proteins directs receptor targeting for invasion of human erythrocytes." EMBO J **22**(5): 1047-1057.

Dutta, S., J. D. Haynes, A. Barbosa, L. A. Ware, J. D. Snavely, J. K. Moch, A. W. Thomas and D. E. Lanar (2005). "Mode of action of invasion-inhibitory antibodies directed against apical membrane antigen 1 of Plasmodium falciparum." Infect Immun **73**(4): 2116-2122.

Dutta, S., J. S. Sullivan, K. K. Grady, J. D. Haynes, J. Komisar, A. H. Batchelor, L. Soisson, C. L. Diggs, D. G. Heppner, D. E. Lanar, W. E. Collins and J. W. Barnwell (2009). "High Antibody Titer against Apical Membrane Antigen-1 Is Required to Protect against Malaria in the Aotus Model." Plos One **4**(12).

Edstein, M. D., B. M. Kotecka, K. L. Anderson, D. J. Pombo, D. E. Kyle, K. H. Rieckmann and M. F. Good (2005). "Lengthy antimalarial activity of atovaquone in human plasma following atovaquone-proguanil administration." Antimicrobial Agents and Chemotherapy **49**(10): 4421-4422.

Edwards, M. J. and N. J. Dimmock (2000). "Two influenza A virus-specific Fabs neutralize by inhibiting virus attachment to target cells, while neutralization by their IgGs is complex and occurs simultaneously through fusion inhibition and attachment inhibition." Virology **278**(2): 423-435.

Ellis, R. D., I. Sagara, O. Doumbo and Y. Wu (2010). "Blood stage vaccines for Plasmodium falciparum: Current status and the way forward." Hum.Vaccin. **6**(8).

Epstein, J. E., K. Tewari, K. E. Lyke, B. K. Sim, P. F. Billingsley, M. B. Laurens, A. Gunasekera, S. Chakravarty, E. R. James, M. Sedegah, A. Richman, S. Velmurugan, S. Reyes, M. Li, K. Tucker, A. Ahumada, A. J. Ruben, T. Li, R. Stafford, A. G. Eappen, C. Tamminga, J. W. Bennett, C. F. Ockenhouse, J. R. Murphy, J. Komisar, N. Thomas, M. Loyevsky, A. Birkett, C. V. Plowe, C. Loucq, R. Edelman, T. L. Richie, R. A. Seder and S. L. Hoffman (2011). "Live attenuated malaria vaccine designed to protect through hepatic CD8 T cell immunity." Science **334**(6055): 475-480.

Faber, B. W., E. J. Remarque, W. D. Morgan, C. H. M. Kocken, A. A. Holder and A. W. Thomas (2007). "Malaria vaccine-related benefits of a single protein comprising Plasmodium falciparum apical membrane antigen 1 domains I and II fused to a modified form of the 19-kilodalton C-terminal fragment of merozoite surface protein 1." Infection and Immunity **75**(12): 5947-5955.

Florens, L., M. P. Washburn, J. D. Raine, R. M. Anthony, M. Grainger, J. D. Haynes, J. K. Moch, N. Muster, J. B. Sacci, D. L. Tabb, A. A. Witney, D. Wolters, Y. Wu, M. J. Gardner, A. A. Holder, R. E. Sinden, J. R. Yates and D. J. Carucci (2002). "A proteomic view of the Plasmodium falciparum life cycle." Nature **419**(6906): 520-526.

Foote, J. and H. N. Eisen (1995). "KINETIC AND AFFINITY LIMITS ON ANTIBODIES PRODUCED DURING IMMUNE-RESPONSES." Proceedings of the National Academy of Sciences of the United States of America **92**(5): 1254-1256.

Forbes, E. K., S. Biswas, K. A. Collins, S. C. Gilbert, A. V. Hill and S. J. Draper (2011). "Combining Liver- and Blood-Stage Malaria Viral-Vectored Vaccines: Investigating Mechanisms of CD8+ T Cell Interference." J Immunol.

Fowkes, F. J., J. S. Richards, J. A. Simpson and J. G. Beeson (2010). "The relationship between anti-merozoite antibodies and incidence of Plasmodium falciparum malaria: A systematic review and meta-analysis." PLoS Med. **7**(1): e1000218.

Freeman, R. R., A. J. Trejdosiewicz and G. A. Cross (1980). "Protective monoclonal antibodies recognising stage-specific merozoite antigens of a rodent malaria parasite." Nature **284**(5754): 366-368.

Gao, X., K. P. Yeo, S. S. Aw, C. Kuss, J. K. Iyer, S. Genesan, R. Rajamanonmani, J. Lescar, Z. Bozdech and P. R. Preiser (2008). "Antibodies targeting the PfRH1 binding domain inhibit invasion of Plasmodium falciparum merozoites." PLoS.Pathog. **4**(7): e1000104.

Garg, S., A. E. Oran, H. Hon and J. Jacob (2004). "The hybrid cytomegalovirus enhancer/chicken beta-actin promoter along with woodchuck hepatitis virus posttranscriptional regulatory element enhances the protective efficacy of DNA vaccines." J Immunol **173**(1): 550-558.

Genton, B., I. Betuela, I. Felger, F. Al-Yaman, R. F. Anders, A. Saul, L. Rare, M. Baisor, K. Lorry, G. V. Brown, D. Pye, D. O. Irving, T. A. Smith, H. P. Beck and M. P. Alpers (2002). "A recombinant blood-stage malaria vaccine reduces Plasmodium falciparum density and exerts selective

pressure on parasite populations in a phase 1-2b trial in Papua New Guinea." Journal of Infectious Diseases **185**(6): 820-827.

Gething, P. W., D. L. Smith, A. P. Patil, A. J. Tatem, R. W. Snow and S. I. Hay (2010). "Climate change and the global malaria recession." Nature **465**(7296): 342-345.

Gilberger, T. W., J. K. Thompson, M. B. Reed, R. T. Good and A. F. Cowman (2003). "The cytoplasmic domain of the Plasmodium falciparum ligand EBA-175 is essential for invasion but not protein trafficking." J Cell Biol **162**(2): 317-327.

Gilson, P. R. and B. S. Crabb (2009). "Morphology and kinetics of the three distinct phases of red blood cell invasion by Plasmodium falciparum merozoites." International Journal for Parasitology **39**(1): 91-96.

Gilson, P. R., T. Nebl, D. Vukcevic, R. L. Moritz, T. Sargeant, T. P. Speed, L. Schofield and B. S. Crabb (2006). "Identification and stoichiometry of GPI-anchored membrane proteins of the human malaria parasite plasmodium falciparum." Mol Cell Proteomics **5**(7): 1286-1299.

Glushakova, S., D. Yin, T. Li and J. Zimmerberg (2005). "Membrane transformation during malaria parasite release from human red blood cells." Curr Biol **15**(18): 1645-1650.

Gomez-Escobar, N., A. Amambua-Ngwa, M. Walther, J. Okebe, A. Ebonyi and D. J. Conway (2010). "Erythrocyte invasion and merozoite ligand gene expression in severe and mild Plasmodium falciparum malaria." J Infect Dis **201**(3): 444-452.

Goodman, A. L. and S. J. Draper (2010). "Blood-stage malaria vaccines - recent progress and future challenges." Ann.Trop.Med.Parasitol. **104**(3): 189-211.

Goodman, A. L., C. Epp, D. Moss, A. A. Holder, J. M. Wilson, G. P. Gao, C. A. Long, E. J. Remarque, A. W. Thomas, V. Ammendola, S. Colloca, M. D. Dicks, S. Biswas, D. Seibel, L. M. van Duivenvoorde, S. C. Gilbert, A. V. Hill and S. J. Draper (2010). "New candidate vaccines against blood-stage Plasmodium falciparum malaria: prime-boost immunization regimens incorporating human and simian adenoviral vectors and poxviral vectors expressing an optimized antigen based on merozoite surface protein 1." Infect Immun **78**(11): 4601-4612.

Gordon, D. M., T. W. McGovern, U. Krzych, J. C. Cohen, I. Schneider, R. Lachance, D. G. Heppner, G. Yuan, M. Hollingdale, M. Slaoui, P. Hauser, P. Voet, J. C. Sadoff and W. R. Ballou (1995). "SAFETY, IMMUNOGENICITY, AND EFFICACY OF A RECOMBINANTLY PRODUCED PLASMODIUM-FALCIPARUM CIRCUMSPOROZOITE-PROTEIN HEPATITIS-B SURFACE-ANTIGEN SUBUNIT VACCINE." Journal of Infectious Diseases **171**(6): 1576-1585.

Greco, W. R., G. Bravo and J. C. Parsons (1995). "The search for synergy: a critical review from a response surface perspective." Pharmacol Rev **47**(2): 331-385.

Greenwood, B. and G. Targett (2009). "Do we still need a malaria vaccine?" Parasite Immunol **31**(9): 582-586.

Grun, J. L. and W. P. Weidanz (1981). "Immunity to Plasmodium chabaudi adami in the B-cell-deficient mouse." Nature **290**(5802): 143-145.

Gupta, S., R. W. Snow, C. A. Donnelly, K. Marsh and C. Newbold (1999). "Immunity to non-cerebral severe malaria is acquired after one or two infections." Nature Medicine **5**(3): 340-343.

Harris, K. S., J. L. Casey, A. M. Coley, R. Masciantonio, J. K. Sabo, D. W. Keizer, E. F. Lee, A. McMahon, R. S. Norton, R. F. Anders and M. Foley (2005). "Binding hot spot for invasion inhibitory molecules on Plasmodium falciparum apical membrane antigen 1." Infect Immun **73**(10): 6981-6989.

Harris, P. K., S. Yeoh, A. R. Dluzewski, R. A. O'Donnell, C. Withers-Martinez, F. Hackett, L. H. Bannister, G. H. Mitchell and M. J. Blackman (2005). "Molecular identification of a malaria merozoite surface sheddase." PLoS Pathog **1**(3): 241-251.

Haynes, B. F., P. B. Gilbert, M. J. McElrath, S. Zolla-Pazner, G. D. Tomaras, S. M. Alam, D. T. Evans, D. C. Montefiori, C. Karnasuta, R. Sutthent, H. X. Liao, A. L. DeVico, G. K. Lewis, C. Williams, A. Pinter, Y. Fong, H. Janes, A. DeCamp, Y. Huang, M. Rao, E. Billings, N. Karasavvas, M. L. Robb, V. Ngauy, M. S. de Souza, R. Paris, G. Ferrari, R. T. Bailer, K. A. Soderberg, C. Andrews, P. W. Berman, N. Frahm, S. C. De Rosa, M. D. Alpert, N. L. Yates, X. Shen, R. A. Koup, P.

Pitisuttithum, J. Kaewkungwal, S. Nitayaphan, S. Rerks-Ngarm, N. L. Michael and J. H. Kim (2012). "Immune-correlates analysis of an HIV-1 vaccine efficacy trial." N Engl J Med **366**(14): 1275-1286.

Hayton, K., D. Gaur, A. Liu, J. Takahashi, B. Henschen, S. Singh, L. Lambert, T. Furuya, R. Bouttenot, M. Doll, F. Nawaz, J. Mu, L. Jiang, L. H. Miller and T. E. Wellems (2008). "Erythrocyte binding protein PfRH5 polymorphisms determine species-specific pathways of Plasmodium falciparum invasion." Cell Host.Microbe **4**(1): 40-51.

Heppner, D. G., J. F. Cummings, C. Ockenhouse, K. E. Kester, J. A. Lyon and D. M. Gordon (2001). "New World monkey efficacy trials for malaria vaccine development: critical path or detour?" Trends Parasitol **17**(9): 419-425.

Hermsen, C. C., S. J. de Vlas, G. J. van Gemert, D. S. Telgt, D. F. Verhage and R. W. Sauerwein (2004). "Testing vaccines in human experimental malaria: statistical analysis of parasitemia measured by a quantitative real-time polymerase chain reaction." Am J Trop.Med Hyg. **71**(2): 196-201.

Hermsen, C. C., D. S. Telgt, E. H. Linders, L. A. van de Locht, W. M. Eling, E. J. Mensink and R. W. Sauerwein (2001). "Detection of Plasmodium falciparum malaria parasites in vivo by real-time quantitative PCR." Mol.Biochem.Parasitol. **118**(2): 247-251.

Hill, A. V. (2006). "Pre-erythrocytic malaria vaccines: towards greater efficacy." Nat.Rev.Immunol. **6**(1): 21-32.

Hill, A. V., A. Reyes-Sandoval, G. O'Hara, K. Ewer, A. Lawrie, A. Goodman, A. Nicosia, A. Folgori, S. Colloca, R. Cortese, S. C. Gilbert and S. J. Draper (2010). "Prime-boost vectored malaria vaccines: progress and prospects." Hum Vaccin **6**(1): 78-83.

Hisaeda, H., A. Saul, J. J. Reece, M. C. Kennedy, C. A. Long, L. H. Miller and A. W. Stowers (2002). "Merozoite surface protein 3 and protection against malaria in Aotus nancymai monkeys." J Infect Dis **185**(5): 657-664.

Hoffman, S. L., L. M. Goh, T. C. Luke, I. Schneider, T. P. Le, D. L. Doolan, J. Sacci, P. de la Vega, M. Dowler, C. Paul, D. M. Gordon, J. A. Stoute, L. W. Church, M. Sedegah, D. G. Heppner, W. R. Ballou and T. L. Richie (2002). "Protection of humans against malaria by immunization with radiation-attenuated Plasmodium falciparum sporozoites." J Infect Dis **185**(8): 1155-1164.

Holder, A. A. (2009). "The carboxy-terminus of merozoite surface protein 1: structure, specific antibodies and immunity to malaria." Parasitology **136**(12): 1445-1456.

Holder, A. A. and R. R. Freeman (1981). "Immunization against blood-stage rodent malaria using purified parasite antigens." Nature **294**(5839): 361-364.

Hviid, L. (2010). "The role of Plasmodium falciparum variant surface antigens in protective immunity and vaccine development." Hum Vaccin **6**(1): 84-89.

Janin, J. (1979). "SURFACE AND INSIDE VOLUMES IN GLOBULAR PROTEINS." Nature **277**(5696): 491-492.

Jeffares, D. C., A. Pain, A. Berry, A. V. Cox, J. Stalker, C. E. Ingle, A. Thomas, M. A. Quail, K. Siebenthall, A. C. Uhlemann, S. Kyes, S. Krishna, C. Newbold, E. T. Dermitzakis and M. Berriman (2007). "Genome variation and evolution of the malaria parasite Plasmodium falciparum." Nat Genet **39**(1): 120-125.

Jiang, L., D. Gaur, J. Mu, H. Zhou, C. A. Long and L. H. Miller (2011). "Evidence for erythrocyte-binding antigen 175 as a component of a ligand-blocking blood-stage malaria vaccine." Proc Natl Acad Sci U S A **108**(18): 7553-7558.

Jones, T. R., D. L. Narum, A. S. Gozalo, J. Aguiar, S. R. Fuhrmann, H. Liang, J. D. Haynes, J. K. Moch, C. Lucas, T. Luu, A. J. Magill, S. L. Hoffman and B. K. Sim (2001). "Protection of Aotus monkeys by Plasmodium falciparum EBA-175 region II DNA prime-protein boost immunization regimen." J Infect Dis **183**(2): 303-312.

Joos, C., L. Marrama, H. E. Polson, S. Corre, A. M. Diatta, B. Diouf, J. F. Trape, A. Tall, S. Longacre and R. Perraut (2010). "Clinical protection from falciparum malaria correlates with neutrophil

respiratory bursts induced by merozoites opsonized with human serum antibodies." PLoS.ONE. **5**(3): e9871.

Jordan-Villegas, A., A. B. Perdomo, J. E. Epstein, J. Lopez, A. Castellanos, M. R. Manzano, M. A. Hernandez, L. Soto, F. Mendez, T. L. Richie, S. L. Hoffman, M. Arevalo-Herrera and S. Herrera (2011). "Immune responses and protection of Aotus monkeys immunized with irradiated Plasmodium vivax sporozoites." Am J Trop Med Hyg **84**(2 Suppl): 43-50.

Jossang, T., J. Feder and E. Rosenqvist (1988). "Photon correlation spectroscopy of human IgG." J Protein Chem **7**(2): 165-171.

Kaneko, O., J. B. Mu, T. Tsuboi, X. Z. Su and M. Torii (2002). "Gene structure and expression of a Plasmodium falciparum 220-kDa protein homologous to the Plasmodium vivax reticulocyte binding proteins." Molecular and Biochemical Parasitology **121**(2): 275-278.

Karlsson, R., L. Fagerstam, H. Nilshans and B. Persson (1993). "Analysis of active antibody concentration. Separation of affinity and concentration parameters." J Immunol Methods **166**(1): 75-84.

Kasturi, S. P., I. Skountzou, R. A. Albrecht, D. Koutsonanos, T. Hua, H. I. Nakaya, R. Ravindran, S. Stewart, M. Alam, M. Kwissa, F. Villinger, N. Murthy, J. Steel, J. Jacob, R. J. Hogan, A. Garcia-Sastre, R. Compans and B. Pulendran (2011). "Programming the magnitude and persistence of antibody responses with innate immunity." Nature **470**(7335): 543-547.

Kennedy, M. C., J. Wang, Y. Zhang, A. P. Miles, F. Chitsaz, A. Saul, C. A. Long, L. H. Miller and A. W. Stowers (2002). "In vitro studies with recombinant Plasmodium falciparum apical membrane antigen 1 (AMA1): production and activity of an AMA1 vaccine and generation of a multiallelic response." Infect Immun **70**(12): 6948-6960.

Khusmith, S., Y. Charoenvit, S. Kumar, M. Sedegah, R. L. Beaudoin and S. L. Hoffman (1991). "PROTECTION AGAINST MALARIA BY VACCINATION WITH SPOROZOITE SURFACE PROTEIN-2 PLUS CS PROTEIN." Science **252**(5006): 715-718.

Khusmith, S., M. Sedegah and S. L. Hoffman (1994). "COMPLETE PROTECTION AGAINST PLASMODIUM-YOELII BY ADOPTIVE TRANSFER OF A CD8+ CYTOTOXIC T-CELL CLONE RECOGNIZING SPOROZOITE SURFACE PROTEIN-2." Infection and Immunity **62**(7): 2979-2983.

Koussis, K., C. Withers-Martinez, S. Yeoh, M. Child, F. Hackett, E. Knuepfer, L. Juliano, U. Woehlbier, H. Bujard and M. J. Blackman (2009). "A multifunctional serine protease primes the malaria parasite for red blood cell invasion." EMBO J **28**(6): 725-735.

Kubler-Kielb, J., F. Majadly, Y. Wu, D. L. Narum, C. Guo, L. H. Miller, J. Shiloach, J. B. Robbins and R. Schneerson (2007). "Long-lasting and transmission-blocking activity of antibodies to Plasmodium falciparum elicited in mice by protein conjugates of Pfs25." Proceedings of the National Academy of Sciences of the United States of America **104**(1): 293-298.

Kumar, S., W. Collins, A. Egan, A. Yadava, O. Garraud, M. J. Blackman, J. A. Guevara Patino, C. Diggs and D. C. Kaslow (2000). "Immunogenicity and efficacy in aotus monkeys of four recombinant Plasmodium falciparum vaccines in multiple adjuvant formulations based on the 19-kilodalton C terminus of merozoite surface protein 1." Infect Immun **68**(4): 2215-2223.

Kumar, S., A. Yadava, D. B. Keister, J. H. Tian, M. Ohl, K. A. Perdue-Greenfield, L. H. Miller and D. C. Kaslow (1995). "Immunogenicity and in vivo efficacy of recombinant Plasmodium falciparum merozoite surface protein-1 in Aotus monkeys." Mol Med **1**(3): 325-332.

Kushwaha, A., P. P. Rao, R. P. Suresh and V. S. Chauhan (2001). "Immunogenicity of recombinant fragments of Plasmodium falciparum acidic basic repeat antigen produced in Escherichia coli." Parasite Immunol. **23**(8): 435-444.

Lai, R. P., M. S. Seaman, P. Tonks, F. Wegmann, D. J. Seilly, S. D. Frost, C. C. LaBranche, D. C. Montefiori, A. K. Dey, I. K. Srivastava, Q. Sattentau, S. W. Barnett and J. L. Heeney (2012). "Mixed adjuvant formulations reveal a new combination that elicit antibody response comparable to Freund's adjuvants." Plos One **7**(4): e35083.

Langhorne, J., F. M. Ndungu, A. M. Sponaas and K. Marsh (2008). "Immunity to malaria: more questions than answers." Nat.Immunol. **9**(7): 725-732.

Layez, C., P. Nogueira, V. Combes, F. T. Costa, I. Juhan-Vague, L. H. da Silva and J. Gysin (2005). "Plasmodium falciparum rhoptry protein RSP2 triggers destruction of the erythroid lineage." Blood **106**(10): 3632-3638.

Lobo, C. A., M. Rodriguez, C. J. Struchiner, M. G. Zalis and S. Lustigman (2006). "Associations between defined polymorphic variants in the PfRH ligand family and the invasion pathways used by P. falciparum field isolates from Brazil." Mol Biochem Parasitol **149**(2): 246-251.

Lopaticki, S., A. G. Maier, J. Thompson, D. W. Wilson, W. H. Tham, T. Triglia, A. Gout, T. P. Speed, J. G. Beeson, J. Healer and A. F. Cowman (2011). "Reticulocyte and erythrocyte binding-like proteins function cooperatively in invasion of human erythrocytes by malaria parasites." Infect Immun **79**(3): 1107-1117.

Lopera-Mesa, T. M., A. Kushwaha, A. Mohmmed and V. S. Chauhan (2008). "Plasmodium berghei merozoite surface protein-9: immunogenicity and protective efficacy using a homologous challenge model." Vaccine **26**(10): 1335-1343.

Lyon, J. A., E. Angov, M. P. Fay, J. S. Sullivan, A. S. Girourd, S. J. Robinson, E. S. Bergmann-Leitner, E. H. Duncan, C. A. Darko, W. E. Collins, C. A. Long and J. W. Barnwell (2008). "Protection Induced by Plasmodium falciparum MSP1(42) Is Strain-Specific, Antigen and Adjuvant Dependent, and Correlates with Antibody Responses." Plos One **3**(7).

MacCallum, R. M., A. C. R. Martin and J. M. Thornton (1996). "Antibody-antigen interactions: Contact analysis and binding site topography." Journal of Molecular Biology **262**(5): 732-745.

Mackinnon, M. J., J. Li, S. Mok, M. M. Kortok, K. Marsh, P. R. Preiser and Z. Bozdech (2009). "Comparative transcriptional and genomic analysis of Plasmodium falciparum field isolates." PLoS Pathog **5**(10): e1000644.

Mahdi Abdel Hamid, M., E. J. Remarque, L. M. van Duivenvoorde, N. van der Werff, V. Walraven, B. W. Faber, C. H. Kocken and A. W. Thomas (2011). "Vaccination with Plasmodium knowlesi AMA1 formulated in the novel adjuvant co-vaccine HT protects against blood-stage challenge in rhesus macaques." PLoS ONE **6**(5): e20547.

Manske, M., O. Miotto, S. Campino, S. Auburn, J. Almagro-Garcia, G. Maslen, J. O'Brien, A. Djimde, O. Doumbo, I. Zongo, J. B. Ouedraogo, P. Michon, I. Mueller, P. Siba, A. Nzila, S. Borrmann, S. M. Kiara, K. Marsh, H. Jiang, X. Z. Su, C. Amaratunga, R. Fairhurst, D. Socheat, F. Nosten, M. Imwong, N. J. White, M. Sanders, E. Anastasi, D. Alcock, E. Drury, S. Oyola, M. A. Quail, D. J. Turner, V. Ruano-Rubio, D. Jyothi, L. Amenga-Etego, C. Hubbart, A. Jeffreys, K. Rowlands, C. Sutherland, C. Roper, V. Mangano, D. Modiano, J. C. Tan, M. T. Ferdig, A. Amambua-Ngwa, D. J. Conway, S. Takala-Harrison, C. V. Plowe, J. C. Rayner, K. A. Rockett, T. G. Clark, C. I. Newbold, M. Berriman, B. Macinnis and D. P. Kwiatkowski (2012). "Analysis of Plasmodium falciparum diversity in natural infections by deep sequencing." Nature.

Marsh, K. and R. J. Howard (1986). "ANTIGENS INDUCED ON ERYTHROCYTES BY PLASMODIUM-FALCIPARUM - EXPRESSION OF DIVERSE AND CONSERVED DETERMINANTS." Science **231**(4734): 150-153.

Marsh, K. and S. Kinyanjui (2006). "Immune effector mechanisms in malaria." Parasite Immunol. **28**(1-2): 51-60.

Maurice, J. M. and S. Davey (2009). State of the world's vaccines and immunization. Geneva, World Health Organization.

McConkey, S. J., W. H. Reece, V. S. Moorthy, D. Webster, S. Dunachie, G. Butcher, J. M. Vuola, T. J. Blanchard, P. Gothard, K. Watkins, C. M. Hannan, S. Everaere, K. Brown, K. E. Kester, J. Cummings, J. Williams, D. G. Heppner, A. Pathan, K. Flanagan, N. Arulanantham, M. T. Roberts, M. Roy, G. L. Smith, J. Schneider, T. Peto, R. E. Sinden, S. C. Gilbert and A. V. Hill (2003). "Enhanced T-cell immunogenicity of plasmid DNA vaccines boosted by recombinant modified vaccinia virus Ankara in humans." Nat Med **9**(6): 729-735.

McGregor, I. A. (1964). "PASSIVE TRANSFER OF HUMAN MALARIAL IMMUNITY." American Journal of Tropical Medicine and Hygiene **13**(1P2): 237-&.

Mikkelsen, R. B., M. Kamber, K. S. Wadwa, P. S. Lin and R. Schmidt-Ullrich (1988). "The role of lipids in Plasmodium falciparum invasion of erythrocytes: a coordinated biochemical and microscopic analysis." Proc Natl Acad Sci U S A **85**(16): 5956-5960.

Miller, L. H., M. F. Good and G. Milon (1994). "Malaria pathogenesis." Science **264**(5167): 1878-1883.

Mitchell, G. H., G. A. Butcher and S. Cohen (1974). "A merozoite vaccine effective against Plasmodium knowlesi malaria." Nature **252**(5481): 311-313.

Miura, K., A. C. Orcutt, O. V. Muratova, L. H. Miller, A. Saul and C. A. Long (2008). "Development and characterization of a standardized ELISA including a reference serum on each plate to detect antibodies induced by experimental malaria vaccines." Vaccine **26**(2): 193-200.

Miura, K., H. Zhou, A. Diouf, S. E. Moretz, M. P. Fay, L. H. Miller, L. B. Martin, M. A. Pierce, R. D. Ellis, G. E. D. Mullen and C. A. Long (2009). "Anti-Apical-Membrane-Antigen-1 Antibody Is More Effective than Anti-42-Kilodalton-Merozoite-Surface-Protein-1 Antibody in Inhibiting Plasmodium falciparum Growth, as Determined by the In Vitro Growth Inhibition Assay." Clinical and Vaccine Immunology **16**(7): 963-968.

Miura, K., H. Zhou, S. E. Moretz, A. Diouf, M. A. Thera, A. Dolo, O. Doumbo, E. Malkin, D. Diemert, L. H. Miller, G. E. D. Mullen and C. A. Longli (2008). "Comparison of Biological Activity of Human Anti-Apical Membrane Antigen-1 Antibodies Induced by Natural Infection and Vaccination." Journal of Immunology **181**(12): 8776-8783.

Molineaux, L., H. H. Diebner, M. Eichner, W. E. Collins, G. M. Jeffery and K. Dietz (2001). "Plasmodium falciparum parasitaemia described by a new mathematical model." Parasitology **122**(Pt 4): 379-391.

Moon, J. J., H. Suh, A. V. Li, C. F. Ockenhouse, A. Yadava and D. J. Irvine (2012). "Enhancing humoral responses to a malaria antigen with nanoparticle vaccines that expand Tfh cells and promote germinal center induction." Proc Natl Acad Sci U S A **109**(4): 1080-1085.

Moorthy, V. S., C. Diggs, S. Ferro, M. F. Good, S. Herrera, A. V. Hill, E. B. Imoukhuede, S. Kumar, C. Loucq, K. Marsh, C. F. Ockenhouse, T. L. Richie and R. W. Sauerwein (2009). "Report of a consultation on the optimization of clinical challenge trials for evaluation of candidate blood stage malaria vaccines, 18-19 March 2009, Bethesda, MD, USA." Vaccine **27**(42): 5719-5725.

Moss, D. K., E. J. Remarque, B. W. Faber, D. R. Cavanagh, D. E. Arnot, A. W. Thomas and A. A. Holder (2011). "Plasmodium falciparum merozoite surface protein (MSP) 119-specific antibodies that interfere with parasite growth in vitro can inhibit MSP1 processing, merozoite invasion and intracellular parasite development." Infect Immun.

Murray, C. J., L. C. Rosenfeld, S. S. Lim, K. G. Andrews, K. J. Foreman, D. Haring, N. Fullman, M. Naghavi, R. Lozano and A. D. Lopez (2012). "Global malaria mortality between 1980 and 2010: a systematic analysis." Lancet **379**(9814): 413-431.

Narum, D. L., J. D. Haynes, S. Fuhrmann, K. Moch, H. Liang, S. L. Hoffman and B. K. L. Sim (2000). "Antibodies against the Plasmodium falciparum receptor binding domain of EBA-175 block invasion pathways that do not involve sialic acids." Infection and Immunity **68**(4): 1964-1966.

Newbold, C. I., R. Pinches, D. J. Roberts and K. Marsh (1992). "PLASMODIUM-FALCIPARUM - THE HUMAN AGGLUTINATING ANTIBODY-RESPONSE TO THE INFECTED RED-CELL SURFACE IS PREDOMINANTLY VARIANT SPECIFIC." Experimental Parasitology **75**(3): 281-292.

Newman, M. A., C. R. Mainhart, C. P. Mallett, T. B. Lavoie and S. J. Smithgill (1992). "PATTERNS OF ANTIBODY SPECIFICITY DURING THE BALB/C IMMUNE-RESPONSE TO HEN EGG-WHITE LYSOZYME." Journal of Immunology **149**(10): 3260-3272.

Nguitragool, W., A. A. Bokhari, A. D. Pillai, K. Rayavara, P. Sharma, B. Turpin, L. Aravind and S. A. Desai (2011). "Malaria parasite clag3 genes determine channel-mediated nutrient uptake by infected red blood cells." Cell **145**(5): 665-677.

Northrup, S. H. and H. P. Erickson (1992). "KINETICS OF PROTEIN PROTEIN ASSOCIATION EXPLAINED BY BROWNIAN DYNAMICS COMPUTER-SIMULATION." Proceedings of the National Academy of Sciences of the United States of America **89**(8): 3338-3342.

O'Neill, P. M., V. E. Barton and S. A. Ward (2010). "The molecular mechanism of action of artemisinin--the debate continues." Molecules **15**(3): 1705-1721.

Ogun, S. A., L. Dumon -Seignovert, J.-B. Marchand, A. A. Holder and F. Hill (2008). "The oligomerization domain of C4-binding protein (C4bp) acts as an adjuvant, and the fusion protein comprised of the 19-kilodalton merozoite surface protein 1 fused with the murine C4bp domain protects mice against malaria." Infection and Immunity **76**(8): 3817-3823.

Olivieri, A., C. R. Collins, F. Hackett, C. Withers-Martinez, J. Marshall, H. R. Flynn, J. M. Skehel and M. J. Blackman (2011). "Juxtamembrane shedding of Plasmodium falciparum AMA1 is sequence independent and essential, and helps evade invasion-inhibitory antibodies." PLoS Pathog **7**(12): e1002448.

Ord, R. L., M. Rodriguez, T. Yamasaki, S. Takeo, T. Tsuboi and C. A. Lobo (2012). "Targeting sialic acid dependent and independent pathways of invasion in Plasmodium falciparum." Plos One **7**(1): e30251.

Osier, F. H., G. Fegan, S. D. Polley, L. Murungi, F. Verra, K. K. Tetteh, B. Lowe, T. Mwangi, P. C. Bull, A. W. Thomas, D. R. Cavanagh, J. S. McBride, D. E. Lanar, M. J. Mackinnon, D. J. Conway and K. Marsh (2008). "Breadth and magnitude of antibody responses to multiple Plasmodium falciparum merozoite antigens are associated with protection from clinical malaria." Infect Immun **76**(5): 2240-2248.

Pandey, K. C., S. Singh, P. Pattnaik, C. R. Pillai, U. Pillai, A. Lynn, S. K. Jain and C. E. Chitnis (2002). "Bacterially expressed and refolded receptor binding domain of Plasmodium falciparum EBA-175 elicits invasion inhibitory antibodies." Mol.Biochem.Parasitol. **123**(1): 23-33.

Pang, X. L., T. Mitamura and T. Horii (1999). "Antibodies reactive with the N-terminal domain of Plasmodium falciparum serine repeat antigen inhibit cell proliferation by agglutinating merozoites and schizonts." Infect Immun **67**(4): 1821-1827.

Plotkin, S. A., W. A. Orenstein and P. A. Offit (2008). Vaccines. Philadelphia, Pa. ; [London], Saunders.

Pol, E., R. Karlsson, H. Roos, A. Jansson, B. Xu, A. Larsson, T. Jarhede, G. Franklin, A. Fuentes and S. Persson (2007). "Biosensor-based characterization of serum antibodies during development of an anti-IgE immunotherapeutic against allergy and asthma." J Mol Recognit **20**(1): 22-31.

Pombo, D. J., G. Lawrence, C. Hirunpetcharat, C. Rzepczyk, M. Bryden, N. Cloonan, K. Anderson, Y. Mahakunkijcharoen, L. B. Martin, D. Wilson, S. Elliott, D. P. Eisen, J. B. Weinberg, A. Saul and M. F. Good (2002). "Immunity to malaria after administration of ultra-low doses of red cells infected with Plasmodium falciparum." Lancet **360**(9333): 610-617.

Porter, D. W., F. M. Thompson, T. K. Berthoud, C. L. Hutchings, L. Andrews, S. Biswas, I. Poulton, E. Prieur, S. Correa, R. Rowland, T. Lang, J. Williams, S. C. Gilbert, R. E. Sinden, S. Todryk and A. V. Hill (2011). "A human Phase I/IIa malaria challenge trial of a polyprotein malaria vaccine." Vaccine **29**(43): 7514-7522.

Potocnjak, P., N. Yoshida, R. S. Nussenzweig and V. Nussenzweig (1980). "MONO-VALENT FRAGMENTS (FAB) OF MONOCLONAL-ANTIBODIES TO A SPOROZOITE SURFACE-ANTIGEN (PB44) PROTECT MICE AGAINST MALARIAL INFECTION." Journal of Experimental Medicine **151**(6): 1504-1513.

Poulsen, T. R., A. Jensen, J. S. Haurum and P. S. Andersen (2011). "Limits for Antibody Affinity Maturation and Repertoire Diversification in Hypervaccinated Humans." Journal of Immunology **187**(8): 4229-4235.

Price, P. W., E. C. McKinney, Y. L. Wang, L. E. Sasser, M. K. Kandasamy, L. Matsuuchi, C. Milcarek, R. B. Deal, D. G. Culver and R. B. Meagher (2009). "Engineered cell surface expression of membrane immunoglobulin as a means to identify monoclonal antibody-secreting hybridomas." Journal of Immunological Methods **343**(1): 28-41.

Pye, D., K. L. Vandenberg, S. L. Dyer, D. O. Irving, N. H. Goss, G. C. Woodrow, A. Saul, C. R. Alving, R. L. Richards, W. R. Ballou, M. J. Wu, K. Skoff and R. F. Anders (1997). "Selection of an adjuvant for vaccination with the malaria antigen, MSA-2." Vaccine **15**(9): 1017-1023.

Rayner, J. C., E. Vargas-Serrato, C. S. Huber, M. R. Galinski and J. W. Barnwell (2001). "A Plasmodium falciparum homologue of Plasmodium vivax reticulocyte binding protein (PvRBP1) defines a trypsin-resistant erythrocyte invasion pathway." J Exp Med **194**(11): 1571-1581.

Recker, M., C. O. Buckee, A. Serazin, S. Kyes, R. Pinches, Z. Christodoulou, A. L. Springer, S. Gupta and C. I. Newbold (2011). "Antigenic variation in Plasmodium falciparum malaria involves a highly structured switching pattern." PLoS Pathog **7**(3): e1001306.

Reddy, S. B., R. F. Anders, J. G. Beeson, A. Farnert, F. Kironde, S. K. Berenzon, M. Wahlgren, S. Linse and K. E. Persson (2012). "High affinity antibodies to Plasmodium falciparum merozoite antigens are associated with protection from malaria." Plos One **7**(2): e32242.

Remarque, E. J., B. W. Faber, C. H. Kocken and A. W. Thomas (2008). "Apical membrane antigen 1: a malaria vaccine candidate in review." Trends Parasitol **24**(2): 74-84.

RichaletSecordel, P. M., N. RaufferBruyere, L. L. H. Christensen, B. OfenlochHaehnle, C. Seidel and M. H. V. VanRegenmortel (1997). "Concentration measurement of unpurified proteins using biosensor technology under conditions of partial mass transport limitation." Analytical Biochemistry **249**(2): 165-173.

Richard, D., L. M. Kats, C. Langer, C. G. Black, K. Mitri, J. A. Boddey, A. F. Cowman and R. L. Coppel (2009). "Identification of rhoptry trafficking determinants and evidence for a novel sorting mechanism in the malaria parasite Plasmodium falciparum." PLoS Pathog **5**(3): e1000328.

Richard, D., C. A. MacRaild, D. T. Riglar, J. A. Chan, M. Foley, J. Baum, S. A. Ralph, R. S. Norton and A. F. Cowman (2010). "Interaction between Plasmodium falciparum Apical Membrane Antigen 1 and the Rhoptry Neck Protein Complex Defines a Key Step in the Erythrocyte Invasion Process of Malaria Parasites." Journal of Biological Chemistry **285**(19): 14815-14822.

Ridley, R. G., B. Takacs, H. Etlinger and J. G. Scaife (1990). "A rhoptry antigen of Plasmodium falciparum is protective in Saimiri monkeys." Parasitology **101 Pt 2**: 187-192.

Riglar, D. T., D. Richard, D. W. Wilson, M. J. Boyle, C. Dekiwadia, L. Turnbull, F. Angrisano, D. S. Marapana, K. L. Rogers, C. B. Whitchurch, J. G. Beeson, A. F. Cowman, S. A. Ralph and J. Baum (2011). "Super-resolution dissection of coordinated events during malaria parasite invasion of the human erythrocyte." Cell Host.Microbe **9**(1): 9-20.

Roberts, D. M., A. Nanda, M. J. Havenga, P. Abbink, D. M. Lynch, B. A. Ewald, J. Liu, A. R. Thorner, P. E. Swanson, D. A. Gorgone, M. A. Lifton, A. A. Lemckert, L. Holterman, B. Chen, A. Dilraj, A. Carville, K. G. Mansfield, J. Goudsmit and D. H. Barouch (2006). "Hexon-chimaeric adenovirus serotype 5 vectors circumvent pre-existing anti-vector immunity." Nature **441**(7090): 239-243.

Rodriguez, M., S. Lustigman, E. Montero, Y. Oksov and C. A. Lobo (2008). "PfRH5: a novel reticulocyte-binding family homolog of plasmodium falciparum that binds to the erythrocyte, and an investigation of its receptor." Plos One **3**(10): e3300.

Roestenberg, M., S. J. de Vlas, A. E. Nieman, R. W. Sauerwein and C. C. Hermsen (2012). "Efficacy of preerythrocytic and blood-stage malaria vaccines can be assessed in small sporozoite challenge trials in human volunteers." J Infect Dis **206**(3): 319-323.

Roestenberg, M., M. McCall, J. Hopman, J. Wiersma, A. J. Luty, G. J. van Gemert, d. V. van, B. van Schaijk, K. Teelen, T. Arens, L. Spaarman, Q. de Mast, W. Roeffen, G. Snounou, L. Renia, d. V. van, C. C. Hermsen and R. Sauerwein (2009). "Protection against a malaria challenge by sporozoite inoculation." N Engl J Med **361**(5): 468-477.

Roestenberg, M., E. Remarque, E. de Jonge, R. Hermsen, H. Blythman, O. Leroy, E. Imoukhuede, S. Jepsen, O. Ofori-Anyinam, B. Faber, C. H. Kocken, M. Arnold, V. Walraven, K. Teelen, W. Roeffen, Q. de Mast, W. R. Ballou, J. Cohen, M. C. Dubois, S. Ascarateil, d. V. van, A. Thomas and R. Sauerwein (2008). "Safety and immunogenicity of a recombinant Plasmodium

falciparum AMA1 malaria vaccine adjuvanted with Alhydrogel, Montanide ISA 720 or AS02." PLoS.ONE. **3**(12): e3960.

Roost, H. P., M. F. Bachmann, A. Haag, U. Kalinke, V. Pliska, H. Hengartner and R. M. Zinkernagel (1995). "EARLY HIGH-AFFINITY NEUTRALIZING ANTIVIRAL IGG RESPONSES WITHOUT FURTHER OVERALL IMPROVEMENTS OF AFFINITY." Proceedings of the National Academy of Sciences of the United States of America **92**(5): 1257-1261.

Rutgers, T., D. Gordon, A. M. Gathoye, M. Hollingdale, W. Hockmeyer, M. Rosenberg and M. Dewilde (1988). "HEPATITIS-B SURFACE-ANTIGEN AS CARRIER MATRIX FOR THE REPETITIVE EPITOPE OF THE CIRCUMSPOROZOITE PROTEIN OF PLASMODIUM-FALCIPARUM." Bio-Technology **6**(9): 1065-1070.

Sabchareon, A., T. Burnouf, D. Ouattara, P. Attanath, H. Bouharountayoun, P. Chantavanich, C. Foucault, T. Chongsuphajaisiddhi and P. Druilhe (1991). "PARASITOLOGICAL AND CLINICAL HUMAN RESPONSE TO IMMUNOGLOBULIN ADMINISTRATION IN FALCIPARUM-MALARIA." American Journal of Tropical Medicine and Hygiene **45**(3): 297-308.

Sachs, J. and P. Malaney (2002). "The economic and social burden of malaria." Nature **415**(6872): 680-685.

Sanderson, F., L. Andrews, A. D. Douglas, A. Hunt-Cooke, P. Bejon and A. V. Hill (2008). "Blood-stage challenge for malaria vaccine efficacy trials: a pilot study with discussion of safety and potential value." Am.J.Trop.Med.Hyg. **78**(6): 878-883.

Sauerwein, R. W., M. Roestenberg and V. S. Moorthy (2011). "Experimental human challenge infections can accelerate clinical malaria vaccine development." Nat Rev Immunol **11**(1): 57-64.

Saul, A. (1987). "Kinetic Constraints on the Development of A Malaria Vaccine." Parasite Immunology **9**(1): 1-9.

Saul, A. and M. P. Fay (2007). "Human immunity and the design of multi-component, single target vaccines." Plos One **2**(9): e850.

Schmidt-Ullrich, R., J. Brown, H. Whittle and P. S. Lin (1986). "Human-human hybridomas secreting monoclonal antibodies to the Mr 195,000 Plasmodium falciparum blood stage antigen." J Exp Med **163**(1): 179-188.

Schofield, L., G. R. Bushell, J. A. Cooper, A. J. Saul, J. A. Upcroft and C. Kidson (1986). "A rhoptry antigen of Plasmodium falciparum contains conserved and variable epitopes recognized by inhibitory monoclonal antibodies." Mol Biochem Parasitol **18**(2): 183-195.

Sheehy, S. H., C. J. Duncan, S. C. Elias, S. Biswas, K. A. Collins, G. A. O'Hara, F. D. Halstead, K. J. Ewer, T. Mahungu, A. J. Spencer, K. Miura, I. D. Poulton, M. D. Dicks, N. J. Edwards, E. Berrie, S. Moyle, S. Colloca, R. Cortese, K. Gantlett, C. A. Long, A. M. Lawrie, S. C. Gilbert, T. Doherty, A. Nicosia, A. V. Hill and S. J. Draper (2012). "Phase Ia clinical evaluation of the safety and immunogenicity of the Plasmodium falciparum blood-stage antigen AMA1 in ChAd63 and MVA vaccine vectors." Plos One **7**(2): e31208.

Sheehy, S. H., C. J. Duncan, S. C. Elias, K. A. Collins, K. J. Ewer, A. J. Spencer, A. R. Williams, F. D. Halstead, S. E. Moretz, K. Miura, C. Epp, M. D. Dicks, I. D. Poulton, A. M. Lawrie, E. Berrie, S. Moyle, C. A. Long, S. Colloca, R. Cortese, S. C. Gilbert, A. Nicosia, A. V. Hill and S. J. Draper (2011). "Phase Ia Clinical Evaluation of the Plasmodium falciparum Blood-stage Antigen MSP1 in ChAd63 and MVA Vaccine Vectors." Mol Ther: Epub 23 Aug 2011, doi:2010.1038.

Sigmundsson, K., G. Masson, R. Rice, N. Beauchemin and B. Obrink (2002). "Determination of active concentrations and association and dissociation rate constants of interacting biomolecules: an analytical solution to the theory for kinetic and mass transport limitations in biosensor technology and its experimental verification." Biochemistry **41**(26): 8263-8276.

Simpson, J. A., L. Aarons, W. E. Collins, G. M. Jeffery and N. J. White (2002). "Population dynamics of untreated Plasmodium falciparum malaria within the adult human host during the expansion phase of the infection." Parasitology **124**(Pt 3): 247-263.

Singh, S., M. M. Alam, I. Pal-Bhowmick, J. A. Brzostowski and C. E. Chitnis (2010). "Distinct External Signals Trigger Sequential Release of Apical Organelles during Erythrocyte Invasion by Malaria Parasites." Plos Pathogens **6**(2).

Singh, S., K. Miura, H. Zhou, O. Muratova, B. Keegan, A. Miles, L. B. Martin, A. J. Saul, L. H. Miller and C. A. Long (2006). "Immunity to recombinant Plasmodium falciparum merozoite surface protein 1 (MSP1): Protection in Aotus nancymai monkeys strongly correlates with anti-MSP1 antibody titer and in vitro parasite-inhibitory activity." Infection and Immunity **74**(8): 4573-4580.

Smith, T., G. F. Killeen, N. Maire, A. Ross, L. Molineaux, F. Tediosi, G. Hutton, J. Utzinger, K. Dietz and M. Tanner (2006). "Mathematical modeling of the impact of malaria vaccines on the clinical epidemiology and natural history of Plasmodium falciparum malaria: Overview." Am J Trop Med Hyg **75**(2 Suppl): 1-10.

Smythe, J. A., M. G. Peterson, R. L. Coppel, A. J. Saul, D. J. Kemp and R. F. Anders (1990). "Structural diversity in the 45-kilodalton merozoite surface antigen of Plasmodium falciparum." Mol Biochem Parasitol **39**(2): 227-234.

Spring, M. D., J. F. Cummings, C. F. Ockenhouse, S. Dutta, R. Reidler, E. Angov, E. Bergmann-Leitner, V. A. Stewart, S. Bittner, L. Juompan, M. G. Kortepeter, R. Nielsen, U. Krzych, E. Tierney, L. A. Ware, M. Dowler, C. C. Hermsen, R. W. Sauerwein, S. J. de Vlas, O. Ofori-Anyinam, D. E. Lanar, J. L. Williams, K. E. Kester, K. Tucker, M. Shi, E. Malkin, C. Long, C. L. Diggs, L. Soisson, M. C. Dubois, W. R. Ballou, J. Cohen and D. G. Heppner, Jr. (2009). "Phase 1/2a study of the malaria vaccine candidate apical membrane antigen-1 (AMA-1) administered in adjuvant system AS01B or AS02A." PLoS ONE **4**(4): e5254.

Sridhar, S., A. Reyes-Sandoval, S. J. Draper, A. C. Moore, S. C. Gilbert, G. P. Gao, J. M. Wilson and A. V. S. Hill (2008). "Single-dose protection against Plasmodium berghei by a simian adenovirus vector using a human cytomegalovirus promoter containing intron A." Journal of Virology **82**(8): 3822-3833.

Srinivasan, P., W. L. Beatty, A. Diouf, R. Herrera, X. Ambroggio, J. K. Moch, J. S. Tyler, D. L. Narum, S. K. Pierce, J. C. Boothroyd, J. D. Haynes and L. H. Miller (2011). "Binding of Plasmodium merozoite proteins RON2 and AMA1 triggers commitment to invasion." Proc Natl Acad Sci U S A **108**(32): 13275-13280.

Stanton, R. J., B. P. McSharry, M. Armstrong, P. Tomasec and G. W. G. Wilkinson (2008). "Re-engineering adenovirus vector systems to enable high-throughput analyses of gene function." Biotechniques **45**(6): 659-+.

Sterkers, Y., C. Scheidig, M. da Rocha, C. Lepolard, J. Gysin and A. Scherf (2007). "Members of the low-molecular-mass rhoptry protein complex of Plasmodium falciparum bind to the surface of normal erythrocytes." J Infect Dis **196**(4): 617-621.

Stoute, J. A., M. Slaoui, D. G. Heppner, P. Momin, K. E. Kester, P. Desmons, B. T. Wellde, N. Garcon, U. Krzych, M. Marchand, W. R. Ballou and J. D. Cohen (1997). "A preliminary evaluation of a recombinant circumsporozoite protein vaccine against Plasmodium falciparum malaria." New England Journal of Medicine **336**(2): 86-91.

Stowers, A., N. Prescott, J. Cooper, B. Takacs, D. Stueber, P. Kennedy and A. Saul (1995). "Immunogenicity of recombinant Plasmodium falciparum rhoptry associated proteins 1 and 2." Parasite Immunol **17**(12): 631-642.

Stowers, A. W., L. H. Chen Lh, Y. Zhang, M. C. Kennedy, L. Zou, L. Lambert, T. J. Rice, D. C. Kaslow, A. Saul, C. A. Long, H. Meade and L. H. Miller (2002). "A recombinant vaccine expressed in the milk of transgenic mice protects Aotus monkeys from a lethal challenge with Plasmodium falciparum." Proc Natl Acad Sci U S A **99**(1): 339-344.

Stowers, A. W., V. Cioce, R. L. Shimp, M. Lawson, G. Hui, O. Muratova, D. C. Kaslow, R. Robinson, C. A. Long and L. H. Miller (2001). "Efficacy of two alternate vaccines based on Plasmodium falciparum merozoite surface protein 1 in an Aotus challenge trial." Infect Immun **69**(3): 1536-1546.

Stowers, A. W., M. C. Kennedy, B. P. Keegan, A. Saul, C. A. Long and L. H. Miller (2002). "Vaccination of monkeys with recombinant Plasmodium falciparum apical membrane antigen 1 confers protection against blood-stage malaria." Infect Immun **70**(12): 6961-6967.

Stowers, A. W. and L. H. Miller (2001). "Are trials in New World monkeys on the critical path for blood-stage malaria vaccine development?" Trends in Parasitology **17**(9): 415-419.

Stubbs, J., K. M. Simpson, T. Triglia, D. Plouffe, C. J. Tonkin, M. T. Duraisingh, A. G. Maier, E. A. Winzeler and A. F. Cowman (2005). "Molecular mechanism for switching of P. falciparum invasion pathways into human erythrocytes." Science **309**(5739): 1384-1387.

Sun, J., D. Li, Y. Hao, Y. Zhang, W. Fan, J. Fu, Y. Hu, Y. Liu and Y. Shao (2009). "Posttranscriptional regulatory elements enhance antigen expression and DNA vaccine efficacy." DNA Cell Biol **28**(5): 233-240.

Suss-Toby, E., J. Zimmerberg and G. E. Ward (1996). "Toxoplasma invasion: the parasitophorous vacuole is formed from host cell plasma membrane and pinches off via a fission pore." Proc Natl Acad Sci U S A **93**(16): 8413-8418.

Swanson, S. J., J. Ferbas, P. Mayeux and N. Casadevall (2004). "Evaluation of methods to detect and characterize antibodies against recombinant human erythropoietin." Nephron Clin Pract **96**(3): c88-95.

Szymczak, A. L., C. J. Workman, Y. Wang, K. M. Vignali, S. Dilioglou, E. F. Vanin and D. A. Vignali (2004). "Correction of multi-gene deficiency in vivo using a single 'self-cleaving' 2A peptide-based retroviral vector." Nat.Biotechnol. **22**(5): 589-594.

Takala, S. L., D. L. Smith, M. A. Thera, D. Coulibaly, O. K. Doumbo and C. V. Plowe (2007). "Short report: rare Plasmodium falciparum merozoite surface protein 1 19-kda (msp-1(19)) haplotypes identified in Mali using high-throughput genotyping methods." Am J Trop Med Hyg **76**(5): 855-859.

Tham, W. H., J. Healer and A. F. Cowman (2012). "Erythrocyte and reticulocyte binding-like proteins of Plasmodium falciparum." Trends Parasitol **28**(1): 23-30.

Tham, W. H., D. W. Wilson, S. Lopaticki, C. Q. Schmidt, P. B. Tetteh-Quarcoo, P. N. Barlow, D. Richard, J. E. Corbin, J. G. Beeson and A. F. Cowman (2010). "Complement receptor 1 is the host erythrocyte receptor for Plasmodium falciparum PfRh4 invasion ligand." Proc Natl Acad Sci U S A **107**(40): 17327-17332.

Tham, W. H., D. W. Wilson, L. Reiling, L. Chen, J. G. Beeson and A. F. Cowman (2009). "Antibodies to Reticulocyte Binding Protein-Like Homologue 4 Inhibit Invasion of Plasmodium falciparum into Human Erythrocytes." Infection and Immunity **77**(6): 2427-2435.

Thera, M. A., O. K. Doumbo, D. Coulibaly, M. B. Laurens, A. Ouattara, A. K. Kone, A. B. Guindo, K. Traore, I. Traore, B. Kouriba, D. A. Diallo, I. Diarra, M. Daou, A. Dolo, Y. Tolo, M. S. Sissoko, A. Niangaly, M. Sissoko, S. Takala-Harrison, K. E. Lyke, Y. Wu, W. C. Blackwelder, O. Godeaux, J. Vekemans, M. C. Dubois, W. R. Ballou, J. Cohen, D. Thompson, T. Dube, L. Soisson, C. L. Diggs, B. House, D. E. Lanar, S. Dutta, D. G. Heppner, Jr. and C. V. Plowe (2011). "A field trial to assess a blood-stage malaria vaccine." N Engl J Med **365**(11): 1004-1013.

Thompson, F. M., D. W. Porter, S. L. Okitsu, N. Westerfeld, D. Vogel, S. Todryk, I. Poulton, S. Correa, C. Hutchings, T. Berthoud, S. Dunachie, L. Andrews, J. L. Williams, R. Sinden, S. C. Gilbert, G. Pluschke, R. Zurbriggen and A. V. Hill (2008). "Evidence of blood stage efficacy with a virosomal malaria vaccine in a phase IIa clinical trial." Plos One **3**(1): e1493.

Tissot, A. C., R. Renhofa, N. Schmitz, I. Cielens, E. Meijerink, V. Ose, G. T. Jennings, P. Saudan, P. Pumpens and M. F. Bachmann (2010). "Versatile virus-like particle carrier for epitope based vaccines." Plos One **5**(3): e9809.

Triglia, T., J. Thompson, S. R. Caruana, M. Delorenzi, T. Speed and A. F. Cowman (2001). "Identification of proteins from Plasmodium falciparum that are homologous to reticulocyte binding proteins in Plasmodium vivax." Infect.Immun. **69**(2): 1084-1092.

Tsai, C. W., P. F. Duggan, A. J. Jin, N. J. Macdonald, S. Kotova, J. Lebowitz, D. E. Hurt, R. L. Shimp, Jr., L. Lambert, L. H. Miller, C. A. Long, A. Saul and D. L. Narum (2009). "Characterization of a

protective Escherichia coli-expressed Plasmodium falciparum merozoite surface protein 3 indicates a non-linear, multi-domain structure." Mol Biochem Parasitol **164**(1): 45-56.

Vaid, A., D. C. Thomas and P. Sharma (2008). "Role of Ca2+/calmodulin-PfPKB signaling pathway in erythrocyte invasion by Plasmodium falciparum." J Biol Chem **283**(9): 5589-5597.

Volkman, S. K., P. C. Sabeti, D. DeCaprio, D. E. Neafsey, S. F. Schaffner, D. A. Milner, J. P. Daily, O. Sarr, D. Ndiaye, O. Ndir, S. Mboup, M. T. Duraisingh, A. Lukens, A. Derr, N. Stange-Thomann, S. Waggoner, R. Onofrio, L. Ziaugra, E. Mauceli, S. Gnerre, D. B. Jaffe, J. Zainoun, R. C. Wiegand, B. W. Birren, D. L. Hartl, J. E. Galagan, E. S. Lander and D. F. Wirth (2007). "A genome-wide map of diversity in Plasmodium falciparum." Nature Genetics **39**(1): 113-119.

Walther, M., S. Dunachie, S. Keating, J. M. Vuola, T. Berthoud, A. Schmidt, C. Maier, L. Andrews, R. F. Andersen, S. Gilbert, I. Poulton, D. Webster, F. Dubovsky, E. Tierney, P. Sarpotdar, S. Correa, A. Huntcooke, G. Butcher, J. Williams, R. E. Sinden, G. B. Thornton and A. V. Hill (2005). "Safety, immunogenicity and efficacy of a pre-erythrocytic malaria candidate vaccine, ICC-1132 formulated in Seppic ISA 720." Vaccine **23**(7): 857-864.

Walther, M., F. M. Thompson, S. Dunachie, S. Keating, S. Todryk, T. Berthoud, L. Andrews, R. F. Andersen, A. Moore, S. C. Gilbert, I. Poulton, F. Dubovsky, E. Tierney, S. Correa, A. Huntcooke, G. Butcher, J. Williams, R. E. Sinden and A. V. Hill (2006). "Safety, immunogenicity, and efficacy of prime-boost immunization with recombinant poxvirus FP9 and modified vaccinia virus Ankara encoding the full-length Plasmodium falciparum circumsporozoite protein." Infect Immun **74**(5): 2706-2716.

Wang, W., E. Q. Wang and J. P. Balthasar (2008). "Monoclonal Antibody Pharmacokinetics and Pharmacodynamics." Clinical Pharmacology & Therapeutics **84**(5): 548-558.

Webster, D. P., S. Dunachie, J. M. Vuola, T. Berthoud, S. Keating, S. M. Laidlaw, S. J. McConkey, I. Poulton, L. Andrews, R. F. Andersen, P. Bejon, G. Butcher, R. Sinden, M. A. Skinner, S. C. Gilbert and A. V. Hill (2005). "Enhanced T cell-mediated protection against malaria in human challenges by using the recombinant poxviruses FP9 and modified vaccinia virus Ankara." Proc Natl Acad Sci U S A **102**(13): 4836-4841.

World Health Organization. (2011). World malaria report. Geneva, World Health Organization.

Yeoh, S., R. A. O'Donnell, K. Koussis, A. R. Dluzewski, K. H. Ansell, S. A. Osborne, F. Hackett, C. Withers-Martinez, G. H. Mitchell, L. H. Bannister, J. S. Bryans, C. A. Kettleborough and M. J. Blackman (2007). "Subcellular discharge of a serine protease mediates release of invasive malaria parasites from host erythrocytes." Cell **131**(6): 1072-1083.